

Investigation of Support Fabrics for Graphene-Based End-of-Life Sensors for Fire Protective
Garments

by

Diana Yehia

A thesis submitted in partial fulfillment of the requirements for the degree of

Master of Science

in

Textiles and Clothing

Department of Human Ecology
University of Alberta

© Diana Yehia, 2021

Abstract

Fire-resistant fabrics used in protective clothing experience a reduction in performance because of ageing. Yet there are generally few visible clues before the loss in performance has reached a dangerous level. To solve this issue, a graphene-based end-of-life (EOL) sensor is being developed at the University of Alberta which will be placed as a patch on the protective clothing's surface. It will indicate when fire-resistant fabric of the protective clothing has reached an unsafe level of performance. My thesis aims to identify the most suitable fabric to serve as a support for the EOL sensor.

The support fabric should be flame resistant and washable. It should also withstand ageing conditions (e.g. temperature, ultraviolet light, and moisture) without degrading. Therefore, a series of FR fabrics made of different materials as well as those that are commonly used for fire protective clothing were subjected to accelerated ageing at specific conditions. The residual mechanical performance was assessed to identify the best candidate for the support fabric.

The final candidate fabric was coated with reduced graphene oxide (rGO) so that the durability of the rGO coating to washing and the quality of bond between the coating and the selected support fabric could be assessed. This was done by monitoring changes in the surface conductivity of the rGO coating and observing changes in the morphology of the coating on the support fabric following multiple laundering cycles.

The fabric substrate is the cornerstone for the development of the graphene-based EOL sensor. The success of the selected fabric substrate and meeting the requirements proposed will allow the manufacturing of the EOL sensor which will be suitable for keeping firefighters safe and ensure that their protective clothing is safe to use.

Acknowledgements

I would like to thank the Aga Khan Foundation for giving me this once-in-a-lifetime opportunity to pursue my education in Canada.

I also would like to express my sincere appreciation and deepest gratitude to Dr. Jane Batcheller and Dr. Patricia Dolez, thank you for believing in me.

I wish to acknowledge the support and great love of my family, my father, Nasser; my mother, Abeer; my siblings, Mazen, Shams and Yazan; and my precious nephew, Youssef. Nashir and Najma Karmali whom I would not be here without their help and constant support. Jo Hindle for being the grandmother I never had.

Lastly, my friends whom I love the most, Zeina, Basel, Reem, Razan, Lamia, Homa, Laura and Pradipika. Thanks for being a part of my life.

This research was supported by NSERC Strategic Project STPGP 521866 – 18, Graphene-based end-of-life sensors for fire protective fabrics.

Table of Contents

1.	INTRODUCTION.....	1
1.1.	Background	1
1.2.	Ageing of fire protective clothing	3
1.3.	Research objectives	5
1.4.	Limitations	6
2.	REVIEW OF LITERATURE.....	7
2.1.	Firefighters' ensemble.....	7
2.2.	Fire-resistant fabrics.....	8
2.2.1.	Fibres used in current outer shell fabrics.....	11
2.2.1.1.	Aramid fibres.....	12
2.2.1.2.	PBI fibres.....	16
2.2.1.3.	PBO fibres	17
2.2.2.	Fibres investigated as candidates for the support fabric for the EOL sensor	19
2.2.2.1.	Glass fibres	20
2.2.2.2.	Cellulosic fibres.....	22
2.2.2.2.1.	FR Cotton fibres	24
2.2.2.2.2.	Regenerated cellulose fibres.....	26
2.2.2.3.	FR Polyester fibres	28
2.2.2.4.	Oxidized PAN fibres	29
2.2.2.5.	Novoloid fibres.....	32
2.2.2.6.	Liquid Crystal Polyester fibres.....	33
2.3.	Conditions causing the ageing of the fabrics used in firefighters' garments.....	34
2.3.1.	Heat and flame	35
2.3.2.	Ultraviolet light	37
2.3.3.	Water	39
2.3.4.	Laundering	41
2.3.5.	Abrasion	44
3.	MATERIALS AND METHODS	47
3.1.	Fabrics tested.....	47
3.2.	Fabric Characterization Methods	48
3.2.1.	Mass	48
3.2.2.	Thickness.....	49

3.2.3.	Fabric count and structure	50
3.2.4.	Fibre content.....	50
3.3.	Determination of the accelerated ageing conditions for the sensor substrate fabric assessment	50
3.3.1.	Thermal ageing conditions	51
3.3.2.	Photochemical ageing conditions.....	53
3.3.3.	Hydrothermal ageing condition.....	55
3.3.4.	Laundrying ageing conditions	57
3.4.	Experimental Design	59
3.4.1.	Thermal test.....	60
3.4.2.	Photochemical test.....	61
3.4.3.	Hydrothermal test.....	62
3.4.4.	Laundrying test.....	64
3.5.	Residual performance assessment methods	65
3.5.1.	Tear strength.....	65
3.5.2.	Tensile strength	68
3.5.3.	Shrinkage.....	72
3.6.	Assessing the strength of the rGO coating	73
3.6.1.	Preparation of the rGO-coated specimens.....	73
3.6.2.	Laundrying of the rGO-coated specimens.....	76
3.6.3.	Electrical conductivity measurement of rGO-coated specimens.....	76
3.6.4.	Surface morphology characterization of the rGO-coated specimens	76
3.7.	Statistical analysis	77
4.	RESULTS AND DISCUSSION	78
4.1.	Fabric characterization	78
4.2.	Effect of accelerated ageing on the mechanical strength of the tested fabrics	82
4.2.1.	Effect of accelerated thermal ageing on the mechanical strength of the tested fabrics.....	85
4.2.2.	Effect of accelerated photochemical ageing on the mechanical strength of the tested fabrics	109
4.2.3.	Effect of accelerated hydrothermal ageing on the mechanical strength of the tested fabrics..	129
4.2.4.	Effect of accelerated laundrying on the mechanical strength of the tested fabrics.....	149
4.3.	Shrinkage.....	165
4.4.	Final selection of the support fabric	170
4.5.	Assessing the strength of the rGO coating	171

5.	SUMMARY AND RECOMMENDATIONS	182
5.1.	Summary	182
5.2.	Recommendations	183
	BIBLIOGRAPHY	185
	APPENDICES.....	205
	Appendix A: Fabrics’ characteristics	205
	Appendix B: Paired samples test and One-way ANOVA test for all fabrics tested after accelerated thermal ageing.....	226
	Appendix C: Paired samples test and One-way ANOVA test for all fabrics tested after accelerated UV ageing 237	
	Appendix D: Paired samples test and One-way ANOVA test for all fabrics tested after accelerated hydrothermal ageing.....	249
	Appendix E: Paired samples test and One-way ANOVA test for all fabrics tested after accelerated laundering.....	256
	Appendix F: Summary of Descriptive Statistics, Levene's Test of Equality of Error Variances, Tests of Between-Subjects Effects, and Multiple Comparisons for shrinkage for all fabrics tested	267

List of Acronyms

Acronym	Explanation
DI	Deionized water
EOL	End-of-life
FE-SEM	Field emission scanning electron microscope
FR	Fire-resistant
FTIR	Fourier transform infrared spectroscopy
GO	Graphene oxide
HM	High modulus
LSCM	Laser scanning confocal microscopes
LOI	Limiting oxygen index
LCP	Liquid crystal polyester
NFPA	National Fire Protection Association
OPF	Oxidized PAN fibre
PAN	Polyacrylonitrile
PBI	Polybenzimidazole
PPTA	Poly-p-phenylene terephthalamide
PBO	Poly-p-phenylene benzobisoxazole
PET	Polyethylene terephthalate
RO	Reverse osmosis water
R_s	Sheet electrical resistance
SEM	Scanning electron microscope
rGO	Reduced graphene oxide
SM	Standard modulus
UV	Ultraviolet
WOB	Without optical brighter

1. INTRODUCTION

1.1. Background

Firefighting is deemed to be one of the most stressful and dangerous professions (Kunadharaju et al., 2011). According to the International Association of Firefighters (2001), the injury rate is three times higher for professional firefighters in comparison to workers in other industrial occupations while on duty. Most on-duty injuries for firefighters include burns, sprains and strains, wounds and bruises, eyes injuries and illness from the inhalation of toxic materials. When heat is transferred to the skin, it gets absorbed and can cause skin burns if the heat transfer, intensity, and time of exposure are sufficient to cause damage (Holcombe, 1981). Besides, the body temperature increases when the heat gain is higher than the heat loss leading to heat stress where skin temperature increases beyond a critical value causing the decrease in the wearer's performance (Rossi, 2014). Fire protective clothing is designed to provide thermal protection and also act as an insulator between the wearer and the ambient environment which may be very hot in a fire situation (Holcombe, 1981). Because fire protective clothing contributes to the safety of firefighters and is considered the first line of defence against fire (Arrieta et al., 2010), fire protective clothing must maintain its performance against hazards throughout its lifetime. However, fire protective clothing can be affected by many environmental conditions, for instance: heat, ultraviolet light (UV), and moisture. These conditions may cause a reduction in the mechanical performance of the fire protective clothing. Unfortunately, visibly assessing the performance of fire protective clothing is generally not possible because, in many cases, large losses in performance can take place before the degradation of the fabric is visible to the naked eye (Rossi et al., 2008). Therefore, the reduction in mechanical performance can not be detected from the fabric appearance alone.

Smart textiles are described as the outcome of functional components being integrated into textiles (Salavagione et al., 2018). These functional components may react with exterior stimulants, store or convect energy, provide drug release, or act as monitors or sensors. In the past two decades, different techniques have been under development to include smart components in textiles (Lee et al., 2016). Initially, smart textiles involved wires attached to the textile to connect processors and batteries. Recently, techniques have become more advanced and smart components can either be integrated in, embodied into, or coated onto the textiles. For example, conductive nanoparticles can be deposited on a textile substrate using different deposition methods such as atomic layer deposition, galvanic deposition, electrochemical deposition and electroless deposition (Hansora et al., 2015). Graphene is one example of these conductive nanomaterials. It has unique thermal, optical, mechanical, electrical, and magnetic properties. Graphene is a two-dimensional (2D) flat monolayer of carbon atoms in the form of a honeycomb network that is the building component of other graphitic materials (Geim & Novoselov, 2007). Graphene's excellent properties and sensitivity to all environmental stimuli makes it an excellent option for a functional component to be integrated into other materials in an attempt to improve their performances or to add smart features (Salavagione et al., 2018). Graphene can be incorporated into textiles in different ways by making a graphene/polymer mixture to form the fibre or by a graphene coating on an already processed fibre or fabric.

At the University of Alberta, a project is underway to develop graphene-based, end-of-life (EOL) sensors for fire protective clothing. Three sensors are being developed: a heat sensor, a UV sensor, and a moisture sensor (NSERC Strategic Project STPGP 521866 – 18, Graphene-based end-of-life sensors for fire protective fabrics). Each sensor consists of several layers, including polymers that are similarly sensitive to the ageing conditions of heat, UV, and

moisture as the outer shell fabrics of firefighters' protective garments, along with a reduced graphene oxide (rGO) coating on a support fabric. The rGO coating will act as a conductive track (Cho et al., 2019) that will eventually be exposed and will lose its conductivity as the polymer component of the sensor is degraded and lost through exposure to the selected ageing conditions. The sensor with its textile substrate will be applied as a patch to specific areas of the outer shell of a firefighter's protective garment. Changes in the electrical conductivity of the sensor will be used to monitor the condition of the outer shell fabrics and will help the users determine if the fire protective clothing is safe to use or not.

1.2. Ageing of fire protective clothing

First responders, such as firefighters, are exposed to a variety of hazards in their work environments, such as thermal, chemical, biological, mechanical, and nuclear hazards (Song et al., 2017a). Firefighters are especially in danger of exposure to thermal hazards, including open flame, radiant heat, steam, hot fluids and surfaces. Therefore, flame-resistant (FR) and thermal-protective clothing is very important for a firefighter's safety. Because of their hazardous duties, such as fighting indoor/outdoor fires or during life-saving interventions, firefighters are required to wear special protective textile materials (Crown & Batcheller, 2016). For structural firefighters, light garments might be sufficient in some situations, but because firefighters are unaware of the hazards they will confront, they usually wear thick and heavy garments. To provide protection against flash fires, any material participating in the garment system must be able to "resist ignition and self-extinguish when the ignition source is removed, limit heat transmission, not melt or shrink, maintain its structural integrity and flexibility and not emit any toxic combustion products during exposure to high heat flux." (Crown & Dale,

2005, p. 702). These requirements are also relevant for other industrial workers where protection against thermal hazards is needed (Crown & Batcheller, 2016).

High-performance fibres are the essential materials for manufacturing fire protective clothing and take an important role in defining its properties and end-uses (Song et al., 2017b). Fabric made from inherently FR fibres or FR treated fabrics are the two options for thermal protective clothing which have been accessible for numerous years (Crown & Batcheller, 2016). These materials provide significant resistance/retardancy against heat and flame (Song et al., 2017b), however, like all materials, they age and may lose their properties over time. According to Rossi et al (2008), when FR fabrics typically used as outer shell in firefighter protective clothing are exposed to high thermal fluxes, a change in attributes occurs which may cause an alteration in performance and change in appearance. This ageing of materials often leads to a reduction in their heat protection and mechanical properties such as tear and tensile strength, and undesirable appearance changes like decolouration. The degradation of a material and the reduction in its performance might happen before or without any visible changes (Rossi et al., 2008; Arrieta et al., 2010). These undesirable changes resulting from ageing can diminish the protective properties of a garment and lead to possible injury from exposure to workplace hazards (Arrieta et al., 2010).

The minimum requirements for the design, performance, testing and certification of new structural and proximity fire fighting protective ensembles and ensemble elements such as coats, trousers, coveralls, helmets, gloves, footwear, and interface components, are specified by the National Fire Protection Association (NFPA) 1971 (2018) - Standard on Protective Ensembles for Structural Fire Fighting and Proximity Fire Fighting. Firefighters' protective clothing must meet the performance requirements established by this standard for use in North

America. The high-performance materials used in these garments are tested and certified to performance requirements when they are new. Since the materials are known to deteriorate as they age, garments are also required to be retired and replaced after a fixed number of years in service. Nevertheless, the date of retirement may not reflect the actual condition of the garment. The EOL sensors under development at the University of Alberta are intended to help predict the condition of the protective clothing materials and provide the end user with a better justification for retiring their protective clothing than just the number of years the garment has been in service.

1.3. Research objectives

This research study is designed to assess and compare the performance of a selection of high-performance fabrics, and to determine the best choice of support fabric for the graphene-based EOL sensor. The chosen support fabric must fulfil some specific requirements. These requirements are:

1. The fabric must resist ageing under specific conditions that are damaging for the fire-protective fabrics currently used as the exterior layer or outer shell fabric of firefighters' protective clothing.
2. The fabric must be able to withstand the same laundering conditions as the outer shell fabric of firefighters' protective clothing.
3. The fabric must have excellent mechanical flexibility and durability.
4. The fabric must be able to be attached (sewn) to the outer shell fabric of firefighters' protective clothing.
5. The fabric must allow for a good quality coating of the rGO conductive tracks of the EOL sensor.

1.4. Limitations

The limitations of this research include:

1. The fabrics chosen for this research were limited to those made from inherently FR fibres and FR treated fabrics.
2. For Fabric O, the quantity of material available was not enough to test more than one specimen for each accelerated ageing condition.

2. REVIEW OF LITERATURE

2.1. Firefighters' ensemble

As stated in the introduction, fire protective ensembles are fundamental for the safety of firefighters and are considered the primary line of defence against hazardous elements like fire, steam, chemicals, and sharp items (McQuerry et al., 2015). A variety of ensembles exist in the market to provide full wearer protection. Structural fire fighting protective ensemble was defined by NFPA 1971 (2018) as “multiple elements of compliant protective clothing and equipment that when worn together provide protection from some risks, but not all risks, of emergency incident operations” (p. 20). The coat, trouser and coverall are garment elements for the structural fire fighting protective ensemble. Other elements such as gloves, hoods, helmets, and footwear are included. Figure 1 shows the composition of a typical firefighters' garment. Each garment of the ensemble normally consists of three layers, each layer with a particular task (Rossi, 2014). The outer shell or the surface layer provides protection against heat and flame, protection against mechanical hazards, and provides some resistance to penetration by liquids. The moisture barrier or the middle layer is intended to prevent liquid penetration and also allow water vapour generated from the body to pass to the outer ambient atmosphere. The function of the thermal liner, or the inside layer closer to the wearer's body, is to protect the body from high heat transfer. As noted by Rossi (2014), fire protective clothing needs to provide a balance between high thermal protection and high thermal comfort, thus materials with suitable thermal resistance as well as water vapour penetrability are needed.

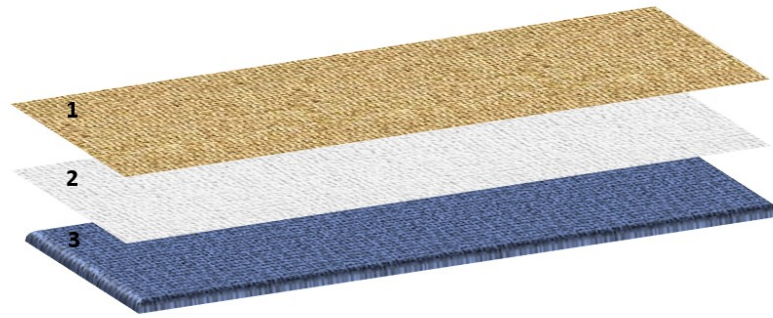


Figure 1. Layers of a typical firefighters' garment: (1) outer shell, (2) moisture barrier, and (3) thermal liner.

2.2. Fire-resistant fabrics

The development of FR textiles first started as treatments for both natural and synthetic fibres, and it is believed that most FR textiles were developed around the time of World War II to improve the safety of military personnel (Horrocks, 2011). Textiles used in fire protective clothing should protect the wearer and provide a level of fire-retardancy/resistance (Horrocks, 2016). Flammability is described as how quickly a fibre or fabric burns or ignites, leading to a fire or combustion (Hirschler et al., 1996, as cited in Song et al., 2017c). Several parameters characterize the flammability behaviour of textile, such as the ignition time, burning rate and the heat release rate resulting from the exposure to an ignition source (Horrocks, 2016). The extent of a fire hazard is determined by these parameters. Other factors related to the textile such as the melting and shrinking characteristics and the emission of smoke and toxic gases, primarily affect the thermal protection level of a given textile. In short exposure intervals, heat leaves a less damaging effect on textile materials if not accompanied by flame. However, the presence of flame induces a chemical reaction, also defined as pyrolysis, wherein gaseous components are released from the degrading material

followed by an oxidation reaction with the ambient atmosphere. This reaction with flame is powerful enough to produce light and heat in the range between 600 and 1000 °C which is an ideal temperature for the burning of textiles. Chemical and physical changes occur in a textile material when exposed to heat, these changes are dependant on the temperature and the chemical composition of the material (Choudhury, 2017).

When synthetic fibres are exposed to high temperatures, they soften when they reach their glass transition temperature, melt when they reach their melting temperature, go through pyrolysis when they reach their pyrolysis temperature and eventually ignite and combust when they reach their combustion temperature (Song et al., 2017b). Combustion is an exothermic process that requires heat, oxygen and sustainable fuel (Choudhury, 2017). When combustion occurs, it includes the release of gases, water vapour and radiant heat/flame (Song et al., 2017b). The minimum oxygen needed to create a combustion reaction is termed LOI (Limiting oxygen index). If a synthetic fibre has an LOI of more than 21% (percentage of oxygen normally present in the ambient atmosphere), the fibre is identified to be inherently FR. Natural fibres such as wool, cotton and viscose and synthetic fibres such as polyester, nylon and acrylic have low LOI values (less than 21%), however, with appropriate chemical modification of these fibres, the LOI can be increased to be more than 21%. These fibres are referred to as chemically modified flame-resistant fibres. More information on chemically modified FR fibres follows.

There are many approaches to render a textile material to be FR, and they vary according to the nature of the material (Song et al., 2017b). For synthetic fibres, one approach involves the incorporation of flame-retardants as polymerization additives or spinning-dope additives. For natural fibres, flame retardants are used in finishing and are applied directly to

the fabric. Textile materials produced using either of these approaches are referred to as chemically modified FR fibres. The flame retardancy of chemically modified FR fibres is not durable and might disappear after repeated washing. According to (Horrocks, 2016), chemically modified FR fibres have a maximum continuous operating temperature of 100 °C “a temperature at which a fabric can still operate constantly without any significant thermal degradation arising.” (Horrocks, 2016, p. 243). For example, FR cotton, FR wool, FR viscose, FR polyester, FR acrylic and FR polypropylene fibres. Another approach for synthetic fibres is the modification at a molecular level, wherein their chemical structure is altered to make them thermally stable without any additional chemicals or special processing to acquire their flame resistance (Song et al., 2017b). The flame retardancy of inherently FR fibres is durable and stays after repeated washing. Inherently FR and inorganic fibres have a continuous operating temperature higher than 150 °C. For example, meta- and para- aramids, novoloid, PBI, PBO, carbon and glass fibres (Horrocks, 2016).

Fire protective garments are made of FR fibres (Fei, 2018). The thermal protection against several hazards such as flash fire, electric arc and molten material is acquired through these products via rendering the material to resist ignition, decreasing the burning rate and heat output, and promoting the production of char. Therefore, altering the mechanism of combustion or stopping the combustion process is an efficient way to reduce the flammability of textile materials (Joseph & Tretsiakova-McNally, 2013). Furthermore, the material is less likely to maintain a self-propagating flame after the elimination of the ignition source (Horrocks, 2016). The function of FR fibres is exhibited through two mechanisms (Song et al., 2017b): gas phase and solid phase. In the gas phase, the flame-retardant material decomposes into free radicals and creates non-volatile compounds, for instance, ester compounds, which will limit the oxygen

needed for combustion either by creating a complex reaction between these compounds and oxygen from the ambient atmosphere or by depositing these compounds on the surface of the fibre in a gas phase. As a result, the pyrolysis and softening of the fibre are delayed and the LOI value increases. In the case of the solid phase, the surface of the fibre changes and this change encourage substantial cross-linking which results in the production of carbonaceous char deposited on the surface of the fibre. This char insulates the fibre beneath from radiant heat/flame and acts like a layer that prevents further burning and production of new fuel. The process of forming the carbonaceous char sometimes is complemented with the formation of water. Through water, the fibre is cooled down and the energy needed for further burning of fibre increases. As a result, the pyrolysis, softening and LOI value of the fibre increase.

Generally, it is worth quoting Horrocks (2016) who clarified the key factors which should be considered while selecting and designing fire protective clothing, such as “the fundamental thermal or burning behaviour of textile fibres, the influence of fabric structure and garment/product shape on the burning behaviour, the geometry in which the textile is used (e.g. vertical or horizontal), the possible selection of non-toxic, smoke-free flame retardant additives or finishes, design of the protective garment, depending on its usage, with comfort properties, the intensity of the ignition source, and the oxygen supply.” (p .240)

2.2.1. Fibres used in current outer shell fabrics

Three main families of inherently FR fibres are currently used as blends in firefighter protective garment outer shell fabrics (Bourbigot, 2008). These fibres are aramids, PBI and PBO and are described in detail below. The performance of fabrics made from blends of these fibres has been used as a benchmark for the selection of the textile substrate for the

graphene-based EOL sensor. The substrate fabric must not compromise the performance of the protective garment and should ideally have better resistance to ageing conditions than the shell fabric.

2.2.1.1. Aramid fibres

In the early 1960s, aromatic polyamides emerged and became a revolutionary substance with many industrial applications (Rebouillat, 2001). Aromatic polyamide-based fibres referred to as aramids were defined by the United States Federal Trade Commission as ‘a manufactured fibre in which the fibre-forming substance is a long-chain synthetic polyamide in which at least 85% of the amide (—CO—NH—) linkages are attached directly to two aromatic rings’ (Rebouillat, 2001, p. 24). Aramid products such as fibres, fibrils, films, paper, particles, and pulps display interesting thermal and mechanical properties (Gabara et al., 2007). Both continuous filament yarns for applications that require high mechanical properties and staple spun yarns for textile applications enjoy a huge demand on the market. DuPont, which remains the largest manufacturer, carried out the fundamental production and the first commercial launch of aramid products. The first aromatic polyamide fibre to be produced is meta-aramid, an MPDI-based (poly (m-phenylene isophthalamide)) fibre with meta-oriented linkages. This fibre was introduced in 1967 by DuPont under the trademark Nomex[®] (Rebouillat, 2001). Para-aramid fibre is a PPTA-based (poly (p-phenylene terephthalamide)) fibre with para-oriented linkages. It was introduced in 1971 by DuPont under the trademark Kevlar[®]. Another key manufacturer of meta-aramid fibres is Teijin in Japan, under the tradename Teijinconex[®]. Teijin also produces two types of para-aramids fibres: PPTA-based, under the tradename Twaron[®], and copolymer-based, under the tradename Technora[®]. Russia also manufactures a small amount of para-aramid fibre, under the tradenames Armos[®] and

Rusar[®]. Both are copolymer-based reliant on a special but expensive monomer (diaminophenylbenzimidazole) (Gabara et al., 2007, p. 979). Figure 2 shows the chemical formulas for meta- and para-aramid fibres.

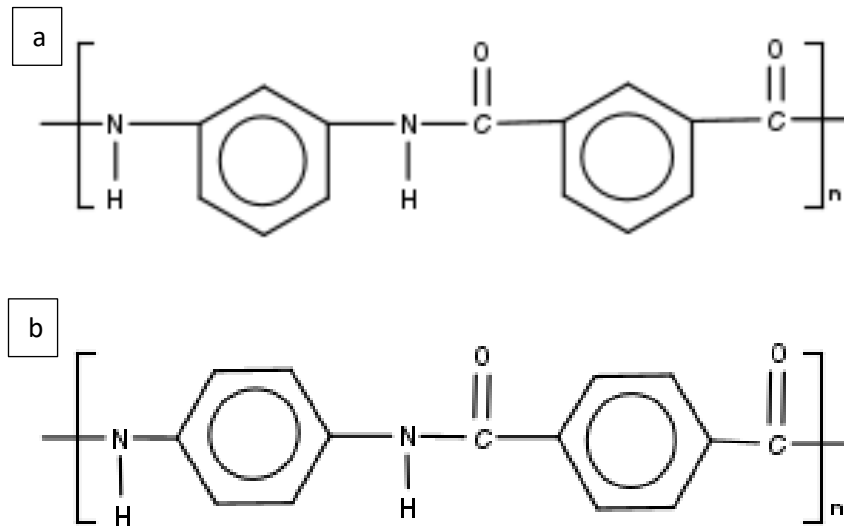


Figure 2. Chemical structure of: (a) meta-aramid fibre, (b) para-aramid fibre.

Meta-aramid has a thermal conductivity that is lower than any other aramid fibre (Bourbigot & Flambard, 2002). The LOI of meta-aramids is between 30 and 32% which means there is not enough oxygen in the ambient atmosphere to sustain combustion. The continuous operating temperature for meta-aramids is 200 °C. At temperatures below 250 °C, meta-aramid fibres maintain their tensile strength (Yang, 2018), but when exposed to 300 °C, the fibres only preserve 60% of their strength. They tend to decay quickly when exposed to a temperature above 371 °C. Weight loss occurs at 450 °C and the fibre completely chars at 600 °C in air (Bourbigot & Flambard, 2002). When a meta-aramid fabric is exposed to a flash fire, a carbonaceous insulation layer, ten times thicker than the main layer, is created (Rebouillat,

2001). When the source of fire is removed, meta-aramid fibres tend to self-extinguish. At ambient conditions, meta-aramid fibres have a moisture regain of 4.5% (Yang, 2018).

Para-aramid is one of the most popular lyotropic aramid fibres (Bourbigot & Flambard, 2002). PPTA is the polymer used to produce para-aramid fibres (Gabara et al., 2007). This polymer forms fibres with very high crystallinity and high orientation. Therefore, the produced fibre has very high strength and high modulus or stiffness (Bourbigot & Flambard, 2002). The LOI for para-aramid is between 28 and 30%. Para-aramid continuous operation temperature is 190 °C. It glows when it is ignited but does not melt, yet it degrades in the open air when the temperature is above 400 °C and chars at 450 °C. When exposed to high temperatures for a long time, para-aramid fibres show excellent thermal stability. According to Yang (2018) at a temperature of 180 °C in dry air, para-aramid fibres exhibit a loss in tensile strength of not more than 16%. At 300 °C, the fibres still possess high strength and modulus, but, at 400 °C, para-aramid fibres lose half of their strength and reach zero at 455 °C. Para-aramids have a moisture regain of 4.0% for high modulus (HM) and 7.0% for standard modulus (SM) fibres.

Polymers used to produce aramid fibres have a high melting point and do not dissolve easily, hence, fibres are produced from polymer solutions (Gabara et al., 2007; Jassal et al., 2020). Highly polar solvents such as N-methyl-2-pyrrolidone (NMP) and dimethylacetamide (DMAc) with or without inorganic salts or acids are used to dissolve polymers. To produce meta-aramids, an isotropic polymer solution is formed by dissolving MPDI polymer in solvents like NMP and DMAc (Gabara et al., 2007; Jassal et al., 2020). To produce para-aramids, a lyotropic polymer solution is formed by dissolving PPTA polymer in solvents with inorganic salts and acid such as sulfuric acid, and copolymerization of the

polymer is performed to increase solubility. Later, polymer solutions are spun into fibres using a spinning process, for instance, wet spinning, dry spinning and dry-jet wet spinning. MPDI-based fibres are less orientated and crystalline than PPTA-based fibres (Gabara et al., 2007). Therefore, meta-aramid fibres exhibit lower strength than para-aramid fibres (Jassal et al., 2020).

The mechanical properties are defined by the molecular chain structure of the fibre (Rebouillat, 2001). Likewise, the molecular orientation around the fibre axis, the number of active areas taken by a single chain and the linearity degree of the chain all contribute to determining the tensile modulus. Rebouillat (2001) also states that the high tensile strength expressed by para-aramid fibres can be linked to the regular polymer chain. On the other hand, meta-aramid fibres exhibit a lower tensile modulus because of their irregular polymer chain. Aramids experience shrinkage of less than 0.1% at 177 °C in air and at 100 °C in water (Jassal et al., 2020). In addition, meta-aramid fabrics are more preferable for protective apparel because they have a more comfortable textile-hand than para-aramids (Gabara et al., 2007). According to Rebouillat (2001) “The stiffness of the PPTA chain is partly associated with the limited rotation of the carbon-nitrogen bond, itself due to the resonance-conjugation existing between the amide and the aromatic groups” (p. 46). The same case does not apply to meta-aramids (Rebouillat, 2001). For this reason, para-aramid fibres have a golden yellow colour in comparison to meta-aramid fibres which have a white colour (Rebouillat, 2001; Jassal et al., 2020).

2.2.1.2. PBI fibres

The aromatic polybenzimidazole (PBI) polymer was developed in the 1960s (Dawkins et al., 2014). A decade later, NASA started incorporating PBI fibres in their applications, including fabrication of brake parachutes, ropes and astronauts' clothing because of its non-flammability and high thermal stability (Dawkins et al., 2014; Coffin et al., 1982). In the early 1980s, PBI fibres were commercially manufactured by Celanese Corporation under the trademark PBI (Song & Su, 2020). Later on, other PBI products surfaced in the market such as films, reinforcement composites, microporous sizing, coating, resins, moulding resins, and paper (Dawkins et al., 2014). PBI was first used as an outer shell fabric in the fire services, generally as a blend with para-aramids, and later in the braking systems of cars in the 1990s. In the 2000s, the use of PBI in the fire protective turnout gear expanded. The outstanding performance displayed by PBI makes it a good choice for fire protective clothing.

PBI polymer is produced according to a two-stage reaction process between two monomers: tetra-aminobiphenyl (TAB) and diphenylisophthalate (DPIP) (Horrocks et al., 2001). The polymer obtained is dissolved in DMAc to make a polymer solution and then spun into fibres at high temperature using a dry-spinning process (Coffin et al., 1982). Drawing of fibres is performed to obtain the desired mechanical properties. The produced fibres are treated with sulfuric acid to reduce shrinkage of fibres when subjected to heat or flame and later spun into staples (Coffin et al., 1982; Horrocks et al., 2001). The thermal stability of PBI takes advantage of the wholly aromatic, ladder-like structure (Dawkins et al., 2014). In addition, the presence of three benzene rings in the repeating unit helps to improve the thermal stability, toughness, and stiffness of the polymer (Dawkins et al., 2014). According to (Horrocks et al., 2001), the thermal stability of PBI fibres increases when treated with sulfuric acid and treated

PBI fibres exhibit a thermal shrinkage of less than 10%. Figure 3 shows the chemical structure of the PBI polymer.

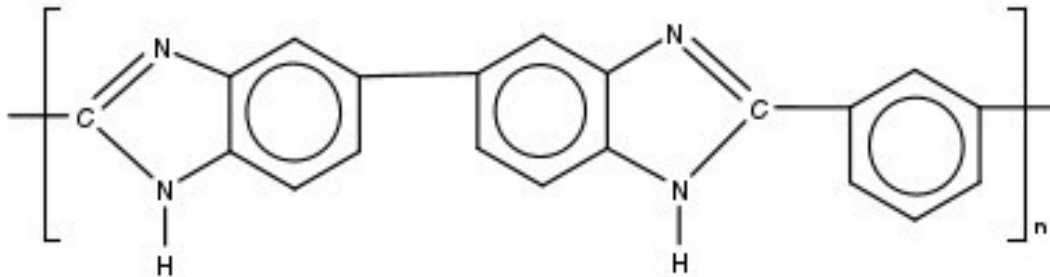


Figure 3. Chemical structure of PBI polymer.

The LOI for PBI is higher than 41% (Bourbigot & Flambard, 2002). PBI fibres have a continuous operating temperature of 250 °C. Moreover, the glass transition temperature for PBI is 450 °C. When exposed to a temperature of 580 °C in the air or a temperature over 1000 °C in nitrogen, PBI starts to degrade. Also, PBI does not burn and when the source of flame is eliminated, it self-extinguishes. Yet, it chars when subjected to high heat flux, but retains its flexibility and experiences a slight shrinkage. Additionally, the moisture regain is around 15% which is higher than most other fibres (Dawkins et al., 2014). The high absorbency of fibres is linked to water forming hydrogen bonds with the hydrogen on the polymer chain's imidazole ring.

2.2.1.3. PBO fibres

The US Air Force Materials Laboratory was the first to produce poly-p-phenylene benzobisoxazole (PBO) fibres (Bourbigot & Flambard, 2002). These fibres showed exceptional properties. Afterward, the chemical company Dow obtained the patent from the Stanford

Research Institute to continue the development of the product. Although handling the polymer is tough because of its rigid rod-like nature, they were able to come up with innovative methods to produce the fibre. However, because of some hurdles related to fibre spinning, Dow joined the Japanese Company Toyobo in 1994 in an attempt to develop a new spinning method to produce PBO fibres. Consequently, a new approach of spinning was developed and the production of PBO fibres emerged in 1998 under the trademark Zylon[®].

PBO is an aromatic heterocyclic rigid-rod polymer and the polymer itself has extremely rigid molecules which lead to an extremely oriented structure (Beers et al., 2001). The monomer 4,6-diamino-1,3-benzenediol dihydrochloride (DABDO) is used in the fabrication of the PBO fibres. The fabrication process involves the condensation polymerization of DABDO and terephthalic acid (TA). The obtained polymer is dissolved in an acidic solvent such as sulfuric acid or poly(phosphoric) acid (PPA) (Abe & Yabuki, 2012). Then, the polymer solution is spun into fibres through a dry-jet wet spinning process and later drawn to control the mechanical properties. PBO fibres exhibit high resistance to flame, creep, chemicals, and abrasion, and have high thermal stability (Beers et al., 2001). Zylon[®] is considered the number one polymer regarding flame resistance and thermal stability (Horrocks et al., 2001). This fibre has a rigid and linearly symmetrical repeating aromatic structure, and the absence of aliphatic CH groups gives it high thermal stability (Figure 4).

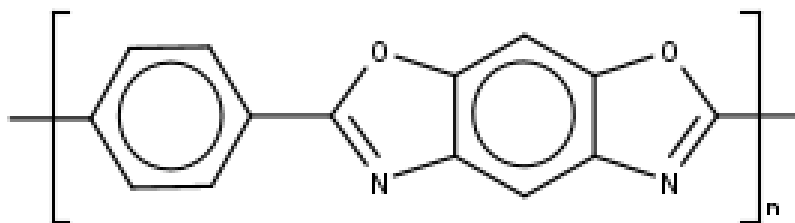


Figure 4. Chemical structure of PBO polymer.

The LOI for PBO fibres is 68% (Bourbigot & Flambard, 2002). PBO's continuous operating temperature in the air is 350 °C. The temperature at which PBO starts to degrade is 600 °C in air and over 700 °C in an inert atmosphere. When an HM Zylon[®] fibre is exposed to temperatures of 300, 400 and 500 °C, the tenacity retention is 65, 50 and 40% respectively (Horrocks et al., 2001). Other researchers found that when PBO fibres were heated for 200 h at 300 °C, in a nitrogen atmosphere, the tensile strength did not change, however, when the heating is in air, the tensile strength is reduced by 40% (Fei, 2018). The moisture regain of HM Zylon[®] is 0.6%, whereas it is 2% in the case of AS Zylon[®].

2.2.2. Fibres investigated as candidates for the support fabric for the EOL sensor

A series of commercially available fabrics were obtained corresponding to different types of fibres which could be relevant as a substrate for the graphene-based EOL sensor. The main selection criterion for these fabrics was to be FR. The selection below gives information about each of these fibre types.

2.2.2.1. Glass fibres

The first known use of glass fibre in textiles was in 1713 by a French physicist who produced the fibres from molten glass and incorporated them as strands into textiles (Martynova & Cebulla, 2018). Also, in the late 19th century, glass fibres are known to have been interwoven with silk for dress fabric, but it was not until the 1930s that glass fibre was produced at an industrial scale. In 1935, thermosetting resins such as polyester were reinforced with glass fibres and used for structural purposes. Fibreglass has been widely used as a reinforcement material ever since because of its good fire resistance and low cost. Glass fibres have high corrosion resistance, and higher stiffness and strength than most textile fibres. The strength can be increased by increasing the fibre surface to volume ratio (Jones, 2001). Therefore, the finer the fibre diameter, the stronger it will be. Glass fibres have flourished in the twentieth century and have been incorporated in many applications, for example, filtration, insulation, and data transmission.

Silicon dioxide (SiO_2), known as silica, is the main element of glass fibres (Martynova & Cebulla, 2018). It is also the main constituent of sand, which is made of small crystals of silica. The silica tetrahedron is formed of one silicon atom surrounded by four oxygen atoms (Figure 5 (a)). In sand, silicon atoms connect through Si-O-Si bonds (Figure 5 (b)). There is no chemical formula to describe glass because it is a combination of silica elements with several metal oxides in different ratios. Hence, the chemical structure is expressed by the percentage content of the oxides.

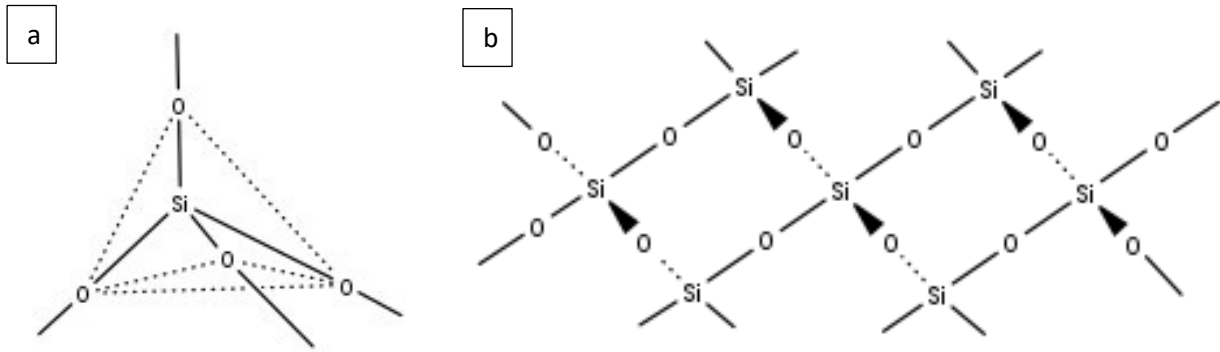


Figure 5. The chemical structure of: (a) silica tetrahedron, (b) crystallized SiO_2 . After (Martynova & Cebulla, 2018).

Glass fibres soften around 650-970 °C (Bourbigot & Flambard, 2002). When exposed to a temperature above 850 °C, the softened glass fibres crystallize. They melt as the temperature rises to between 1225-1360 °C. There are two main categories of glass fibres depending on the final use of the product: either inexpensive fibres for general use or expensive fibres for exclusive use (Martynova & Cebulla, 2018). Only 10% of today's manufactured glass fibres are for exclusive use, the remaining 90% is E-grade glass fibres. The letter E stands for the electrical property, and these fibres have low electrical conductivity. They also have very high resistance against heat and moisture (Gong & Chen, 2000). According to Martynova & Cebulla (2018), there are two types of E-Glass, one with boron which is more common, and the second type without boron. When E-glass contains boron, the silicon oxide content ranges between 52-56%. When it does not contain boron, the percentage is higher and ranges between 59-61%. Both types of E-glass, contain other metal oxides such as aluminum oxide (12-15%), calcium oxide (21-23%), and magnesium oxide (1-3.5%). The percentage of titanium oxide depends on the E-glass type. For non-boron-containing E-glass, the percentage ranges between 0.5-1.5% while it is lower for boron-containing E-glass and ranges around 0.4-0.6%. Both types

of E-glass fibres have similar mechanical and physical properties. They show good strength, and really good chemical, and electrical resistance. However, glass fibres have lower strength and modulus than aramids and carbon fibres, yet higher density (Gabara et al., 2007). Notwithstanding the above, because of its low cost, glass fibres are commonly used for reinforcement applications. Yet, the use of glass fibres in the heat and flame resistance textiles application is limited because of their brittle characteristics (Horrocks, 2016).

2.2.2.2. Cellulosic fibres

Cellulose-based fibres are used to produce all types of textile products from high-end fashion to industrial markets because of several desirable properties they provide such as excellent hand, softness, comfort, strength and toughness (Kotek, 2007). There are two types of cellulosic fibres (Hu et al., 2020). Firstly, natural fibres which originate from plants such as seeds (e.g. cotton), bast (e.g. flax, jute, hemp) and leaf (e.g. sisal), and secondly, manmade fibres which use cellulose as a raw material (e.g. viscose, modal and rayon). Natural cellulosic fibres display high moisture absorption, high strength and modulus but have low elongation and elasticity. In contrast, regenerated cellulose fibres have low strength and modulus and high elongation, yet high moisture absorption and low elasticity (Pritchard et al., 2000). The basic monomer of natural and regenerated cellulosic fibres is a two-glucose repeating unit known as cellobiose (Jiang, 2020). Figure 6 shows the chemical structure.

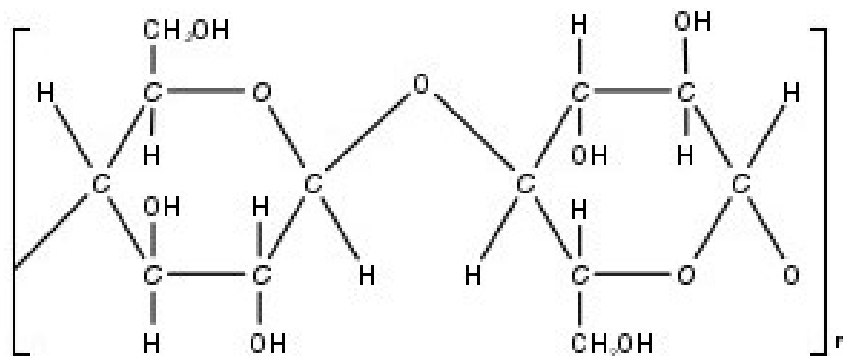


Figure 6. Chemical structure of the cellulose polymer.

According to Shafizadeh (1985), the pyrolysis reaction of cellulose involves three pathways depending on the temperature of exposure and is described as follows: at low temperatures, the glycosyl units in cellulose decompose and lead to the production of water, carbon, carbon dioxide and the formation of char. At high temperatures, the cleavage of the glycosyl units in cellulose leads to the depolymerization of the molecule and the release of the flammable and volatile product levoglucosan. Finally, direct and intense exposure to heat or radiation at high temperatures leads to the diffusion of the substrate and the breakdown of the molecule to lower weight molecules resulting in the production of gaseous products such as carbon, carbon dioxide, water, hydrogen and hydrocarbons. These reactions affect the physical and chemical properties of the fibres and their impact becomes more severe as the temperature and time of exposure increase.

Although cellulose-based textiles are highly flammable, burn quickly and ignite rapidly when triggered by a fire, they can be rendered FR (Horrocks & Kandola, 1998). There are three groups of FR cellulosic textiles: cotton, regenerated cellulose and blends of cellulosic fibres with other fibres (Joseph & Tretsiakova-McNally, 2013). Pyrolysis of cellulose-based material, as described above, includes depolymerization, bond scission and the release of highly

flammable volatiles such as hydrocarbons, alcohols, aldehydes and ketones. By using flame retardants, char formation is urged, and decomposition and emission of highly flammable gases are reduced (Bhat, 2013). The earliest attempts to make cellulosic fabrics FR involved using water-soluble chemicals placed on cotton fabrics to slow down the burning process and eventually cause the fabric to self-extinguish (Burrow, 2013). Yet, this finish did not establish permanent flame retardancy because it was removed when the fabric was laundered or wetted. Later, other FR finishes were developed, which bound to the cellulosic structure and formed a merged network within the fibre structure. These finishes are permanent and are not removed when the fabric is washed. According to (Burrow, 2013), rendering cellulosic fabrics FR by these methods can increase the stiffness of the fabric and reduce the comfort properties of the fabric.

Regenerated cellulosic fibres can be rendered FR using two approaches: firstly, by adding the flame retardant to the cellulosic polymer solution before extruding the fibre, or secondly, by covering the fibre with the flame retardants after extruding the cellulosic polymer. According to Burrow (2013), fibres manufactured with FR additives have the same comfort and other properties as non-FR cellulosic fibres. In the next subsections, I will discuss in more detail the two types of cellulosic fibres assessed as potential candidates for the sensor fabric substrate, these are the most commonly used in the fire protective clothing industry: FR cotton and FR viscose.

2.2.2.2.1. FR Cotton fibres

Cotton consists of long chain cellulose polymers containing carbon, hydrogen and oxygen (Miraftab, 2000). Cotton is naturally generated and is also biodegradable. As well, it

offers distinct physical properties and aesthetic characteristics that make it very popular and in high demand for many end-uses. Some of the most important characteristics of cotton fibres are high moisture absorbency, high wet modulus, and a good handle. Cotton is involved in many applications, for example, sleepwear, sportswear, underwear, casual and formal wear as a result of its durability, high wearing comfort, high heat, and alkali resistance (Yang, 2013). However, cotton is considered one of the most flammable textile fibres. The LOI for cotton is 18.4%, which places it in the very flammable fibres category. Its tendency to ignite, burn and produce an afterglow, brings a high risk of burn injuries which can be fatal in many cases. For instance, children's sleepwear made of 100% cotton or cotton-rich blends were considered highly flammable and exhibit huge risks of fire injuries or death (Horrocks et al., 2004, as cited in Yang, 2013). For this reason, in the late 1960 and early 1970s, governmental regulations in several countries pushed researchers to develop flame retardants for cotton textiles such as children's sleepwear. Later, other regulations appeared for clothing textiles and home furnishing where cotton is commonly used (Yang, 2013). Untreated cotton will experience combustion when ignited in the presence of oxygen and high temperature (Wakelyn et al., 2007). Though, cotton can be rendered FR using durable or nondurable flame retardant finishes according to the intended end-use. Most nondurable flame retardants are based on borax, boric acid, diammonium phosphate or sodium phosphate dodecahydrate. As mentioned previously, these flame retardants can easily be removed by water and have a very low resistance to laundering, however, most of these flame retardants can withstand several nonaqueous laundering cycles using a dry-cleaning solvent. On the other hand, the main durable flame retardants are phosphorus-based. THPC-based (tetrakis(hydroxymethyl)phosphonium chloride) flame retardants are the most effective. One example is THPCOH which has good durability and resistance to several aqueous launderings, however, it tends to release

formaldehyde during the drying process which can have a hugely damaging effect on the textile workers' health. This problem can be solved by using phosphonium salt before applying the flame retardant on cotton and using a better hooding during the drying process. Less commercialized durable flame retardants are available because of a requirement established by the US for children's sleepwear. The requirement is the durability of the flame retardant for 50 hot water laundering and drying cycles. Other reasons such as the process control and application difficulties, the high cost and limited availability of the flame retardants, and health issues, limited their use. Semidurable flame retardants for cotton fibres such as APP (ammonium phosphate, ammonium polyphosphates), THPX (tetra(hydroxymethyl)phosphonium salt) and MDPA (N-methylol dimethylphosphonopropionamide) were developed between 1950 and 1980 and are still in the use today (Horrocks, 2011). Furthermore, attempts to improve the performance of these flame retardants along with addressing their impact on health and the environment have been the main concentration for the past two decades. Also, FR cotton starts to degrade around 300 °C and reaches its peak degradation at 376 °C with complete charring at 410 °C (Yang & He, 2011).

2.2.2.2.2. Regenerated cellulose fibres

Commercially available - regenerated cellulose - fibres include viscose, modal and lyocell (Burrow, 2013). Despite the fact that all three fibre types are 100% cellulose, different processes of manufacturing are followed which results in different properties. The viscose process is used to produce viscose fibres. The cellulose used to produce viscose fibres is mostly extracted from wood pulp, sometimes from cotton, and bamboo pulp. Sodium hydroxide is first used to steep the pulp. The following step involves converting it to cellulose xanthate by adding carbon disulphide. Later, sodium hydroxide is used again to dissolve the cellulose xanthate,

and the viscous golden liquid obtained is viscose. Next, the solution is filtered and extruded from spinnerets into a bath containing different types of acids that will convert the cellulose xanthate back to cellulose by reacting with the sodium hydroxide in the liquid viscose. The manufactured fibre is then stretched while it is in the plastic state to improve the crystallization and orientation with the fibre axis. The final step is to cut the fibres into measured lengths to produce staple spun yarns, filaments, or tows. Modal fibres are produced using the modal process which is a modified version of the viscose process. However, an additive is added to the spinning solution allowing the produced fibre to have higher stretch, orientation, and strength than normal viscose and higher modulus than cotton. Fibres produced using the modal process have better properties than fibres produced using the viscose process. The lyocell process is the newest method for producing regenerated cellulose, and fibres produced have higher strength than viscose and cotton. The FR additives are added to the spinning solution before spinning the fibre to render them FR.

Lenzing™ FR is produced using the modal process (Burrow, 2013). It was first produced in 1976, by dispersing a phosphate-based additive in the cellulose solution before extrusion. Since this additive is embedded into the fibre, it can not be eliminated when washed or subjected to abrasion, thus it gives the fibre the characteristic of being inherently FR. Furthermore, additives are encased with cellulose and will not be removed by washing or abrasion. Figure 7 shows Exolit® 5060 which is an organophosphate additive used to produce Lenzing™ FR fibres. The additive is situated under the fibre's surface, and the particles are aligned along the fibre axis. As a result, when the Lenzing FR fibre is exposed to high heat, the additive starts to decompose before the cellulose in the fibre.

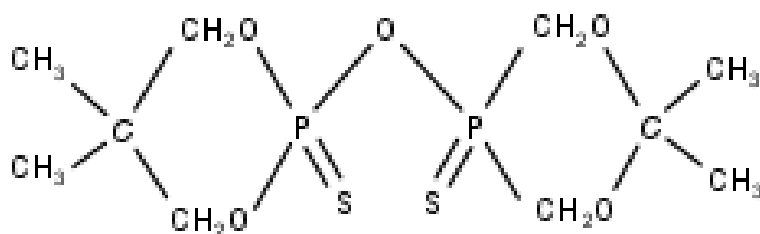


Figure 7. Chemical structure of Exolit[®] 5060. After (Burrow, 2013).

2.2.2.3. FR Polyester fibres

Polyethylene terephthalate (PET) fibres are the most common type of polyester for textile applications (Bourbigot, 2008). These fibres are used widely in the production of many textile products, including clothing, upholstery, curtains, and bedding. Yet these fibres are flammable and burn with melting. The development of inherently FR polyester fibres started in the 1960s (Horrocks, 2016). Many FR polyester fibres were developed at that time but only a few had good feedback from the end market, such as Trevira CS[®] which continues to show great success in the home furnishing market. Trevira CS[®] is produced by incorporating a phosphorus-containing reactive comonomer such as 2-carboxyethyl(methyl)phosphinic acid (Figure 8 (a)), 2-carboxyethyl(phenyl)phosphinic acid (Figure 8 ((b)) or their cyclic anhydrides (Figure 8 (c)), into a PET chain (Figure 8 (d)) (Joseph & Tretsiakova-McNally, 2013). The flame retardants are introduced before the spinning process of the synthetic fibre, through copolymerization or polymer backbone grafting (Alongi et al., 2013).

Hoechst was the first manufacturer to develop Trevira CS[®] (Horrocks, 2016). Its continuous use temperature is 100 °C. It does not promote charring but has a low tendency to

produce flammable molten drops. The LOI of Trevira CS[®] is between 28 and 30% depending on the amount of phosphorus-based flame retardant used (Bajaj, 2000).

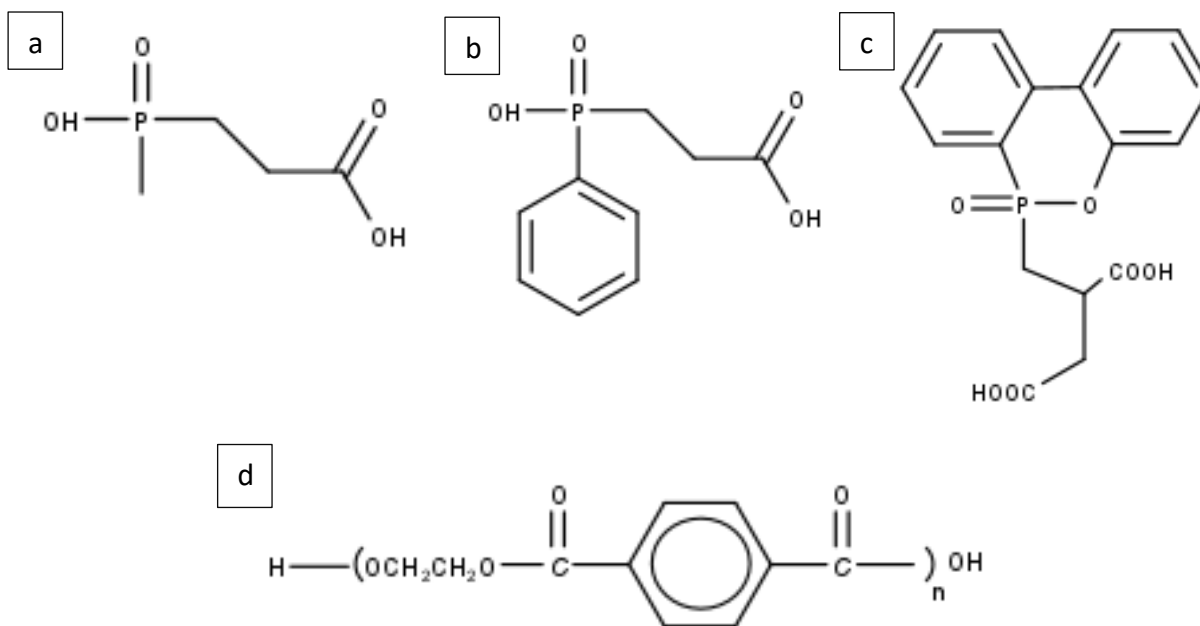


Figure 8. Chemical structure of: (a, b, and c) phosphorus-containing reactive comonomers, (d) PET. After (Vigneswaran et al, 2014; Joseph & Tretsiakova-McNally, 2013).

2.2.2.4. Oxidized PAN fibres

The development of carbon fibres has been on-going for the last 50 years (Lavin, 2001). Rayon-based carbon fibres were the first to surface but they are no longer produced. Another organic precursor used to produce carbon fibres under controlled conditions of pyrolysis and cyclisation is polyacrylonitrile (PAN) (Horrocks & Kandola, 2013). These precursors go through a stabilization process to form the fibre, and the fibre produced is oxidized PAN fibre (OPF) (Bourbigot & Flambard, 2002). Many companies produce OPF, for

example, Pyromex[®] in Japan, and PANOX[®] in the UK and Germany. PAN-based carbon fibres are the most common among all carbon fibres and were first manufactured during the 1960s and 1970s (Lavin, 2001). These fibres are not stiff nor strong. Figure 9 shows the chemical structure of OPF.

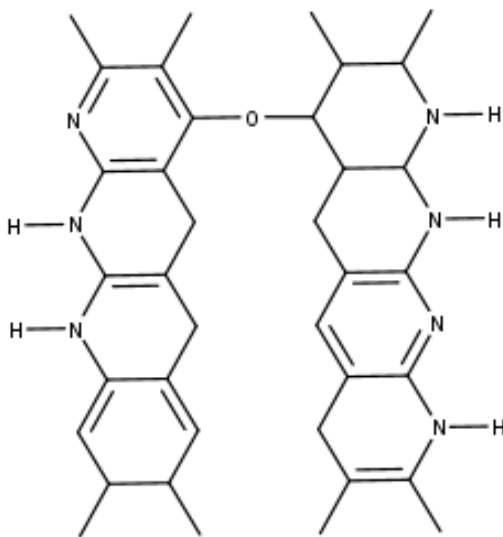


Figure 9. Chemical structure of OPF. After (Bourbigot & Flambard, 2002).

The burning of OPF fibres occurs readily because of the large amount of highly flammable volatiles emitted and leading to the high flammability of these fibres (Hall et al., 1994b). However, the incorporation of flame retardant comonomers enhances the flame retardancy and reduces the burning rate of fibres. The flame retardancy is linked to the char-forming tendency of all flame retardants and their ability to minimize flammable volatiles produced during the first step of acrylonitrile copolymer pyrolysis. Oxidation, cyclization, and dehydrogenation are three chemical reactions occurring in PAN fibres while undergoing the pre-oxidation stage (Sun et al., 2020). Cyclization and dehydrogenation cause the production

of heat and low-molecular weight products, which leads to a major change in the composition of the fibres and the formation of a ladder-type structure.

Manufacturing PAN-based fibres involves a low-temperature stabilisation process followed by a high-temperature carbonization process (Liu et al., 2015). This gives good thermal stability to the fibres because of the cyclization of the polymer when the fibres are pre-heated at a temperature of 200-300 °C during the stabilisation process. The high Young's modulus of PAN-based fibres is because of the carbonization of the polymer that causes the crystallites to be ordered and oriented in the direction of the fibre axis (Frank et al., 2017). The produced fibres have a low tensile strength at the initial stage. Further heat treatment of PAN-based precursors under tension at temperatures above 200 °C in an oxidizing environment initiates various thermally activated processes such as the crosslinking of the molecular chains by oxygen bonds and the reorganization of its polymer chains. OPF contains hydroxyl groups which, when exposed to temperatures ranging from 400 to 500 °C during carbonization process, go through crosslinking condensation reactions (Huson, 2017). A high-rate carbonization process initiates defects in the fibre, but when done at a low rate, large amounts of nitrogen are eliminated, and this leads to an increase in the fibre tensile strength. As a result, the thermally stable cyclized sections, which are initiated by the stabilisation and cyclization reactions during the formation of the fibre, are rearranged and coalesced. The resulting carbon fibre contains 98 wt% carbon, 1-2 wt% nitrogen and 0.5 wt% hydrogen.

OPF is considered the strongest compared to all carbon fibres (Lavin, 2001). It also may be thermally treated to increase its modulus and strength. In PAN fibres, the ether bridges reduce the thermal stability of the fibre but increase the char formation, thus slow the burning process (Bourbigot & Flambard, 2002). The LOI for carbon fibres is 45-60% and the

continuous operation temperature is 200 °C. The fibre starts to decompose at a temperature above 300 °C. Also, this fibre does not melt when exposed to direct fire.

2.2.2.5. Novoloid fibres

Novoloid fibres are manufactured in Japan and go by the tradename Kynol[®] (Horrocks et al., 2001). They chemically consist of 76% carbon, 18% oxygen, and 6% hydrogen, and are phenolic resin-based. Figure 10 shows the chemical structure of Kynol[®]. It is obtained by crosslinking reaction between formaldehyde and phenol to create an amorphous, three-dimensional cross-linked single network structure (Hearle, 2009; Bourbigot & Flambard, 2002).

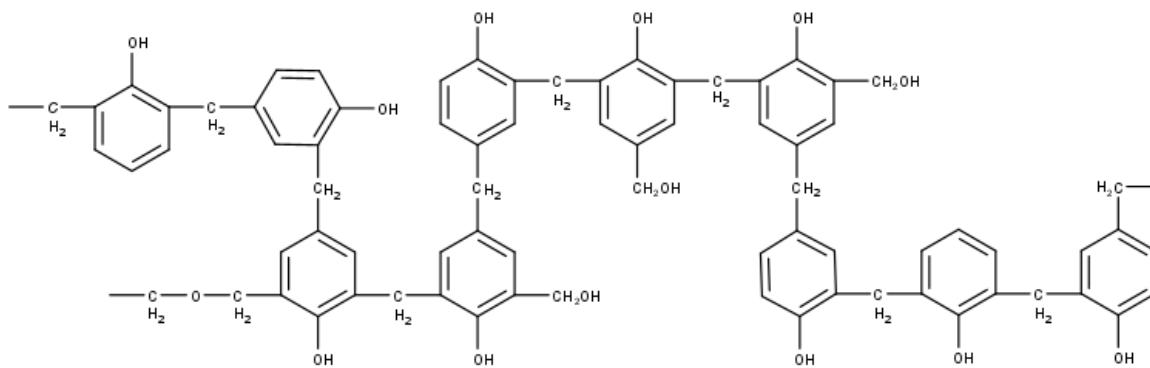


Figure 10. The chemical structure of Kynol. After (Bourbigot & Flambard, 2002).

The LOI of Kynol[®] is between 30 and 34% (Bourbigot & Flambard, 2002). Its continuous operating temperature is 200 °C. The degradation and weight loss start around 450 °C. When exposed to flame, the fibre does not melt but it chars with little or no smoke until it fully carbonizes at 700 °C. The moisture regain for this fibre is 6% (Horrocks et al, 2001). Kynol[®] exhibits many qualities, for example, outstanding thermal and electrical insulation, high

heat resistance and high chemical resistance, not to mention the release of nontoxic gases while burning. Thus, it is used in many applications such as cables, composites, industrial sealings, industrial packaging, heat insulation and FR equipment. For instance, when comfort and protection against a hazard (thermal or chemical) are required, Kynol[®] garments, hood and gloves are used.

2.2.2.6. Liquid Crystal Polyester fibres

Liquid crystal fibres were first manufactured by DuPont in the 1960s where they developed polyamide-based fibres, such as Kevlar[®] (Sloan, 2017). The success of aramids drove researchers to use other polymers in the same process. Liquid crystal polyester (LCP) was developed by Kuraray and is commercialized under the trademark Vectran[™]. Figure 11 shows the chemical structure of Vectran[™]. This fibre is based on two monomers: 4-hydroxy benzoic acid (HBA) and 6-hydroxy naphthoic acid (HNA) which are used in different ratios and exposed to different thermal treatments to produce the fibre (Pegoretti & Traina, 2018). The most common ratio for this fibre is 3:1 of HBA and HNA, respectively, which leads to good mechanical properties and a melting point above 330 °. Vectran[™] was first used in the tire industry but because of the fast production process needed for the tire industry and its high cost, it was excluded from that business (Sloan, 2017). Yet because of its superior properties like high thermal stability, low shrinkage, and resistance to abrasion, it has now found applications in the manufacturing of cables, ropes, optical fibre reinforcement, fishing nets and fire protective clothing (Pegoretti & Traina, 2018).

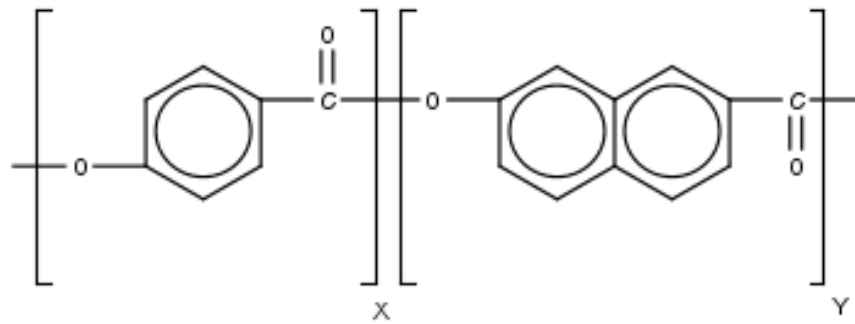


Figure 11. The chemical structure of Vectran™. After (Sloan, 2017).

The glass transition temperature of Vectran™ is close to 70-80 °C (Pegoretti & Traina, 2018). Its maximum operating temperature is around 270-330 °C above which melting starts to happen. It has a strength of 1-3 GPa, a modulus of 50-100 GPa and an elongation at break of 1-3%. The LOI for Vectran™ is similar to aramids, between 28 and 30% (Sloan, 2017). Because it is polyester-based, Vectran™ is considered hydrophobic and has near-zero moisture regain. Also, this fibre is stable against common acids and bleach solutions used in industrial laundering. Sloan (2017) also stated that the abrasion resistance of Vectran™ is excellent and is enhanced when it is in a damp state.

2.3. Conditions causing the ageing of the fabrics used in firefighters' garments

Firefighters' protective garments are intended to shield and protect them from hazards while on duty. These garments are made of high-performance fibres and exhibit exceptional properties. However, the various conditions the garments are exposed to while in-service, for example, heat and flame, UV, moisture, abrasion, and cleaning, may affect their performance. These conditions cause for instance a reduction in their mechanical performance, such as tensile and tear strength (Dolez et al., 2019; Dolez, P. I., 2019a; Arrieta et al., 2011a;

Dolez & Malajati, 2020). The changes in performance, which are common in textile materials, are influenced by not only the type of exposure, but also the duration, intensity, temperature, and frequency of the exposure. These exposures will ultimately affect the lifetime of the fire protective garment. In the following sections, the most common causes of degradation in firefighters' protective garments are described.

2.3.1. Heat and flame

Firefighters are constantly exposed to heat fluxes and high temperatures while on duty (Rezazadeh & Torvi, 2011). These conditions degrade fabrics. Factors contributing to the effect of thermal exposure on fire protective garment elements include the exposure duration, temperature, and frequency, along with the intensity of the heat flux. A series of research studies have looked at the effect of thermal exposure on fabrics using different methods and exposure durations. Different parameters related to the tested fabrics were assessed after ageing, for example, changes in tensile strength, tear strength, mass per unit area, surface morphology, colour, flexibility, and dimension have all been assessed (Dolez et al., 2019; Arrieta et al., 2011b; Arrieta et al., 2010; Liu et al., 2015; Li et al., 2019a; Sloan, 2017).

The first layer of a fire protective clothing system to encounter thermal hazards is the outer shell fabric (Song & Lu, 2013). The function of the outer shell fabric is to protect the wearer from ambient conditions and shield the underlayers to make sure they stay undamaged (Song et al., 2017c). The thermal resistance of fire protective clothing is dependant on the nature of the outer shell fabric. As a result of exposure to heat, degradation in the outer shell fabric might occur, causing a deterioration in its mechanical efficiency, which might contribute to burn injuries (Barker, 2005). In some instances, the strength of the outer shell fabric may be

so low as to be at the point where the fabric suffers from rips because of normal motions performed by firefighters, leading to the rupture of the outer shell fabric and exposing the underlayers to the heat source. In this case, the fire protective clothing fails its purpose.

Thermal energy transfer happens in three forms (Rossi, 2003): radiation, convection, and conduction. According to Krasny (1986, as cited in Rossi, 2003), in most fire settings, radiation makes up over 80% of the thermal energy with a possibility of convection and conduction also contributing. The intensity of radiant heat can reach 40 kW/m² in domestic fires and over 200 kW/m² in large, fuelled fires (Schoppee et al., 1986, as cited in Rossi, 2003). Thermal hazards encountered by firefighters are classified into three main categories (Song & Lu, 2013): routine, hazardous, and emergency. According to Song & Lu (2013), routine conditions involve a temperature lower than 100 °C and heat flux lower than 4 kW/m². Hazardous conditions involve a temperature between 100-300 °C and heat flux between 4-25 kW/m². Emergency conditions include a temperature between 300-1100 °C and heat flux between 25-208 kW/m². According to Hoschke (1981), routine conditions correspond to a hot summer day in which no special clothing is necessary. On the other hand, hazardous conditions correspond to what firefighters encounter outside a burning building wherein a turnout uniform is required. Emergency conditions or a flashover are encountered by firefighters in which they are in direct contact with fire and special protective equipment is necessary.

The temperature recorded near firefighters during a building firefighting training ranged between 50 and 130 °C on the ground, and between 100 and 190 °C at 1 m above the ground with a radiant heat flux ranging between 5 and 10 kW/m² (Rossi, 2003). At some point, one measurement reached 278 °C with a radiant heat flux of 26 kW/m². However, these values varied according to the number of times the doors and windows were open during the fire. On

the other hand, the temperature in a flashover can reach up to 1000 °C (Song & Lu, 2013). The heat flux could be 50 kW/m² if it occurred in a large room, and 100 kW/m² if it occurred in what is equivalent to a public theatre (Horrocks, 2014). Whereas heat fluxes in wildfires can reach up to 100 kW/m² (Mäkinen, 2005).

In summary, studies have shown that exposure to heat and flame is a significant hazard for firefighters and one that causes degradation of their clothing, hence, a fire protective clothing system that is efficient at resisting degradation caused by thermal exposure is essential to ensure the safety of firefighters.

2.3.2. Ultraviolet light

Firefighters are exposed to UV radiation while on duty (Rezazadeh & Torvi, 2011). This condition degrades fabrics. Factors contributing to the effect of UV exposure on fire protective clothing elements include the intensity and wavelength of the light source, exposure duration, temperature, along with the moisture content of the fabric (Rubeziene et al., 2012). A series of research studies have looked at the effect of UV exposure on fabrics using different methods and exposure durations. Different parameters related to the tested fabrics were assessed after ageing, for example, changes in tensile strength, tear strength, and surface morphology (Dolez, P. I., 2019a; Rubeziene et al., 2012; El Aidani et al., 2013; Walsh et al., 2006; Gu, 2005; Sloan, 2017).

Fibre deterioration can be a result of exposure to solar radiation (Rubeziene et al., 2012). The deterioration is dependant on the amount of energy absorbed by the fibre, therefore, the deterioration is high when the absorbed energy is high. The solar spectrum is made up of visible and infrared radiation (IR), both are responsible for heating materials, and UV radiation

causes the degradation of materials. UV radiation is more damaging than visible radiation and degrades textile materials at a faster rate. According to Rubeziene et al. (2012), the UV spectra is in the range between 100 and 400 nm and is divided into three areas: UV-A: 315 to 400 nm, UV-B: 280-315 nm and UV-C: 100 to 280 nm. UV-C gets absorbed by the ozone layer before reaching the earth's surface (Alebeid & Zhao, 2017). However, UV-B and UV-A reach the earth's surface and cause critical health concerns and lead to photodegradation of textiles and other materials.

When UV hits textiles, it gets reflected and scattered, absorbed and/or transmitted (Alebeid & Zhao, 2017). If a textile absorbs UV light, and if the UV energy is high enough to break the molecular bonds, a photochemical reaction known as photolysis occurs and causes photodegradation and weakening of fibres (Tucker et al., 1980). If a textile does not absorb UV easily, and if it contains photosensitizers such as impurities, delustering agents and dyes, a secondary photochemical reaction known as photosensitization occurs where these photosensitizers absorb UV and leave electrons in an excited state within the chemical bond and convert absorbed water or oxygen to hydroxyl radicals which leads to changes in the chemical and physical properties of the fibres (Tucker et al., 1980; Rezazadeh & Torvi., 2011). Both the intensity of the radiation source and the fabric spectral absorptivity affect the amount of energy absorbed by the fabric. The high area-to-volume ratio of fibres makes them susceptible to degradation triggered by light. This degradation results in the deterioration of textiles' mechanical properties such as tear and tensile strength.

There are many accelerated weathering testers that use a variety of artificial light sources such as carbon arc, xenon arc and fluorescent lamps (Izdebska, 2016). Enclosed carbon arc (wavelength output below 350 nm) and sunshine carbon arc (wavelength output about 390

nm) have been in use since the 1900s (Brennan & Fedo, 1994). Enclosed carbon arc is believed to imitate sunlight better than sunshine carbon arc. Xenon arc has been in use since the mid-1900s. Currently, xenon arc lamps are the most commonly used artificial light sources for accelerated weathering testing and are believed to give the best imitation of natural sunlight (Millington, 2018). Fluorescent UV lamps operate differently from arc type light sources in which they only produce the wavelength range to match the most damaging wavelength of sunlight. Different fluorescent lamps exist in the market, for instance, FS-40 lamp (output in the UV-B spectrum with some UV-A), UVB-313 lamp (higher and more stable output than FS-40 lamp) and UVA-340 lamp (output in the UV-A spectrum with some UV-B). In addition, according to NFPA 1851 (2014), degradation of fibres through exposure to fluorescent light is less severe than degradation from exposure to sunlight.

In summary, studies have shown that exposure to UV is a significant hazard for firefighters' protective clothing systems and causes their degradation, hence, a fire protective clothing system with good UV resistance is essential to ensure the safety of firefighters.

2.3.3. Water

Firefighters are exposed to water while on duty (Rezazadeh & Torvi., 2011). According to Lawson et al. (2004), the presence of moisture in a fire protective clothing system can be a result of internal or external sources. Internal moisture is associated with the wearer's body sweat. On the other hand, external moisture is related to the firefighting activities such as spraying water, walking through a swamp and/or a lake, and other natural conditions such as rain and dew. Fabrics saturated with water and sweat cause performance deterioration of fire protective clothing elements (Barker, 2005). The degree of moisture sorption in the fabric,

location, duration, and source of exposure affect the heat transfer through fire protective fabrics (Zhang et al., 2017). A series of research studies have looked at the effect of moisture on fabrics using different methods and exposure durations. Different parameters related to the tested fabrics were assessed after ageing, for example, changes in tensile strength and tear strength (Arrieta et al., 2011a; Udayraj et al., 2016; Rossi et al., 2004; Zhang et al., 2018; Lawson et al., 2004).

External moisture is accumulated on the outer shell fabric (Song et al., 2017d). There are two types of hot water exposure associated with structural fire hazards: hot-water splashes and hot-water immersion (Mandal et al., 2016). Firefighters might encounter hot-water splashes from pipelines or water extinguishers reaching a high temperature. Knees, elbows, and lower parts of the legs are most likely to be affected by hot-water immersion. This exposure to hot water can affect the fire protective clothing and cause a decrease in its performance. According to Mandal et al. (2016), the air permeability and thickness of the fabric along with the temperature and angle of the hot water splashes affect the performance of the fabric when exposed to these hazards. Also, water immersion with compression has a larger impact on the performance of the fabrics than hot-water splashes. The hot water transfer happens in both cases, but in terms of water immersion, conductive heat transfer also occurs.

The presence of moisture in fabrics can be in the form of bound water or free water (Udayraj et al., 2016). Bound water is water absorbed by fibres in a fabric. When fibres reach a saturated state wherein fibres can not absorb any more water, water starts to occupy the empty spaces between fibres, and this is defined as free water. Moisture in fire protective clothing not only affects the performance of the fabric but also affects the physiological comfort of the firefighter. Some fibres used for manufacturing fire protective fabrics undergo a degradation

process because of exposure to moisture and this phenomenon is termed hydrolysis (Arrieta et al., 2011a). Hydrolysis causes a deterioration of the mechanical properties of fibres. This reaction includes water attacking the amide bonds in aramid fibres which leads to chain scission. However, the interaction with water occurs in the amorphous regions and the presence of amorphous regions enhances moisture absorption (Parimala et al., 1990). Hence, highly crystalline fibres such as Kevlar[®] are less susceptible to hydrolysis. (Arrieta et al., 2011a). In addition, for Kevlar[®] to undergo hydrolysis, there is a need for catalyst such as a base or an acid to initiate a chemical reaction. When a hydrolysis degradation ensues, the catalyst attacks the amide linkage leading to chain scission which will negatively affect the molecular weight and the mechanical properties. Zylon[®] is stable in dry conditions but degrades in the presence of moisture and temperature (Forster et al., 2011). The degradation mechanism of Zylon[®] starts with the opening of the benzoxazole ring followed by chain scission leading to mechanical damage and the reduction in the molar mass.

In summary, studies have shown that repeated exposure of firefighters' protective clothing systems to hot or cold water while on duty will wet materials and cause a reduction in their thermal insulation which will lead to their degradation, hence, in the long term, this will diminish their thermal performance and threaten the safety of firefighters.

2.3.4. Laundering

To maintain the cleanliness of textiles, including firefighters' protective clothing, they generally go through some form of maintenance or restoration process such as dry-cleaning, laundering, bleaching, or scrubbing fabrics to remove dirt and soil (Rezazadeh & Torvi, 2011; Slater, 1991, p. 10). Laundering is a strong procedure that incorporates hot water,

detergent and mechanical agitation which can cause shrinkage and the reduction in the mechanical properties of textiles such as tear and tensile strength, thermal properties such as thermal protective performance, and water/oil repellency properties (Rezazadeh & Torvi, 2011; Slater, 1991, p. 10; Saville, 1999). The effect of the chemical action on fibres is dependant on the detergent chemistry, the water itself and the temperature of water used. The mechanical action involves abrasive forces that result from the contact between the wall of the machine and the textile load as well as between the individual pieces of textiles (Slater, 1991, p. 10). A series of research studies have looked at the effect of laundering on fabrics using different methods and numbers of cycles. Different parameters related to the tested fabrics were assessed after ageing, for example, changes in tensile strength, tear strength, and weight, (Dolez & Malajati, 2020; Zambrano et al., 2019; Vanderschaaf et al., 2015).

NFPA 1851 (2014) - Standard on Selection, Care, and Maintenance of Protective Ensembles for Structural Fire Fighting and Proximity Fire Fighting, has three cleaning levels: routine, advanced and specialized. Routine cleaning is the end user's responsibility and should be performed on soiled fire protective garment elements without taking them out of service. It may be done using a brush or by hand in a sink. When routine cleaning fails to clean the fire protective garment elements, advanced cleaning is advised. Advanced cleaning should be done by the manufacturer, an organization trained by the manufacturer, a verified organization or by an authorized Independent Service Providers (ISP) and requires industrial cleaning machines with controlled conditions. NFPA 1851 (2014) asks for advanced cleaning at least once a year (Stull & Stull, 2019). According to NFPA 1851 (2014), there are many requirements related to advanced cleaning, for instance, the machine should not be overloaded, the water temperature should not exceed 40 °C, the use of a mild detergent with a pH between 6.0 and 10.5 pH, and

a washing machine with a capacity of drum RPM (revolutions per minute) in which the G-force does not surpass 980 m/s^2 . In addition, the outer shell fabric or any reflective component should not be cleaned with a brush or any abrasive cleaning tools. Specialized cleaning is proposed for unusual contamination, for instance, hazardous chemicals and dangerous substances. It requires special cleaning agents and special cleaning procedures.

The newest version of NFPA 1851 (2020) asks for advanced cleaning once every six months, hence, at least two advanced cleanings per year. A programmable washer/extractor machine is required for cleaning the fire protective garment elements and should allow adjustments of water temperature and level, along with cycle type and time. The evaluation of the effectiveness of the cleaning process should be taken into consideration, however, if the effectiveness of the cleaning method was not verified, a disinfecting and sanitizing process is required whenever the fire protective garment elements are infected with body fluids or infectious materials. According to NFPA 1851 (2020), the washer/extractor machine should not be overloaded or underloaded. Otherwise, the water temperature, detergent pH, and drum RPM are the same as identified in NFPA 1851 (2014). When the protective garment elements are not adequately cleaned via advanced cleaning, specialized cleaning is advised.

Chemicals emitted in situations encountered by firefighters such as smoke particulates, gas emissions and dense deposits pose serious risks to the health of firefighters (Fabian et al, 2010). It was recently shown that these chemicals may get through the firefighter's protective clothing (Keir et al., 2017). Both NFPA 1851 (2014) and NFPA 1851 (2020) mandate that the fire protective garment elements undergo advanced cleaning whenever it is contaminated with combustion products such as fire gases and smoke particulates (Stull & Stull, 2019). The associated number of washes will vary depending on the fire station location

and the firefighter's role (Stull & Stull, 2018). In some instances, it is estimated that up to 25 laundering cycles per year could be performed on fire protective clothing to remove toxic substances and prevent them from getting on the skin of the firefighters. Several studies have looked at the effect of laundering on fabrics used in protective clothing (Dolez & Malajati, 2020; Mäkinen 1992). For example, Mäkinen (1992) found that when four different fabrics: FR viscose blend (65% FR viscose, 30% Nomex[®] and 5% Kevlar[®]), FR cotton, FR wool, and an aramid fabric, were exposed to 50 laundering cycles, an increase in the water absorption and a decrease in both the FR treatment and the air permeability of the fabrics were noticed. Another laundry study by Dupont (2001) found that FR cotton only maintained 50% of its tear strength after 50 industrial laundering cycles while Nomex[®] IIIA preserved around 90% of its tear strength after 100 industrial laundering cycles and around 25% after 200 industrial laundering cycles. These studies confirm the damaging effects of multiple washing processes on textiles materials.

In summary, studies have shown that laundering of firefighters' protective clothing systems and exposure to hot or cold water, abrasion and cleaning agents through maintenance procedures necessary for the cleanliness and safety of the firefighters' protective clothing, will lead to their degradation, hence, after multiple laundry cycles, it will diminish their thermal performance and threaten the safety of firefighters.

2.3.5. Abrasion

Abrasion has been identified as another cause of the degradation of fire protective garments (Rezazadeh & Torvi, 2011). Wear or abrasion of textiles is a slow, continuous and insidious degradative process while in use, which might at first only cause a change in

appearance, however, it will eventually lead to the deterioration of the fabric and the decrease in further abrasion resistance, tear strength, and flammability properties which might put the wearer at risk (Mäkinen, 1992; Textor et al., 2019). Moreover, the frictional forces between garments and external surfaces or between different garment pieces, initiate microcracks in the fibres which will develop into more significant cracks with time (Slater, 1991, p. 30).

Factors contributing to the effect of abrasion on fire protective clothing systems are the intensity and frequency of the mechanical action. A series of research studies have looked at the effect of abrasion on fabrics using different methods and cycle numbers. Different parameters related to the tested fabrics were assessed after ageing, for example, changes in tensile strength, tear strength, and weight (Textor et al., 2019; Vanderschaaf et al., 2015; Slater, 1991).

In a study by Vanderschaaf et al., (2015) looking at the effect of multiple abrasion and laundering cycles on the protective clothing fabrics, visual signs of abrasion were found to include a change in colour, frosting, thinning and the formation of small holes in the fabric. Loss in strength also occurred with abrasion and varied in extent depending on the fabric composition. When abrasion was combined with laundering a 3/1 twill weave FR cotton fabric (88% cotton and 12% nylon) exhibited a loss in tensile strength of 57% after 25 wear/laundrying cycles, while a 2/1 twill weave tri-blend fabric (48% modacrylic, 37% lyocell and 15% para-aramid) experienced a loss in tensile strength of 22%, and a plain weave Nomex[®] fabric (93% meta-aramid, 5% para-aramid and 2% anti-static fibre) suffered a loss in tensile strength of 24%.

In summary, studies have shown that abrasion or wear is a significant cause of degradation to firefighters' protective clothing systems, hence, a fire protective clothing system with good abrasion resistance is essential to ensure the safety of firefighters.

3. MATERIALS AND METHODS

3.1. Fabrics tested

A series of fabrics were selected for the study. Some of these fabrics are currently used as outer shell fabrics for firefighter protective clothing. They are made of blends of meta- and para-aramid, PBI and PBO fibres. Others have been identified as potential candidates as the substrate for the graphene-based EOL sensors. They include glass fibres, natural and regenerated cellulosic fibres, polyester, oxidized PAN, LCP and novoloid fibres. All of these fabrics are inherently FR or treated to be FR. Table 1 lists fabrics, with their trade names, colour when relevant, and identification code used in this study. More information about each fabric is provided in Section 4.1 and Appendix A.

Table 1. List of fabrics included in the study.

Identification code	Fabric name
A	Brigade™ 750 – natural
B	Agility™ – light gold
C	Pioneer™ – gold
D	Armor AP™ – gold
E	Gemini™ XT – naturel
F	Kombat™ Flex – gold
G	PBI Max™ – gold (6.0 oz)
I	Flameflex 275– graphite
L	CarbonX Repel
M	LENZING™ FR
N	Zylon®
O	NF Arc™
T	Fiberglass Cloth (Style 7500)
U	Vectran™

Specimens were prepared based on the test method used to measure their residual performance. Tearing strength was measured for fabrics A, B, C, D, E, F, G, I, L, M, N and O (see section 3.5.1). Tensile strength was measured instead of tearing strength for fabrics T and U because these fabrics slipped and could not be torn using the clamps and equipment available for testing (see section 3.5.2).

3.2. Fabric Characterization Methods

3.2.1. Mass

Mass was measured following the standard test method ASTM D3776/D3776M (2020) - Standard Test Methods for Mass Per Unit Area (Weight) of Fabric. Five die-cut specimens with a radius of 2.5 cm were taken from different locations in the sample, for a total area of 98.2 cm² (Figure 12). Specimens were brought to moisture equilibrium in the standard atmosphere for textile testing (65 ± 5% RH at 20 ± 2 °C) before being weighed using a Mettler Toledo PJ3000 balance (Mettler-Toledo, New Zealand, capacity 3100g, readability 0.01g). In the case of Fabric O, the information provided by the fabric supplier was used since there was insufficient fabric to test. The mass per unit area for all other fabrics was calculated using the following Equation 1:

$$\text{Mass} \left(\frac{\text{g}}{\text{m}^2} \right) = \frac{\text{Mass of 5 specimens (g)}}{\text{Total area of 5 specimens (cm}^2\text{)}} \times 10,000 \quad (1)$$

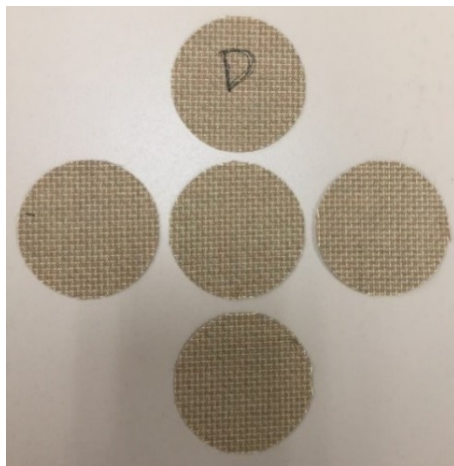


Figure 12. Die-cut specimens (example of Fabric D).

3.2.2. Thickness

Thickness was measured following the standard test method ASTM D1777 (2019) - Standard Test Method for Thickness of Textile Materials. A Thickness Compression Recovery Tester (Model CS-55) (Custom Scientific Instruments, Inc, NJ, USA) was used with a presser foot diameter of 28.7 mm and pressure of 1.0 kPa. The specimen was placed with the face side up on the anvil of the thickness gauge. Then the presser foot was gradually lowered into contact with the specimen. Dial readings (with an accuracy of 0.001 inch) were taken for the conditioned fabrics at five different locations. In the case of Fabric O, the information provided by the fabric supplier was used since there was insufficient fabric to test. The mean thickness was calculated using Equation 2:

$$\text{Thickness (mm)} = \text{Thickness (inches)} \times 25.4 \quad (2)$$

3.2.3. Fabric count and structure

Fabric count was measured following the standard test method ASTM D3775 (2017) - Standard Test Method for Fabric Count of Woven Fabric. Five counts over one centimetre in each fabric dimension (warp × weft) were taken using a traversing thread counter and the mean fabric count was calculated for each fabric. A Leica EZ4 educational stereomicroscope was used to observe and photograph each fabric structure.

3.2.4. Fibre content

Fibre content was provided for each fabric by the fabric supplier and was confirmed following the standard test method AATCC TM20 (2018) - Test Method for Fiber Analysis: Qualitative (visual and microscopical examination). For fabrics that were blends, I used this method to determine where the different fibres are present in the fabric. For example, if the fabric had filaments and staple spun yarns, these were examined to determine which fibres made up these yarns. The first step was preparing the glass slide for the microscopical examination: 1) separating the fibres by untwisting the yarns and cutting them, 2) placing a small number of fibres on a glass slide, 3) teasing the fibres apart, 4) adding a drop of mineral oil, and 5) covering with a coverslip. The second step is comparing the microscopic appearance of the fibres to reference photomicrographs to determine their generic fibre type.

3.3. Determination of the accelerated ageing conditions for the sensor substrate

fabric assessment

In this study, the fabrics investigated as potential candidates for the sensor substrate were subjected to accelerated ageing conditions to mimic conditions that are encountered by

firefighters while on duty. The purpose of this assessment was to identify fabrics that can resist ageing conditions that are known to be damaging to the shell fabrics of firefighters' clothing. In this way, it was possible to identify candidates for the support fabric for the EOL sensor that will have better ageing properties than the shell fabrics of the FR clothing. The longer life expectancy of the support fabric will ensure that it does not fail before the shell fabric and the support fabric will not interfere with the operation of the EOL sensor. The ageing conditions used in this study were taken from research that was previously undertaken by Dolez et al. (2019); Dolez (2019a); Arrieta et al. (2011a); Dolez & Malajati (2020) who investigated the effect of different accelerated ageing conditions on the mechanical performance of fire protective fabrics used as the outer shell of firefighters' clothing. Ageing conditions that were selected and are described in the following sections, have shown in previous research to reduce the tearing strength of the shell fabrics to just below the minimum performance requirement specified in NFPA 1971 (2018) of 100 N.

3.3.1. Thermal ageing conditions

The thermal ageing conditions used in this study are based on those reported by researchers who subjected seven FR fabrics to thermal ageing conditions at different temperatures (150, 190, 210, 235, 300 °C) and recorded the residual tear strength at regular intervals for up to 500 h (Dolez et al., 2019). Figure 13 shows an example of the results obtained for a Kevlar[®]/Nomex[®]/PBO fabric (similar in fibre content to Fabric B in this study). Based on the criterion of a final tearing strength of 100 N, I identified the thermal ageing conditions that were found to bring the most thermally-resistant fabric to this value. Based on the initial tear strength values reported for the fabrics and the percentage change in strength reported in the paper, the residual strength corresponding to 100 N was computed. To do this, the data

expressing the residual tear strength as a function of the ageing time for each temperature were used and the ageing time to reach the NFPA criterion of 100 N for each fabric was found by interpolation using a linear approximation (example in Figure 13). The results for all seven fabrics from the study by Dolez et al. (2019) are shown in Table 2 for the ageing temperature of 235 °C. This temperature was selected for the current study based on the oven capability and the need to keep the ageing time within a reasonable time period. The most thermally resistant outer shell fabric at this temperature was Kevlar[®]/Nomex[®]/PBO, which took 42 h for its tearing strength to diminish to the NFPA minimum requirement of 100 N. This combination of ageing time (42 h) and temperature (235 °C) was used for the thermal ageing conditions used to assess the sensor substrate fabric candidates.

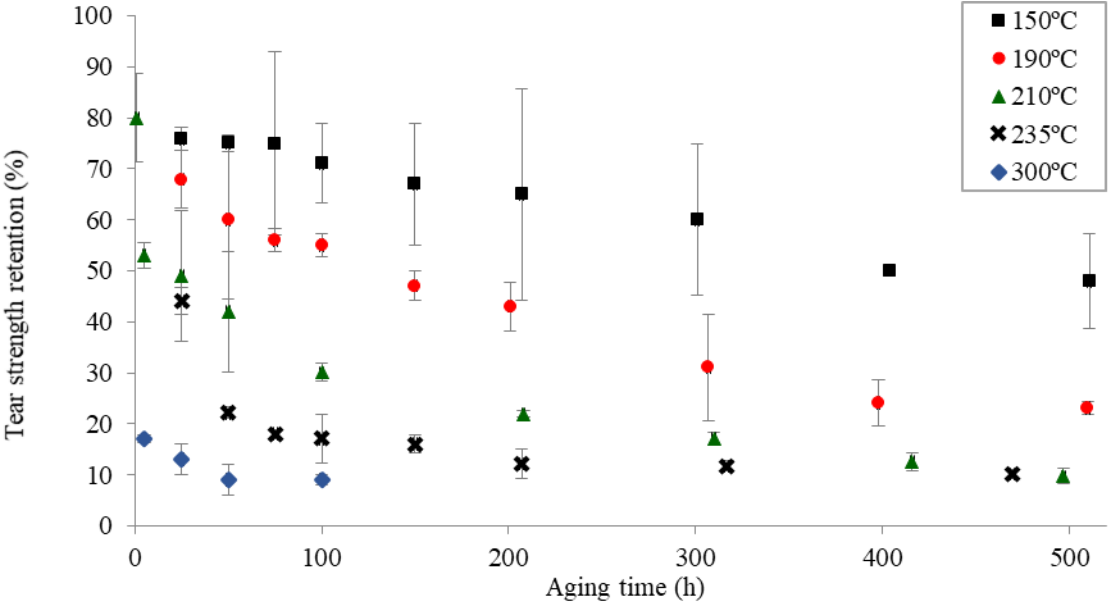


Figure 13. Tear strength retention for a Kevlar[®]/Nomex[®]/PBO fabric after thermal ageing at different temperatures as a function of the ageing time (data from Dolez et al., 2019).

Table 2. Computation of the time to reach the NFPA 1971 minimum requirement for tear strength as a result of thermal ageing of seven outer shell fabrics at 235 °C (original data from Dolez et al., 2019).

Fabric	Tear strength retention (%) corresponding to 100 N	Ageing time (hours)
100% Kevlar [®]	27	5
Nomex [®] IIIA	76	4
Kevlar [®] /Nomex [®]	80	3
Kevlar [®] /Nomex [®] /PBO	29	42
Kevlar [®] /Basofil	71	12
100% Nomex [®]	81	38
Kevlar [®] /PBI	44	5

3.3.2. Photochemical ageing conditions

Similar to the thermal ageing conditions, the UV ageing conditions for this thesis are based on the conditions used by a researcher who subjected seven FR fabrics to UV accelerated ageing using a fluorescent UV tester at a temperature of 80 °C and different UV intensities (0.55, 1.00, 1.55 W/m² at a wavelength of 340 nm). The researcher recorded the residual tear strength of the fabrics at regular intervals for up to 500 h of exposure (Dolez, 2019a). Figure 14 shows the results obtained for a Kevlar[®]/PBI fabric (similar in fibre content to Fabric F in this study). Based on the criterion of a final tearing strength of 100 N, I identified the ageing conditions that were found to bring the most UV-resistant fabric to this value. To do this, the data expressing the residual tear strength as a function of the ageing time for each UV intensity were used and the ageing time to reach the NFPA criterion of 100 N for each fabric

was found by interpolation using a linear approximation (example in Figure 14). The results for all seven fabrics are shown in Table 3.

To keep the ageing time within a reasonable time period, I selected to use a UV intensity of 1.00 W/m^2 . At this intensity, the most UV-resistant fabric was found to be Kevlar[®]/PBI, with an ageing time of 243 h. This time, at an intensity of 1.00 W/m^2 at 340 nm and $80 \text{ }^\circ\text{C}$, was thus selected for the photochemical ageing conditions used to assess the resistance of the sensor substrate fabric candidates to photochemical ageing.

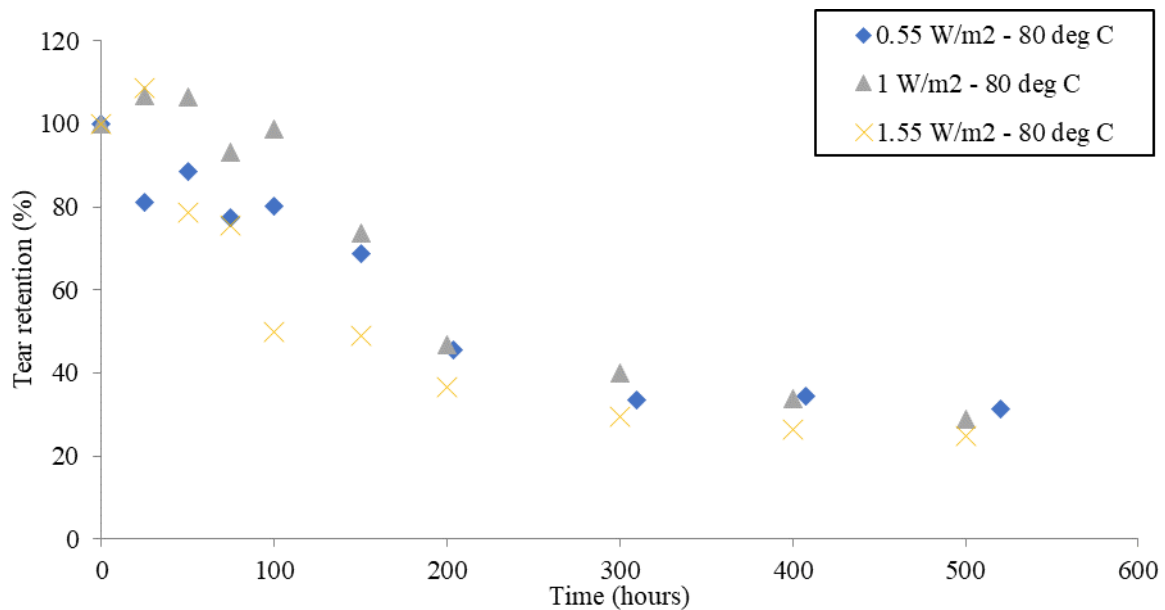


Figure 14. Tear strength retention for a Kevlar[®]/PBI fabric after photochemical ageing at different intensities as a function of the ageing time (data from Dolez, 2019a).

Table 3. Computation of the time to reach the NFPA 1971 minimum requirement for tear strength as a result of photochemical ageing at 80 °C for seven outer shell fabrics (original data from Dolez, 2019a).

Fabric	Tear strength retention (%) corresponding to 100 N	Ageing time (hours)		
		@ 0.55 W/m ²	@ 1.00 W/m ²	@ 1.55 W/m ²
100% Kevlar [®]	27	271	167	95
Nomex [®] IIIA	76	49	29	22
Kevlar [®] /Nomex [®]	80	113	33	40
Kevlar [®] /Nomex [®] /PBO	29	335	201	97
Kevlar [®] /Basofil	71	100	17	44
100% Nomex [®]	81	45	3	7
Kevlar [®] /PBI	44	225	243	146

3.3.3. Hydrothermal ageing condition

In the case of hydrothermal ageing, only data for a Kevlar[®]/PBI fabric (similar in fibre content to Fabric F in this study) was available for consideration from a study by Arrieta et al. (2011a). The fabric had been subjected to hydrolytic ageing at three temperatures (50, 60 and 80 °C) and two levels of relative humidity (RH) -60 and 80%- for up to 31 days (Arrieta et al., 2011a). Tensile tests were performed on yarns extracted from the fabric. The yarn's initial strength was 34 N (Figure 15). Since the initial tensile strength of this fabric is 1214 N (Arrieta et al, 2010), the NFPA 1971 (2018) minimum requirement for outer shell fabric tensile strength of 623 N corresponds to a fabric residual strength of about 50%. If the assumption is made that the same ratio applies for the yarn strength, it means that the NFPA 1971 minimum requirement

is reached for a yarn strength of about 17 N. Based on the data shown in Figure 15, this value corresponds to an ageing time of 31 days at 80 °C and 60% RH.

Since access to a moisture chamber was not possible, hydrothermal ageing was conducted by immersing the fabric in water at 80 °C. The data of Arrieta et al. (2011a) had shown no effect of RH on the ageing results, which led them to conclude that hydrolytic ageing is controlled by the diffusion of water inside the fibres rather than by the relative humidity. To compensate for the lack of data regarding moisture ageing behaviour of outer shell fabrics, it was decided to assess the hydrothermal ageing of the support fabrics at three different durations: 15, 24 and 31 days.

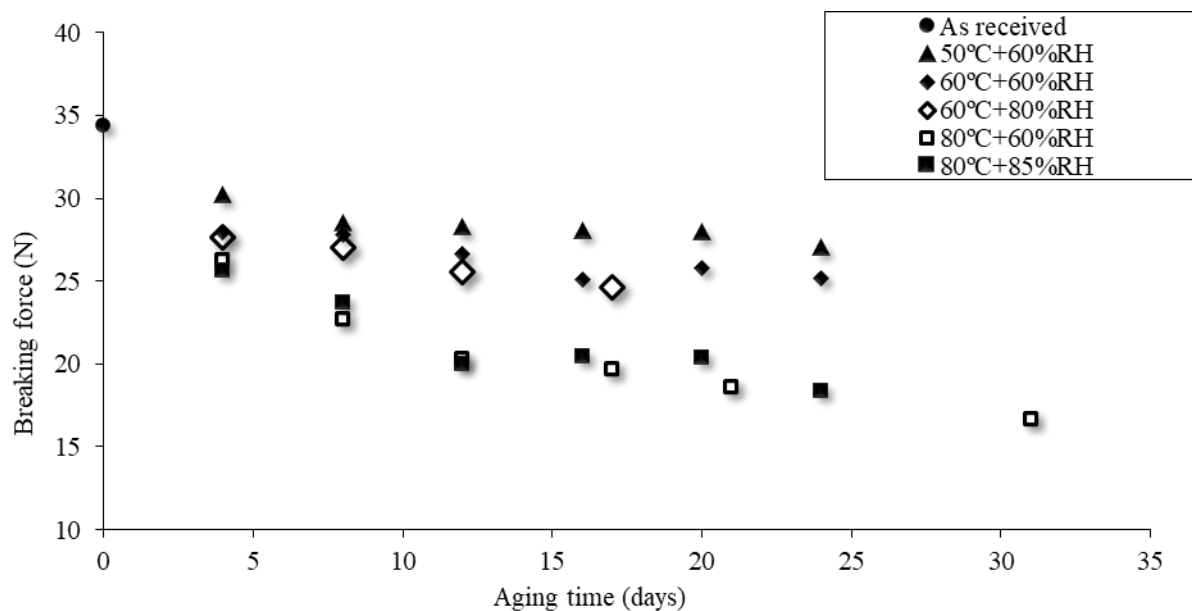


Figure 15. Variation in breaking force of a yarn extracted from a Kevlar[®]/PBI fabric exposed to hydrolytic ageing at different temperatures and relative humidity as a function of the ageing time (data from Arrieta et al., 2011a).

3.3.4. Laundering ageing conditions

Similar to the thermal ageing and photochemical ageing conditions, the laundering ageing conditions for this thesis are based on the conditions used by researchers who subjected seven FR fabrics to accelerated laundering (Dolez & Malajati, 2020). These researchers used a domestic washing machine and dryer to expose the fabrics to 10, 20, 35, and 50 laundering cycles at 60 °C (Dolez & Malajati, 2020) and measured the residual tear strength following the multiple laundering cycles. Figure 16 shows the data for all the fabrics tested in their study. Based on the criterion of a final tearing strength of 100 N, I identified the laundering conditions that were found to bring the most resistant fabric to this value. To do this, the data expressing the residual tear strength as a function of the number of cycles for all fabrics were used and the ageing time to reach the NFPA minimum requirement for each fabric was found by interpolation using a linear approximation (example in Figure 16). The results for all the fabrics are shown in Table 4.

For most of the fabrics, the minimum requirement was not reached after 50 washing/drying cycles (fabrics still had tearing strengths in excess of 100 N). However, it was decided to use 50 cycles to assess the resistance to laundering of the sensor substrate fabric candidates to have a number of cycles comparable to the previous research. In addition, because of the limited amount of material available for Fabric O, an accelerated laundering test using small specimens and a Launder-Ometer[®] was used following ISO 105-C06 (2010) - Tests for colour fastness - Part C06: Colour fastness to domestic and commercial laundering using the procedure (C1M) rather than a domestic washing machine and tumble drier. According to the test method, one 45 min cycle of the Launder-Ometer[®] test is equivalent to 5 domestic washes,

the sensor fabric substrate candidates were therefore subjected to 10 cycles at 60 °C. Between cycles, the fabrics were laid flat to air dry on screens.

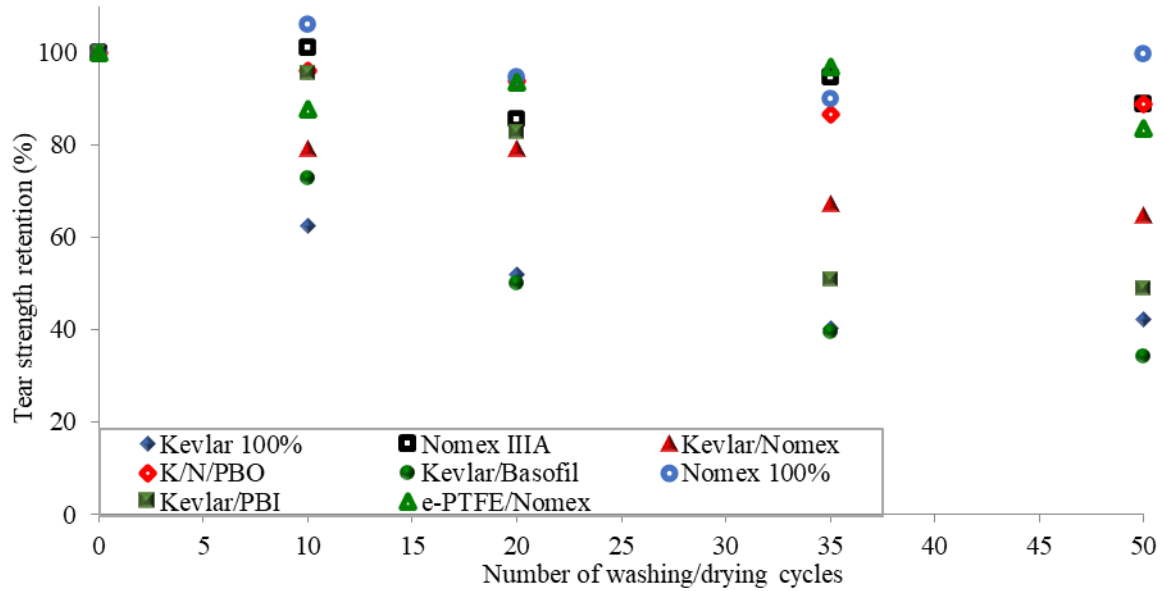


Figure 16. Tear strength retention as a function of the number of washing/drying cycles for seven outer shell fabrics and a moisture barrier (data from Dolez & Malajati, 2020).

Table 4. Computation of the number of laundering cycles to reach the NFPA 1971 minimum requirement for tear strength for seven outer shell fabrics (original data from Dolez & Malajati, 2020).

Fabric	Tear strength retention (%) corresponding to 100 N	Number of cycles
100% Kevlar [®]	27	>50
Nomex [®] IIIA	76	>50
Kevlar [®] /Nomex [®]	80	<50
Kevlar [®] /Nomex [®] /PBO	29	>50
Kevlar [®] /Basofil	71	<50
100% Nomex [®]	81	>50
Kevlar [®] /PBI	44	>50

3.4. Experimental Design

To find a support fabric for the sensor that resists severe ageing conditions, the selected fabrics were subjected to heat, UV, water, and laundering using the ageing conditions described in the previous section. The dependent variables for all conditions are the residual tear/tensile strength after ageing as well as shrinkage after laundering. The independent variables are the fabrics tested (14 fabrics) as well as the variables specific to each ageing treatment. For thermal ageing, the additional independent variables are the temperature of the oven (1 level) and the duration (1 level). For photochemical ageing, the additional independent variables are the wavelength (1 level), the intensity (1 level), the temperature (1 level) and the duration (1 level). For hydrothermal ageing, the additional independent variables are the temperature of the oven (1 level) and the duration (3 levels). For laundering, the additional

independent variables are the number of cycles (10 levels), and the washing and drying conditions (1 level each).

3.4.1. Thermal test

Two Heratherm™ OGH ovens (120 V, 60 Hz) (Thermo Scientific, Inc, MA, USA) were employed in this part of the study. The temperature of the ovens was set to 235 °C. Specimens were attached to the oven shelves in a hanging position using copper wire hooks (Figure 17) while leaving some space between them and the oven walls. The specimens attached to the oven shelves were placed in the conditioning room for 24 h. The two ovens were pre-heated for two hours until they reached the required temperature. At that time, the shelves with the preconditioned specimens were inserted into the ovens. The specimens were exposed to thermal ageing for 42 h. After 42 h, the shelves were removed from the ovens and the specimens were allowed to cool down in ambient conditions. They were then transferred to the conditioning room to condition and ultimately tested for tear/tensile strength.

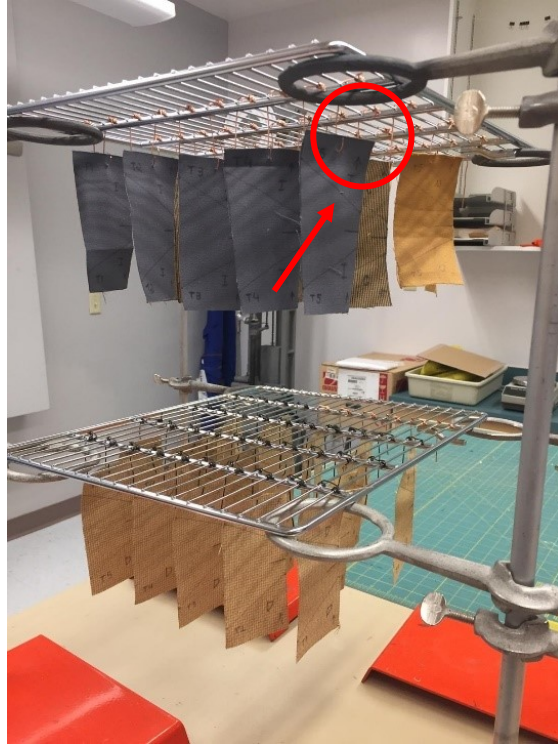


Figure 17. Specimens attached to the shelves and placed on racks.

3.4.2. Photochemical test

The Atlas UV tester (AMETEK, Inc, IL, USA) was employed with fluorescent lamps corresponding to the UVA range (315-400 nm). The conditions applied were intensity of 1 W/m^2 at 340 nm and a temperature of $80 \text{ }^\circ\text{C}$. It is important to note that it was a dry test so there was no control over humidity. The exposure lasted for 243 h, which correspond to 10 days. The test was conducted according to the standard test method AATCC TM186 (2015) - Weather Resistance: UV Light and Moisture Exposure.

The UV tester was calibrated and set to the conditions before beginning the exposure. For the tearing test, I wanted a portion of the fabric to be strong enough to be mounted in the grips of the tensile tester. For this reason, specimens were secured inside the holders with the cardboard masks to restrict the area of the photochemical exposure for each specimen to

the area that would be subjected to the tearing or tensile test while protecting the remainder of the specimen that would be held by the grips of the tester (Figure 18). The mounted specimens were then positioned in the UV tester. After the exposure time of 243 h, the holders were removed from the ageing chamber, and the specimens were taken out of the holders, conditioned, and later tested for tear/tensile strength.

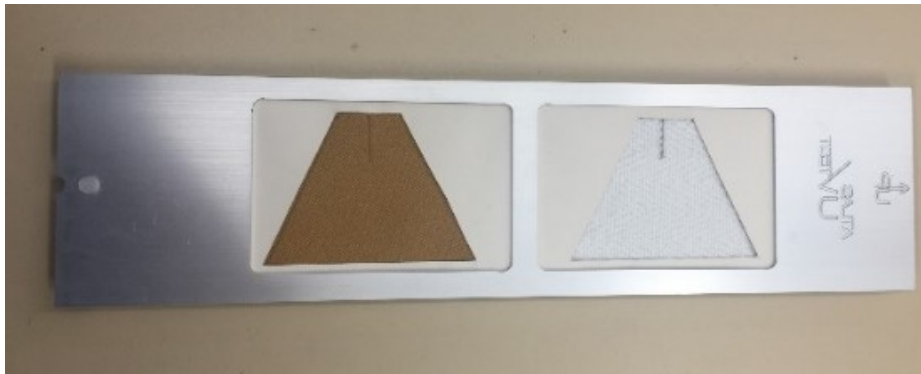


Figure 18. Specimens inside a specimen holder.

3.4.3. Hydrothermal test

Two Heratherm™ OGH ovens (120 V, 60 Hz) (Thermo Scientific, Inc, MA, USA) were employed in this part of the study. The temperature of the ovens was set to 80 °C. According to the procedure developed for the study, the specimens were pre-wetted with reverse osmosis (RO) water using a tray and a metal roller. Then, the specimens corresponding to each ageing duration were rolled together and inserted inside 500 ml flasks (Figure 19). Each type of fabric was placed in a separate flask. Then, the flasks were filled with RO water at 80 °C so as to completely cover all specimens. Heat resistant stoppers with two holes were inserted to close the flasks and the flasks were placed in the pre-heated ovens (Figure 20). Because of the use of cold water for the pre-wetting of the specimens, a period of about 10 min was needed

for the water inside the flasks to reach 80 °C again. A thermometer was used to monitor the temperature of the water inside the flasks. When that temperature was reached again, the ageing time was started. RO water at 80 °C was added every other day to the flasks to compensate for the water evaporation. After each ageing period, specimens were collected from the flasks, and laid flat to air dry on drying screens (Figure 21). When dry, they were conditioned and tested for tear/tensile strength.

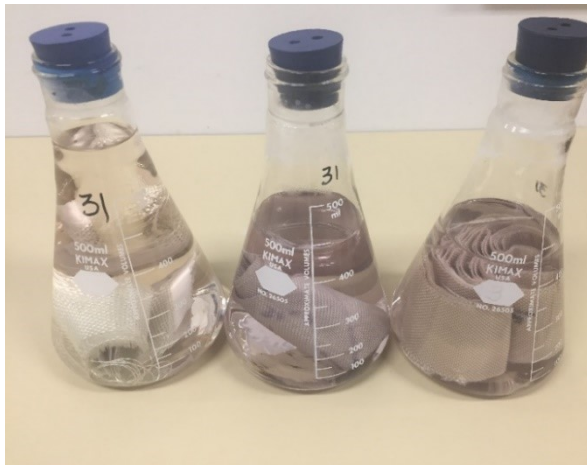


Figure 19. Specimens inside flasks.



Figure 20. The positioning of flasks inside the oven.



Figure 21. Drying screen.

3.4.4. Laundering test

The Launder-Ometer[®] (Model LHD-EF) (Atlas Electric Devices Co, IL, USA) was employed in this part of the study. Specimens were subjected to 10 laundering cycles. The test was carried out according to the standard test method ISO 105-C06 (2010) - Tests for colour fastness — Part C06: Colour fastness to domestic and commercial laundering using the procedure C1M. The temperature of the launder-Ometer[®] was set to 60 °C for 45 min for each cycle. A detergent solution of 0.4% weight to volume of AATCC 1993 Standard Reference Detergent without optical brightener (WOB) was premixed with RO water and left to stir with a magnetic stirrer for 30 min before each wash. The wash solution along with 50 metal balls were placed inside each canister. For canisters containing 5 specimens, 150 ml of the detergent solution was used while for canisters with only 1 specimen, 50 ml of detergent solution was used. Different fabrics were placed in separate canisters.

The Launder-Ometer[®] was filled with water and pre-heated for one hour until it reached the required temperature. Then, the canisters containing the detergent solution, the metal balls, and the specimens were positioned inside the machine and the rotor was turned on. Specimens were subjected to one 45-minute cycle of laundering per day. After each washing cycle, the specimens were removed from the canisters, rinsed three times using RO water, gently pad-dried using a towel and placed on a drying screen to dry overnight. These steps were repeated 10 times. The specimen shrinkage in the warp direction was measured on dry specimens after each cycle. At the end of the last cycle, the dry specimens were conditioned and later tested for tear/tensile strength.

3.5. Residual performance assessment methods

3.5.1. Tear strength

The initial and residual tear strength of specimens of fabrics A, B, C, D, E, F, G, I, L, M, N and O was determined following ASTM D5587 (2015) - Standard Test Method for Tearing Strength of Fabrics by Trapezoid Procedure. A modification was made to the size of the specimens because of limitations in the fabric quantity available. The specimen size used was 55 × 110 mm (Figure 22) instead of 75 x 150 mm as defined in the ASTM D5587 (2015) standard. The other geometrical characteristics of the specimen (trapezoid angle, length of the smaller base, and notch length) were kept the same. This decision was based on the results of a study that concluded that there is no statistical difference in the tear strength in the warp direction for this smaller 55 × 110 mm specimen size as long as the other geometrical characteristics of the specimen are left unchanged (Munevar et al., 2020). Other studies have reported results with smaller specimen sizes for tear strength using the trapezoidal test method (El Aidani et al., 2011; Nguyen-Tri et al., 2014; Dolez et al., 2019). Tests were only carried out in the warp direction, also because of limitations in the fabric quantity available for the study. Generally, five replicates were tested in agreement with the ASTM D5587 (2015) standard. However, in some instances (Fabric O), we only had enough material to test one specimen per condition.

The tear strength measurement test was carried out on an Instron tension and compression strength tester (Model 5565) (Instron Corporation, Inc, MA, USA), with two clamps holding the specimens along the oblique edges of the trapezoidal tearing zone. Specimens were conditioned for at least 24 h before each tearing test and the test was conducted

in a conditioned environment ($65 \pm 5\%$ RH at 20 ± 2 °C). The initial separation between the clamps was 25 mm.

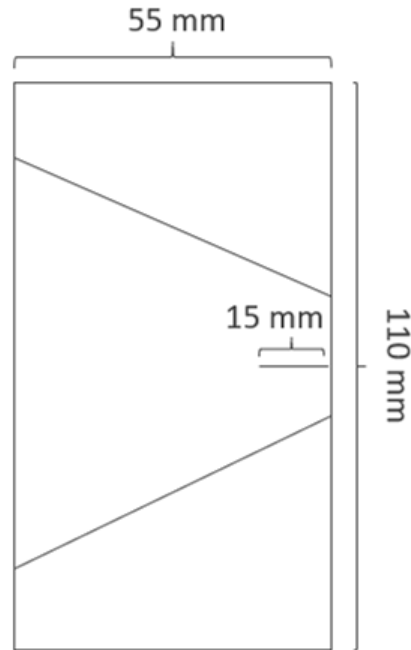


Figure 22. Illustration of the specimen shape and dimensions.

During the tear test according to the trapezoid procedure, the upper jaw moves away from the fixed lower jaw at a constant rate of 300 mm/min. As the distance between the clamps increases, a force is applied to the yarns at the leading edge of the slit and the tearing of the specimen begins. The force necessary to initiate and propagate the tear across the specimen is recorded. The test stops when the specimen is completely torn apart (Figure 23 (a, b, c)). The tearing strength for each specimen is determined according to the ASTM D5587 (2015) standard and is given by the average of the five highest peaks over the tearing distance. The average tear strength of the five specimens was computed along with the standard deviation for most fabrics.

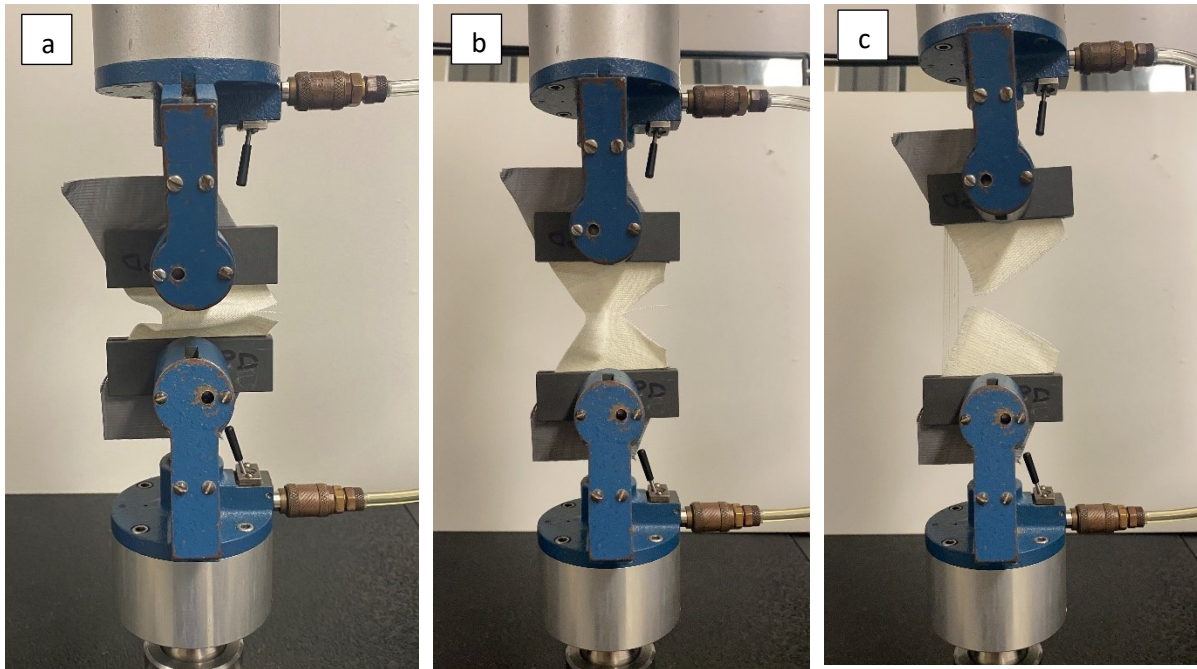


Figure 23. Test setup for tear strength measurement: (a) before tearing, (b) halfway tearing, (c) complete tearing.

Several of the fabrics included in this study are high-performance fabrics and have very high tear strength. Thus, many specimens experienced slippage in the grips (Figure 24 (a)). Because of the high strength and smoothness of the yarns in some of the fabrics, the clamps were not able to hold a good grip on the specimens, so the whole specimen or some of the yarns slipped from the clamps rather than tearing. To solve this problem, different approaches were attempted, for instance using different clamps (rubber-faced, serrated and smooth surfaces covered with sandpaper) and covering the clamped edges of the specimens with duct tape. Eventually, the combination of rubber-faced clamps and duct tape (IPG: Intertape polymer group) on the specimens solved the problem of specimen slippage for most materials (Figure 24 (b)).

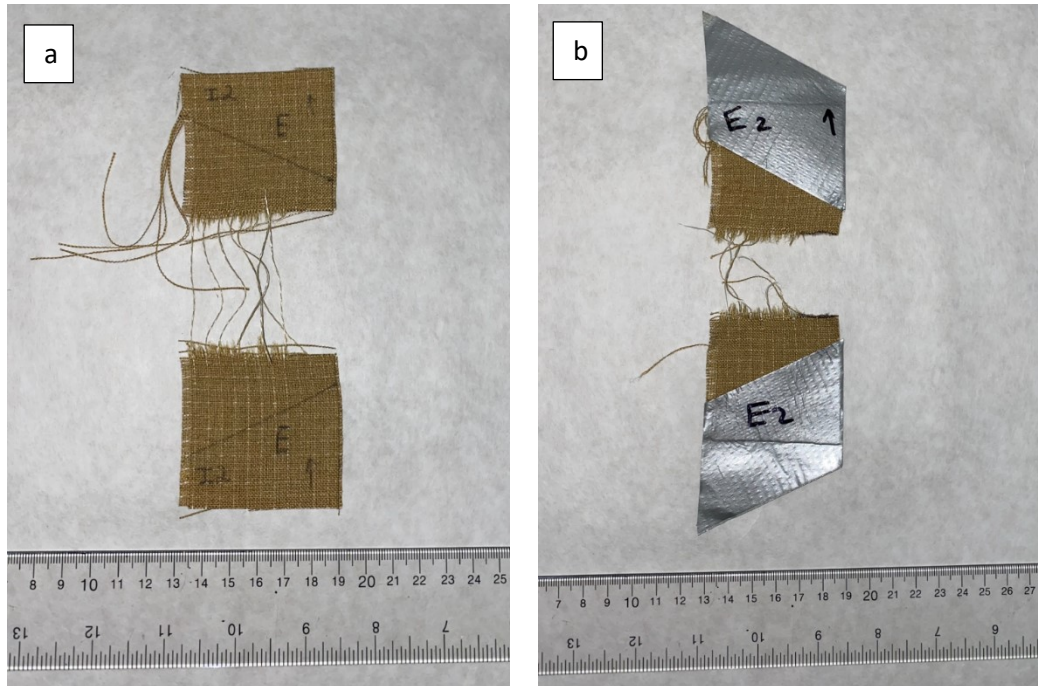


Figure 24. Specimen from Fabric E after tearing test: (a) suffering of slippage, (b) tearing without slippage (with duct tape).

3.5.2. Tensile strength

For fabrics T and U, the effect of ageing was assessed using tensile strength measurements rather than tear strength. The initial and residual tensile strengths of the fabrics were determined following ASTM D5035 (2019) - Standard Test Method for Breaking Force and Elongation of Textile Fabrics (Strip Method). An Instron tension and compression strength tester (Model 5565) (Instron Corporation, Inc, MA, USA) was used, at a rate of extension of 20 mm/min. Specimens were conditioned for at least 24 h before each tensile test and the test was conducted in a conditioned environment ($65 \pm 5\%$ RH at 20 ± 2 °C). A specimen size of 50×160 mm was used for fabric T and for the accelerated UV aged specimens for Fabric U. For the unaged condition as well as after thermal, hydrothermal, and laundering ageing for fabric U, 50×320 mm long specimens were used instead to allow securing them with a metal

rod in the grips and prevent slippage (see more details below). Each specimen was ravelled to a warp yarn count of 16 yarns which corresponded to a ravelled width of ~25 mm (Figure 25). Rubber-coated clamps were used with an initial separation of 75 mm. The tests were carried only for the warp direction of both fabrics.

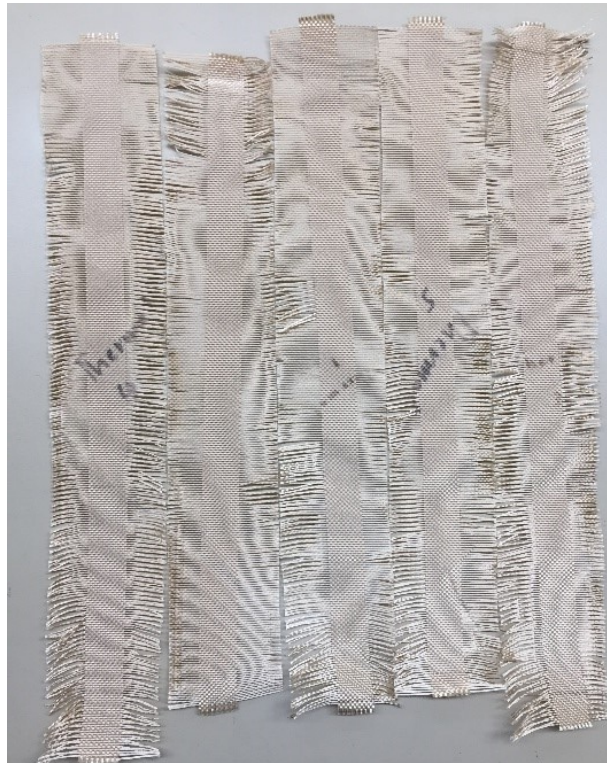


Figure 25. Example of ravelled specimens of Fabric (U) after thermal exposure.

As the test proceeds, the upper jaw moves away from the fixed lower jaw at a constant rate of 20 mm/min. As the distance between the clamps increases, the force applied increases until breakage of the specimen takes place. The breaking strength for each specimen is determined by the force at breakage. The average breaking strength of five specimens was computed along with the standard deviation.

As a result of the high strength and smoothness of the filament yarns of the two fabrics T and U, slippage of the specimens in the clamps was initially observed. As a result, different strategies to prevent slippage were applied for each fabric. In the case of Fabric T (low count, glass fabric with filament yarns), where the loose structure of the fabric allowed the yarns to slip from the clamps, another fabric with a very low melting temperature (polypropylene) was melted on the edges of the specimens to prevent movement of the yarns from the cut edges and to help the clamps get hold of the specimens (Figure 26). This procedure was performed for specimens before the ageing treatments were applied, except for the thermally aged specimens because of the potential that the melted polypropylene would not survive the ageing treatment. For thermally aged specimens, duct tape was applied after the thermal ageing treatment was completed. In the case of Fabric U (low count, LCP fabric with filament yarns), a longer specimen length was used to allow for the ends of each specimen to wrap around a metal rod positioned outside each clamp before being taken back into the clamp and held a second time by the clamps (Figure 27). Unless stated otherwise, the same configuration for the clamping of the specimens was used when comparing aged and unaged specimens.

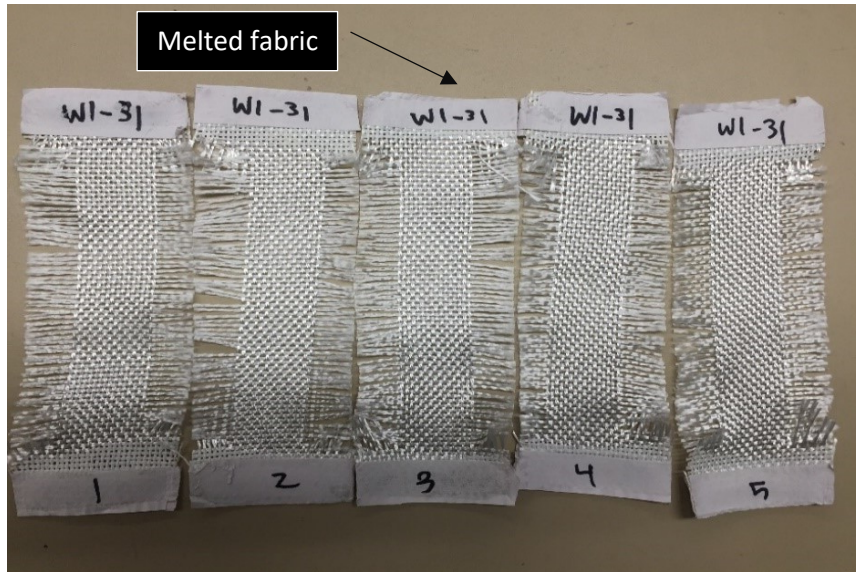


Figure 26. Melted polypropylene fabric on the edge of fabric T specimens.



Figure 27. Tensile strength test for Fabric U, using a long specimen length wrapped around and a metal rod outside the upper and lower clamps.

3.5.3. Shrinkage

Fabric shrinkage was estimated by making two reference marks on the specimens at a distance of 80 mm from each other along the warp direction (Figure 28). The percentage (%) of shrinkage was calculated for the warp direction using Equation 3:

$$\text{Shrinkage (\%)} = \frac{B - A}{A} \times 100 \quad (3)$$

Where A is the initial distance between two reference points, i.e. before laundering, and B is the distance between the two reference points measured after laundering and drying. The measurement for shrinkage was performed after every two laundering cycles on each replicate, and the average percentage shrinkage and standard deviation for each fabric were calculated. Hence, the shrinkage of the fabrics was measured 5 times in total over 10 laundering cycles.

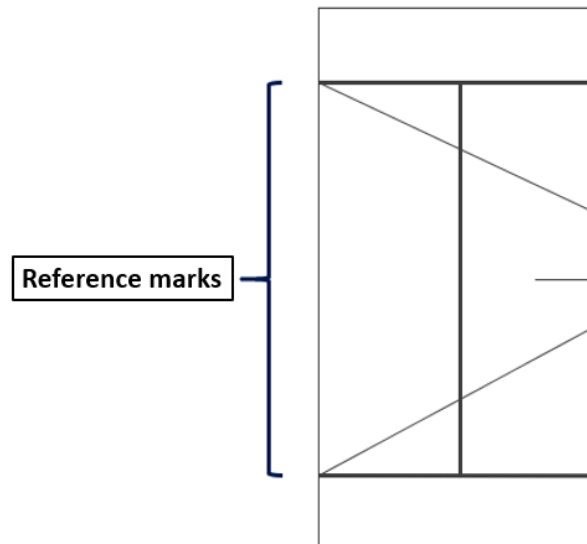


Figure 28. Illustration of a specimen with the reference marks situated 80 mm apart.

3.6. Assessing the strength of the rGO coating

The electrically conductive layer used in the graphene-based EOL sensor may be affected by the ageing conditions and gradually lose its conductivity (Cho et al., 2019). Verifying the quality of the bonding between the graphene layer prepared with graphene oxide (GO) ink and the selected support fabric is critical to ensure the proper functioning of the EOL sensor.

For this purpose, rGO-coated specimens were prepared and subjected to accelerated laundering. After each laundering cycle, the conductivity of the rGO layer on the fabric specimen was measured.

3.6.1. Preparation of the rGO-coated specimens

The preparation of the rGO-coated specimens was performed according to a previous study where rGO conductive coatings and tracks were successfully prepared on a meta-aramid fabric (Cho et al., 2019). Twelve pieces with dimensions of 8×8 cm were hand-cut from the fabric identified as the best candidate for the sensor substrate (Section 4.4). The fabric was used as received.

Specimens were coated using the dip and dry method described by Cho et al. (2019). According to this approach, the fabric specimens were dipped into the GO solution for 15 min (Figure 29). Figure 30 shows the heat press machine (Carver, Inc, IN, USA) used to dry the specimens at $107\text{ }^{\circ}\text{C}$ for 2 min (Figure 31). For the drying operation, the specimen was inserted between two films of Kapton in order to avoid being damaged by direct contact with the press hot plates.

The following step involves reducing the GO. With GO, the plane of carbon atoms is filled with defects and oxygen-containing functional groups (Pei & Cheng, 2012). The reduction of GO will lead to the healing of structural defects and the removal of oxygen-containing groups. Hence, higher electrical conductivity is achieved. For the reduction step, the specimens were immersed in 400 ml of water mixed with 10 grams of L-AA (L-ascorbic acid) powder in a glass bottle. The bottle was tightly sealed and placed in an oven (Symphony-VWR, Vacuum brand 2 C) at 90 °C for 4 h (Figure 32). After 4 h in the oven, the specimens were left to flat-dry for 24 h. The flakes of rGO were visible on the surface of the dried specimens (Figure 33). In accordance with the protocol developed by Cho et al. (2019), flakes not strongly attached to the fabric surface were exfoliated using a piece of adhesive tape. The dip-dry-reduce-exfoliate process was repeated 10 times until 10 layers of rGO were prepared on each fabric specimen. The 12 rGO-coated specimens were given the codes coated-1 to coated-12.



Figure 29. Specimen after dipping in GO.



Figure 30. Drying of specimen using the heated press.



Figure 31. Dried specimen.



Figure 32. Reducing GO-coated specimens in L-AA.

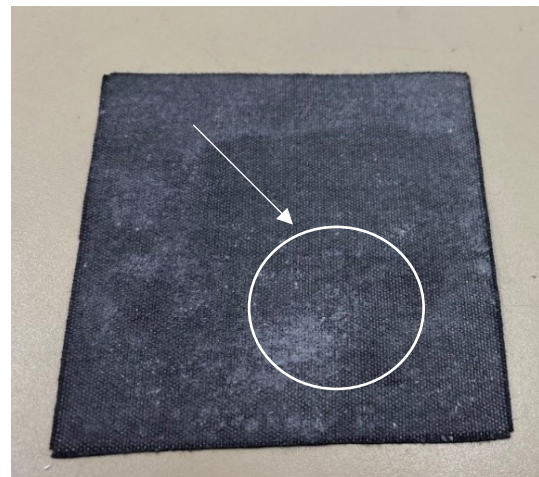


Figure 33. Loosely attached rGO flakes on the surface of the specimen.

3.6.2. Laundering of the rGO-coated specimens

Accelerated laundering was performed on the rGO-coated specimens using the Launder-Ometer[®] (see section 3.3.4) to assess the strength of the coating on the fabric. The temperature of the water bath was set to 40 °C and the Launder-Ometer[®] was run for 30 min for each wash cycle. A detergent solution of 0.4% weight to volume of AATCC 1993 Standard Reference Detergent (WOB) was premixed with RO water and left to preheat and stir with a magnetic stirrer for 30 min before each wash. Each canister contained one specimen with 50 ml of pre-heated detergent solution along with 50 metal balls. The specimens were subjected to up to three laundering cycles.

3.6.3. Electrical conductivity measurement of rGO-coated specimens

A four-point-probe resistivity measurement system (Pro4 4000, Lucas Labs, CA, USA) was employed to measure the sheet electrical resistance (R_s) of the rGO-coated specimens. Five measurements were made on each face of the specimens. The average value and standard deviation were calculated. The measurement was performed for each specimen in the initial condition (e.g. before laundering) as well as after 1, 2 or 3 laundry cycles depending on the case.

3.6.4. Surface morphology characterization of the rGO-coated specimens

Field emission scanning electron microscope (FE-SEM) was employed to characterize the surface morphology of some of the rGO-coated specimens in the initial

condition and after a selected number of laundering cycles¹. Images were taken with different levels of magnification at five different locations for each selected specimen.

3.7. Statistical analysis

The strength between unaged and aged specimens for all fabrics tested is compared and analyzed for significant differences using The Paired Samples T-Test using Microsoft[®] Excel[®] Version 2101. One-way ANOVA test is used to analyze the significant differences in the change in strength between fabrics in order to compare their performance, as well as shrinkage after laundering using Statistical Package for the Social Sciences (SPSS). The effect of all accelerated ageing conditions on the mechanical strength, as well as shrinkage after laundering for all fabrics tested were investigated. The details of the results of the statistical analysis performed to assess the effect of ageing conditions on the fabrics' performance are provided in appendix B for thermal ageing, C for photochemical ageing, D for hydrothermal ageing, E for laundering, and F for shrinkage.

¹ The FE-SEM imaging was performed by PhD student Md. Saiful Hoque.

4. RESULTS AND DISCUSSION

4.1. Fabric characterization

A summary of the fabric characteristics including, fabric structure, thickness, mass, fibre content, fabric count and yarn structure is presented in Table 5. This table includes all 14 fabrics evaluated in this study, identified by their letter codes and tradenames.

A full detailed description of the fabric characteristics supplemented with images of fabrics, yarns, and fibres is presented separately for each fabric in Appendix A. After close visual examination of each fabric, it was observed that the fibres used in the warp and weft yarns are similar in appearance within each fabric. Hence, photomicrographs of the fibres from only one direction (warp yarns) are presented for each fabric.

Table 5. Summary of the fabric characteristics.

Code	Name	Structure	Thickness (mm)	Mass (g/m ²)	Fibre content (supplier)	Fabric count (yarn/cm)		Yarn structure
						Wa	We	
A	Brigade™ 750 – natural	plain weave	0.6	257	93% Nomex [®] , 5% Kevlar [®] and 2% anti- static carbon (a)	28	27	Y1: staple 2-ply
B	Agility™ – light gold	2/1 twill weave	0.5	226	60% Kevlar [®] , 20% Nomex [®] and 20% PBO (b)	19	18	Y1: staple 2-ply
C	Pioneer™ – gold	2/1 twill weave	0.48	227	60% Kevlar [®] and 40% Nomex [®] (c)	18	18	Y1: staple 2-ply Y2: staple 2-ply
D	Armor AP™ – gold	broken twill weave	0.4	222	65% Kevlar [®] and 35% Nomex [®] (d)	24	24	Y1: staple 2-ply Y2: filament singles
E	Gemini™ XT – naturel	plain weave	0.48	246	55% Kevlar [®] , 37% PBI and 8% LCP (a)	16	15	Y1: filament singles + staple singles

								Y2: staple 2-ply
F	Kombat™ Flex – gold	2/1 twill weave	0.5	234	64% Kevlar® and 36% PBI (d)	18	17	Y1: filament singles + staple singles Y2: staple 2-ply
G	PBI Max™ 6.0 oz – gold	2/1 twill weave	0.38	214	65% Kevlar® and 35% PBI (a)	24	22	Y1: filament singles Y2: staple 2-ply
I	Flameflex 275– graphite	2/1 twill weave	0.5	84	63% cotton, 34% polyester and 3% EOL (XLANCE®) (e)	28	17	Y1: staple singles
L	CarbonX Repel	2/1 twill weave	0.58	278	50% oxidized PAN, 17% Kevlar®, 30% FR rayon and 3% anti-static polyester (f)	25	25	Y1: staple 2-ply
M	LENZING™ FR	3/1 reverse twill weave	1.7	556	100% FR viscose (g)	13	7	Y1: staple 3-ply
N	Zylon®	2/1 twill weave	0.55	333	100% PBO (h)	27	22	Y1: staple 2-ply

O	NF Arc™	plain weave	0.33	170	30% oxidized PAN, 40% Kevlar® and 30% novoloid (i)	32	22	Y1: staple 3-ply
T	Fiberglass Cloth (Style 7500)	plain weave	0.45	317	100% fiberglass (j)	7	6	Y1: filament 2-ply
U	Vectran™	plain weave	0.68	289	100% LCP (k)	10	10	Y1: filament singles

a Honeywell. <https://www.honeywellfirstresponder.com/~media/epresence/firstresponder/literature/pdf/selector%20guides/fabric%20selector.ashx?la=es-mx>

b Personal communication: Agility™ Datasheet, Tencate.

c Personal communication: Pioneer™ Datasheet, Tencate.

d Global turnout gear fabrics. https://s7d9.scene7.com/is/content/minesafetyappliances/Globe_Material_Selection_Guide_08.18

e Flameflex 275 Datasheet, Carrington textiles. <https://www.carrington.co.uk/en/fabric/flameflex-275>

f CarbonX Datasheet, TEXTECH. https://www.tradingsolutionsw.com/wp-content/uploads/2020/03/Data_Sheet_CR-80-1.pdf

g LENZING™ FR, ivodex. <https://www.lenzingindustrial.com/Application/protective-wear>

h Zylon Datasheet, Toyobo. <https://www.toyobo-global.com/seihin/kc/pbo/zylon-p/bussei-p/technical.pdf>

i Personal communication: Steve Zawislak, Amex. https://www.norfab.com/download_pdf.php?id=325

j Fiberglass Cloth (Style 7500) Datasheet, Freeman manufacturing & supply company. <https://www.freemansupply.com/datasheets/Style7500.pdf>

k Vectran™, Kuraray. <https://www.kuraray.com/products/vectran>

4.2. Effect of accelerated ageing on the mechanical strength of the tested fabrics

The strength (tear or tensile depending on the fabric) of the aged specimens was measured and compared to the strength of unaged specimens. The objective was to characterize the effect of each accelerated ageing condition on these important mechanical properties. Figure 34 shows the effect of the different accelerated ageing conditions on the mechanical strength of all fabrics tested. The behaviour of the fabrics differed depending on the accelerated ageing condition. Some fabrics experienced a change (increase or decrease) in their strength (tear or tensile strength) following exposure to the different accelerated ageing conditions. Others appeared to show no effect in some instances.

To facilitate the analysis of the fabrics' behaviour to ageing, the selected fabrics were grouped based on their fibre content. These groups are shown in Table 6. Group 1 includes fabrics composed mainly of aramid fibres, Nomex[®] and Kevlar[®]. Group 2 includes fabrics composed of Kevlar[®] and PBI fibres. Group 3 comprises oxidized PAN-based fabrics. Group 4 includes fabrics containing PBO fibres. Group 5 includes fabrics composed of FR cellulosic fibres (natural or regenerated). Group 6 includes fabrics that did not fit into the other groups and consists of a fiberglass fabric and an LCP fabric. For each accelerated ageing condition, the change in mechanical strength of the fabrics is discussed separately for each of the fabric groups.

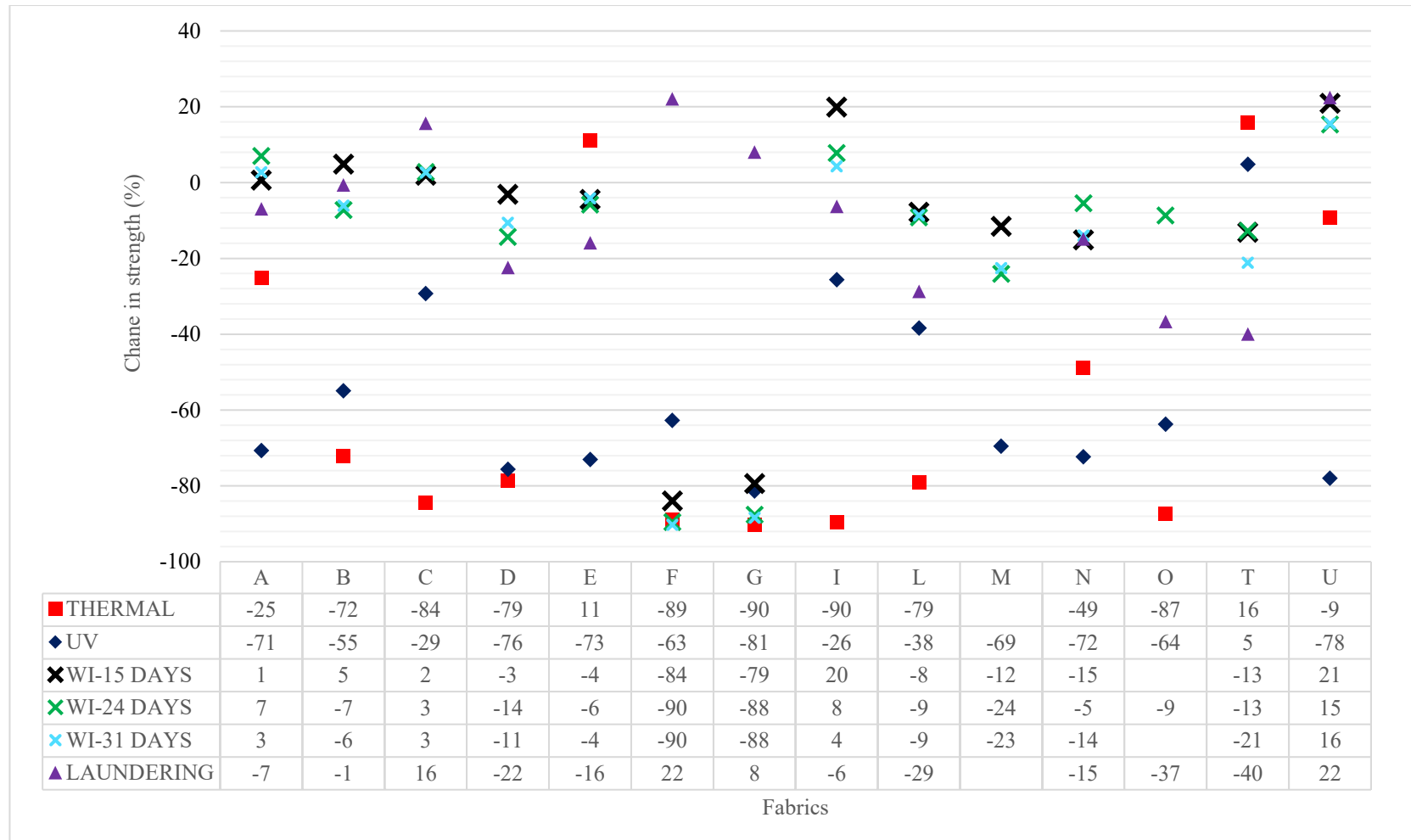


Figure 34. Percent change in mechanical strength after exposure to the different accelerated ageing conditions (A-O: tear strength, T-U: tensile strength).

Table 6. Fabric groups.

Group	Code	Fabric	Fibre content (%)
1	A	Brigade™ 750 – natural	93% Nomex®, 5% Kevlar® and 2% anti-static carbon
	C	Pioneer™ – gold	60% Kevlar® and 40% Nomex®
	D	Armor AP™ – gold	65% Kevlar® and 35% Nomex®
2	E	Gemini™ XT – naturel	55% Kevlar®, 37% PBI and 8% LCP
	F	Kombat™ Flex – gold	64% Kevlar® and 36% PBI
	G	PBI Max™ 6.0 oz – gold	65% Kevlar® and 35% PBI
3	L	CarbonX Repel	50% oxidized PAN, 17% Kevlar®, 30% FR rayon and 3% anti-static polyester
	O	NF Arc™	30% oxidized PAN, 40% Kevlar® and 30% novoloid
4	B	Agility™ – light gold	60% Kevlar®, 20% Nomex® and 20% PBO
	N	Zylon®	100% PBO
5	I	Flameflex 275 – graphite	63% cotton, 34% polyester and 3% EOL (XLANCE®)
	M	LENZING™ FR	100% FR viscose
6	T	Fiberglass Cloth (Style 7500)	100% fiberglass
	U	Vectran™	100% LCP

4.2.1. Effect of accelerated thermal ageing on the mechanical strength of the tested fabrics

The strength (tear or tensile depending on the fabric) of the thermally aged specimens was measured and compared to the strength of unaged specimens. The objective was to characterize the effect of accelerated thermal ageing on this important mechanical property. Figure 35 shows the strength values before and after ageing as well as the corresponding change in mechanical strength for all the fabrics tested. Differences in behaviour can be observed between the fabrics. Some exhibited a fairly similar decrease in strength as a result of ageing while a couple of fabrics experienced an increase. The effect of thermal ageing on the mechanical strength of the fabrics is discussed separately for the six fabric groups identified in Table 6.

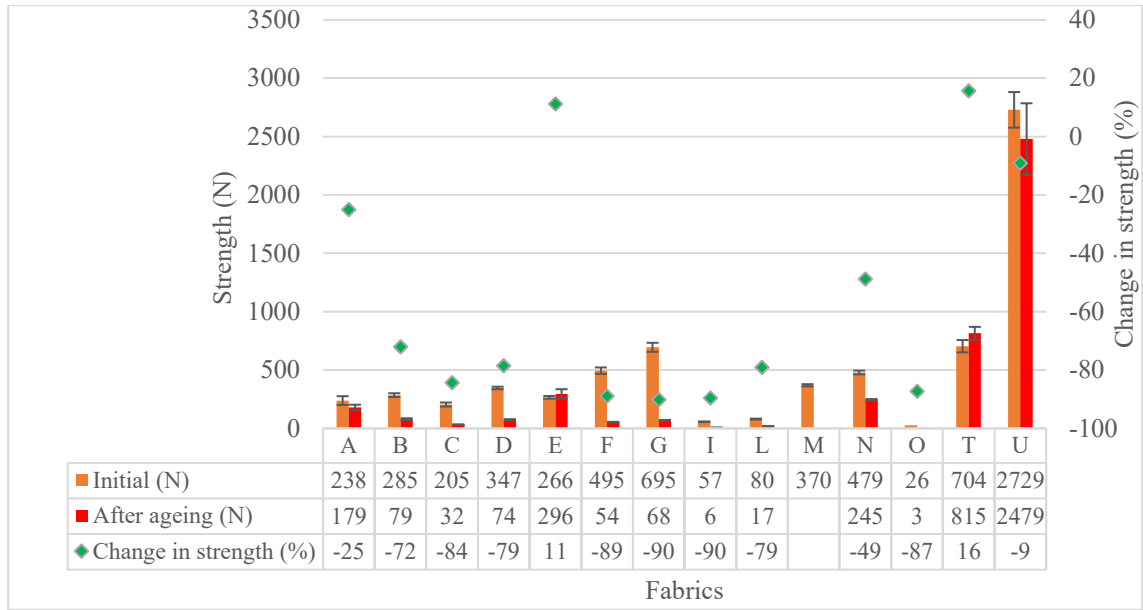


Figure 35. Average initial mechanical strength, average residual mechanical strength after thermal ageing at 235 °C for 42 h, and corresponding percent change in mechanical strength for all fabrics (A-O: tear strength, T-U: tensile strength).

Group 1 fabrics

The thermal ageing behaviour of Group 1 fabrics was characterized by tear strength. The results are shown in Figure 36. This group includes Fabrics A, C and D. These fabrics consist of blends of Nomex[®] and Kevlar[®], as well as a small amount of anti-static carbon fibres in Fabric A.

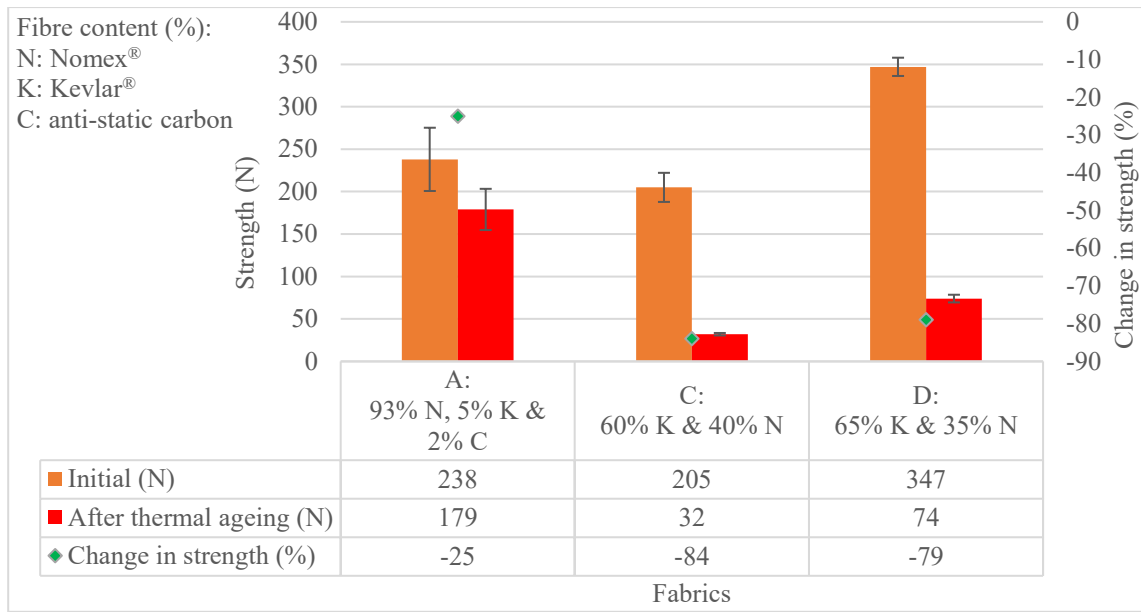


Figure 36. Average initial tear strength, average residual tear strength after thermal ageing at 235 °C for 42 h, and corresponding percent change in tear strength for Group 1 fabrics.

The differences in tear strength measured after thermal ageing for Fabric A, C and D are statistically significant, with a p value of .036 for Fabric A and p values of $< .001$ for Fabric C and D. The decrease in strength is 25% for Fabric A, 84% for Fabric C and 79% for Fabric D. The Nomex[®] content in Fabric A is 93% while it is 40% and 35% for Fabric C and D, respectively. The lower loss in tear strength for Fabric A is attributed to the higher Nomex[®] content in comparison to the other two fabrics which include greater quantities of Kevlar[®]. Moreover, Nomex[®] continuous operating temperature is 200 °C, whereas it is 190 °C for Kevlar[®] (Bourbigot & Flambard, 2002). Therefore, fabrics with higher Nomex[®] content have been found to withstand thermal ageing better than fabrics containing a higher content of Kevlar[®] (Dolez et al., 2019).

Various studies in the literature have investigated the effect of thermal ageing on Kevlar[®] and Nomex[®] fibres and fabrics. For instance, in a study conducted by Ozgen and

Pamuk (2014) 100% Kevlar[®] and 100% Nomex[®] plain weave fabrics were subjected to accelerated thermal ageing. Fabrics were left in a hanging position in an oven for 2, 10, 20 and 30 days at 220 °C, and 1, 2, 5 and 10 days at 300 °C, and the effect of the accelerated thermal ageing on the weight and tear strength of the fabrics evaluated. In the case of the 100% Kevlar[®] fabric, 30 days of ageing at 220 °C led to approximately 5% reduction in mass, and between 92 and 95% reduction in tensile strength in both directions of the fabric. For 10 days of ageing at 300 °C, the authors reported a 9% reduction in mass and a 95% reduction in tensile strength. On the other hand, for the 100% Nomex[®] fabric, 30 days of ageing at 220 °C led to a 4.3% reduction in mass, and between 3 and 4% reduction in tensile strength in both directions. After 10 days of ageing at 300 °C, the reduction in mass was 5% and the reduction in tensile strength was around 2-6%. To make the closest comparison possible with the conditions used in this study, thermal ageing at 220 °C for 2 days led the 100% Kevlar[®] fabric to lose between 56 and 69% of its tensile strength in the warp and weft directions, respectively, whereas it only led to a loss in tensile strength between 3 and 0.5 % in the warp and weft directions for the 100% Nomex[®] fabric. The authors found the change in strength after thermal ageing to be much less for Nomex[®] than for Kevlar[®] and for both of the fabrics, the tensile strength and mass continued to decrease as the ageing time and temperature increased.

Fabrics with similar fibre content as those included in Group 1 were also tested for tear strength in a study where firefighter outer shell fabrics were left in a hanging position and aged using an electrical convection oven at five different temperature: 150, 190, 210, 235 and 300 °C, for times of up to 500 h (Dolez et al., 2019). Their Fabric #2 (similar to Fabric A in terms of fibre content) had a small weight loss which occurred between 250 and 410 °C, and was attributed to the decomposition of the water-repellent finish, whilst the largest weight loss

happened between 410 and 550 °C and was attributed to the decomposition of Nomex[®]. The tear strength retention in their Fabric #2 was 70% at 150 °C after 510 h, and 52% at 235 °C after 100 h. On the other hand, for a fabric made of 100% Nomex[®], the tear strength retention was almost 80% at 150 °C after 500 h, and around 51% at 235 °C after 100 h. The tear strength retention in their Fabric #3 containing 60% Kevlar[®] and 40% Nomex[®] (similar to Fabric C in terms of fibre content) was 65% at 150 °C after 512 h, and 32% at 235 °C after 100 h. Finally, for a fabric made of 100% Kevlar[®], the tear strength retention was only 35% at 150 °C after 500 h, and 6% at 235 °C after 100 h. They reported that fabrics with higher Nomex[®] content tended to have better tear strength retention compared to fabrics with higher Kevlar[®] content. A comparison between the results reported by Dolez et al (2019) and the results of this study was conducted. Fabric A exhibits a tear strength retention of 75% after 42 h at 235 °C, whereas Fabric #2 had a residual tear strength of 63% after being exposed to the same ageing conditions. Fabric C exhibited a tear strength retention of 16% after 42 h at 235 °C, whereas Fabric #3 had a residual tear strength of 48% after the exposure to the same conditions. There is a relatively good agreement for the Nomex[®] IIIA fabric (Fabric A and Fabric #2), while the results are quite different for the 60/40% Kevlar[®]/Nomex[®] blend fabric (Fabric C and Fabric #3). This may be attributed in part to differences in the testing protocols between the two studies. They used a specimen's size of 51 × 102 mm, whereas, in this study, it was 55 x 110 mm. In addition, their specimens were not conditioned before testing. There may also have been changes in the fabric characteristics since there are about 10 years between their manufacturing times.

Another study looked at the mechanical properties of Kevlar[®] fibres after thermally treating them in a tubular resistance furnace at evaluated temperatures: 150, 350 and 520 °C for 0.5 to 260 h (Parimala & Vijayan, 1993). A 60% decrease in tensile strength after 3 h at 350

°C, and after 250 h at 150 °C was observed. The decrease in tensile strength was attributed to the diminishing of the crystallinity and the weakening of the van der Waals forces in the Kevlar[®] structure.

In terms of the effect of thermal ageing on Nomex[®], a study was conducted where a thermal treatment was carried out on Nomex[®] fibres and their residual properties were measured (Jain & Vijayan, 2002). The fibres were enclosed in quartz tubes, placed in a furnace, and exposed to thermal ageing for 1000 h at 200, 300, 350, and 400 °C. Heat exposure triggered the deterioration of the fibres and affected their characteristics, such as tensile strength, weight, and crystallinity. It also led to surface damage, with peel-offs, holes, defects, and groove-like openings. The authors reported a reduction in the fabric performance.

Another investigation was performed to assess the effect of thermal ageing on a 60/40% Kevlar[®]/PBI blend fabric reinforced with continuous Kevlar[®] filaments at 190, 220, 275, and 320 °C for up to 1000 h (Arrieta et al., 2011b). The high crystallinity of Kevlar[®] is related to three factors: first, the aligned rigid-rod chains resulting in large domains of extended molecules, second, the sheet-like structure because of the significant degree of hydrogen bonds between the highly oriented chains in the *b* direction, and third, the van der Waals forces between the sheet-like crystalline domains in the *a* direction (Jassal et al., 2020; Arrieta et al., 2011b). Raman spectroscopy of the thermally aged Kevlar[®] fibres showed a decrease in crystallinity and the growth of the amorphous region, whereas X-ray diffraction showed an increase followed by a decrease in the crystalline region (Arrieta et al., 2011b). It was hypothesized that two processes occurred in the fibre after thermal ageing. Firstly, a growth of the Kevlar[®] polymer crystallite size in the *bc* direction like what was observed through X-ray diffraction, and secondly, a decrease in crystallinity as well as the loosening of the crystalline

structure in the a direction of the fibre because of the weakening of the van der Waals forces which explained the disappearance of the change in crystallinity through Raman spectroscopy. It was hypothesized that the effect of the loosening of the crystalline structure in the a direction has a bigger effect in comparison to the growth of the crystallite size in the bc direction which explained the loss in tensile strength after thermal ageing.

These different studies confirm that fabrics with a higher percentage of Nomex[®] exhibit a lower loss in mechanical performance in comparison with fabrics with a higher percentage of Kevlar[®] when undergoing the same conditions of thermal ageing. Thus, the better resistance to thermal ageing of Fabric A can be linked to its higher Nomex[®] content. Fabric C and Fabric D are relatively similar regarding fibre content. However, there was a statistically significant difference in the change in tear strength between the two fabrics with a p value of .010 (details in Appendix B- Table B16). The woven structure of Fabric C consists of staple spun yarns (one Kevlar[®] staple spun yarn after every two Kevlar[®]/Nomex[®] staple spun yarn). On the other hand, Fabric D is woven with staple spun yarns and filament yarns (one Kevlar[®] filament yarn after every four Kevlar[®]/Nomex[®] staple spun yarns in the woven structure). The higher strength exhibited by Fabric D both before and after ageing is related to the filament yarns used in this fabric. Less force was required to tear Fabric C (no filament yarns) compared to the higher load needed to tear Fabric D (20% filament yarns). Figure 37 shows the differences in the tearing behaviour for the two fabrics before and after thermal ageing. Fabric D has an initial tearing curve that continues to rise over the test and indicates the sharing of the force by adjacent yarns during the test. The tearing behaviour of Fabric C did not change between the initial and thermally-aged conditions (Figure 37 (a,b)) and shows a pattern of individual yarns breaking as the tearing force moved through the fabric and similar strengths (peaks in the graph)

for the yarns being torn. However, the tearing behaviour of Fabric D was different between the initial and thermally-aged conditions (Figure 37 (c,d)). In the initial condition (Figure 37 (c)), the high peaks represent filament yarns, and since filament yarns tend to offer higher strength than staple spun yarns (Alagirusamy & Das, 2015). These filament yarns also led to better yarn mobility due to their slippery surface properties, hence the yarns were able to join together to resist the force which contributed to a higher tearing resistance. In the thermally-aged condition of Fabric D (Figure 37 (d)), the filament yarns broke as they were encountered during tearing and the initial benefit provided by the filament yarns was lost because of their reduced strength following thermal ageing. The change in the tearing behaviour in Fabric D accounts for the much greater tearing resistance in this fabric over Fabric C which showed a similar tearing behaviour both before and after thermal ageing.

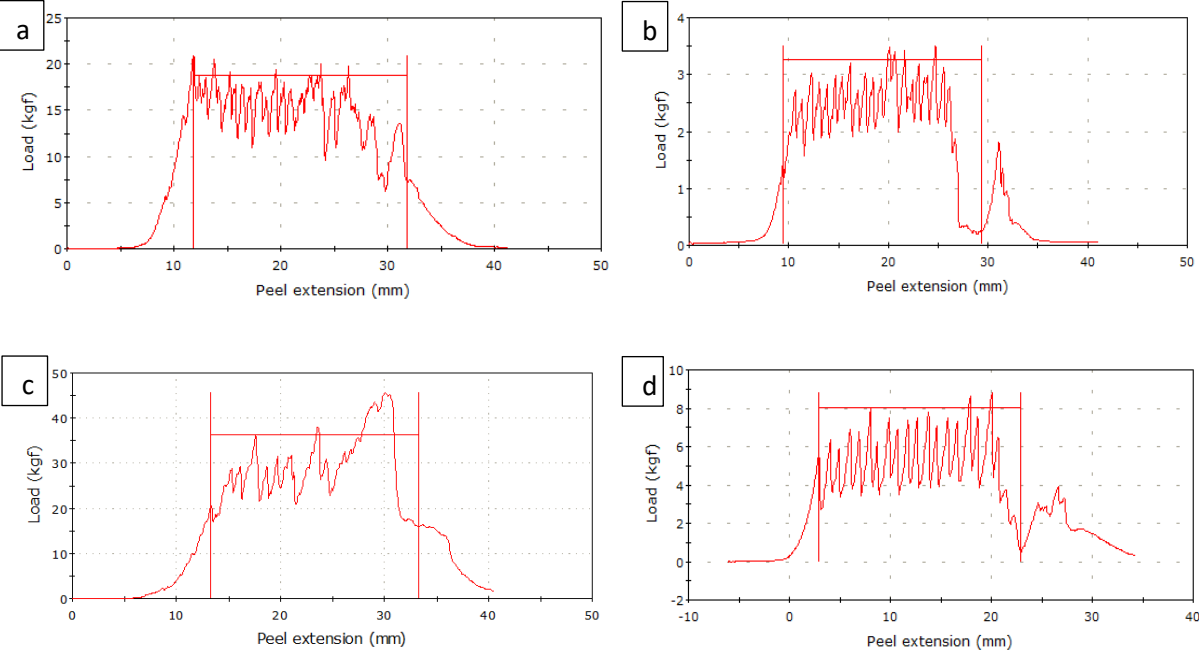


Figure 37. Tearing behaviour of specimens taken from: Fabric C (a: initial, b: thermally-aged), Fabric D (c: initial, d: thermally-aged).

Results from this study are in agreement with the literature about the thermal ageing behaviour of Nomex[®] and Kevlar[®] containing fabrics. The differences in behavior of the Group 1 fabrics are associated with their fibre contents and their yarn structures.

Group 2 fabrics

The thermal ageing behaviour of Group 2 fabrics was characterized by tear strength. The results are shown in Figure 38. This group includes Fabrics E, F and G. These fabrics consist of blends of Kevlar[®] and PBI fibres. In the case of Fabric E, it also contains a small amount of LCP filaments (one LCP filament yarn after every seven Kevlar[®]/PBI staple spun yarn in the woven structure).

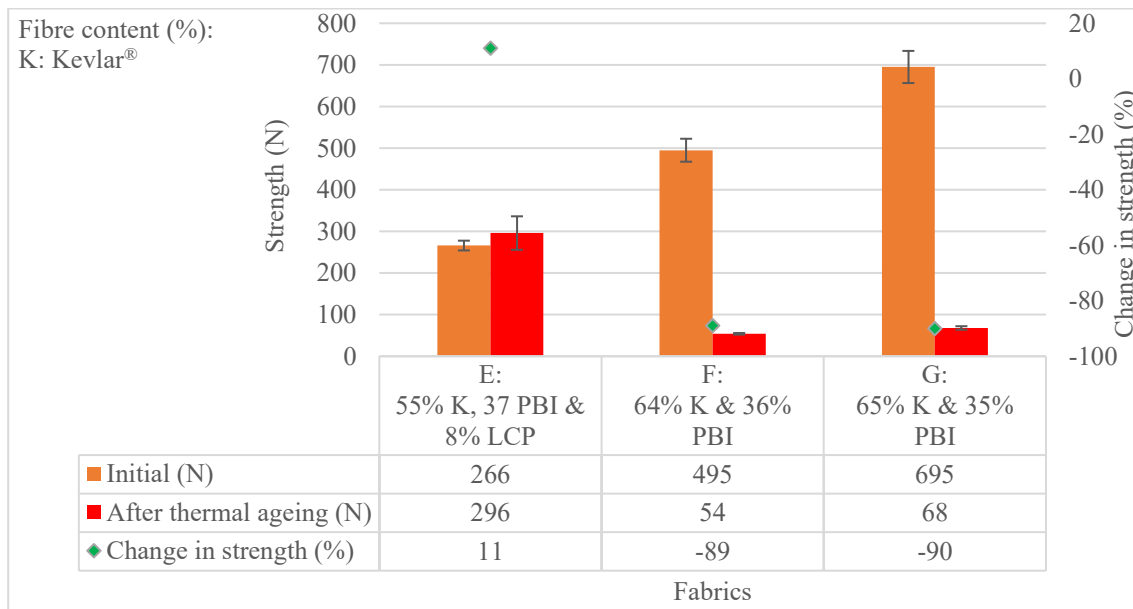


Figure 38. Average initial tear strength, average residual tear strength after thermal ageing at 235 °C for 42 h, and corresponding percent change in tear strength for Group 2 fabrics.

In the case of Fabric E, which consists of 55% Kevlar[®], 37% PBI, and 8% LCP, there was no change in tear strength (p value of .153). On the other hand, there was a statistically

significant difference in tear strength between the initial and the thermally-aged conditions with a p value of $< .001$ for Fabrics F and G. The loss in tear strength for these fabrics is 89 and 90%, respectively. There was no statistically significant difference in the change in tear strength between the two fabrics with a p value of .492 (details in Appendix B- Table B16).

These results agree well with other studies on the ageing behaviour of Kevlar[®] and PBI fibres. The ageing of Kevlar[®] fibres was already described in the section above relative to Group 1 fabrics. In the case of PBI fibres, a study looked at the effect of thermal ageing at 190, 220, 275, and 320 °C for up to 1000 h on a 60/40% Kevlar[®]/PBI blend fabric (Arrieta et al., 2011b). A decrease in the glass transition temperature was observed and associated with the chain scission of the PBI molecules following thermal ageing. Consequently, this led to a decrease in the molecular weight and contributed to the reduction in tensile strength.

In another study, the thermo-oxidative ageing behaviour of an 85/15 % PBI/Ultem1000 film was studied through exposure to a thermal treatment at 80 °C for 24 h (Musto et al., 1993). Using Fourier transform infrared spectroscopy (FTIR), the authors detected several new oxidized groups, which pointed towards the cleavage of the imidazole rings in the polymer chemical structure. The results confirm that Kevlar[®] and PBI fibres can be affected severely by thermal ageing.

My results are also in agreement with studies looking at the thermal ageing of fabrics with similar fibre content. For instance, a 60/40% Kevlar[®]/PBI blend fabric was exposed to temperatures up to 320 °C for up to 500 h in an electric convection oven (Arrieta et al., 2010). The residual tensile strength was measured to assess the effect of thermal ageing on the fabric's mechanical properties. The fabric only maintained 50% of its tensile strength after

12 days at 190 °C. A similar loss in strength was noted after less than 1 h at 320 °C. The breaking strength continued to decrease as the temperature and ageing time increased.

Another study with the same Kevlar[®]/PBI blend fabric (Fabric #7) involved the measurement of tear strength retention after the fabric was aged at five different temperatures: 150, 190, 210, 235, and 300 °C for a duration of up to 500 h (Dolez et al., 2019). It is important to clarify that, in this study, the specimens were not conditioned before testing for tear strength and the tear strength specimen sizes are slightly different (51 × 102 mm in their study), whereas in this study, it was 55 x 110 mm. The authors reported a tear strength retention of 70% after 550 h at 150 °C, and 22% at 235 °C after 100 h. The tear strength retention was 27% under the same conditions as in my study (42h of ageing at 235 °C). By comparison, Fabrics F and G, which have a relatively similar fibre content to each other and to Fabric #7 of the previous study, showed a tear strength retention of 11 and 10%, respectively.

In the case of Fabric E, thermal ageing did not affect the fabric like the other two fabrics. The woven structure of Fabric E consists of one LCP filament yarn after every seven Kevlar[®]/PBI staple spun yarns, while the woven structures of Fabrics F and G consist of one Kevlar[®] filament yarn every two Kevlar[®]/PBI staple spun yarns. The better performance exhibited by Fabric E can be linked to the presence of the LCP filament yarns. LCP fibres have high thermal stability and can retain their performance up to their melting point which is in the range of 275-375 °C (Pegoretti & Traina, 2018). Moreover, closer examination showed that the Kevlar[®]/PBI staple spun yarns in Fabric E were affected by thermal ageing just like what happened with similar yarns in Fabrics F and G, whereas the LCP filaments were not affected. Therefore, when the tearing test was performed on Fabric E, the Kevlar[®]/PBI staple spun yarns broke, yet the LCP filaments did not break but rather slipped from the fabric structure and

grouped together to resist the tearing force which essentially maximized the residual tear strength (see Figure 39).

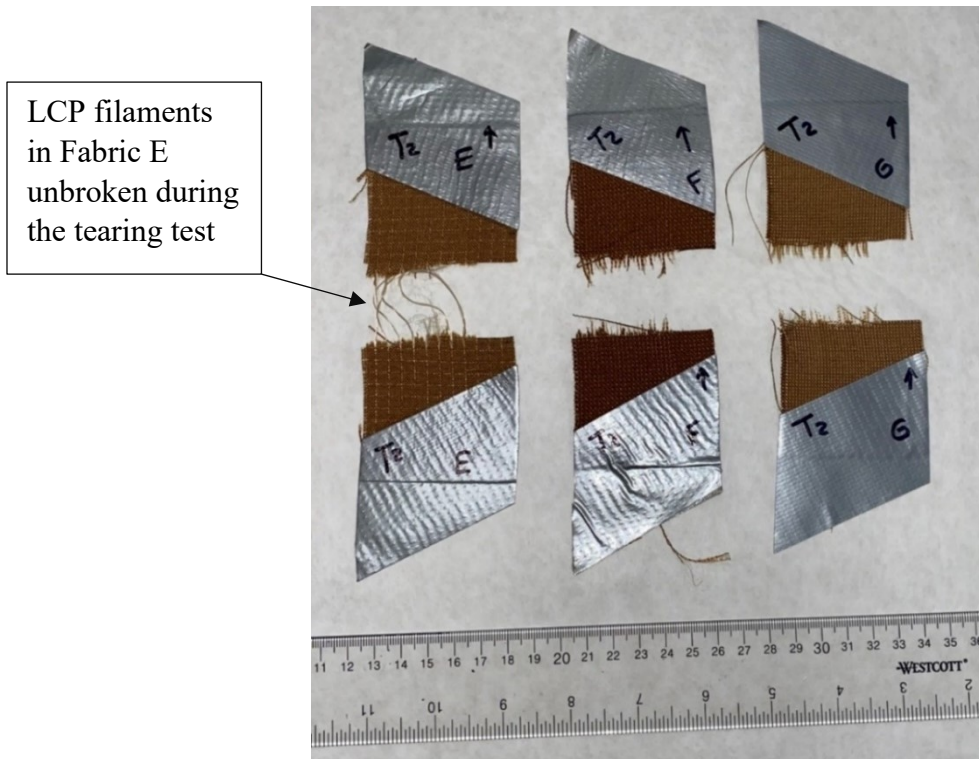


Figure 39. Thermally aged specimens from Fabric E, F and G after tearing.

The results obtained for Group 2 fabrics can thus be mainly explained by the fabric fibre content and they agree with the existing literature.

Group 3 fabrics

The thermal ageing behaviour of Group 3 fabrics was characterized by tear strength. The results are shown in Figure 40. This group includes Fabrics L and O. These fabrics mainly consist of oxidized PAN and Kevlar[®] fibres. Fabric L also includes FR rayon and anti-static polyester. Fabric O contains novoloid.

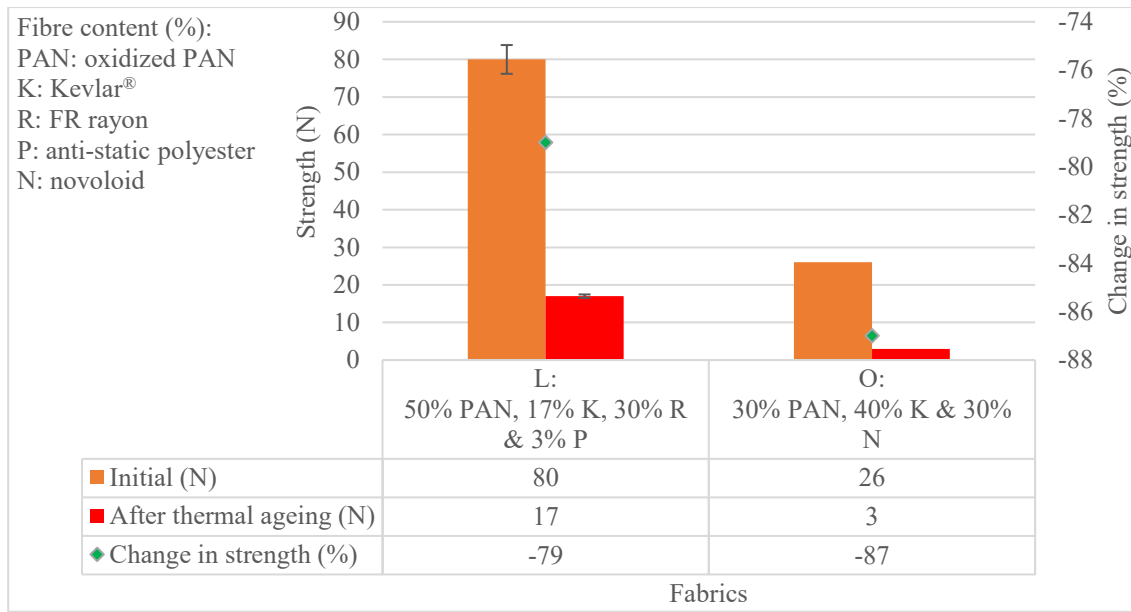


Figure 40. Average initial tear strength, average residual tear strength after thermal ageing at 235 °C for 42 h, and corresponding percent change in tear strength for Group 3 fabrics.

The loss in tear strength for Fabric L and O after thermal ageing is 79 and 87%, respectively. There was a statistically significant difference in tear strength between the initial and the thermally-aged condition for Fabric L, with a *p* value of < .001. Statistical analysis was not conducted on Fabric O because only one specimen per condition was tested because of fabric limitations. The OPF content in Fabric L and O is 50 and 30%, respectively.

Fabric L contains polyester and FR rayon in addition to oxidized PAN. Polyester fibres melt at 280 °C (Jaffe & East, 2007). Exposure to a heat source causes polyester fibres to soften and shrink (Burrow, 2013). For its part, FR viscose has been reported to experience thermal degradation between 220 to 290 °C (Yao et al., 2019). PAN fibres tend to form a char while undergoing pyrolysis which limits the production of flammable volatiles and contributes to their flame retardancy properties (Bajaj, 2000). According to Bajaj & Sengupta (1992), oxidized PAN fibres perform well in fire protective clothing. Hall et al. (1994a) state that when

PAN fibres are exposed to 200 °C, the flame retardant starts to melt and eventually fuses to the polymer chain at 300 °C, this reaction leads to the production of polyphosphoric acids which deposit on the surface, and protect the polymer from further decomposition.

Fabric O contains 30% novoloid fibres and novoloid goes through gradual carbonization when heated (Bajaj, 2000). Moreover, heating triggers further polymerization, crosslinking, and thermal degradation of the fibres, and eventually leads to the production of high flame and heat resistant char (Horrocks, 2014). However, it was reported that this fibre is reactive at 150 °C (Horrocks et al., 2001). Others have also reported that novoloid suffers a weight loss when exposed to 250 °C without the presence of oxygen, and completely carbonizes at 700 °C (Bourbigot & Flambard, 2002).

Very limited information has been found on the effect of thermal ageing on Group 3 fabrics. However, the decrease in strength as a result of thermal ageing at 235 °C for 42 h obtained for fabrics included in Group 3 can be explained by the fibre content of the fabrics and is in agreement with the existing literature.

Group 4 fabrics

The thermal ageing behaviour of Group 4 fabrics was characterized by tear strength. The results are shown in Figure 41. This group includes Fabric B and N. These fabrics consist of PBO fibres, blended with para- and meta-aramid fibres in the case of Fabric B.

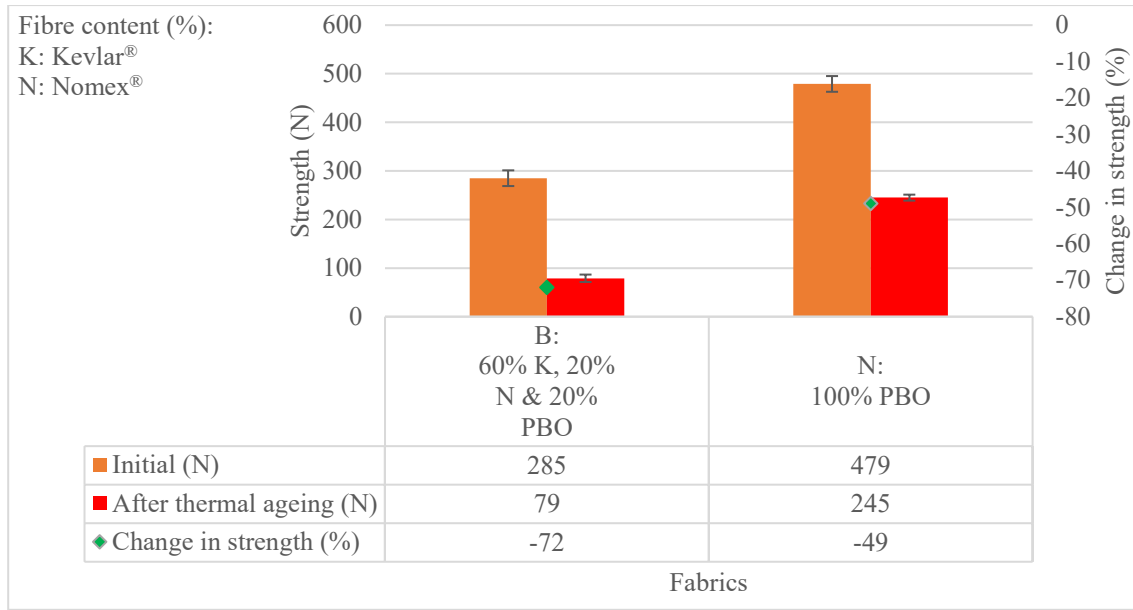


Figure 41. Average initial tear strength, average residual tear strength after thermal ageing at 235 °C for 42 h, and corresponding percent change in tear strength for Group 4 fabrics.

There was a statistically significant difference in tear strength between the initial and thermally-aged conditions for Fabric B and N, with *p* values of < .001 for both fabrics. Fabric B and Fabric N experienced a reduction in tear strength of 72 and 49%, respectively.

Researchers have shown that PBO exhibits high thermal-oxidative stability that allows it to resist heat up to about 600 °C in air and 700 °C in an inert atmosphere (Bourbigot & Flambard, 2002). On the other hand, weight losses of 10 and 22% were detected when the researchers exposed PBO fibres to a thermal treatment in air for 200 h at 343 °C and 371 °C, respectively. At temperatures between 700 and 1400 °C under a nitrogen atmosphere, PBO fibres go through a carbonization process (Hao et al., 2019). Above 750 °C, they undergo structural changes leading to the reduction in both the tensile strength and initial young’s modulus.

Another study was conducted to monitor gases such as CO, CO₂ and H₂O emitted by thermally degraded PBO fibres at 600 and 800 °C in a furnace under air (Bourbigot et al., 2001). From FTIR analysis, the researchers concluded that the low amount of evaporated gases from the PBO fibres was because of its high thermal stability. In addition, the resulting char structure of PBO fibres can trap free radicals making them resistant to oxidation.

A similar trend was obtained in a study on pyrolyzed PBO fibres in argon atmosphere with a heating rate of 10 °Cmin⁻¹ at temperatures ranging between 25-800 °C (Tamargo-Martínez et al., 2004). Thermogravimetry (TG) and differential thermal analysis (DTA) showed a reduction in mass of 1% at 100 °C because of water loss. Only a small mass loss occurred before 570 °C and the mass loss started to happen at 660 °C, with a major mass loss at 777 °C because of the deterioration of the fibres. Elemental analysis detected chemical changes in the polymer structure in which the content of carbon increased while the percentages of nitrogen, hydrogen, and oxygen decreased. Additionally, Raman spectroscopy showed no change until 500 °C. Above that temperature, bands indicated a conversion into carbonaceous materials. The band vanishes around 700-720 °C. Correspondingly, X-ray diffraction revealed that the polymer backbone broke down in the same 700-720 °C temperature range. In terms of fibre morphology, the nanofibrils became thinner and more defined (with a dimension of 5 to 15 nm) at 660 °C. At 720 °C, the fibre surface becomes oriented with more elongated plates (with a dimension of 5 to 20 nm). This morphology was dominant at 800 °C.

According to the previously mentioned research studies which have looked at the effect of thermal exposures on PBO fibres (Bourbigot & Flambard, 2002; Bourbigot et al., 2001; Tamargo-Martínez et al., 2004), PBO fibres are not expected to undergo any major changes in strength, mass, morphology, or emission of gases below a temperature around 700

°C. Hence, under my test conditions at 235 °C for 42 h, I did not expect a considerable degradation of fabrics with a high content of PBO.

The effect of thermal ageing on the tear strength of a fabric similar to Fabric B in terms of fibre content (Fabric #4) has been looked at in a study where they exposed fabrics to five different temperatures: 150, 190, 210, 235, and 300 °C for times up to 500 h (Dolez et al., 2019). The authors reported a tear strength retention of 48% at 150 °C after 511 h, and 17% at 235 °C after 100 h. The decomposition of the fabric was studied by thermogravimetric analysis in nitrogen. A small weight loss was observed below 410 °C. It was attributed to the decomposition of the finish. The weight loss between 410 and 520 °C was linked to the decomposition of Nomex[®]. The largest loss happened at 580 °C and was associated with the decomposition of Kevlar[®]. The loss between 650 and 800 °C was related to the decomposition of PBO. The authors attributed it to the fact that PBO has a stable C-O linkage in the heterocyclic rings in the backbone and a heterocyclic rigid conformation of the molecules, which gives it a higher degradation temperature in comparison with Kevlar[®] and Nomex[®] (Dolez et al., 2019). To compare with my conditions, a tear strength retention of 29% was obtained for Fabric #4 after 42 h at 235 °C, similar to the tear strength retention of 28% exhibited by Fabric B in my study.

Finally, there was a statistically significant difference in the change in tear strength between the two fabrics with a *p* value of .001. The difference in behaviour between Fabric B and Fabric N can be attributed to the difference in PBO content in the fabrics. Fabric N is made of 100% PBO fibres whereas Fabric B consists of 60% Kevlar[®], 20% Nomex[®] and only 20% PBO. The difference in thermal ageing performance between the three types of fibres can be

seen in their respective continuous operating temperature values (Bourbigot & Flambard, 2002): 310 °C for PBO, 200 °C for Nomex[®], and 190 °C for Kevlar[®].

My results for the PBO/aramid blend fabric are thus in agreement with the literature regarding the better resistance to thermal ageing of PBO compared to aramid fibres. However, Fabric N, consisting of 100% PBO lost more strength than expected during the thermal ageing test and this was unexpected from the studies cited above.

Group 5 fabrics

The thermal ageing behaviour of Group 5 fabrics was characterized by tear strength. The results are shown in Figure 42. This group includes Fabrics I, and M. These fabrics are cellulose-based. Only Fabric I survived the accelerated thermal ageing. Thus, it was only possible to perform the tear strength test after thermal ageing on this fabric. This fabric is treated with an FR finish and consists of 63% cotton, 34% polyester, and 3% EOL (XLANCE[®]). According to the manufacturer (XLANCE, n.d.), XLANCE[®] is a polyolefin-based elastic yarn. Fabric M contains 100% FR viscose.

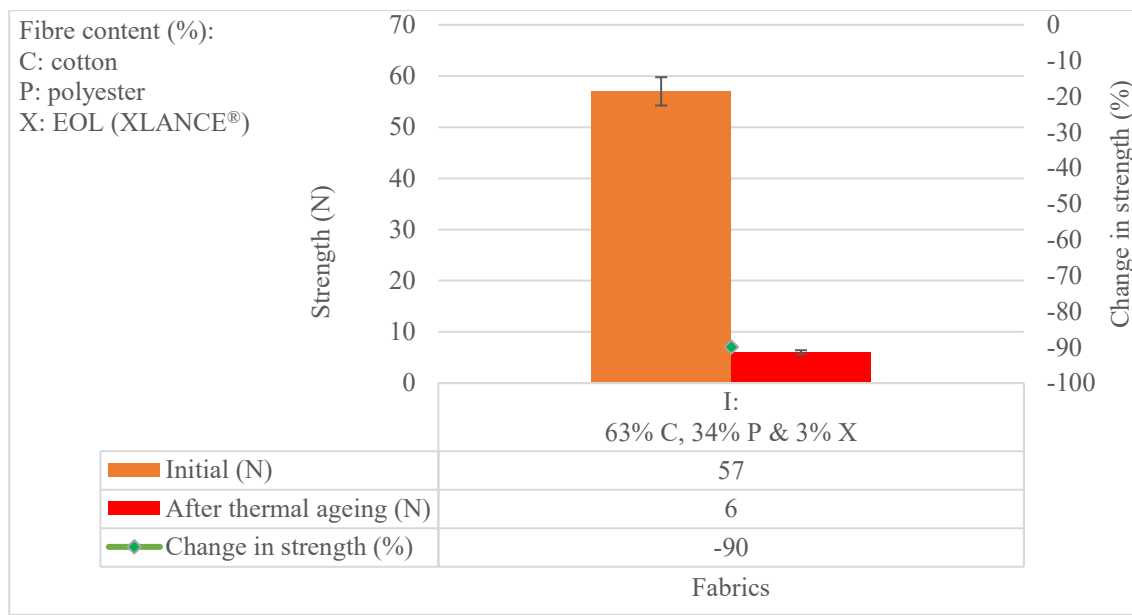


Figure 42. Average initial tear strength, average residual tear strength after thermal ageing at 235 °C for 42 h, and corresponding percent change in tear strength for Group 5 fabrics.

The results provide a strong evidence of the negative effect of heat exposure on cellulose-based fabrics. There was a statistically significant difference in tear strength between the initial and thermally aged condition for Fabric I, with a p value of $< .001$. Fabric I experienced a loss in tear strength of 90% which was similar to the change noted in the Kevlar/PBI blend Fabrics F and G.

The pyrolysis reaction of cellulose can be classified into two groups according to the temperature of exposure (Barker & Drews, 1985). At temperatures lower than 250 °C, it involves the production of non-flammable gases and non-volatile char such as water and carbon dioxide. At temperatures higher than 250 °C, it involves depolymerization, and leads to the release of flammable and volatile products such as the primary product (levoglucosan) and other secondary products. According to Barker & Drews (1985), the physical and chemical properties of cellulosic-based fibres are affected by these reactions. For instance, the strength

of fibres decreases as the temperature and time of exposure increase. Other highly flammable compounds such as hydrocarbons, alcohols, aldehydes, and ketones are also formed (Lecoeur et al., 2001).

The thermal degradation of FR cotton fabrics containing 3, 4, and 5 wt% of GP-108 fire retardant in aqueous solution was assessed by heating them in a nitrogen atmosphere at temperatures ranging between 40 to 700 °C with a heating rate of 10 °C/min (Li et al., 2019a). The FR cotton fabrics maintained an average mass of 95% up to 250 °C. This 5% loss was associated with the evaporation of adsorbed water. The fabrics experienced a maximum weight loss of around 17% at temperatures close to 287 °C. This slight loss in mass was linked to the flame retardant promoting the formation of char and hence preventing further degradation.

Fabric I also contained polyester fibres. The melting temperature of polyester is 280 °C (Jaffe & East, 2007). Polyester undergoes thermal degradation when heated above 300 °C, followed by the emission of highly flammable volatiles (Joseph & Tretsiakova-McNally, 2013). Melting and shrinking away from the fire source are also reactions exhibited by FR polyester (Burrow, 2013). The flame retardancy of polyester fibres can be improved by adding an additive to the polymer solution (Perez et al., 2006). This can cause a plasticizing effect, surface segregation and blooming, which will eventually affect the mechanical strength of the fibre and its elongation at break.

In the case of Fabric M, which consists of 100% FR viscose, we observed severe dimensional changes, complete colour change, and full charring as a result of the 42 h exposure to 235 °C (Figure 43 (b)) compared to its initial condition (Figure 43 (a)). A weight loss of more than 40% has been reported for FR Lenzing fibres exposed to temperatures ranging between 200 and 400 °C (Gu, 2009). In addition, FR viscose thermal degradation ranges from

220 to 290 °C, with the deposition of residues (Yao et al., 2019). This explains the result obtained with Fabric M.

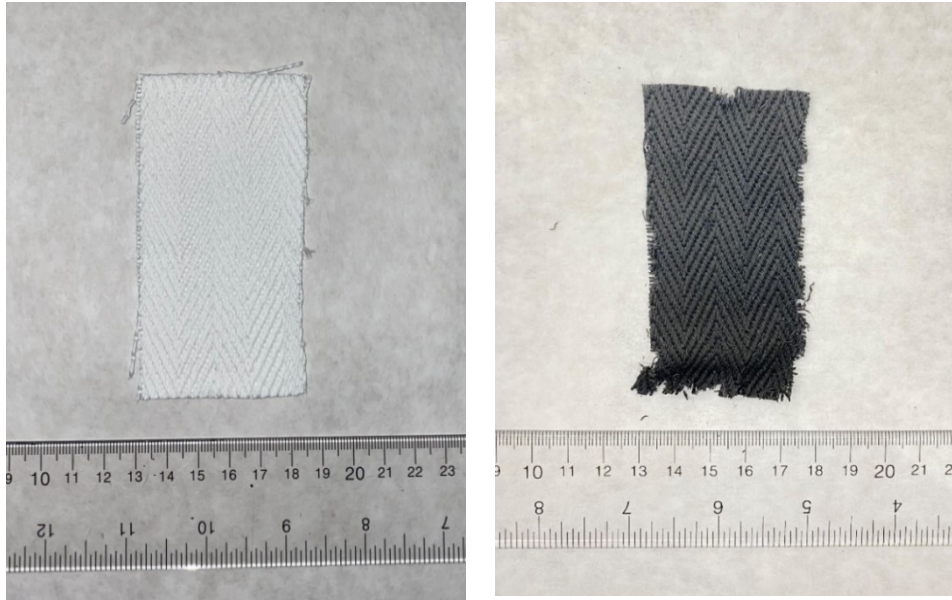


Figure 43. Fabric M: (a) initial condition, b) after thermal ageing.

The cellulose-based fabrics tested did not resist the accelerated thermal ageing at 235 °C for 42 h. This behaviour can be associated with their fibre content and is in agreement with the literature.

Group 6 fabrics

Other fabrics were included in this study. For instance, Fabrics T and U. The thermal ageing behaviour of Group 6 fabrics was characterized by tensile strength. The results are shown in Figure 44. Fabric T is made of fibreglass and Fabric U is 100% LCP.

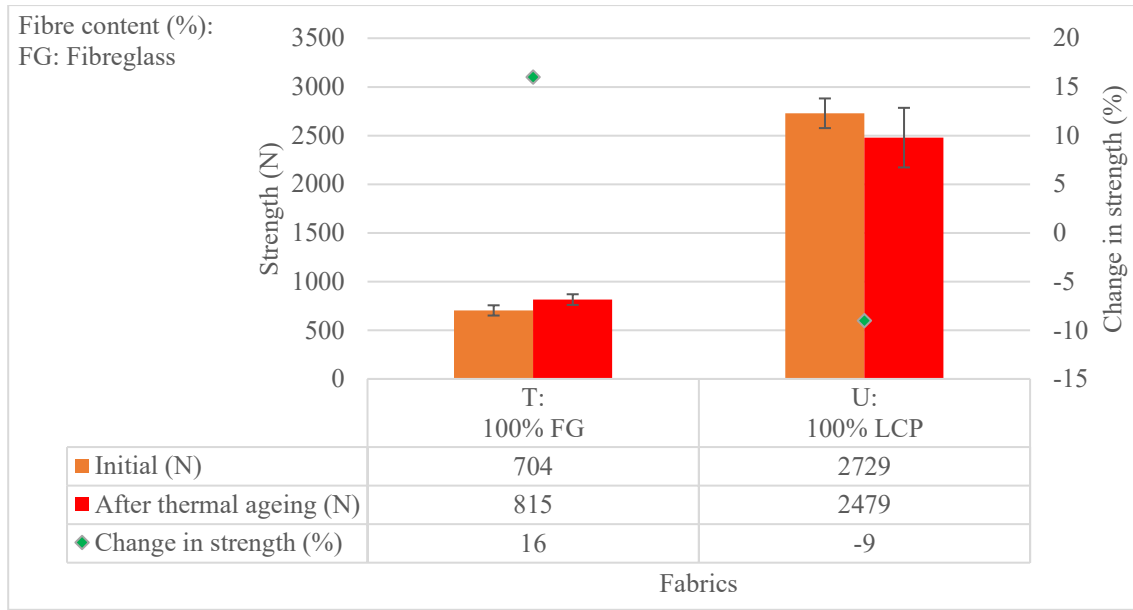


Figure 44. Average initial tensile strength, average residual tensile strength after thermal ageing, and corresponding percent change in tensile strength for Fabrics T and U.

There was a statistically significant difference in tensile strength between the initial and the thermally-aged conditions for Fabric T, with a p value of .012. On the other hand, Fabric U experienced a loss in tensile strength of 9%. However, this loss is not statistically significant with a p value of .141.

Accounts have been found in the literature where researchers exposed glass fibres to elevated temperatures for various times and measured the effect on the fibre's mechanical performance. For instance, Khazanov et al. (1995) associated the increase in strength of glass fibres at high temperature with the high elastic and plastic deformation of the fibres. When heated, the elastic modulus increases three to seven times, depending on the structure of the glass fibres, and ultimately was associated with the healing of microcracks and microdefects on the surface of fibres.

Khazanov et al. (1995) also reported the results of other studies that associated glass fibre's higher strength with a deep variation in structure when the fibres are drawn into fine filaments. The molecular orientation and the chain structure also contribute to the fibres' strength. Another explanation for glass fibres' strength is the hardened surface layer. The isotropic structure of high strength glass fibres can be attributed to the high cooling rate of the glass melt while forming the fibres which prevent them from having microdefects and microcracks.

In another study, E-glass fibres were exposed to different temperatures ranging between 100 and 600 °C for 4 h (Thomas, 1960). The authors did not observe a change in strength for temperatures below 300 °C. However, a decline in strength started above 300 °C, and the fibres lost 65% of their strength after 4 h at 400 °C. On the other hand, Cameron (1968) reported a loss in E-glass fibre strength of 60% after 65 h at 273 °C. In contrast, according to Sinclair (2015), glass fibres can be thermally stable to a temperature up to 450 °C.

In the case of Fabric T, it is difficult to explain this slight increase in the fabric tensile strength observed after 42 h of ageing at 235 °C, however, the result obtained from this study aligns with results from other research studies which have confirmed that the degradation of glass fibre requires a higher temperature than 235 °C.

The result obtained for Fabric U agrees well with existing studies on the thermal behaviour of LCP fibres. LCP fibres have a high thermal tolerance and can retain most of their performance up to their melting point in the range of 275-375 °C (Pegoretti & Traina, 2018). It has been reported that after 30 days of thermally treating LCP fibres at 195 °C, a loss in strength of 24% was measured. When exposed to temperatures above the melting point, LCP fibres suffer a weight loss of 20% at 450 °C and nearly 50% at 550 °C (Fette & Sovinski, 2004). The

decrease in strength with exposure to heat is because of the activation of amorphous regions within the crystalline regions (Sloan, 2017). LCP fibres exhibit the features of thermoplastics and thermosets. More specifically, the fibre is spun as a thermoplastic, but the molecular weight and polymer structure are formed by solid-state polymerization. Hot air shrinkage of less than 0.2% occurred in SM LCP fibres when exposed to hot air at 180 °C for 30 h. On the other hand, long-term exposure of LCP fibres at 250 °C in dry air resulted in a loss in strength of 90-80% after 300 h. This is a higher temperature and longer exposure duration in comparison to conditions used in this study. This explains why we did not measure a significant difference in the tensile strength before and after the thermal treatment for Fabric U.

In addition, a close examination of the surface of Fabric U after the thermal ageing treatment showed that the fabric became brittle and its tactile feel or hand changed. Images of the fabric before (Figure 45 (a)) and after (Figure 45 (b)) the heat treatment only showed colour change. On the other hand, images of yarns at a higher magnification (Figure 46) showed a change in the yarn's diameter as a result of the fibres fusing together. This observation points towards a partial melting of the fibres during the thermal ageing treatment.

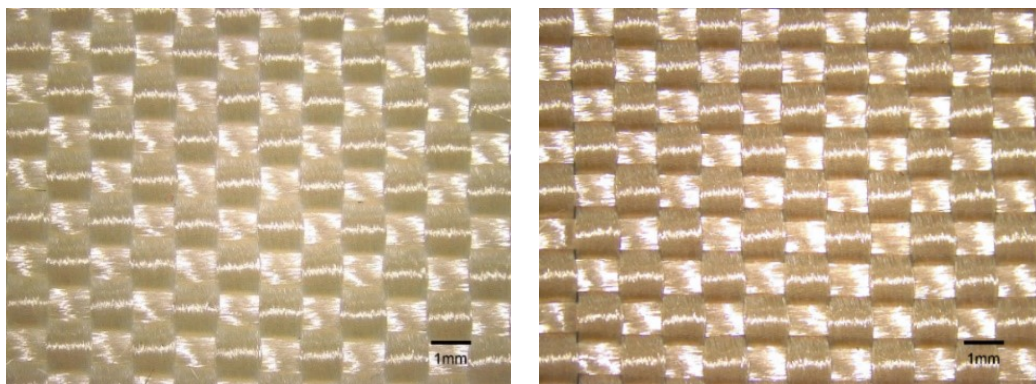


Figure 45. Fabric U: (a) initial condition, b) after thermal ageing.

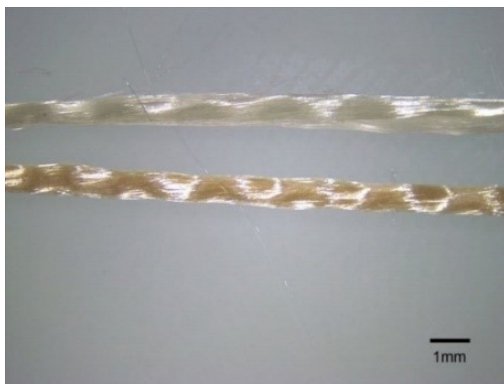


Figure 46. Fabric U – unaged (top) and thermally aged (bottom) yarns.

4.2.2. Effect of accelerated photochemical ageing on the mechanical strength of the tested fabrics

The strength (tear or tensile depending on the fabric) of the photochemically aged specimens was measured and compared to what had been obtained for the unaged specimens. The objective was to characterize the effect of accelerated photochemical ageing on this important mechanical property. Figure 47 shows the strength values before and after ageing as well as the corresponding change in mechanical strength for all the fabrics tested. Differences in behaviour can be observed between the fabrics. Most fabrics exhibited relatively large decreases in strength as a result of photochemical ageing except one fabric which displayed a slight increase. The effect of photochemical ageing on the mechanical strength of the fabrics is discussed separately for the six fabric groups identified in Table 6.

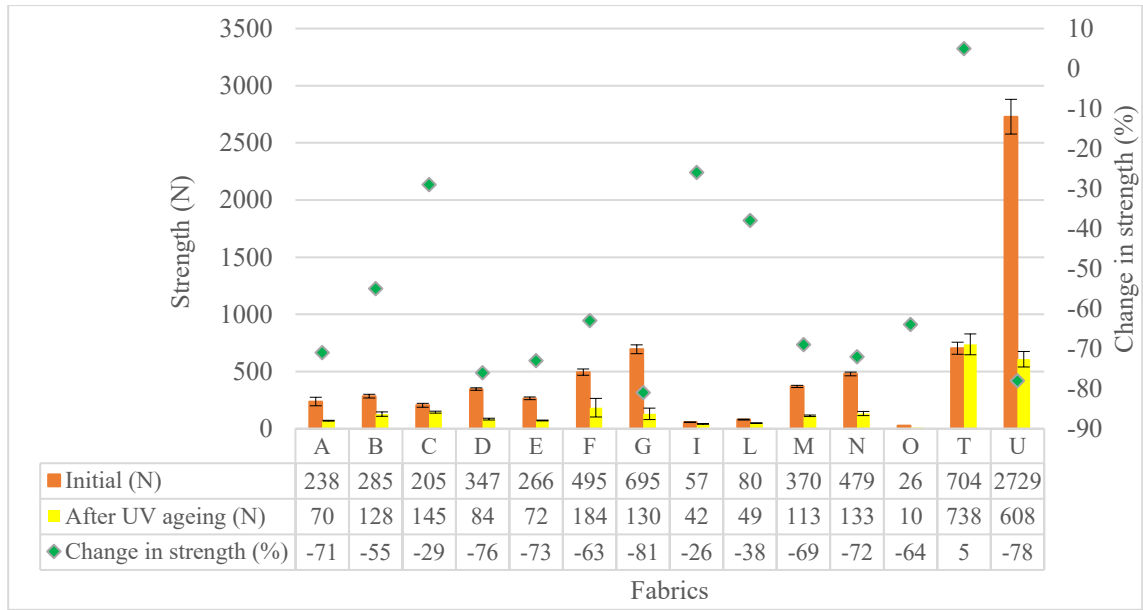


Figure 47. Average initial mechanical strength, average residual strength after photochemical ageing, and corresponding percent change in strength for all fabrics (A-O: tear strength, T-U: tensile strength).

Group 1 fabrics

The photochemical ageing behaviour of Group 1 fabrics was characterized by tear strength. The results are shown in Figure 48. This group includes Fabrics A, C and D. These fabrics consist of blends of Nomex[®] and Kevlar[®], as well as a small amount of anti-static carbon fibres in Fabric A.

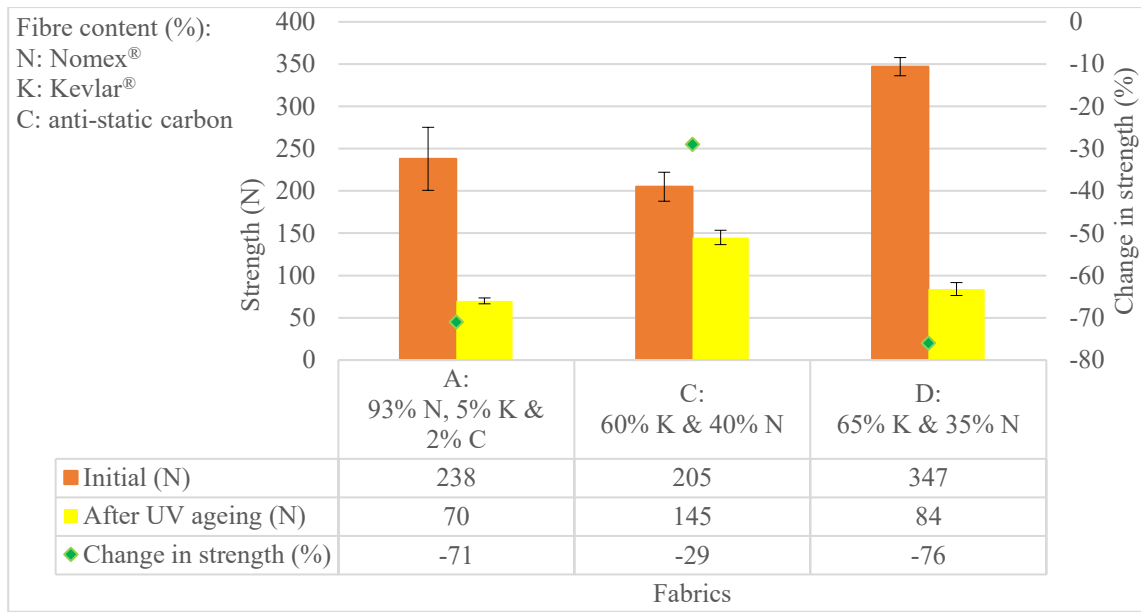


Figure 48. Average initial tear strength, average residual tear strength after photochemical ageing and corresponding percent change in tear strength for Group 1 fabrics.

The differences in tear strength measured after photochemical ageing for Fabric A, C and D are statistically significant, with p values of $< .001$ for all three fabrics. The loss in tear strength because of photochemical ageing for Fabrics A, C and D is 71, 29 and 76%, respectively. The Nomex® content in Fabric A is 93% while it is 40% and 35% for Fabric C and D, respectively.

Published studies have shown that fabrics with a higher Nomex® content tend to be more susceptible to photodegradation compared to fabrics containing a high content of Kevlar®. This has been attributed to the fact that Nomex® fibres have a small skin area with limited difference between the structure of the skin and the core (Houshyar et al., 2018). On the other hand, Kevlar® fibres present a skin-core structure with a high crystalline core and a less ordered skin. As a result, Kevlar® is less susceptible to photodegradation in comparison to Nomex® because the chemical degradation happens more easily in disordered regions and para aramids

have small polymer fraction (Dobbe et al, 1977, as cited in Nazaré et al., 2012). The enol form of the amide group in para aramids increases the conjugation and delocalization of absorbed energy and renders them to be more resistant to photodegradation in comparison to meta aramids (Carlsson et al., 1975, as cited in Nazaré et al., 2012). It is important to note that UV irradiation has a negative effect on the aramid polymer chain structure and leads to chain cleavage and surface deterioration (Houshyar et al., 2018).

In terms of the effect of UV ageing on Nomex[®], a UV ageing treatment was carried out on the Nomex[®] side of a firefighter protective clothing moisture barrier composed of an expanded polytetrafluoroethylene (e-PTFE) membrane laminated to a Nomex[®] fabric (El Aidani et al., 2013). The ageing treatment involved various temperatures: 50, 70 and 80 °C, with different fluorescent UV light intensities ranging between 0.35 to 1.35 W/m² at a wavelength of 340 nm for several ageing times up to 400 h. Chemical modifications occur in the polymer networks when exposed to UV irradiation, these modifications include crosslinking, chain scission, the formation of free radicals and functional groups. These structural changes result in an alteration in the mechanical properties and morphology of the material. The first 200 h of UV ageing at 80 °C with an intensity of 1 W/m² led the membrane to suffer from a rapid decrease in tear strength. By the time the ageing reached 250 and 300 h, the specimens only retained about 30% of their original strength. This decrease was related to a reduction observed in the molecular weight and the glass transition temperature, and changes in the fabric morphology. The authors observed an increase in the crystallinity of the Nomex[®] fibres with the increase in ageing time. This was attributed to the fact that chain scission shortened the polymer lengths, and within the amorphous regions eventually allowed for crystallization of the shorter polymer chains in these areas. Although they thought the increase

in crystallinity should lead to an improvement in the mechanical properties, the chain scission and decrease in the polymer chain lengths caused a reduction in the molecular weight, which was identified as the reason for the decline in the mechanical properties. Additionally, scanning electron microscope (SEM) was used to analyze the changes in the surface morphology of the Nomex[®] fibres before and after ageing. The UV irradiation affected the surface of the Nomex[®] fibres, with a transition from smooth to rough, as well as the formation of cracks, holes and broken fibres. The authors also observed broken fibres, which eventually caused the deterioration in the mechanical performance.

In a study by Gu (2005), Kevlar[®] filaments were subjected to UV irradiation using a UV lamp emitting light with a wavelength ranging between 315 and 400 nm (intensity not provided by the author) for a time duration of 1 to 6 h. Data analysis was conducted to look at the effect of accelerated UV ageing on their tensile strength. The filaments had an initial strength of 38 cN. After 6 h of UV irradiation, microcracks appeared on the surface of the filaments which displayed a residual strength of about 33 cN. The strength decreased further as the ageing time increased.

The effect of accelerated UV ageing on the mechanical properties of a 60/40% Kevlar[®]/PBI blend fabric was assessed after exposure to UV ageing in a Q-LAB QUV Accelerated Weathering Tester with an irradiance intensity ranging between 0.35 to 1.55 W/m² at a wavelength of 340 nm for 4 to 35 days with variable temperatures: 50, 60, 70 and 80 °C (Arrieta et al., 2011a). A loss in tensile strength of around 50% was reported after the longest duration of exposure at all temperatures. At 80 °C for 300 h and intensity of 0.68 W/m², the breaking force of yarns dropped from 34 N to 21 N which equals to a loss in tensile strength by

38%. The loss in strength was attributed to the photodegradation of Kevlar[®], wherein light induced an oxidation reaction in the fibre and led to the cleavage of the amide bond.

Another study on a fabric similar to Fabric A in terms of fibre content involved the measurement of tear strength and tensile strength, and the analysis of the fabric morphology after the exposure to accelerated UV ageing using a NIST SPHERE weathering device with an output intensity of 480 W/m² using a mercury arc lamp system emitting a UV wavelength between 290 and 450 nm at 50 °C and 50% RH for 66 days (Davis et al., 2010). The authors reported a tear strength loss of 43% after one day of UV ageing. The reduction in tear strength reached 80% after 7 days and 87% after 13 days. A similar behaviour was obtained for tensile strength, and the reduction was 40, 80 and 89% after 1, 7 and 13 days, respectively. After 13 days of UV ageing, the fibre surface had become rougher with around 10% of surface pitting. The fractured ends of fibres were imaged using a laser scanning confocal microscope (LSCM). While the unaged fibres showed ductile failure at the fracture surfaces, the mechanism of failure transitioned from ductile (necking) to brittle (sharp cleavage) after UV ageing. The fibre roughness, surface pitting and fractured surfaces indicate a degradation of the fibres because of UV ageing.

These different studies confirm that fabrics with a higher percentage of Nomex[®] exhibit a higher loss in mechanical performance in comparison with fabrics with a higher percentage of Kevlar[®] when undergoing the same conditions of UV ageing. Thus, the lower resistance to UV ageing of Fabric A can be linked to its higher Nomex[®] content. Fabric C and Fabric D are relatively similar regarding fibre content. However, there was a statistically significant difference in the change in tear strength between Fabrics C and D with a *p* value of <.001 (details in Appendix C- Table C17). The woven structure of Fabric C consists of staple

spun yarns (one Kevlar[®] staple spun yarn after every two Kevlar[®]/Nomex[®] staple spun yarn). On the other hand, Fabric D is woven with staple spun yarns and filament yarns (one Kevlar[®] filament yarn after every four Kevlar[®]/Nomex[®] staple spun yarns in the woven structure). The higher strength exhibited by Fabric D before ageing is related to the filament yarns used in this fabric. Less force was required to tear Fabric C (no filament yarns) compared to the higher load needed to tear Fabric D (20% filament yarns). Figure 49 shows the differences in the tearing behaviour for the two fabrics before and after photochemical ageing. Before ageing (Figure 49 (c)), Fabric D has an initial tearing curve that continues to rise over the test and indicates the sharing of the force by adjacent yarns during the test. However, this behaviour changed after ageing, with individual yarns breaking as the tearing force moved through the fabric and similar strength peaks recorded across the graph for the yarns being torn (Figure 49 (d)). On the other hand, the tearing behaviour observed on Fabric C did not change between the initial and UV-aged conditions with similar strength peaks recorded across the graph for the yarns being torn (Figure 49 (a,b)). However, after photochemical ageing, more load was required to tear Fabric C (no filament yarns) compared to the lower load needed to tear Fabric D. Therefore, it can be hypothesized that the better tearing resistance exhibited by Fabric C is linked to the Kevlar[®] staple spun yarns breaking after every two Kevlar[®]/Nomex[®] staple spun yarns in the woven structure rather than one Kevlar[®] filament yarn every four Kevlar[®]/Nomex[®] staple spun yarns in Fabric D woven structure, which caused Fabric C to exhibit a higher tearing resistance.

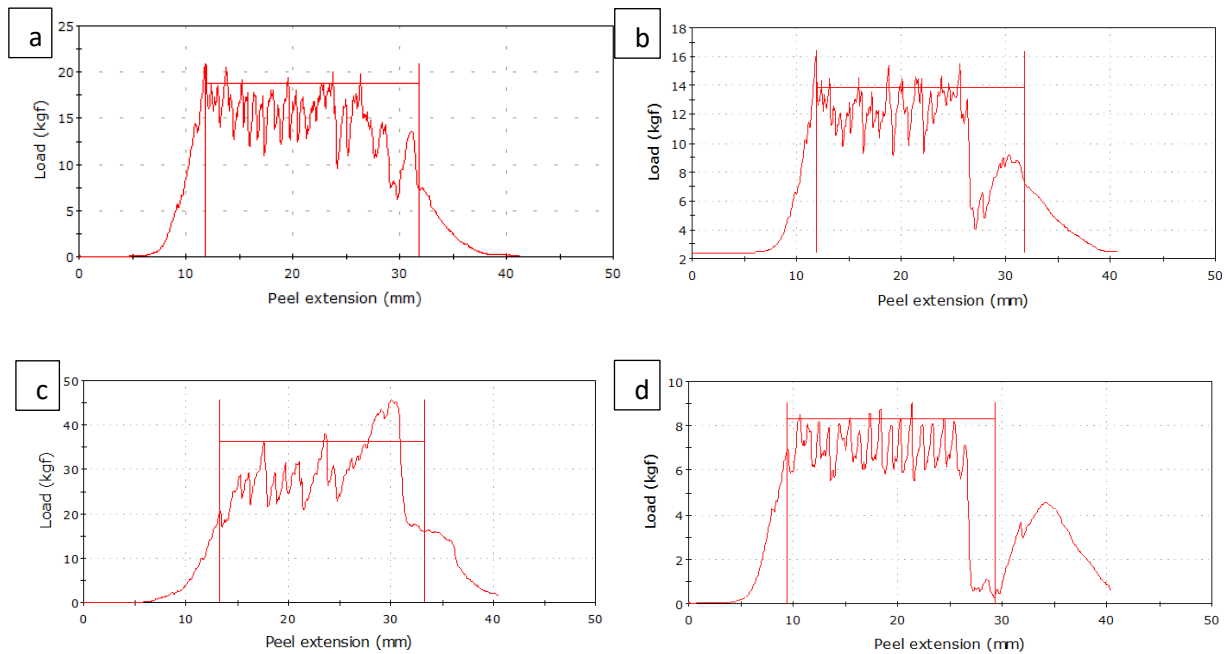


Figure 49. Tearing behaviour of specimens taken from: Fabric C (a: initial, b: photochemically -aged), Fabric D (c: initial, d: photochemically -aged).

Data from previous works support the findings of this study regarding the fact that fabrics with a high percentage of Nomex[®] are more susceptible to photodegradation and exhibit a higher loss in mechanical performance in comparison with fabrics with a high percentage of Kevlar[®], although both fibres are degraded by UV light. The results obtained in terms of the effect of photochemical exposure on the strength of Group 1 fabrics can thus be associated with their fibre content including the fibre composition and structure of select yarns in Fabrics C and D.

Group 2 fabrics

The photochemical ageing behaviour of Group 2 fabrics was characterized by tear strength. The results are shown in Figure 50. This group includes Fabrics E, F and G. These fabrics consist of blends of Kevlar[®] and PBI fibres. In the case of Fabric E, it also contains a

small amount of LCP filaments (one LCP filament yarn after every seven Kevlar[®]/PBI staple spun yarn in the woven structure).

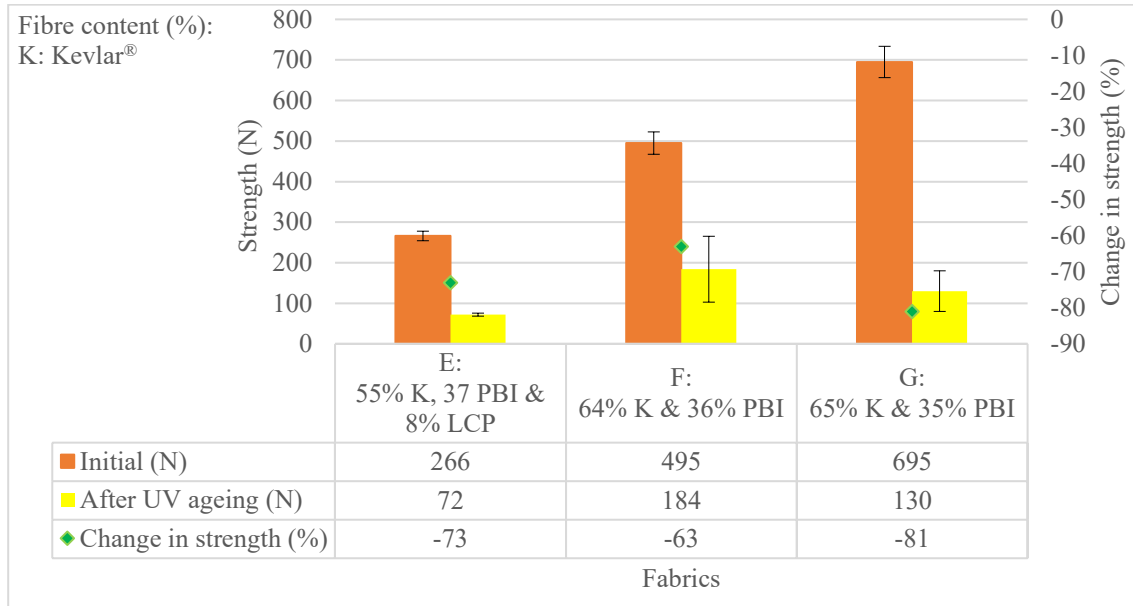


Figure 50. Average initial tear strength, average residual tear strength after photochemical ageing, and corresponding percent change in tear strength for Group 2 fabrics.

The differences in tear strength measured after photochemical ageing for Fabric E, F and G are statistically significant, with p values of $< .001$ for Fabrics E, F and G. The loss in strength because of photochemical ageing for the three fabrics is 73, 63 and 81%, respectively. The content of Kevlar[®] and PBI is 55 and 37%, respectively, for Fabric E. It is 64 and 36%, respectively, for Fabric F. And it is 65 and 35%, respectively, for Fabric G.

The effect of UV ageing on Kevlar[®] fibres has already been described in the section relative to Group 1 fabrics. PBI fibres are similar in structure to Kevlar[®] fibres with a skin-core structure with a high crystalline core and a less ordered skin (Nazaré et al., 2012). They are thus considered as fairly robust against UV irradiation (Carlsson et al., 1975, as cited in Nazaré et al., 2012). It has been also suggested that PBI fibres are resistant to photodegradation because

of the wholly aromatic, ladder-like structure (Arrieta et al., 2011a). PBI behaves similarly to Kevlar[®] when exposed to UV irradiation, hence is less sensitive to photodegradation in comparison with Nomex[®] (Houshyar et al., 2016).

A 60/40% Kevlar[®]/PBI blend fabric with a fibre content similar to Fabric F and G was subject to UV ageing using a mercury arc lamp system in NIST sphere-based weathering machine with an output intensity of 480 W/m² (between 290 and 450 nm) for up to 66 days at 50 °C and 50% RH (Davis et al., 2010). The authors reported a tear strength loss of 54% after 6 days of UV ageing. The loss increased to 70% after 14 days. The decrease in tensile strength was less severe, and the reduction was around 38 and 51% after 6 and 14 days, respectively. LSCM imaging was conducted on the fabric after 14 days of UV exposure. If the Kevlar[®] fibres suffered from surface pitting and surface roughening, fewer physical effects were observed on the UV-aged PBI fibres. The authors concluded that the PBI fibres were less affected by UV radiation and were able to maintain most of their strength.

The mechanical properties of a 60/40% Kevlar[®]/PBI blend fabric were investigated after exposure to UV ageing in a Q-LAB QUV Accelerated Weathering Tester with an irradiance intensity ranging between 0.35 to 1.55 W/m² for 4 to 35 days at variable temperatures of 50, 60, 70 and 80 °C and a wavelength of 340 nm (Arrieta et al., 2011a). The reduction in tensile strength tested on the Kevlar[®]/PBI yarns was as high as 50% after the longest duration of exposure at all temperatures. A reduction by 38% was observed after around 300 h at 80 °C at 0.68 W/m². The loss in strength was linked to the susceptibility of Kevlar[®] to photodegradation.

In a study by Brown et al. (1975), they assessed the tensile strength of a PBI fabric made of continuous filament yarns after exposure to solar radiation for 16 weeks. PBI

continuous filament strips were sealed in Pyrex ampoules with different atmospheres of oxygen, water vapour, methyl mercaptan, and under vacuum and later exposed to solar radiation. The researchers indicated that PBI is inherently photochemically stable because of its stable structure. However, in the presence of oxygen, a significant reduction in tensile strength by 60% occurs after 4 weeks. The tensile strength loss reached 90% after 16 weeks.

A 60/40% Kevlar[®]/PBI blend fabric was subjected to UV exposure in a weather-O-meter using a xenon lamp at an irradiance of 0.24 W/m² at 340 nm, a temperature of 40 °C, and a relative humidity of 50% for 1, 3, 5, and 7 days (Houshyar et al., 2016). The authors observed a change in the polymer structure because of photo-oxidation. The degradation started with chain scission leading to the generation of free radicals and resulting in the breakage of the amide backbone linkage. After 7 days of UV exposure, the fabric had experienced a reduction in tear strength and tensile strength of 84 and 45%, respectively. SEM images of the photoaged specimens revealed that the skin of the PBI fibre was the first to degrade, then cracks started to appear on the surface, and later diffused to the core. These reactions led to the production of brittle failure surfaces in the fibres after mechanical testing.

There was no statistically significant difference in the change in tear strength between Fabrics E, F and G with *p* values of >.001 (details in Appendix C- Table C17). However, in the case of Fabric E, the loss in strength can also be attributed to the presence of the LCP filaments, since LCP fibres have poor UV resistance and are believed to be more susceptible to photodegradation in comparison with aramids (Pegoretti & Traina, 2018).

Previous studies confirmed my findings about the negative effect of photochemical ageing on Kevlar[®] and PBI fibres. The results obtained in terms of the effect of photochemical exposure on the strength of Group 2 fabrics can thus be associated with their fibre content.

Group 3 fabrics

The photochemical ageing behaviour of Group 3 fabrics was characterized by tear strength. The results are shown in Figure 51. This group includes Fabrics L and O. These fabrics mainly consist of oxidized PAN and Kevlar[®] fibres. Fabric L also includes FR rayon and anti-static polyester, and Fabric O contains novoloid.

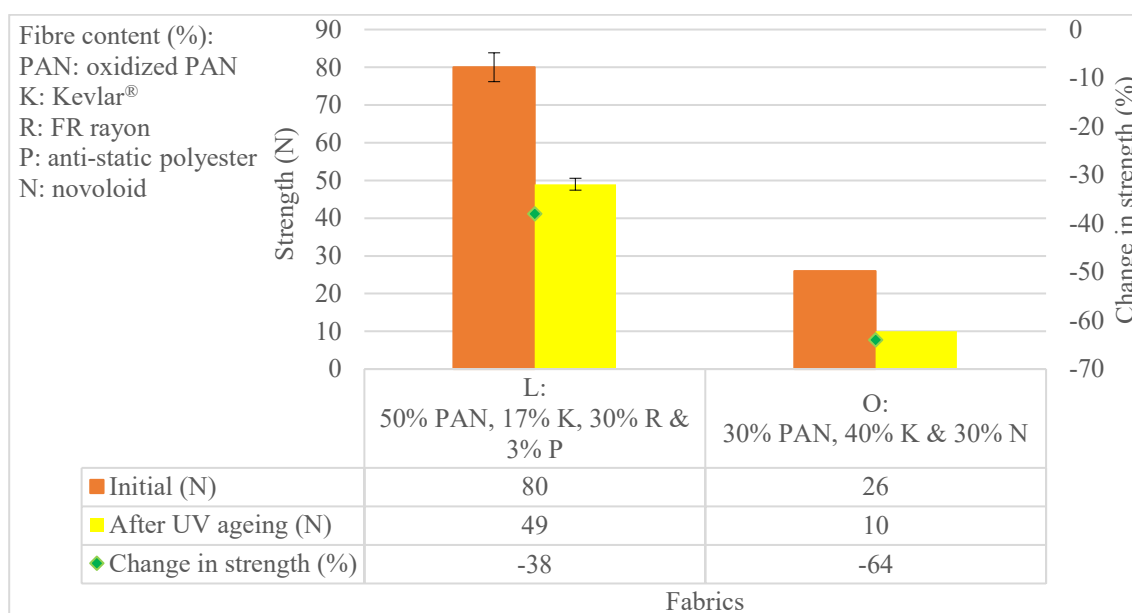


Figure 51. Average initial tear strength, average residual tear strength after photochemical ageing, and corresponding percent change in tear strength for Group 3 fabrics.

In the case of Fabric L, which consists of 50% oxidized PAN and 17% Kevlar[®], 30% FR rayon and 3% polyester, there was a statistically significant difference between the initial and the UV-aged conditions (p value < .001). On the other hand, statistical analysis was not conducted on Fabric O because only one specimen was tested. The reduction in tear strength for Fabric L and O was 38 and 64%, respectively. The photochemical ageing behaviour of

Kevlar[®] fibres has already been described in the section relative to the photochemical ageing of Group 1 fabrics.

In a study by Stephenson et al. (1961a), gaseous products such as hydrogen, methane, acrylonitrile, and hydrogen cyanide, emitted from a PAN polymer (Acrylan) after UV treatment were analyzed. PAN samples were sealed in quartz tubes in an inert atmosphere and underwent UV irradiation using a mercury-arc lamp at 253.7 nm for 200 h. Such gases are by-products of reactions like chain scission and crosslinking in the polymer backbone. However, PAN fibres are considered more resistant to UV ageing in comparison with some other polymers such as PET, nylon 66, and polyethylene. Another study looked at the tensile strength of Acrylan PAN fibres after exposure to UV treatment using a mercury-arc lamp at 253.7 nm (Stephenson et al., 1961b). The fibres were subjected to UV ageing in vacuum and nitrogen atmosphere. A quick change in the colour of the fibre was detected, but there was no change observed in the fibre surface. The degradation was more rapid in the case of the nitrogen atmosphere in comparison with the vacuum. The authors concluded that PAN maintains its tensile strength after exposure to a high dosage of UV light and performs better than most polymers.

In another study, a carbon filament was exposed to UV irradiation using UV lamp over a 315 to 400 nm wavelength range for an ageing time between 1 to 6 h (Gu, 2005). The carbon filament experienced a decrease in tensile strength. The initial tensile strength of the filament was 16 cN, and the residual strength after 6 h of UV treatment was around 12 cN. The author attributed it to the fact that the UV rays have enough energy to break the main C-C bond in the carbon fibres. SEM images revealed a change in the fibre structure. For instance, grooves seemed to flatten on the surface of the filament, and some parts broke away leaving much wider

grooves. This study points toward a breakage of the carbon bond, followed by a reduction in the molecular weight, which will eventually lead PAN fibres to exhibit lower mechanical properties after UV exposure. But no information is provided by the author on the irradiance used in the experiments.

For its part, Fabric L, which consists of PAN, Kevlar[®], FR rayon and anti-static polyester in ratios of 50, 17, 30 and 3%, respectively, exhibited a loss in strength of 38%. This change in strength with UV exposure can be attributed to the blend of fibres including regenerated cellulose fibres. In the case of FR rayon, UV resistance is similar to other cellulosic fibres describe later under Group 5 fabrics.

Fabric O includes 30% of novoloid in addition to oxidized PAN and Kevlar[®] fibres. Novoloid is considered to be UV resistant according to FiberLine (n.d.). Other sources such as the Polymer Properties Database (n.d.) referred to novoloid as a fibre with good UV stability because of its high degree of aromaticity and its three-dimensional cross-linked structure. Yet, it may not be as UV resistant as oxidized PAN and Kevlar[®] fibres as Fabric O seems to have experienced a larger reduction in strength compared to Fabric L.

In conclusion, the presence of PAN and Kevlar[®] fibres appeared to positively affect the resistance to photochemical ageing of Group 3 fabrics.

Group 4 fabrics

The photochemical ageing behaviour of Group 4 was characterized by tear strength. The results are shown in Figure 52. This group includes Fabrics B and N. These fabrics consist of PBO fibres, blended with para- and meta-aramid fibres in the case of Fabric B.

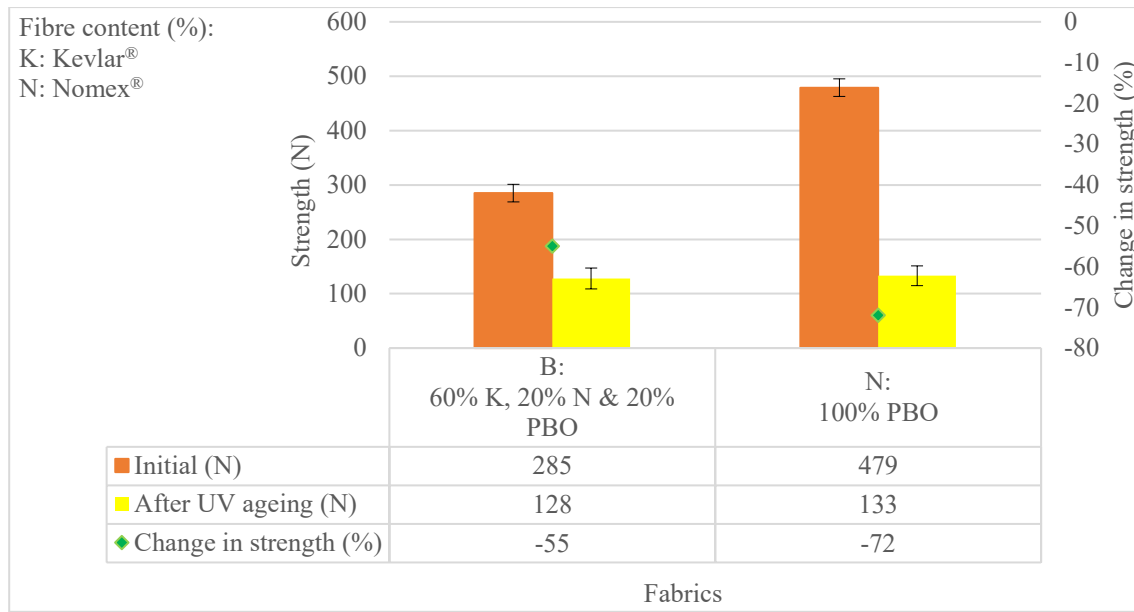


Figure 52. Average initial tear strength, average residual tear strength after photochemical ageing, and corresponding percent change in tear strength for Group 4 fabrics.

The differences in tear strength measured after photochemical ageing for both Fabric B and N are statistically significant, with p values of $< .001$. The reduction in tear strength for Fabric B and Fabric N is 55 and 72%, respectively. The PBO content is 20% for Fabric B, and 100% for Fabric N.

The ageing behaviour of meta- and para-aramid fibres, which are present in Fabric B, has already been described in the section relative to the photochemical ageing of Group 1 fabrics. In a study by Walsh et al. (2006), PBO fibres were exposed to UV radiation in a Weather-Ometer using a xenon-arc lamp to simulate natural sunlight at an intensity of 750 W/m² and 50 °C. SEM images revealed a disruption in the fibre surface orientation and the loss of small bits from the shell of the fibre. The damage was attributed to the degradation of PBO through several reactions: 1) the alteration of the polymer backbone chemical structure; 2) the disordering of the oxazole ring and later rearrangement to form an amide linkage; 3) chain

scission; and/or, 4) crosslinking. The degradation of the polymer also resulted in a loss of strength. The researchers noted a reduction in tensile strength starting after 100 h of UV exposure and reaching a loss of 40% after 300 h (Walsh et al., 2006).

Another study looked at the UV ageing behaviour of Zylon[®] fibres in the dark and using laboratory lighting (Niu et al., 2018). Four different spools of Zylon[®] strands were aged under lab light (in transparent plastic bags) for 270 days and compared to the same strands aged without light (using black bags). There was no variation in strength for the Zylon[®] aged in the dark: the strands were able to maintain their tensile strength after 8 years. On the other hand, Zylon[®] strands aged under laboratory light suffered a loss in tensile strength by 37% after six months and 44% after seven months. The researchers reported a degradation of the PBO fibres, with the re-arrangement of the molecular chain, the growth of the amorphous region, and the formation of debris and defects on the surface of the fibres.

Both fabrics in Group 4 experienced a reduction in tear strength after photochemical ageing. These results are in line with previous studies regarding the sensitivity of PBO and aramid fibres to UV light.

Group 5 fabrics

The photochemical ageing behaviour of Group 5 fabrics was characterized by tear strength. The results are shown in Figure 53. Fabrics I and M are included in this group. These fabrics are cellulose-based. Fabric I is treated with an FR finish and consists of 63% cotton, 34% polyester, and 3% EOL (XLANCE[®]). Fabric M is 100% FR viscose.

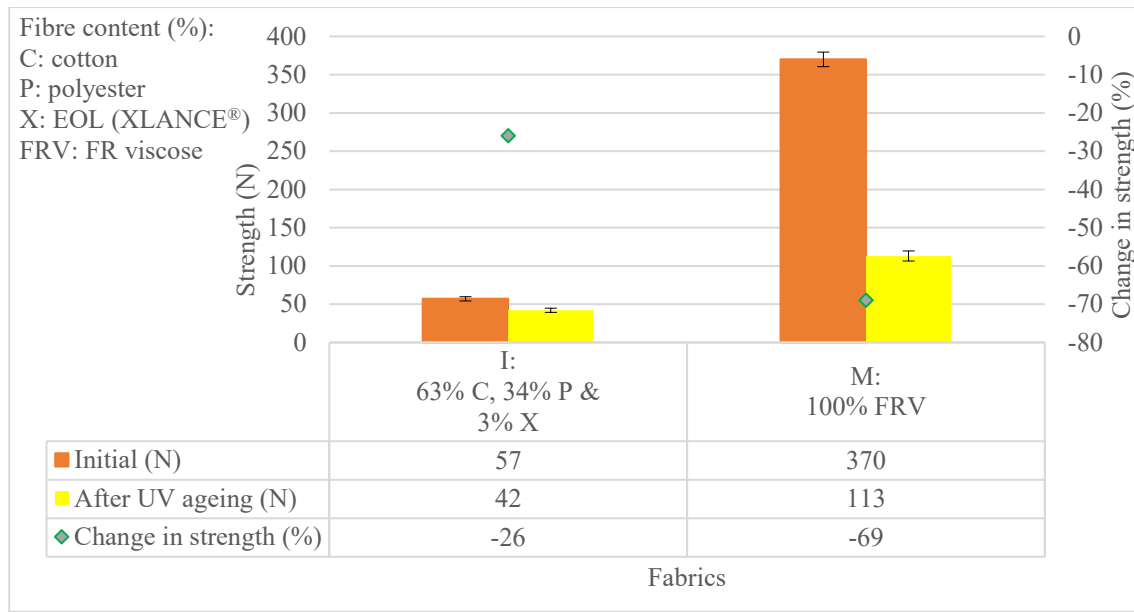


Figure 53. Average initial tear strength, average residual tear strength after photochemical ageing, and corresponding percent change in tear strength for Group 5 fabrics.

The photochemical ageing triggered a loss in tear strength by 26 and 69% for Fabric I and M, respectively. There was a statistically significant difference in tear strength between the initial and UV aged conditions for Fabric I and M, with p values of $< .001$ for both fabrics.

Cellulose-based fabrics do not absorb near UV light and are not prone to photodegradation (Tucker et al., 1980). However, they are damaged through photosensitization. Impurities, delustering additives, and dyestuff might exist in the fabric and absorbs light, and hence cause a chemical reaction between excited molecules and cellulose molecules and cause the breakage of the cellulose chain. In contrast, a study by Rowell & Stout (2007) revealed that cellulose-based fabrics can suffer from photodegradation (Rowell & Stout, 2007). The chemical structure of a cellulose polymer consists of a long chain of repeated molecular patterns that are joined together through glycosidic ether linkages (Fynn & Dean, 1951). UV light of sufficient energy may attack and break the linkages leading to shorter molecular chains. Cotton

is almost entirely composed of cellulose. This structure gives cotton its fibrous qualities. However, UV irradiation alters the chemical structure of cotton, changing its fibrous qualities and reducing its strength.

A study photoaged bleached cotton print cloth using a Weather-Ometer with a xenon arc lamp for 1, 3 and 6 days (Yatagai & Zeronian, 1994). The researchers applied a 2 h cycle with 102 min of light at 41 °C and 18 min dark at 25 °C. Quartz filters were used on the Xenon lamp which allowed UV wavelengths as low as 190 nm to be included in the light exposure. This allowed for photolytic degradation of the cotton cellulose through the absorption of radiation of 260 nm. The mechanical performance was evaluated through tensile strength tests. The authors reported a tensile strength retention of 90% after 1 day, 71% after 3 days and 39% after 6 days. The tensile strength loss was attributed to DP reduction (Yatagai & Zeronian, 1994). The test conditions for my work included UV in the range of 300 to 400 nm and would not have caused photolysis of the cotton cellulose as occurred in this study.

In the case of polyester, a study subjected bright fibres to outdoor exposure and compared it with exposure behind a glass window (Fung, 2000). It took 3.7 months for the fibres to lose 50% of their strength under outdoor exposure and 24 months to reach the same level when exposed to light behind glass window. The presence of photometal ions in polyester fibres because of delustering additives are thought to contribute to its sensitivity to UV light and to initiate oxidative reactions (Gupta, 2005; King, 2012). However, the loss is dependant on the amount of delustering additives existing in the fibres, therefore, less delustering additives means higher resistance to photodegradation (Tucker et al., 1980).

Fabric I is a dark fabric, and hence the loss in strength can be attributed to the presence of dyestuffs and pigments in the fabric. In terms of the regenerated cellulose fibres

used in Fabric M, SEM images of UV aged viscose rayon fabric (70% viscose from bamboo, 25% cotton, and 5% spandex) showed the development of small, dark speckled areas on some fibres (Brinsko et al., 2016). It was found that these freckle areas might be internal air or gas pocket. The information found regarding the fact that cellulose-based fabrics are prone to photodegradation (Rowell & Stout, 2007) may also apply.

Looking at previous studies and the results from my study, we can conclude that cellulose-based fabrics offer moderate resistance to UV irradiation.

Group 6 fabrics

Other fabrics were included in this study. For instance, Fabrics T and U. The photochemical ageing behaviour of Group 6 fabrics was characterized by tensile strength. The results are shown in Figure 54. Fabric T is made of fibreglass and Fabric U is 100% LCP.

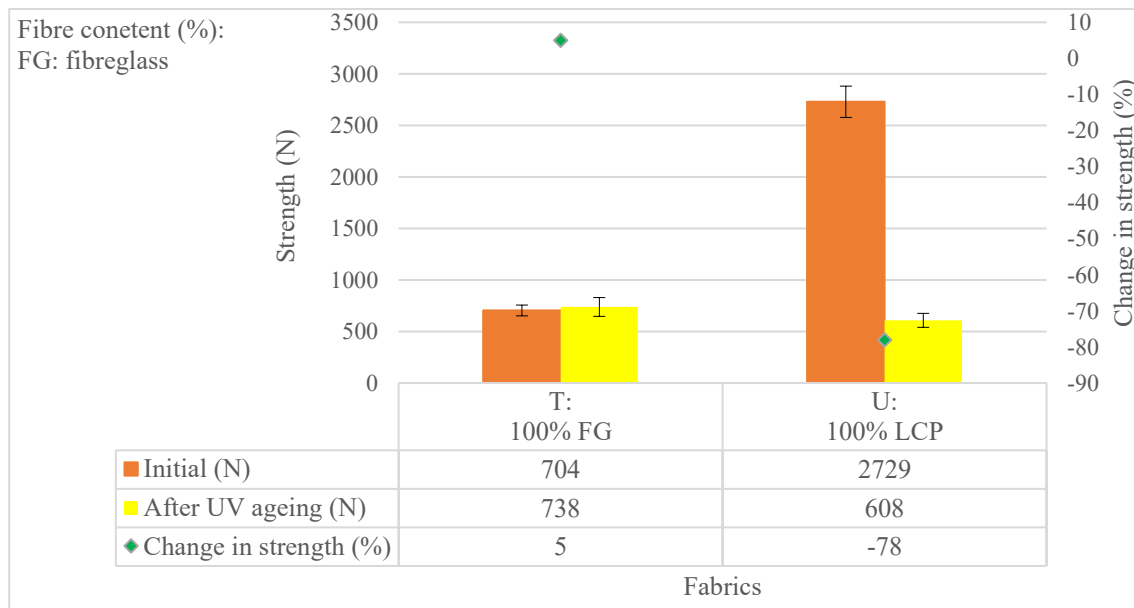


Figure 54. Average initial tensile strength, average tensile strength after photochemical ageing, and corresponding percent change in tensile strength for Fabrics T and U.

In the case of Fabric T, there was no significant change in tensile strength (p value of .491). The loss in strength for Fabric U because of UV exposure is 78%. This loss is statistically significant with a p value of $< .001$.

A previous study conducted with E-glass filaments measured the residual tensile strength after exposure to UV irradiation between 315 and 400 nm (intensity not provided by the author) for a time ranging from 1 to 6 h (Gu, 2005). The original tensile strength of a single glass filament was 19 cN. The author reported that 1 h of UV treatment was enough to have a significantly damaging effect on the fibre, leading to a residual strength of around 15 cN. After 5 h of UV ageing, the residual tensile strength was around 7 cN. The author attributed this decrease in mechanical performance with UV ageing to the fact that glass has several bonds that could be susceptible to photodegradation and breakage. The filaments showed micro-cracks on their surface. These findings seem to indicate that UV irradiation affects glass fibres. However, since the author did not report the value of irradiance used, it is not possible to compare these results with my findings.

In the conditions used in my study, the fibreglass fabric appears to resist photodegradation.

In the case of LCP fibres, contradicting information was found in the research literature. Exposing LCP fibres to sunlight is reported to lead to a quick degradation (Sloan, 2017). After prolonged UV exposure, LCP fibres do not maintain their minimum performance criteria. Nevertheless, the degradation of LCP-based fabrics is dependant on different variables such as the fabric's weave and count, yarn's twist level, size, diameter, and if there are any finishes or coatings. It has been mentioned that LCP fibres are more susceptible to photodegradation than aramids (Pegoretti & Traina, 2018). According to Kuraray (2014),

exposing a rope of LCP fibres with a diameter of 6 mm a 12x1 braid configuration to simulated sunlight using a xenon-arc lamp leads to a tenacity retention of almost 70% after over 600 h. Likewise, aramids showed a similar trend by retaining around 80% of their tenacity. On the other hand, single-end 1500 denier LCP fibres exposed to simulated sunlight using a carbon-arc lamp exhibited a tenacity retention by almost 20% after 500 h. However, aramids showed a tenacity retention of around 55% under the same conditions. In contrast, a study conducted by NASA showed no difference in the UV resistance of LCP and Kevlar 49 (Fette & Sovinski, 2004).

Findings from previous studies support the result obtained from this study that UV light causes the photodegradation of LCP fabrics.

4.2.3. Effect of accelerated hydrothermal ageing on the mechanical strength of the tested fabrics

The strength (tear or tensile depending on the fabric) of the hydrothermally aged specimens was measured after 15, 24 and 31 days at 80°C and compared to what had been obtained for the unaged specimens. The objective was to characterize the effect of accelerated hydrothermal ageing on this important mechanical property. Figure 55 shows the strength values before and after ageing as well as the corresponding change in mechanical strength for all of the fabrics tested. Differences in behaviour can be observed between the different fabrics. Some fabrics exhibited a similar slight decrease in strength, while a few others demonstrated a severe decrease in strength as a result of ageing, however, several fabrics were not affected. The effect of hydrothermal ageing on the mechanical strength of the fabrics is discussed separately for the six fabric groups identified in Table 6.

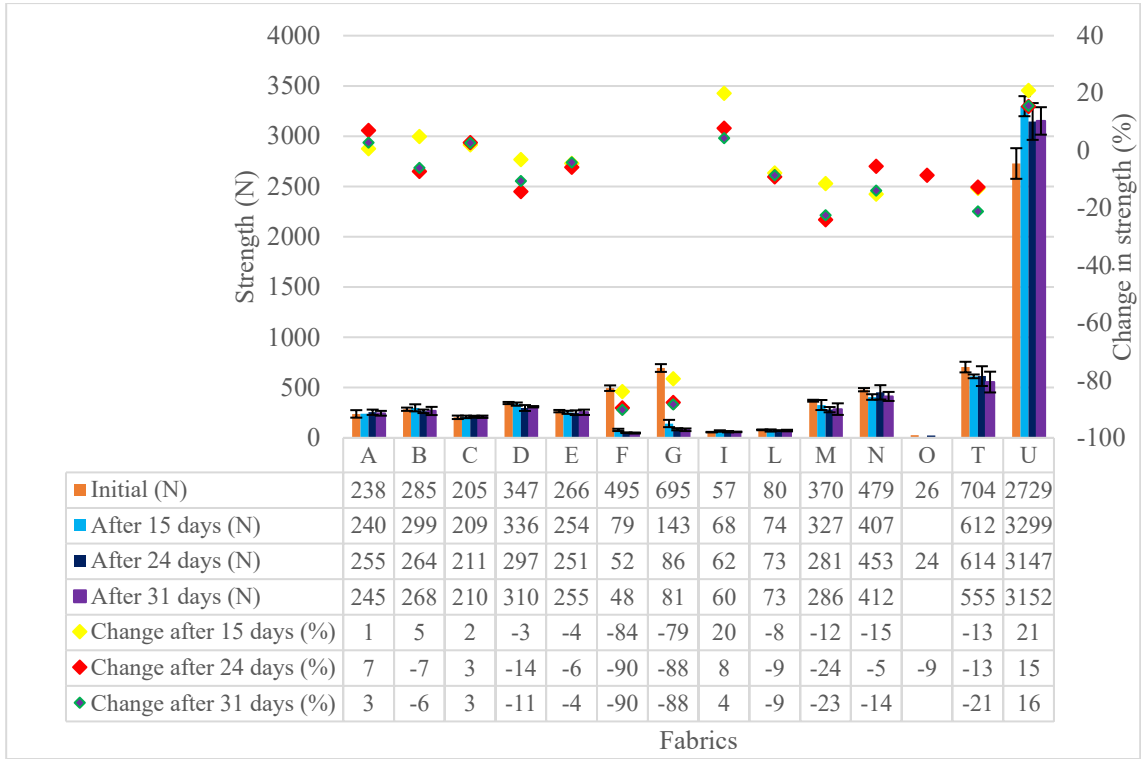


Figure 55. Average initial mechanical strength, average residual mechanical strength after 15, 24 and 31 days of hydrothermal ageing at 80 °C, and corresponding percent change in mechanical strength for all fabrics (A-O: tear strength, T-U: tensile strength).

Group 1 fabrics

The hydrothermal ageing behaviour of Group 1 fabrics was characterized by tear strength. The results are shown in Figure 56. This group includes Fabrics A, C and D. These fabrics consist of blends of Nomex[®] and Kevlar[®], as well as a small amount of anti-static carbon fibres in Fabric A.

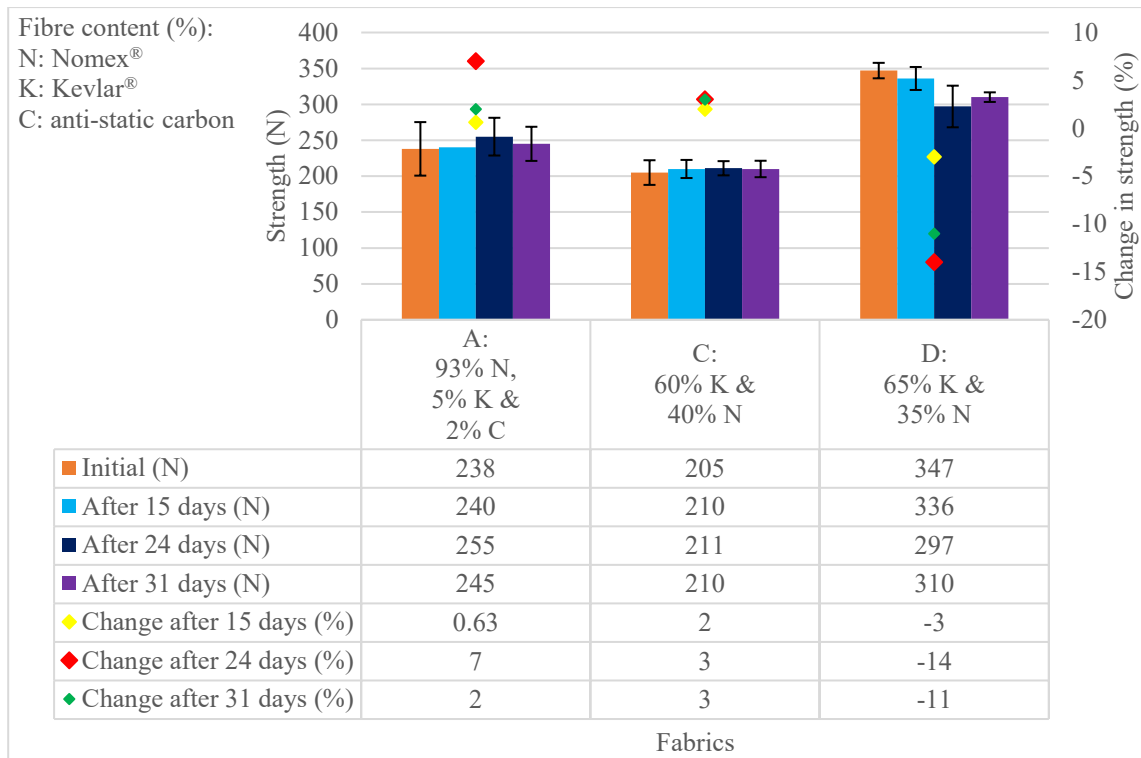


Figure 56. Average initial tear strength, average residual tear strength after 15, 24 and 31 days of hydrothermal ageing at 80 °C, and corresponding percent change in tear strength for Group 1 fabrics.

The differences in tear strength measured after hydrothermal ageing for 15, 24 and 31 days for Fabric A and C are not statistically significant, with p values $> .05$. In the case of Fabric D, the change in tear strength is not statistically significant after 15 days (p value of .248), however, it is statistically significant after 24 and 31 days with p values of .037 and .001, respectively (details in Appendix D).

The tensile strength of Kevlar[®] 129 fibres was looked at in a study where the fibres were subjected to hydrothermal ageing through immersion in DI water at different temperatures: 60, 70, 80 and 90 °C for 12 weeks (Li et al., 2012). After 12 weeks of ageing at 60 °C and 70 °C, the tensile strength retention of the fibres was 59 and 62%, respectively. In

the case of ageing at 80 °C for 2, 4, 8 and 12 weeks, the tensile strength retention was 90, 73, 47 and 41%, respectively. Besides, the tensile strength retention was only 32% at 90 °C after 12 weeks. Furthermore, the authors reported a decrease in strength as the temperature and time of exposure increased. An investigation of the crystalline structure showed some recrystallization and a slight increase in crystallinity because of Kevlar[®] fibre hydrolysis. FTIR analysis pointed towards the chain scission of the amide bonds. The fibres became brittle with the formation of microfibrils and cracks. The hydrolysis reaction was observed to happen at the core of the fibre rather than in the skin, with the skin suffering less deterioration than the core even though the skin has more contact area with water than the core. This behaviour was attributed to the Kevlar[®] fibre's unique core-skin structure. On the contrary, other authors have mentioned that the interactions between the amide bonds and water molecules are restricted to the polymer chains on the surface of the fibre since the water molecules do not enter the cell of the crystalline lattice (Shubha et al., 1993). On the other hand, Nomex[®] fibre's structure is different from Kevlar[®], wherein it has a small skin area with limited difference between the structure of the skin and the core (Houshyar et al., 2018). Therefore, the degradation reaches the core more easily.

Another study about a 60/40% Kevlar[®]/PBI blend fabric involved the measurement of tensile strength after the fabric was hydrothermally aged in an environmental chamber at three different temperatures: 50, 60 and 80 °C, with two levels of RH - 60 and 80% - for times ranging between 4 and 31 days (Arrieta et al., 2011a). A reduction in tensile strength of 50% occurred after 31 days at 80 °C, and this loss was associated with the degradation of Kevlar[®] triggered by exposure to moisture. The authors reported that the temperature alone did not have an effect on the mechanical properties of the fabric but, when combined with moisture,

degradation seemed to accelerate, leading to an increase in the loss in tensile strength. The moisture absorption of Kevlar[®] fibres showed a linear relationship with relative humidity. FTIR analysis was carried out on specimens aged at 60 °C with 80% RH for 4 and 12 days. It showed that the hydrolysis reaction affected the amide bonds in the Kevlar[®] fibres. Since Kevlar[®] fibres are spun in a sulfuric acid solution, traces of this solution are thought to remain in the fibres and act as a catalyst for the hydrolysis reaction; this will cause chain scission and the production of amine groups and carboxylic acid.

Another study of Nomex[®] 410 paper undergoing hydrothermal ageing was conducted in an oven at 180 °C for 168, 504 and 672 h with two levels of RH -10 and 70%- (Li et al., 2019b). The authors verified that the hydrolysis reaction consists of chain breakage, leading to the formation of polar groups.

According to DuPont (2019), exposure of Nomex[®] staple spun yarn or filament yarns to DI water at 99 °C for 10 h leaves no effect on the strength of the yarns. Moreover, exposure of Kevlar[®] filament yarns to water at 65°C for more than 200 days leaves no effect on their strength (DuPont, 2017). With this in mind, it can be concluded that both Nomex[®] and Kevlar[®] have similar resistance to hydrolysis. In contrast, others have suggested that fabrics with higher Kevlar[®] content are more susceptible to hydrolysis compared to fabrics with higher Nomex[®] content (Dolez & Malajati, 2020). The hydrogen bonds in Kevlar[®] might break when exposed to water and not be able to reform easily when dry due to its rigid polymer chains and stiff phenylene rings. On the other hand, Nomex[®] has a more flexible structure with an irregular chain conformation which allows it to reform easily (Dolez & Malajati, 2020).

It was expected for Fabric C and D to perform similarly because of the similarity in fibre content. However, there was a difference in behaviour between the two fabrics after 24

and 31 days. Close examination of the fabrics of Group 1 after hydrothermal ageing showed that all yarns in all three fabrics broke while tearing (Figure 57). This makes it difficult to explain the difference in results between Fabric C and Fabric D. However, the slight loss in strength in Fabric D was statistically significant only after 24 and 31 days of hydrothermal ageing.

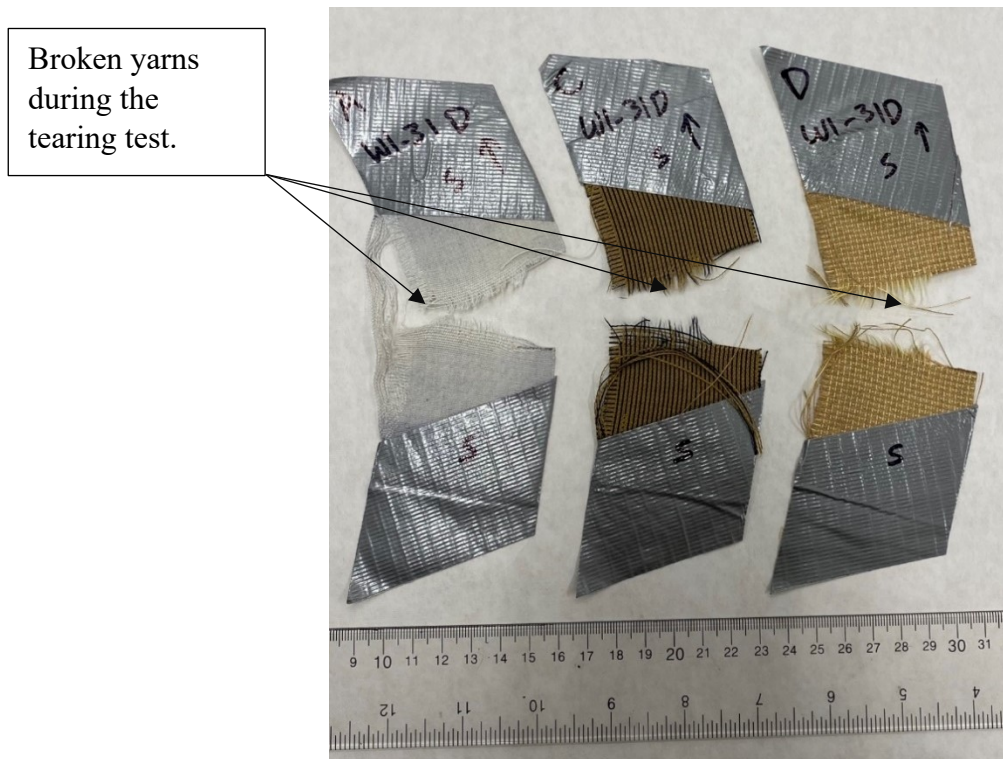


Figure 57. Hydrothermally aged specimens (31 days) from Fabric A, B and C after tearing.

Looking at the data from previous studies, some have suggested that hydrothermal ageing is more likely to affect Kevlar[®] compared to Nomex[®] fibres, however, others suggested that it leaves a similar effect on both fibre types. Therefore, according to the results from this study, it can be concluded that hydrothermal ageing at 80 °C for up to 31 days does not appear to have a severe effect on the strength of Nomex[®] and Kevlar[®] fibres.

Group 2 fabrics

The hydrothermal ageing behaviour of Group 2 fabrics was characterized by tear strength. The results are shown in Figure 58. This group includes Fabrics E, F and G. These fabrics consist of blends of Kevlar[®] and PBI fibres. In the case of Fabric E, it contains a small amount of LCP filaments (one LCP filament yarn after every seven Kevlar[®]/PBI staple spun yarn in the woven structure).

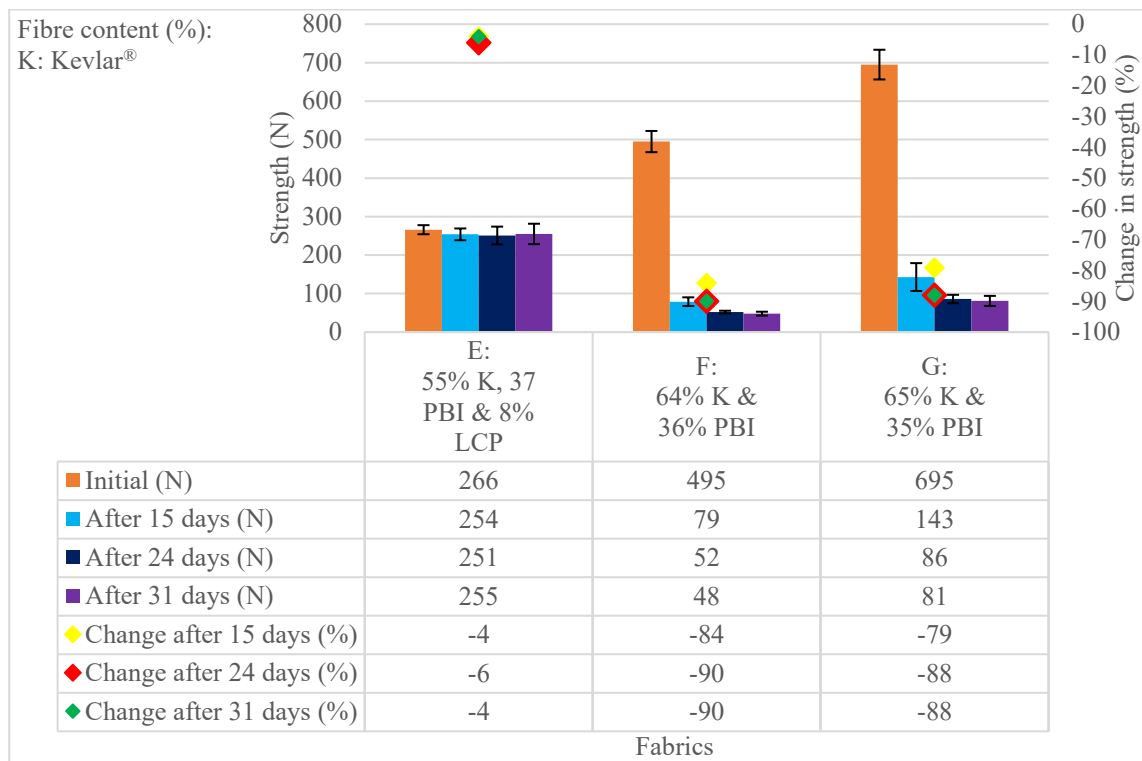


Figure 58. Average initial tear strength, average residual tear strength after 15, 24 and 31 days of hydrothermal ageing at 80 °C, and corresponding percent change in tear strength for Group 2 fabrics.

In the case of Fabric E, which consists of 55% Kevlar[®], 37% PBI, and 8% LCP, there was no change in tear strength after 15, 24 and 31 days with *p* values of .207, .218 and .416, respectively. On the other hand, there was a statistically significant difference in tear strength between the initial and hydrothermally-aged conditions after 15, 24 and 31 days for

Fabric F and G with p values of $<.001$ for the two fabrics (details in Appendix D). The loss in tear strength after immersion in water for 15, 24 and 31 days was 84, 90 and 90%, respectively, for Fabric F. It was 79, 88 and 88%, respectively, for Fabric G. The similar behaviour of Fabrics F and G can be attributed to the fact that these two fabrics have a similar fibre content: with 64% Kevlar[®] and 36% PBI for Fabric F, and 65% Kevlar[®] and 35% PBI for Fabric G.

The effect of hydrothermal ageing on Kevlar[®] fibres has already been described in the section relative to Group 1 fabrics. In the case of PBI fibres, they have a high moisture regain of 15% at 20 °C and 65% RH (Horrocks et al., 2001). This high-water uptake is associated with water molecules bonding to the PBI polymer (Brooks et al., 1993). On the other hand, because of the completely aromatic, ladder-like structure of PBI fibres, it is expected to have exceptional thermal and chemical stability. Therefore, PBI fibres are believed to be resistant to hydrolytic ageing (Arrieta et al., 2011a).

The tensile strength of PBI polymer samples was assessed after exposure to two hydrothermal ageing treatments. First, by immersing specimens in DI water for 7 days at 60 °C, and second, by exposing specimens to a hot water treatment at 288 °C for 2 days in a turbulent steam environment (Liu et al., 2016). Since PBI is known to be prone to moisture absorption, samples were dried before conducting the water immersion experiment. The authors used two drying procedures: first, at 90 °C for 7 days to reduce future thermally induced degradation, second, at 150 °C for 3 days to remove moisture and speed up the drying procedure. The dried samples had an initial tensile strength of 87 MPa. After water immersion at 60 °C for 7 days, the tensile strength was 65 MPa. After 2 days of the 288 °C hot water treatment, the tensile strength was 69 MPa. The fractured surface showed flaws such as cracks and air bubbles, which were associated with the degradation of PBI triggered by the hot water

treatment. Water causes major swelling in PBI, which has a severe effect on its mechanical behaviour. This is because water molecules interact strongly with the hydrophilic groups in PBI, contributing to a reorganization of the intermolecular hydrogen bonding between the polar groups in the PBI network. The presence of moisture triggers the deterioration of the material. The reduction of the material's mechanical properties can be attributed to hydrolysis, swelling, crosslinking, and morphological changes (Liu et al., 2016). Lastly, the researchers concluded that water is able to initiate the deterioration of PBI only when combined with a high temperature. The decrease in tensile strength increased as both moisture content and temperature increased.

In another study, a rip-stop weave fabric, which consisted of 60/40% Kevlar[®]/PBI blend with similar fibre content as Fabric F and G and an initial tear strength of 81 N, was exposed to a temperature of 50 °C with 50% RH for a time up to 56 days in NIST sphere-based weathering device (Nazaré et al., 2012). After the longest exposure time of 56 days, no significant change in tear strength was recorded. Arrieta et al. (2011a), who studied the effect of hydrothermal ageing on a 60/40% Kevlar[®]/PBI blend fabric in an environmental chamber at different temperatures, reported a reduction in tensile strength of 50% after 31 days at 80 °C. In my study, a reduction of 90 and 88% occurred in Fabric F and G after 31 days of ageing at 80 °C. These fabrics are relatively similar in fibre content to the 60/40% Kevlar[®]/PBI blend fabric of the Arrieta et al. (2011a) study.

In the case of Fabric E, hydrothermal ageing did not affect the fabric like the other two fabrics. The woven structure of Fabric E consists of one LCP filament yarn after every seven Kevlar[®]/PBI staple spun yarn in the woven structure. On the other hand, Fabric F and G woven structure consist of one Kevlar[®] filament yarn every two Kevlar[®]/PBI staple spun yarn.

This better performance exhibited by Fabric E can be linked to the presence of the LCP filaments yarns. In fact, LCP is hydrophobic and shows a near-zero water moisture regain (Sloan, 2017). Moreover, closer examination showed that the Kevlar®/PBI staple spun yarns in Fabric E were affected by the hydrothermal ageing just like what happened with yarns in Fabrics F and G, whereas the LCP filaments were not. Moreover, when the tearing test was performed on Fabric E, the Kevlar®/PBI staple spun yarns broke, yet the filaments did not break but rather slipped from the fabric structure which essentially maximized the residual tear strength (see Figure 59).

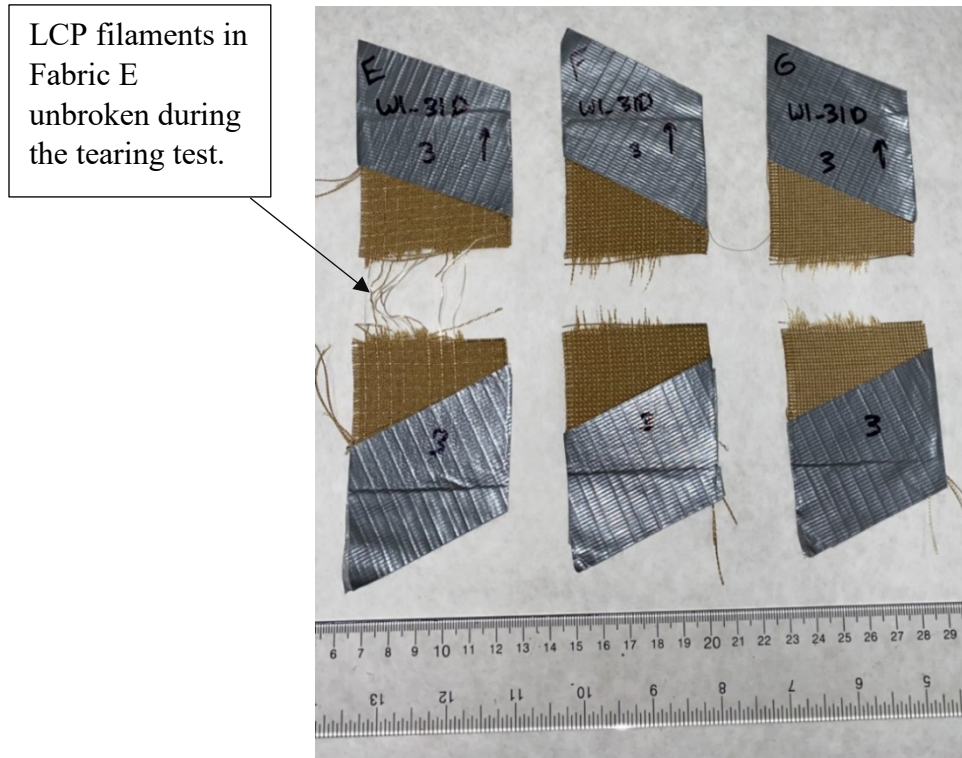


Figure 59. Hydrothermally aged specimens (31 days) from Fabric E, F and G after tearing.

Looking at previous studies and the results from my study, we can conclude that both Kevlar® and PBI fibres undergo hydrolysis when exposed to moisture and heat for

extended periods of time. This conclusion regarding the hydrothermal aging behavior observed with the fabrics of Group 2 appears to contradict the results obtained for Group 1 fabrics, where there was very little to no effect of hydrothermal aging. No explanation has been found so far for this apparent discrepancy.

Group 3 fabrics

The hydrothermal ageing behaviour of Group 3 fabrics was characterized by tear strength. The results are shown in Figure 60. This group includes Fabrics L and O. These fabrics mainly consist of oxidized PAN and Kevlar[®] fibres. Fabric L also includes FR rayon and anti-static polyester. Fabric O contains novoloid.

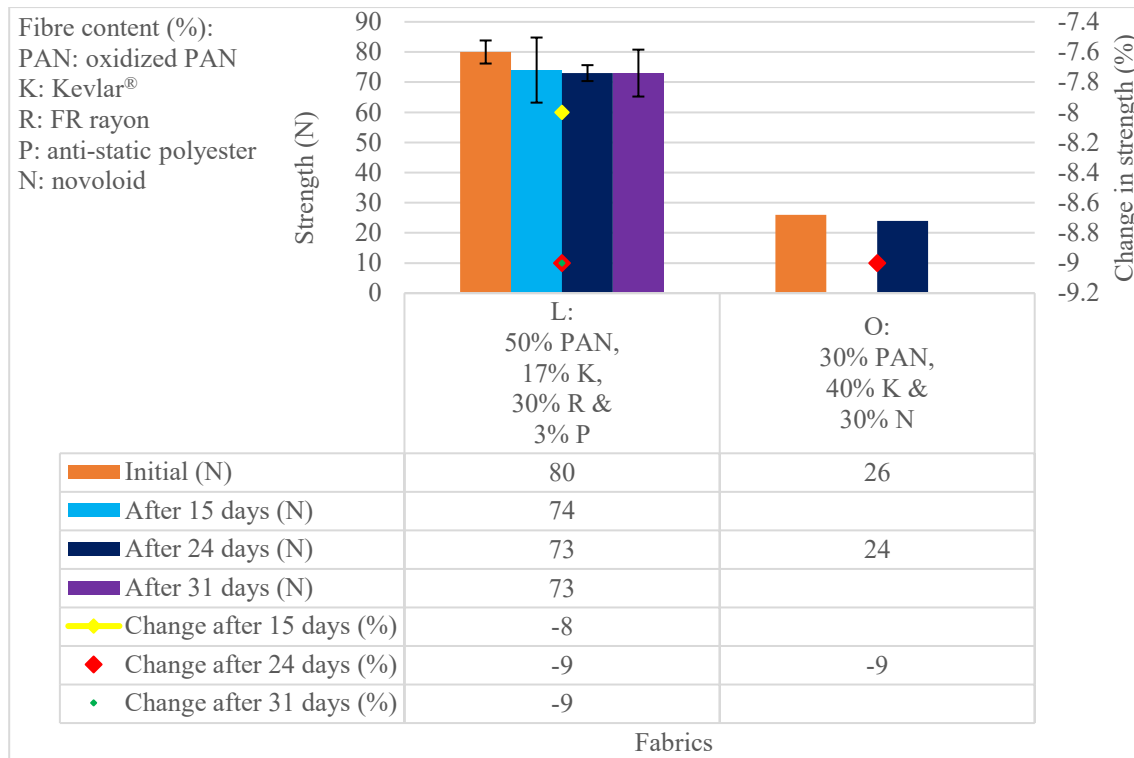


Figure 60. Average initial tear strength, average residual tear strength after 15, 24 and 31 days of hydrothermal ageing at 80 °C, and corresponding percent change in tear strength for Group 3 fabrics.

The change in tear strength for Fabric L was not statistically significant after 15 and 31 days with p values of .257 and .115, respectively. However, it was statistically significant after 24 days with a p value of .008 (details in Appendix D). On the other hand, Fabric O demonstrated a minor decrease in tear strength by 9% after 24 days of hydrothermal ageing, however, statistical analysis was not conducted on this fabric since only one specimen was tested.

The effect of hydrothermal ageing on Kevlar® fibres has already been described in the section relative to Group 1 fabrics. Regarding PAN, no study on the hydrothermal ageing of PAN fibres alone was identified in the literature. Only results for PAN fibres embedded into

polymer matrices were found. For example, a study looked at the change in mechanical properties of a carbon fibre/polycarbonate (CF/PC) composite after immersion in DI water at 80 °C for 100 and 400 h (Tanaka et al., 2013). After 400 h, the CF/PC composite exhibited a decrease in tensile strength and modulus because of the disappearance of the resin. In general, it is believed that carbon fibres have remarkable high moisture resistance (Song et al., 2017b).

Very limited information has been found also on the effect of hydrothermal ageing conditions on the other components of the Group 3 fabrics. Polyester has no wicking ability and has a low moisture regain between 0.4 and 0.8% (Bendak & El-Marsafi, 1991). Thus, the moisture does not get absorbed in the fibres and stays on their surface. Moreover, the poor water absorbency of polyester fibres and their ability to be packed tightly prevent water penetration (Deopura & Padaki, 2015). Rayon is a hygroscopic fibre (Senthil Kumar & Suganya, 2017). It is even more moisture absorbent than cotton. And cellulose-based fibres have been shown to be susceptible to hydrolysis (Testa et al., 1994). Finally, novoloid fibres have a moisture regain of 6% at 20 °C and 65% RH (Horrocks et al., 2001). But no information has been found on their susceptibility to water.

Fabric L may have been protected by the presence of polyester. Regarding Fabric O, not enough experimental data and background information exist to help draw conclusions on its hydrothermal ageing behaviour.

Group 4 fabrics

The hydrothermal ageing behaviour of Group 4 fabrics was characterized by tear strength. The results are shown in Figure 61. This group includes Fabrics B and N. These fabrics consist of PBO fibres, blended with para- and meta-aramid fibres in the case of Fabric B.

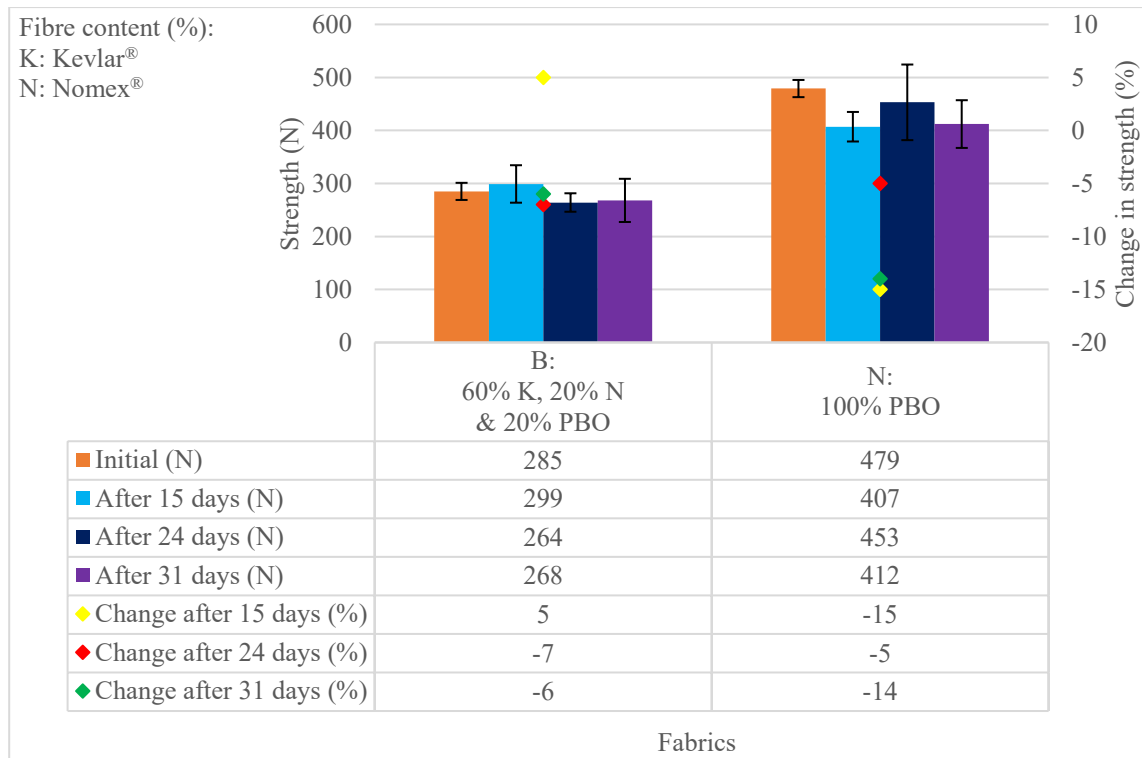


Figure 61. Average initial tear strength, average residual tear strength after 15, 24 and 31 days of hydrothermal ageing at 80 °C, and corresponding percent change in tear strength for Group 4 fabrics.

The differences in tear strength measured after hydrothermal ageing for 15, 24 and 31 days for Fabric B are not statistically significant with p values of .449, .232 and .403, respectively. In the case of Fabric N, there was a statistically significant difference in tear strength between the initial and hydrothermally-aged conditions after 15 and 31 days with p values of .001 and .014, respectively. However, the change in strength after 24 days was not statistically significant with a p value of .445 (details in Appendix D).

The effect of hydrothermal ageing on Kevlar® and Nomex® fibres have already been described in the section relative to Group 1 fabrics. Regarding PBO, a study looked at the mechanical and morphology changes in PBO yarns obtained from hydrothermally aged ballistic

panels used in body armours (Chin et al., 2007). The panels were aged in an environmental chamber at 50 °C and 60% RH for 84 days followed by another treatment at 60 °C with 37% RH for an additional 73 days, and later stored in a chamber for 332 days at 25 °C with 5% RH. The strength decreased from an initial value of 4.8 GPa to 3.64 GPa after 84 days at 50 °C and 60% RH. When the conditions changed to 60 °C and 37% RH for the next 73 days, there was a further loss in tensile strength by 40%, with a drop to 3.08 GPa, however, storing for 332 days at 25 °C with 5% RH initiated a loss in strength less than 4%. Another experiment was conducted by sealing PBO fibres in a tube and placing them in an oven at 55 °C to see if the small amount of residual moisture contained in the PBO fibres would initiate degradation or not. Only a slight decrease in tensile strength by 4% occurred after 210 days, which led the researchers to conclude that the moisture normally contained in PBO fibres does not initiate degradation. Moreover, no opening of the benzoxazole ring was observed which indicated that inherent moisture in PBO does not cause degradation. According to Chin et al. (2007), exposure to high relative humidity was thought to generate a hydrolysis reaction in PBO fibres, involving the breakdown of the structure, opening of the benzoxazole rings, and formation of carboxylic acid and leading to a decrease in the polymer molecular weight. The hydrolysis of the benzamide group shifted the structure from rigid-rod to a polyamide-type, with a reduction in strength. Atomic force microscopy (AFM) revealed how the surface of the fibre changed from being smooth (unaged) to rough (aged) which confirmed the degradation because of hydrothermal ageing. After the initial opening of the oxazole ring and the formation of the new structure similar to but not the same as para-aramid, the hydrothermal ageing ultimately led to complete breakage of the polymer chain (Hart, 2005). A technical datasheet by Toyobo (2005) revealed that AS (as spun) and HM Zylon fibres have a moisture regain of 2.0 and 0.6%, respectively, which is lower compared to aramids (around 4.5%).

The difference in behaviour between these previous studies and my results, which did not show any significant effect of hydrothermal ageing on the mechanical performance of PBO-based fabrics, may be attributed to differences in the duration of the ageing treatment as well as the fact that the ageing protocol in my study involved immersing the specimens in water.

Group 5 fabrics

The hydrothermal ageing behaviour of Group 5 fabrics was characterized by tear strength. The results are shown in Figure 62. This group includes Fabrics I and M. These fabrics are cellulose-based. Fabric I is treated with an FR finish and consists of 63% cotton, 34% polyester, and 3% EOL (XLANCE®). Fabric M is 100% FR viscose.

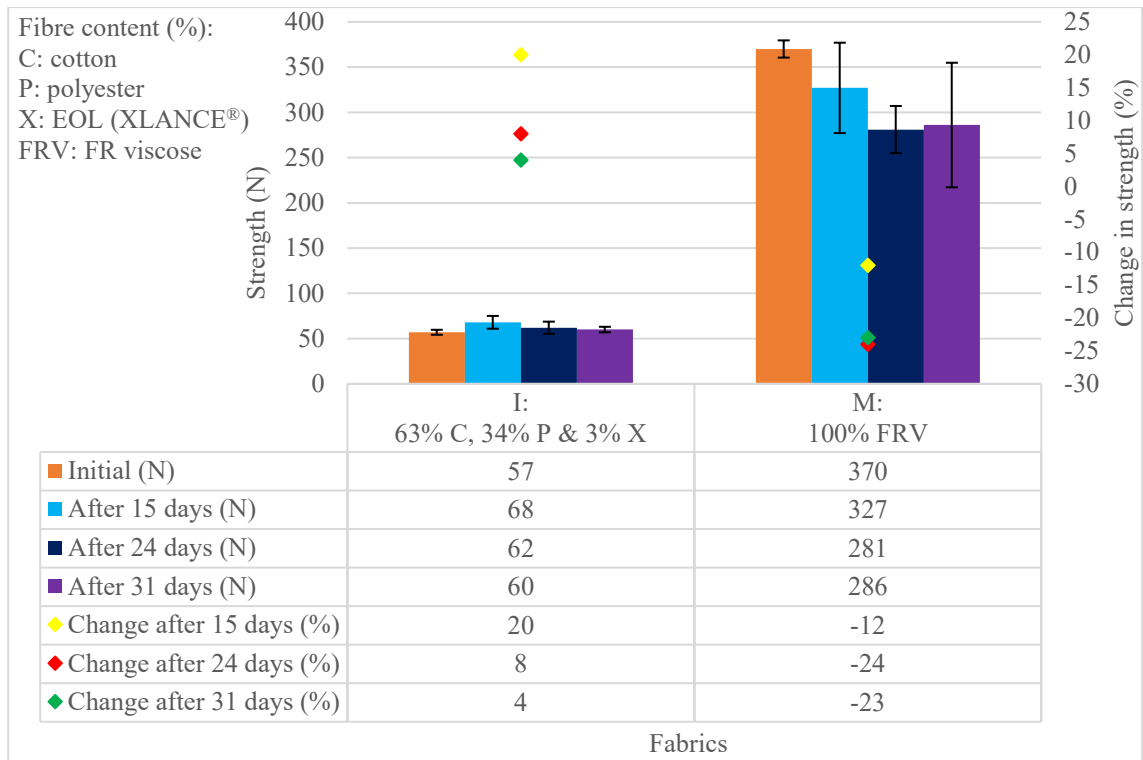


Figure 62. Average initial tear strength, average residual tear strength after 15, 24 and 31 days of hydrothermal ageing at 80 °C, and corresponding percent change in tear strength for Group 5 fabrics.

For Fabric I, the effect of hydrothermal ageing on tear strength measured after 15 days, an increase in strength, is statistically significant, with a p value of .010. No statistically significant change in tear strength was recorded after 24 and 31 days (p values of .209 and .218, respectively). On the other hand, the difference in tear strength measured for Fabric M after hydrothermal ageing for 15 days is not statistically significant (p value of .100) while it is statistically significant after 24 and 31 days with p values of $< .001$ and .014, respectively (details in Appendix D).

Cotton fibres are porous and hydrophilic, and when immersed in water, they swell and the internal pores of fibres get filled with water (Wakelyn et al., 2007). Furthermore, cotton

fibres have a high-water absorbency because of the high number of polar -OH groups in their chemical structure (Song et al., 2017b). Cotton has been shown to be sensitive to hydrolytic ageing, with chain scission in the cellulose molecule (Testa et al., 1994). Regenerated cellulose fibres are also hygroscopic and more moisture absorbent than cotton (Senthil Kumar & Suganya, 2017). Viscose rayon fibres have a very high water absorbency of 100%, swell and suffer from shrinkage when they are wet (Wakelyn et al., 2007).

In terms of the other fibres found in Group 5 fabrics, polyester is hydrophobic with low moisture regain of 0.4% (Deopura & Padaki, 2015). However, it is subject to hydrolytic ageing because of the presence of the hydrolysis-sensitive ester groups leading to chain scission (Bellenger et al., 1995).

Looking at the results from my study, the cellulose-based fabrics included in Group 5 did not appear to be strongly affected by the hydrothermal ageing treatment applied here.

Group 6 fabrics

Other fabrics were included in this study. For instance, Fabrics T and U. The hydrothermal ageing behaviour of Group 6 fabrics was characterized by tensile strength. The results are shown in Figure 63. Fabric T is made of fibreglass and Fabric U is 100% LCP.

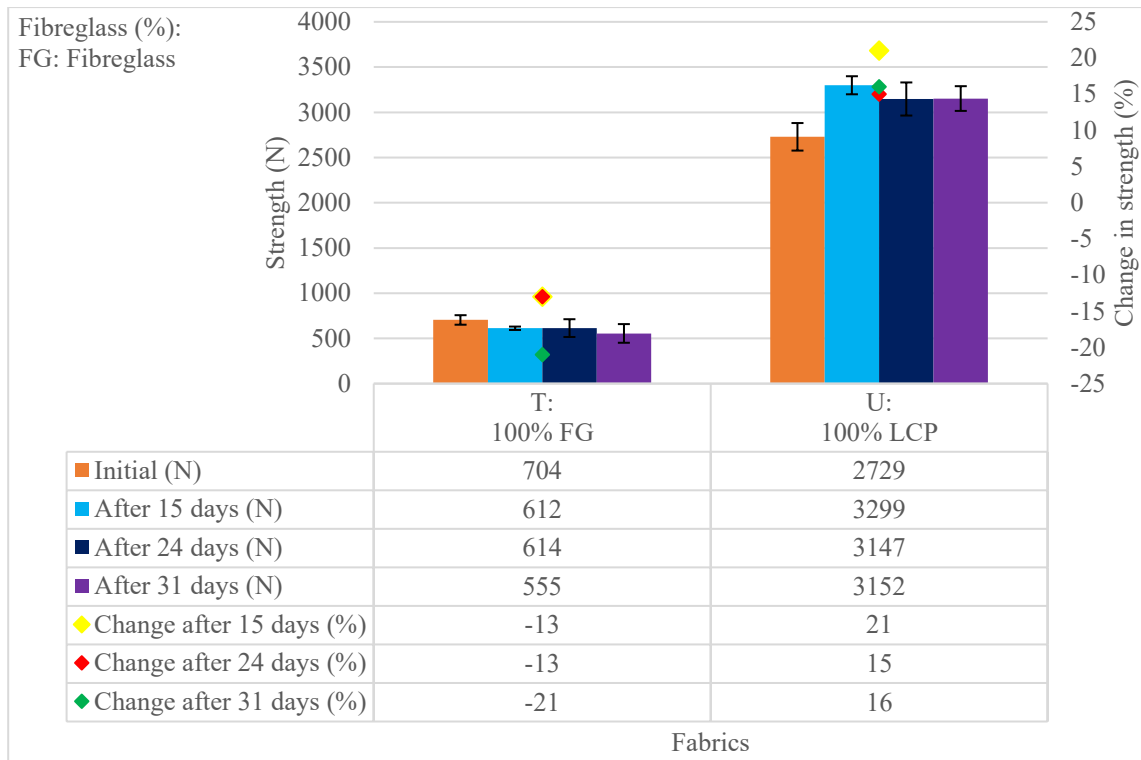


Figure 63. Average initial tensile strength, average residual tensile strength after 15, 24 and 31 days of hydrothermal ageing at 80 °C, and corresponding percent change in tensile strength for Fabric T and Fabric U.

The difference in tensile strength between the initial and hydrothermally-aged conditions of Fabric T was statistically significant after 15 and 31 days with p values of .006 and .021, respectively. However, the change in strength was not statistically significant after 24 days with a p value of .109. On the other hand, Fabric U exhibited a statistically significant change in tensile strength after hydrothermal ageing, with an increase by 21, 15 and 16% between the initial and the 15, 24 and 31 days of hydrothermally-aged conditions with p values of $< .001$, .004 and .002, respectively (details in Appendix D).

Static fatigue determines the lifetime of E-glass fibres (Jones & Huff, 2009). However, the presence of moisture combined with load can reduce their lifetime. Static fatigue

degradation occurs in three stages: the first stage is the growth of cracks, the second stage is the reaction between the load and environment, which leads to the increase in the crack growth rate. At the third stage, stress has less effect on the crack growth, hence, more load is required to initiate more cracks. In a study by Aveston et al. (1980), the authors characterized the effect of moisture on the stress corrosion of E-glass fibres in two conditions: ambient atmosphere and immersed in DI water. They found the reduction in tensile strength was more rapid when the fibres were exposed to atmospheric moisture compared to when they were immersed in water. Moisture caused the weakening of the fibres through crack growth initiation. Finally, Khazanov et al. (1995) reported that water contributes to the depolymerization of glass fibres' surface layers. This will lead to the breakage of the hydrogen bonds and cause a dihydroxylation reaction on the surface. On the other hand, silica fibres are included in the “first hydrolytic class” of materials, hence have a high-water resistance (Khazanov et al., 1995).

Not many studies about the effect of hydrothermal ageing on glass fibres were identified. However, what was found supports the results of my study that glass fibres resist hydrothermal ageing when immersed in water.

Some studies exist on the hydrolytic behaviour of LCP fibres. LCP fibres are hydrolytically stable and show near-zero equilibrium moisture absorption, similar to other polyester-based fibres, which are hydrophobic (Sloan, 2017). Dry LCP fabrics, under atmospheric conditions, accumulate less than 0.1% of moisture (Pegoretti & Traina, 2018). This very low equilibrium moisture content is an advantage of LCP fibres compared with aramids (Sloan, 2017). For instance, LCP fibres did not exhibit any decrease in mechanical strength after 1 month of water immersion at 50 °C (Pegoretti & Traina, 2018).

Another study has looked at the effect of water immersion on the tensile strength of LCP fibres at different temperatures: 40, 60, 80 and 100 °C for 30 days (Abu Obaid et al., 2015). Until 60 °C, LCP fibres demonstrated no change in tenacity. A decrease in tenacity of 6% was measured after 30 days at 80 °C. It reached 12% at 100 °C. Since there was no sign of chemical degradation or thermal oxidation, the researchers tentatively attributed this small decrease in strength to disturbances in the molecular structure of the LCP fibres. On a molecular level, the ester linkages in the chemical structure of LCP fibres did not form hydrogen bonds with water, thus reducing the potential of hydrothermal ageing.

My results for Fabric U agreed with previous studies that show good resistance to the hydrothermal ageing for LCP fabrics.

4.2.4. Effect of accelerated laundering on the mechanical strength of the tested fabrics

The strength (tear or tensile depending on the fabric) of the laundered specimens was measured after 10 accelerated laundering cycles and compared to what had been obtained for the unaged specimens. The objective was to characterize the effect of accelerated laundering on this important mechanical property. Figure 64 shows the strength values before and after ageing as well as the corresponding change in mechanical strength for all the fabrics tested. No data are included for Fabric M. Since Fabric M did not survive thermal ageing, it was decided not to subject it to the laundering treatment. Differences in behaviour can be observed between the fabrics. Some fabrics exhibited a more or less modest decrease in strength as a result of laundering, while the exposure to 10 laundering cycles did not seem to affect the strength of

others. The effect of accelerated laundering on the mechanical strength of the fabrics is discussed separately for the six fabric groups identified in Table 6.

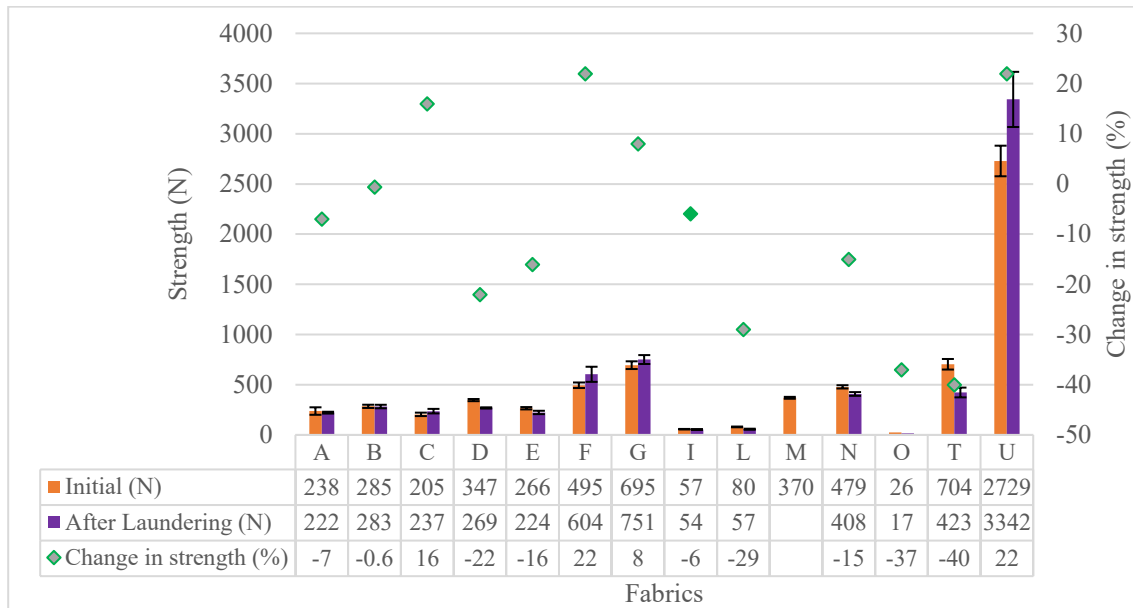


Figure 64. Average initial mechanical strength, average residual mechanical strength after 10 laundering cycles, and corresponding percent change in mechanical strength for all fabrics (A-O: tear strength, T-U: tensile strength).

Group 1 fabrics

The ageing behaviour of Group 1 fabrics after 10 laundering cycles was characterized by tear strength. The results are shown in Figure 65. This group includes Fabrics A, C and D. These fabrics consist of blends of Nomex[®] and Kevlar[®], as well as a small amount of anti-static carbon fibres in Fabric A.

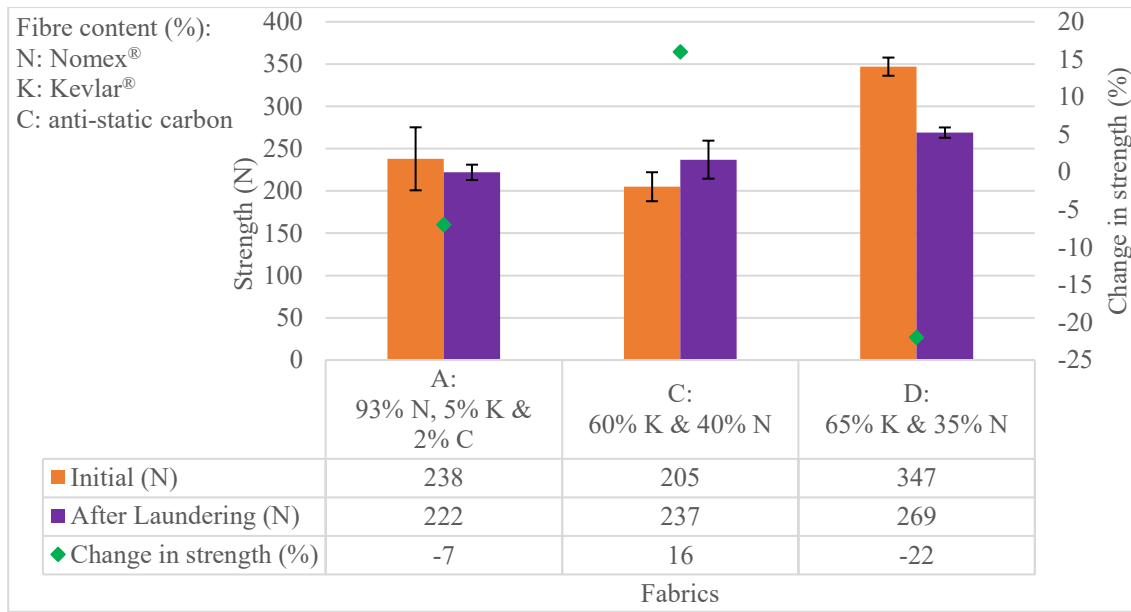


Figure 65. Average initial tear strength, average residual tear strength after 10 laundering cycles, and corresponding percent change in tear strength for Group 1 fabrics.

In the case of Fabric A, no statistically significant change in tear strength occurred (p value of .496). On the other hand, the change in tear strength for Fabric C and D is statistically significant with p values of .035 and $< .001$, respectively. Fabric C experienced a 16% increase in strength whereas Fabric D experienced a decrease of 22%. Fabric A has a very high content of Nomex of 93% whereas it is 40 and 35% for Fabric C and Fabric D, respectively.

The results obtained here can be compared with previously reported findings on the effect of repeated laundering on fire protective fabrics. A collection of seven FR fabrics typically used as outer shell in firefighter protective clothing were subjected to up to 50 washing/drying cycles at 60 °C and their tear strength was assessed after 10, 20, 35, and 50 cycles (Dolez & Malajati, 2020). A 100% Nomex[®] fabric retained almost all of its tear strength after 50 washing/drying cycles whereas a 100% Kevlar[®] fabric exhibited a 58% loss. On the

other hand, a fabric similar to Fabric A in terms of fibre content (Fabric #2) experienced an 11% loss in strength after it was subjected to 50 laundering cycles. This behaviour was linked to the high Nomex[®] fibre content of the fabric, since the meta-aramid molecule, with the phenylene and amide units in a meta configuration, has an irregular chain conformation and a more flexible structure than in Kevlar[®] which has rigid polymer chains and stiff phenylene rings. However, a fabric similar to Fabric C in terms of fibre content (Fabric #3) which contains 60% Kevlar[®], the authors reported a reduction in tear strength by 35% after 50 washing/drying cycles, which increased with the number of the laundering cycles. This effect was associated with the sensitivity to hydrolysis of the amide bond in the Kevlar[®] molecule structure. Moreover, the linear backbone in Kevlar[®] facilitates hydrogen bonding between adjacent molecules, leading to high chain packing and crystallinity, and adding to the high tensile strength of the fibre. However, researchers hypothesized that when Kevlar[®]-based fabrics are exposed to moisture, these hydrogen bonds might break and not be able to reform easily when the fabric is dry. This actively demonstrates that Kevlar[®]-based fabrics are more susceptible to hydrolysis in comparison to Nomex[®]-based fabrics. To compare with results obtained from this study, there was an agreement between the two studies about the effect of laundering on the ageing behaviour of Nomex[®] IIIA (Fabric A and Fabric #2), and between Fabric D and Fabric #3. However, the tear strength of Fabric C increased by 16% after 10 laundering cycles in the Launder-Ometer[®]. These seemingly contradictory results may be attributed in part to the difference in the laundering and drying procedures. For instance, in their study, domestic laundering and tumble drying was used, however, in this study, a Launder-Ometer[®] and flat drying were employed.

Another study also involving a Nomex[®] fabric similar to Fabric A in terms of fibre content performed various series of abrasion/laundry cycles (5, 10, 15, 20 and 25) on the fabric specimens (Vanderschaaf et al., 2015). The fabric experienced a slight increase in mass attributed to relaxation shrinkage after the first cycles and remained relatively stable for the rest of the cycles. A minor increase in thickness from the abrasion procedures applied was also observed over time. After 25 abrasion/laundry cycles, the fabric experienced a loss in strength of 24%. As well, SEM images revealed tangled fibres and broken fibre ends on the fabric's surface. In another study, SEM images were presented of a 100% Nomex[®] knitted fabric, which had been exposed to 30 washes using a domestic washing machine and dried using a tumble dryer (Couvrette, 2015). The researcher observed stray fibres and foreign matter accumulating on the surface of the fabric.

Finally, according to Dupont (2019), a little decrease in tensile strength of fabrics consisting of Nomex[®] fibre can be observed after several laundering cycles. Nomex[®] IIIA fibres lose roughly 10% and 25% of their tensile strength after 100 and 200 industrial laundering cycles, respectively. In this study, 10 cycles in the Launder-Ometer[®] which equals to 50 domestic laundering cycles were performed, and this treatment is less severe and involves less abrasion in comparison to 100 or 200 industrial laundering cycles.

The better resistance of Fabric A to laundering can be linked to its higher Nomex[®] content. On the other hand, the difference in the change in tear strength between Fabric C and D was not statistically significant with a *p* value of .095. This might be attributed to the similarity in fibre content between the two fabrics (details in Appendix E- Table E16). Nonetheless, the two fabrics expressed different behaviour (increase or decrease) in tear strength. It can be theorized that the difference is related to the finishes applied on the fabrics.

Finishes prevent yarn mobility, which reduces tearing resistance. However, when removed, yarn mobility increases and allows yarn to join together and break at once which contributes to a better strength. The removal of the finish might have happened in Fabric C but not in the case of Fabric D. Another explanation for the difference in behaviour can be explained using the tearing graphs. Figure 66 shows the differences in the tearing behaviour for the two fabrics before and after the laundering treatment. Fabric D has an initial tearing curve that continues to rise over the test and indicates the sharing of the force by adjacent yarns during the test coupled with the high strength provided by the filament yarns (Figure 66 (d)). The filament yarns also led to better yarn mobility due to their slippery surface properties, hence the yarns were able to join together to resist the force which contributed to a higher tearing resistance. However, the tearing behaviour of Fabric D change between the initial and laundered conditions (Figure 66 (c)) and showed a pattern of individual yarns breaking as the tearing force moved through the fabric with lower strengths (peaks in the graph) for the yarns being torn. However, the tearing behaviour of Fabric C was different between the initial and laundered (Figure 66 (a,b)). In the initial condition (Figure 66 (a)), it can be noticed from the tearing graph that yarns were breaking in sequence. However, after laundering, yarns appeared to have higher strength (peaks in the graph) indicating that the yarns behaviour changed (Figure 66 (b)). It can be linked to the Kevlar[®] staple spun yarns breaking after every two Kevlar[®]/Nomex[®] staple spun yarns in the woven structure of Fabric C which exhibited a higher tearing resistance in comparison to the Kevlar[®] filament yarns breaking after every four Kevlar[®]/Nomex[®] staple spun yarns in Fabric D woven structure.

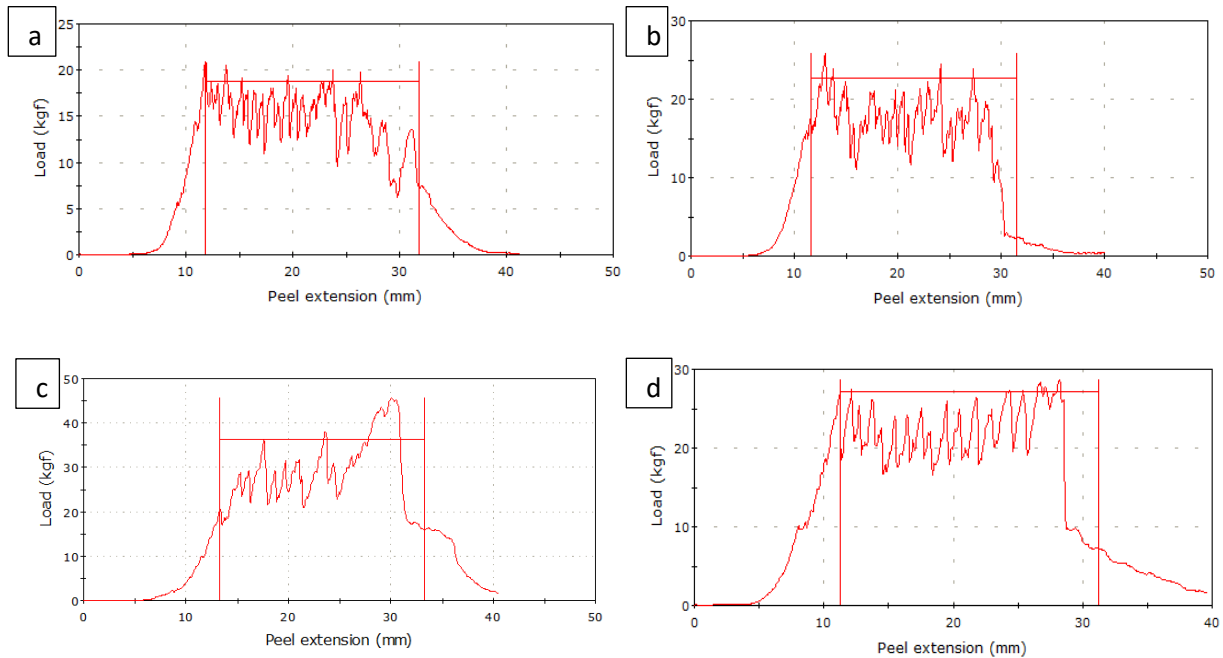


Figure 66. Tearing behaviour of specimens taken from: Fabric C (a: initial, b: laundered), Fabric D (c: initial, d: laundered).

When comparing the data from these previous studies with the results of my study, it is important to note that different techniques were used for washing and drying. These previous studies were conducted with domestic or industrial washing machines and tumble dryers while my study involved the use of a Launder-Ometer[®] and flat drying. Some studies demonstrated that laundering does not have a severe effect on fabrics with high Nomex[®] content while it is more likely to affect fabrics with high Kevlar[®] content. Other studies showed that both fibres should perform similarly when subjected to laundering.

Group 2 fabrics

The ageing behaviour of Group 2 fabrics after 10 laundering cycles was characterized by tear strength. The results are shown in Figure 67. This group includes Fabrics E, F and G. These fabrics consist of blends of Kevlar[®] and PBI fibres. In the case of Fabric E,

it also contains a small amount of LCP filaments (one LCP filament yarn after every seven Kevlar®/PBI staple spun yarn in the woven structure).

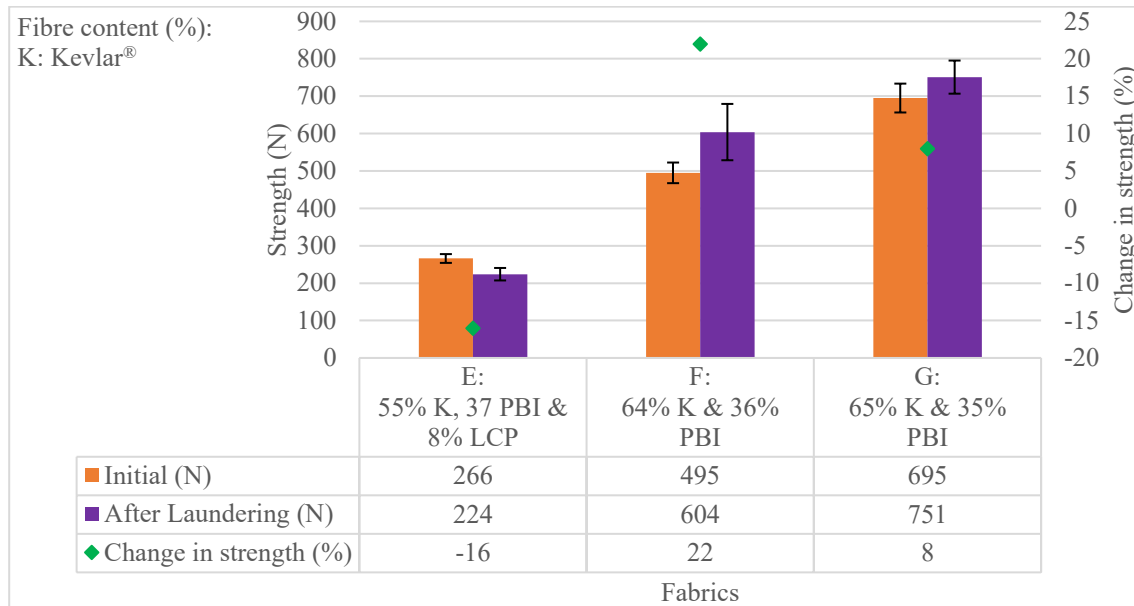


Figure 67. Average initial mechanical strength, average residual mechanical strength after 10 laundering cycles, and corresponding percent change in tear strength for Group 2 fabrics.

In the case of Fabric E and Fabric F, the change in tear strength is statistically significant with p values of .002 and .016, respectively. The strength of Fabric E decreased by 16% after 10 laundering cycles, whereas it increased by 22% for Fabric F. In the case of Fabric G, no statistically significant change in tear strength was obtained (p value of .065).

The effect of laundering on Kevlar® fibres has already been described in the section above relative to Group 1 fabrics. Results for a fabric similar to Fabric F and G in terms of fibre content (Fabric #7) have been reported where the tear strength was measured after 10, 20, 35, and 50 washing/drying cycles at 60 °C (Dolez & Malajati, 2020). The fabric exhibited a loss in tear strength of 49% after 50 washes/drying cycles. The loss in strength was attributed to the

sensitivity of Kevlar[®] to hydrolysis. However, in this study, different results were obtained for Fabrics F and G. The reason behind the differences might rely on the accelerated ageing procedures used. They performed 50 cycles of domestic laundering and tumble drying whereas in this study, a Launder-Ometer[®] and flat drying were used and 10 cycles were assumed to be equivalent to 50 domestic washing cycles.

The decrease in strength obtained here for Fabric E is surprising since it has a lower Kevlar[®] content compared to the three other fabrics of Group 2 (55% vs. 64-65% for Fabric F and G, respectively). In addition, it did not experience a decrease in strength after thermal and hydrothermal ageing, whereas the two other fabrics did. Regarding Fabrics F and G, the difference in the change in tear strength was not statistically significant with a *p* value of 1.0 (details in Appendix E- Table E16). Closer examination showed that all of the yarns broke during the tearing of Fabric E - the LCP filament yarns and the Kevlar[®]/PBI staple spun yarns in the woven structure of Fabric E all broke as they were encountered during the tearing test. However, in Fabrics F and G, while the Kevlar[®]/PBI staple spun yarns in the woven structures broke, the Kevlar[®] filament yarns did not break and instead ended up sliding together and breaking at the same time which contributed to a higher tearing strength for these fabrics after washing (see Figure 68). The reason for the decrease in the strength of the LCP filament yarns of Fabric E may lie in the effect of the mechanical stresses created by the tumbling action in the presence of the metal balls during the accelerated washing procedure.

Unbroken
filament yarns
during the
tearing test.

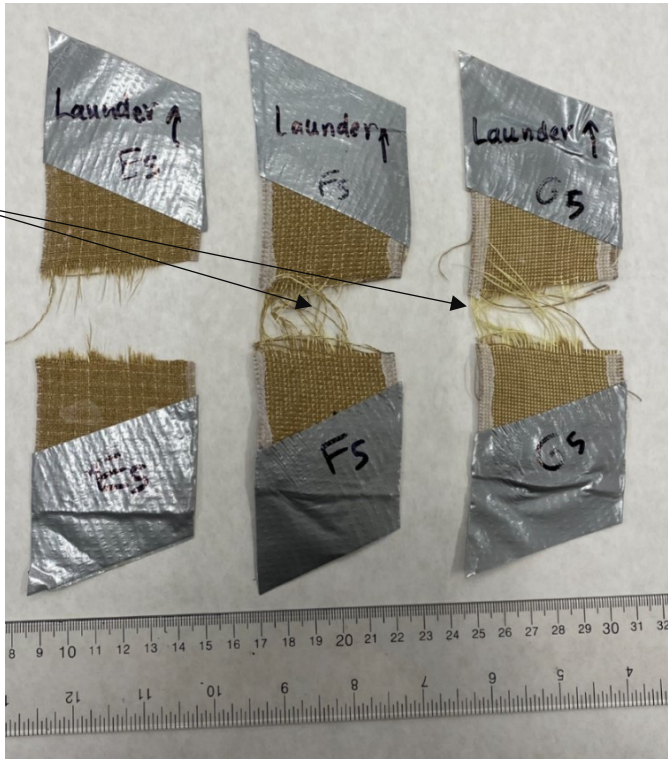


Figure 68. Specimens after 10 laundering cycles from Fabric E, F and G after tearing.

Group 3 fabrics

The ageing behaviour of Group 3 fabrics after 10 laundering cycles was characterized by tear strength. The results are shown in Figure 69. This group includes Fabric L and O. These fabrics mainly consist of oxidized PAN and Kevlar[®] fibres. Fabric L also includes FR rayon and anti-static polyester. Fabric O contains novoloid.

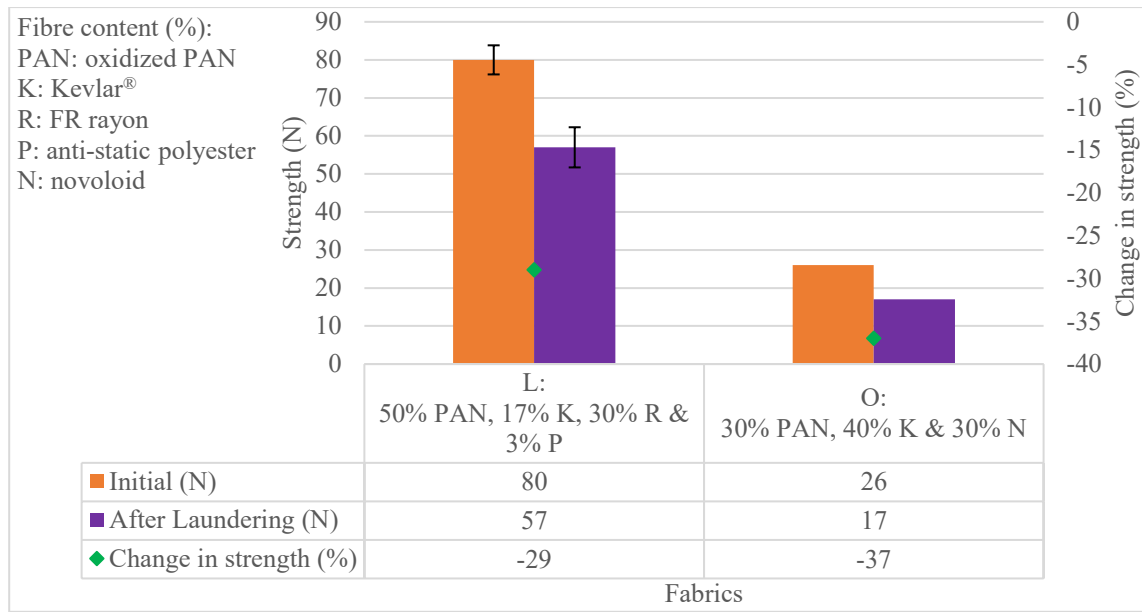


Figure 69. Average initial mechanical strength, average residual mechanical strength after 10 laundering cycles, and corresponding percent change in tear strength for Group 3 fabrics.

Fabric L strength loss of 29% was statistically significant with a p value of $< .001$.

Fabric O lost 37% of its initial tear strength after 10 laundering cycles, but because only one specimen was tested, no statistical analysis was performed.

The effect of repeated launderings on Kevlar[®] fibres was described earlier in the section relative to Group 1 fabrics. On the other hand, very little information was found in the literature about the effect of repeated launderings on oxidized PAN, FR rayon, polyester or novoloid. Very limited information has also been found on the effect of hydrothermal ageing conditions on these fibres (see section 4.2.3). However, according to a brochure for Fabric L provided by TEXTECH (n.d.), this fabric should be washed in cold water with a mild detergent. In the case of Fabric L, the loss in strength might be a result of washing in hot water. However, it can be hypothesized that the sensitivity to moisture of the Group 3 fabrics is also related to the presence of Kevlar[®] fibres.

Group 4 fabrics

The ageing behaviour of Group 4 fabrics after 10 laundering cycles was characterized by tear strength. The results are shown in Figure 70. This group includes Fabrics B and N. These fabrics consist of PBO fibres, blended with para- and meta-aramid fibres in the case of Fabric B.

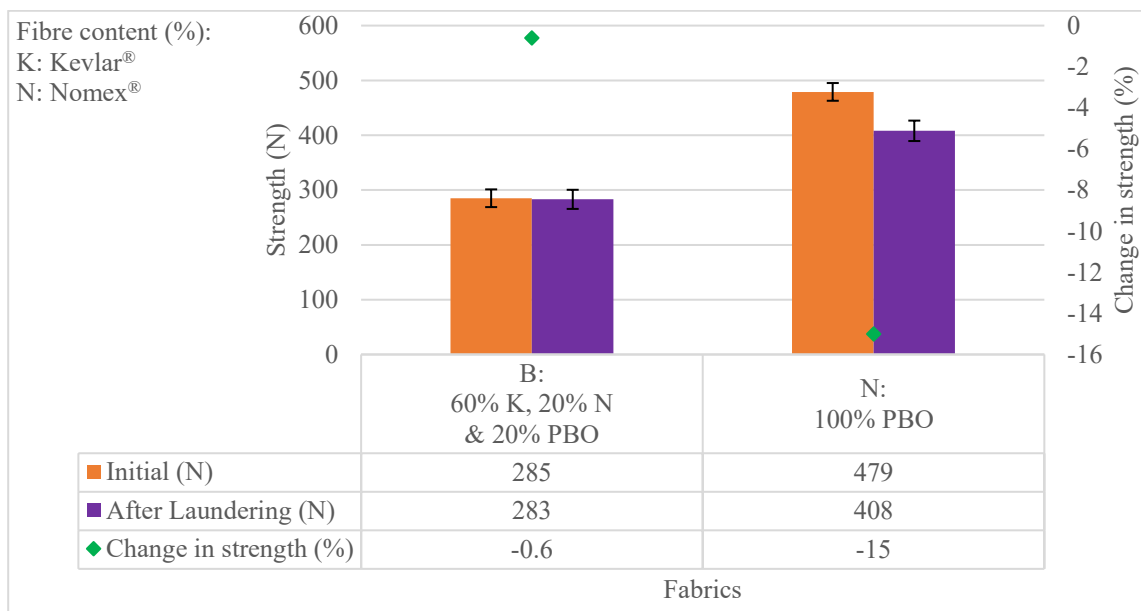


Figure 70. Average initial mechanical strength, average residual mechanical strength after 10 laundering cycles, and corresponding percent change in tear strength for Group 4 fabrics.

In the case of Fabric B, there was no statistically significant change in tear strength (p value of .869). On the other hand, Fabric N showed a loss in tear strength of 15% which is statistically significant with a p value of $< .001$.

The effect of laundering on Kevlar® and Nomex® fibres has already been described in the section above relative to Group 1 fabrics. In a study by Dolez & Malajati (2020) the tear strength of fire protective fabrics was assessed after 10, 20, 35, and 50 washing/drying cycles

at 60 °C. A fabric (Fabric #4) with the same fibre content as Fabric B exhibited a 10% loss in tear strength after 50 washing/drying cycles. According to the researchers, the good results were unexpected since PBO is known to be sensitive to hydrolysis. They thought perhaps a high level of polymerization for the PBO fibres used in the fabric were responsible for the good results.

Although the original tensile strength of PBO is higher than that of aramids, PBO is more susceptible to hydrolysis (Shaw, 2012). Chemical and physical changes occur in PBO after exposure to high temperatures and humidity due to the opening of the benzoxazole ring followed by a hydrolysis reaction. Therefore, the lower performance obtained for Fabric N compared to Fabric B can possibly be related to its higher PBO content.

Group 5 fabrics

The ageing behaviour of Group 5 fabrics after 10 laundering cycles was characterized by tear strength. The results are shown in Figure 71. Fabrics I and M. These fabrics are cellulose-based. Only Fabric I was subjected to repeated launderings because Fabric M did not survive thermal ageing, and hence it was decided not to subject it to the laundering treatment. This fabric is treated with an FR finish and consists of 63% cotton, 34% polyester, and 3% EOL (XLANCE®).

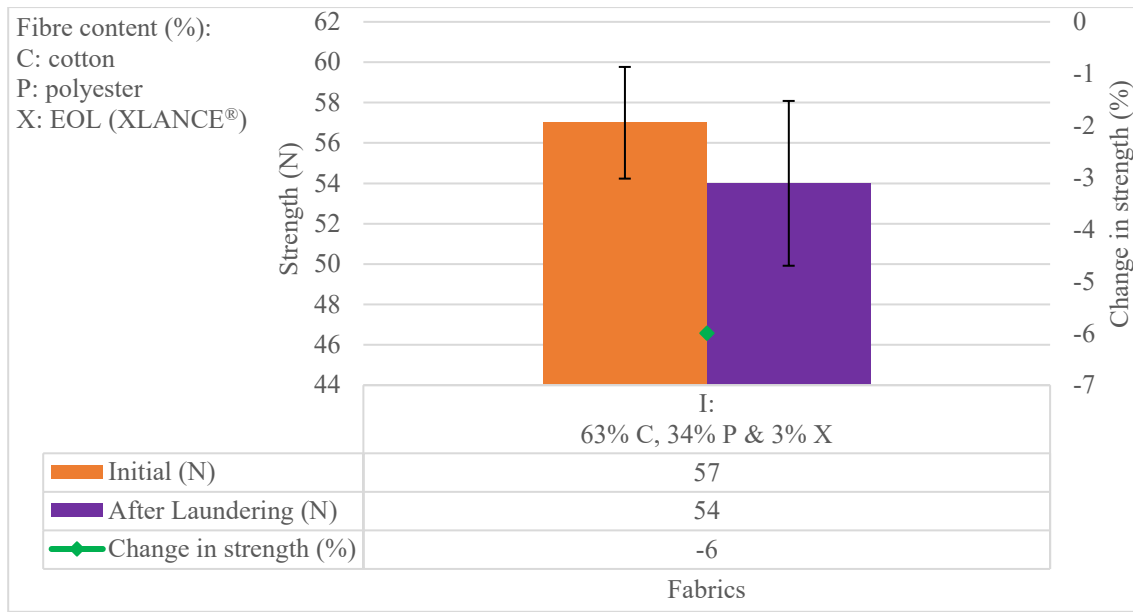


Figure 71. Average initial mechanical strength, average residual mechanical strength after 10 laundering cycles, and corresponding percent change in tear strength for Group 5 fabrics.

No statistically significant difference in tear strength was measured for Fabric I after 10 laundering cycles (p value of .144).

A study looked at the effect of accelerated laundering on the physical properties of an 88/12% cotton/nylon fabric (Vanderschaaf et al., 2015). The fabric was tested in several conditions: no treatment, after one wash, and after 5, 10, 15, 20 and 25 cycles of abrasion followed by a wash between each abrasion treatment. The fabrics exhibited a reduction in mass, suggesting the loss in fibres because of abrasion. This reduction increased as the number of abrasion/laundry cycles increased. SEM imaging showed no difference between the fabric after one wash and 25 abrasion/laundry cycles. It was assumed that the fibres broken during the abrasion treatment were washed away during laundering. The fabric only maintained 43% of its original tensile strength after 25 abrasion/laundry cycles. The loss in tensile strength is most

likely related to the abrasion cycles performed on the fabric leading to the deposition of broken fibres on the surface of the fabric which ultimately got washed away after laundering.

In conclusion, results obtained for Group 5 fabrics are in agreement with the literature which suggests that both polyester and cotton have good resistance to laundering.

Group 6 fabrics

Other fabrics were included in this study. For instance, Fabrics T and U. The ageing behaviour of Group 6 fabrics after 10 laundering cycles was characterized by tensile strength. The results are shown in Figure 72. Fabric T is made of fibreglass and Fabric U is 100% LCP.

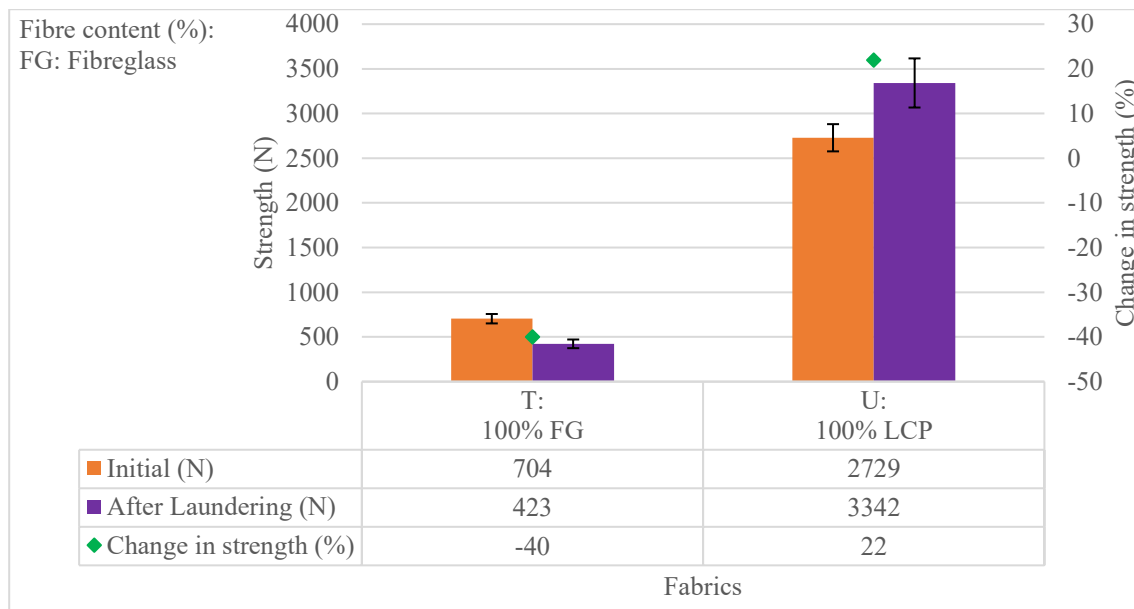


Figure 72. Average initial mechanical strength, average residual mechanical strength after 10 laundering cycles, and corresponding percent change in tensile strength for Fabric T and U.

Fabric T exhibited a decrease of 40% in tensile strength, this decrease is statistically significant with a p value of $< .001$. On the other hand, Fabric U exhibited a statistically significant increase in tensile strength by 22% after 10 laundering cycles with a p value of $.002$.

No previous reports about the effect of repeated laundering on glass fibres have been identified in the literature. However, exposure to water at elevated temperature has been reported to have a negative effect on glass fibres and to cause the loss in strength as mentioned in section 4.2.3. Besides, after subjecting Fabric T to 10 laundering cycles, we were able to make several observations, which could explain the loss in strength measured. The fabric initially displayed a loose structure with smooth yarns and high yarn mobility (Figure 73 (a)). After laundering, the surface of the fabric became fuzzy with the presence of broken fibre ends (Figure 73 (b)). The mechanical stresses created by the tumbling action in the presence of the metal balls caused the filament glass fibres to break, and portions of the fibres were washed away after each of the laundering cycles, which led to a loss in the fabric weight. In addition, the broken fibre ends caused the yarns to become entangled on the fabric surface and these yarns had to be untangled by applying some forces after each laundering cycle to flatten the fabric specimens. These two phenomena could explain the reduction in strength observed.

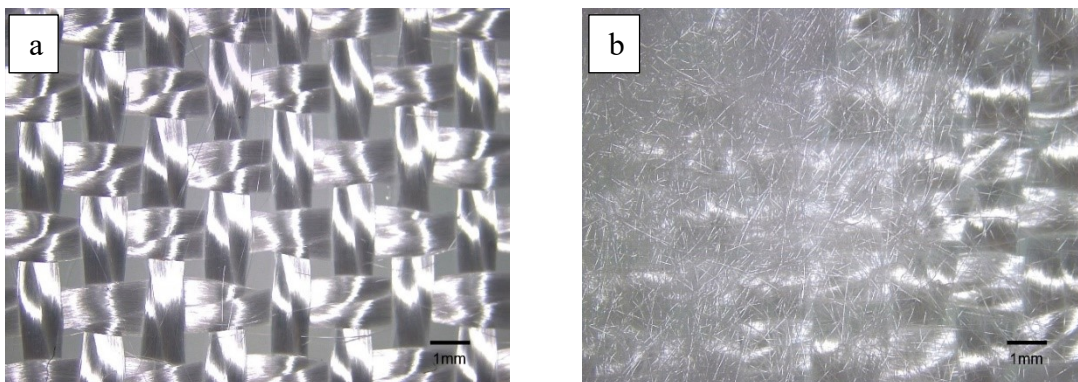


Figure 73. Fabric T: (a) initial condition, (b) after 10 laundering cycles.

Regarding Fabric U, LCP fibres have been reported to have excellent resistance to damage and shrinkage during industrial laundering procedures (Sloan, 2017). The LCP fabric

in this study was one of the four fabrics that showed an increase in strength following 10 laundering cycles.

4.3. Shrinkage

Fabric shrinkage was measured in an attempt to characterize the effect of laundering on the dimensional stability of all fabrics tested. Shrinkage was calculated after every 2 laundering cycles on all specimens, hence a total of 5 measurements were conducted for the 10 laundering cycles applied. Figure 74 shows the shrinkage values after 2, 4, 6, 8 and 10 laundering cycles for all the fabrics tested. Differences in behaviour can be observed between the fabrics. Most fabrics exhibited a fairly similar shrinkage as a result of the laundering procedure while a few others did not demonstrate any shrinkage. Shrinkage measurements were not performed on Fabric M. Since it did not survive thermal ageing, it was decided not to subject it to the laundering treatment. Statistical analysis was performed on the shrinkage data. The details of the results are provided in Appendix F.

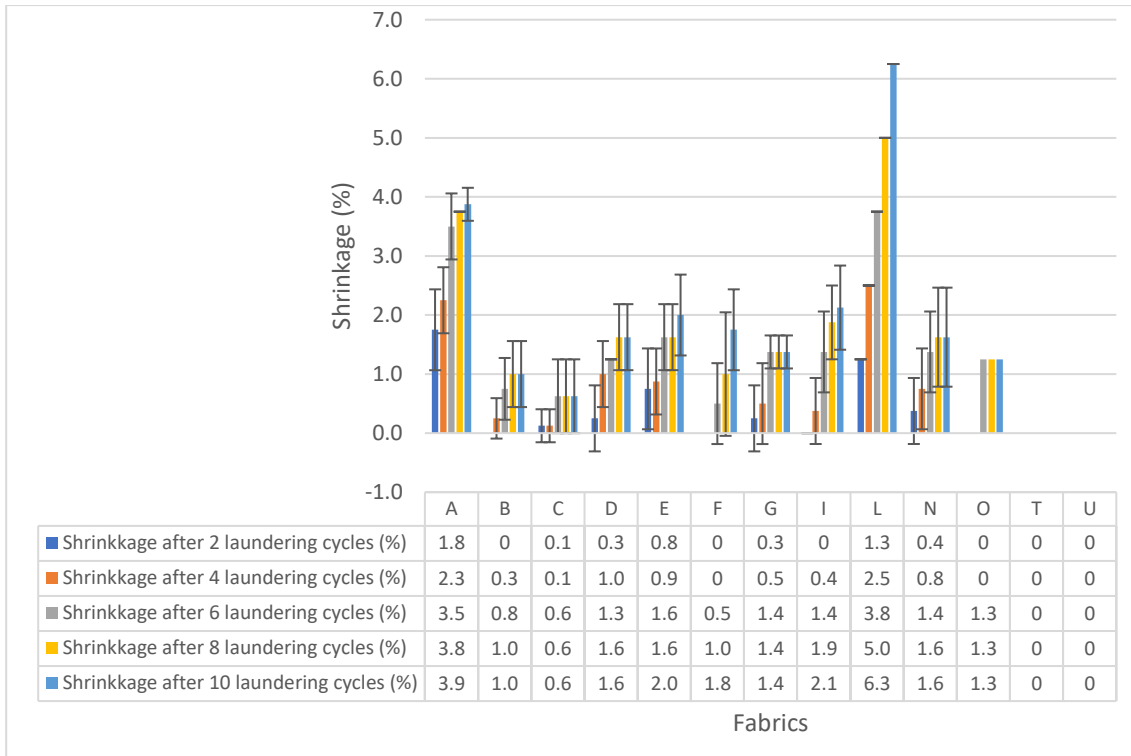


Figure 74. Percent dimensional change (shrinkage) in the warp direction corresponding to 2, 4, 6, 8 and 10 laundering cycles for all the fabrics.

Dimensional stability is the ability of a fabric to resist dimensional changes (Miles, 2003, as cited in Ng et al., 2012). These changes might occur when a fabric is subjected to moisture and/or heat. Dimensional changes are more likely to be a decrease in dimensions (shrinkage) rather than an increase (stretch), as well, it might be reversible or irreversible (Ng et al., 2012). Fabric shrinkage is a problem that can occur during a fabric finishing process or after laundering. There are four main types of shrinkage: relaxation shrinkage, swelling shrinkage, hygral expansion, and felting shrinkage. With the first few launderings of a fabric following manufacturing, relaxation shrinkage commonly occurs. Since the fabrics in the study were all being laundered for the first time and the level of shrinkage was low (< 2% for most fabrics) the shrinkage can be attributed to relaxation of the fabric structures. Swelling shrinkage

generally occurs in fabrics that consist of high moisture-absorbing fibres (Ng et al., 2012). Both hygral expansion and felting shrinkage are associated with wool fibres and are not relevant to this study.

Relaxation shrinkage happens when the forces applied while manufacturing a fabric are released via wetting, hence the fabric returns to its relaxed dimensions (Collier & Tortora, 2001). This type of shrinkage is irreversible (Ng et al., 2012). According to Collier and Tortora (2001), relaxation shrinkage typically occurs after the first few laundering cycles. The amount of relaxation shrinkage that occurs depends on the amount of stretch applied during manufacturing. In woven fabrics, relaxation shrinkage is more common in the warp direction than the weft direction because warp yarns undergo more tension while manufacturing in comparison to weft yarns.

The dimensional stability requirement for FR garments identified in NFPA 1971 (2018) is no more than 5% shrinkage after 5 laundering/drying cycles performed according to the standard test method AATCC TM135- Dimensional Changes of Fabrics after Home Laundering. This is because it has been established that shrinkage of more than 5% will affect the garment's insulation qualities as well as the firefighters' mobility.

Group 1 includes Fabric A, C and D (Nomex[®] and Kevlar[®] blends). Fabric A shrinkage of 3.9% after 10 laundering cycles is statistically significant (p values $< .05$). In the case of Fabric C, no statistically significant shrinkage occurred after 10 laundering cycles (p values $> .05$). On the other hand, Fabric D exhibited a statistically significant shrinkage of 1.6% after 10 laundering cycles (p values $< .05$). According to the literature, fabrics made of Nomex[®] fibres experience low shrinkage and maintains their dimensional stability after several laundering cycles (Dupont, 2019). However, exposure to heat and moisture release the inner

fibre stresses. For instance, exposure to boiling water results in a shrinkage of 3.8% after 100 exposures. For their part, Kevlar[®] fibres do not shrink in hot water (Dupont, 2017). The greater shrinkage in Fabric A might be attributed to the high Nomex[®] content. However, it is also likely that Fabric A had a greater relaxation potential than the other fabrics evaluated. Fabric A may have been stretched more in manufacturing, giving it greater relaxation potential. Differences in textile finishing can also affect shrinkage more so than fibre content. For example, fabrics with water-repellant finishes may be stabilized by the finish and resist shrinkage in laundering and dyed fabrics may have undergone some relaxation during the dyeing process, making them less likely to shrink in laundering.

Group 2 includes Fabric E, F and G (Kevlar[®] and PBI blends), with higher percentage of Kevlar[®] in the fabrics. This group demonstrated a low shrinkage after 10 laundering cycles. In the case of Fabric E, a statistically significant shrinkage of 2% occurred after 10 laundering cycles (p values $< .05$). In the case of Fabric F, it did not exhibit any statistically significant shrinkage after 10 laundering cycles (p values $> .05$). 10 laundering cycles caused a statistically significant shrinkage of 1.4% in Fabric G (p values $< .05$). The lower shrinkage in Group 2 fabrics might be attributed to the higher percentage of Kevlar[®] in comparison with Group 1 fabrics, besides, the shrinkage of PBI fibres is less than 1% in boiling water (Horrocks et al., 2001).

Group 3 includes Fabric L and O (oxidized PAN-based). Fabric L exhibited the highest shrinkage of all tested fabrics, with a maximum shrinkage of 6.2% after 10 laundering cycles (no p value). The high shrinkage of Fabric L might be attributed to the 30% FR rayon fibre content as viscose rayon is sensitive to wet shrinkage, which can lead to problems of dimensional stability after laundering (Chen, 2015). In addition, Fabric L is dyed with a dark

colour, and the wax marker used to make the reference marks came off after each laundering cycle, hence, it was hard to make a definite measurement of shrinkage. In the case of Fabric O, a shrinkage of 1.2 % happened after 3 laundering cycles; no further changes were measured after that. This moderate shrinkage is likely the result of fabric relaxation.

Group 4 includes Fabric B and N (PBO-based). Fabric B did not exhibit any statistically significant shrinkage after 10 laundering cycles (p values $> .05$). It may be attributed to the 60% Kevlar[®] and 20% Nomex[®] fibre content. In the case of Fabric N, which is 100% PBO, there was also no statistically significant shrinkage after 10 laundering cycles (p values $> .05$).

Group 5 includes Fabric I (cotton and polyester blend). Fabric I displayed a statistically significant shrinkage of 2.1% after 10 laundering cycles (p values $< .05$). Cellulosic fibres such as cotton and rayon have a high moisture absorbency and thus tend to swell in water, which can cause shrinkage and dimensional instability (Collier & Tortora, 2001). Polyester on the other hand does not swell in water and exhibits minimal shrinkage in laundering (Deopura & Padaki, 2015).

Finally, Fabric T (100% fibreglass) and Fabric U (100% LCP) exhibited no shrinkage after 10 laundering cycles. Glass fibres exhibit exceptional dimensional stability and will not shrink in water (Guo et al., 2020; Giwa et al., 2013), as well as the very good dimensional stability exhibited by LCP fibres (Sloan, 2017). For instance, SM- and HM- LCP fibres shrink by less than 0.2% when exposed to boiling water at 180 °C for 30 min.

It is important to note that the purpose of this study was not to study the effect of laundering on the dimensional stability of fabrics but only to make sure that no fabric would

experience a level of shrinkage that would interfere with the sensor operation. In addition, the size of specimens was smaller than is normally used for accurately determining dimensional change during laundering.

4.4. Final selection of the support fabric

None of the fabrics tested in this study preserved their strength after exposure to all four ageing conditions. No simple solution is thought to be available to limit degradation because of thermal ageing. On the other hand, the resistance to photodegradation or hydrolysis could potentially be improved with a surface treatment applied on the fabric. As a result, a first selection was made based on the performance of the fabrics when exposed to thermal ageing. Three potential candidates were left after excluding all the fabrics which showed extensive amount of damage because of thermal ageing: Fabric A, T and U.

Ultimately, Fabric A was selected as the best option as a fabric substrate for the end-of-life sensors. The next paragraphs explain the reasons for this choice.

Fabric A is made of Nomex[®] IIIA. It showed a 25% loss in tear strength after thermal ageing which was considered acceptable in comparison with the other fabrics currently used as the outer shell of firefighters' clothing, which lost between 70 and 90% of their strength after exposure to the heat treatment. The tear strength of Fabric A was not affected by hydrothermal ageing or laundering. On the other hand, Fabric A was strongly affected by UV irradiation and lost 70% of its mechanical strength. However, the fabric could be protected against the effects of UV radiation by a surface treatment using UV blockers or absorbers such as carbon black (Hawkins, 1984) or titanium dioxide or zinc oxide nanoparticles (Dolez, 2019b).

Fabric T is a fibreglass fabric. The fabric was not negatively affected by exposure to heat or UV. On the other hand, a reduction in strength between 25 and 40% was observed after hydrothermal ageing and laundering. In addition, during laundering, the surface of the fabric became fuzzy with the presence of broken fibres (see Figure 73). These were eventually washed away with repeated laundering cycles. This behaviour was attributed to the brittleness of the glass fibres, which cannot be successfully laundered and additionally may not withstand the mechanical stresses experienced by the firefighters' protective clothing in service. This fabric was thus not retained as a substrate for the EOL sensors.

Fabric U is composed of LCP. While its UV resistance was limited, there was no major effect of the heat, hydrothermal and laundering treatments on its mechanical strength. However, the fabric became brittle, and its tactile feel or hand changed after thermal ageing. Images of the fabric before (see Figure 45 (a)) and after (see Figure 45 (b)) the heat treatment only showed a colour change. On the other hand, images of the yarns at a higher magnification (see Figure 46) showed a change in the yarn's diameter, possibly because of a partial melting of the fibres during the thermal ageing treatment. As a result, this fabric was not selected as a substrate for the graphene-based EOL sensors.

4.5. Assessing the strength of the rGO coating

The surface resistance R_s was measured for all 12 rGO-coated specimens in the initial condition (i.e. before laundering). Figure 75 presents the initial R_s values for both faces of all 12 rGO-coated specimens. The specimens exhibited relatively similar R_s values. The average R_s values are 1146 and 1216 Ohm/sq for Face-1 and Face-2, respectively. The highest R_s values were reported for specimen coated-3 and the lowest surface R_s values for coated-5.

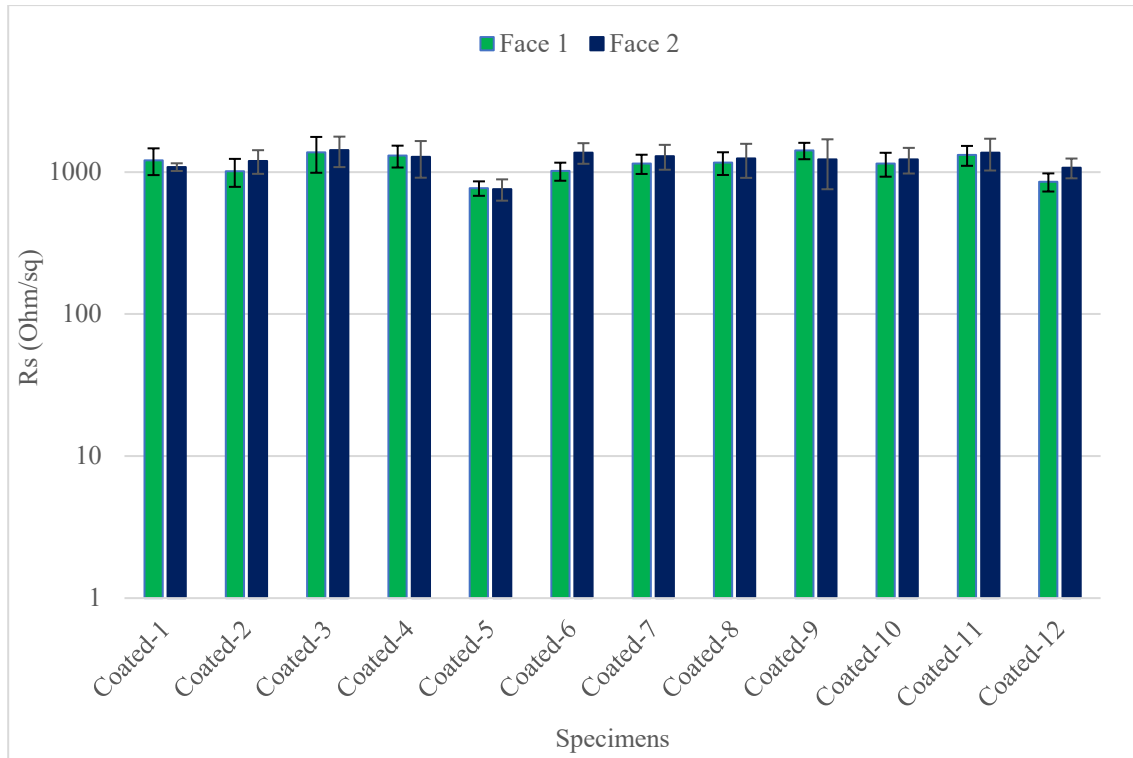


Figure 75. Average initial R_s values for both faces for all 12 rGO-coated specimens.

One specimen was set aside for FE-SEM imaging for further comparison with laundered specimens. Specimen coated-10 was selected since it had the closest R_s values to the average of the 12 specimens. Figure 76 shows the FE-SEM images of specimen coated-10. With the smooth rGO layers deposited on the surface of the fabric (Figure 76 (a)), the fibres were barely visible. This indicates the success of the preparation of the rGO coating, with rGO flakes wrapped around the fibres, in agreement with what has been reported by Cho et al. (2019), and layers building up on the surface of the fabric. With 10 layers of rGO coating, the surface features of the fibres have disappeared (Figure 76 (b)). Moreover, the low magnification image reveals the uniformity of the coating of the surface of the fabric with no signs of cracking (Figure 76 (a)).

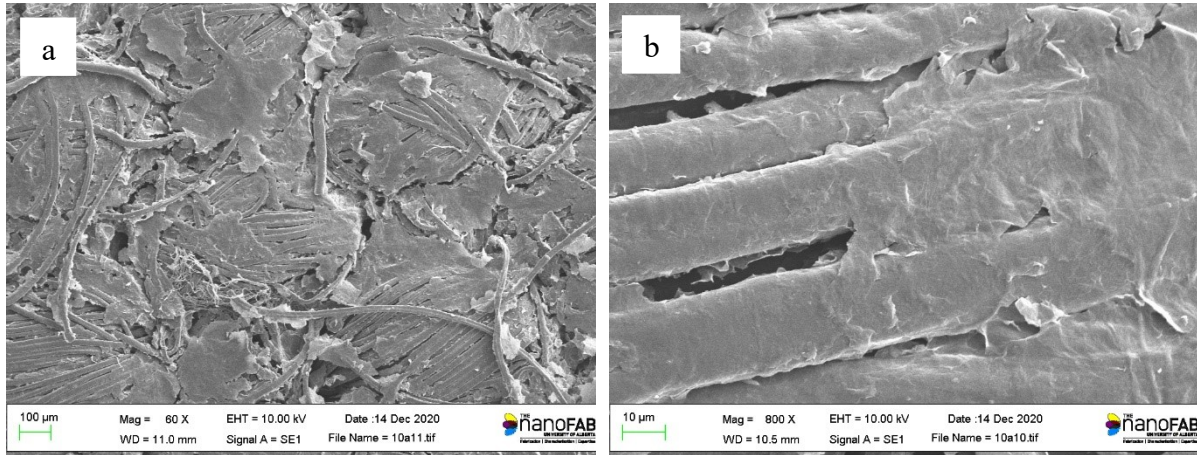


Figure 76. FE-SEM images of specimen coated-10 in the initial condition ($60\times$ and $800\times$ magnification).

The other 11 specimens (coated-1, -2, -3, -4, -5, -6, -7, -8, -9, -11 and -12) underwent a first laundering cycle. The residual R_s values for both faces for all 11 rGO-coated specimens after the first laundering cycle are shown in Figure 77. As a general rule, the laundering cycle negatively affected the rGO coating. Most specimens only demonstrated a moderate increase in the R_s values. The highest increase was observed for coated-6 with 75% and the lowest for coated-1 with 25%. On the other hand, one specimen (coated-11) exhibited a massive increase of two orders of magnitude in R_s , indicating a failure in the rGO coating as a result of one cycle of laundering.

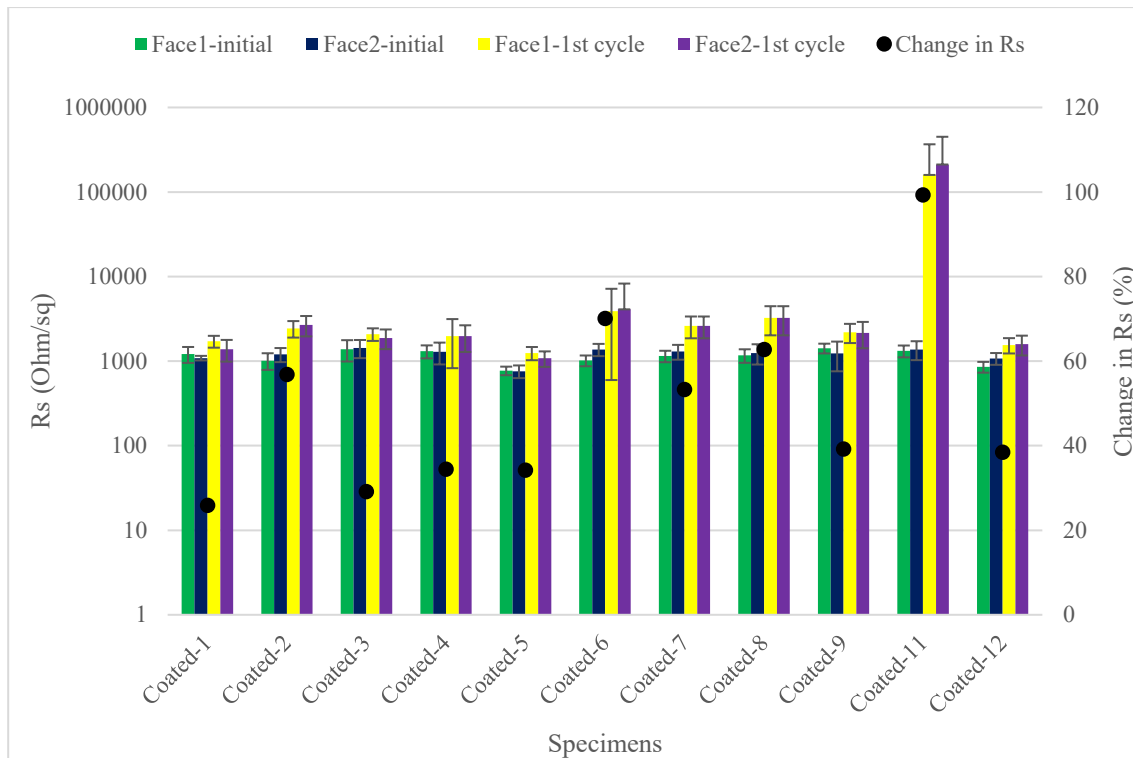


Figure 77. Average initial R_s values for both faces, average residual R_s values for both faces after the first laundering cycle, and corresponding percent change in R_s values for 11 rGO-coated specimens.

Specimen coated-9 was chosen for FE-SEM imaging for comparison with the initial condition (specimen coated-10). Figure 78 shows the corresponding FE-SEM images. Fewer rGO sheets can be seen on the surface of the fabric and the fibres are more visible (Figure 78 (a)). In addition, the rGO coating shows cracks and sheets appear to be peeling off of the surface of the fibres. Besides, evidence of rGO flakes loosely bonded to the surface of the fibres can be noticed. These flakes are more likely to be washed away after further laundering because of their poor bonding to the fibre surface (Figure 78 (b)). The higher R_s values obtained for coated-9 after the 1st laundering cycle in comparison to the initial R_s values can be associated with the loosening of the rGO coating from the fibre and fabric surface.

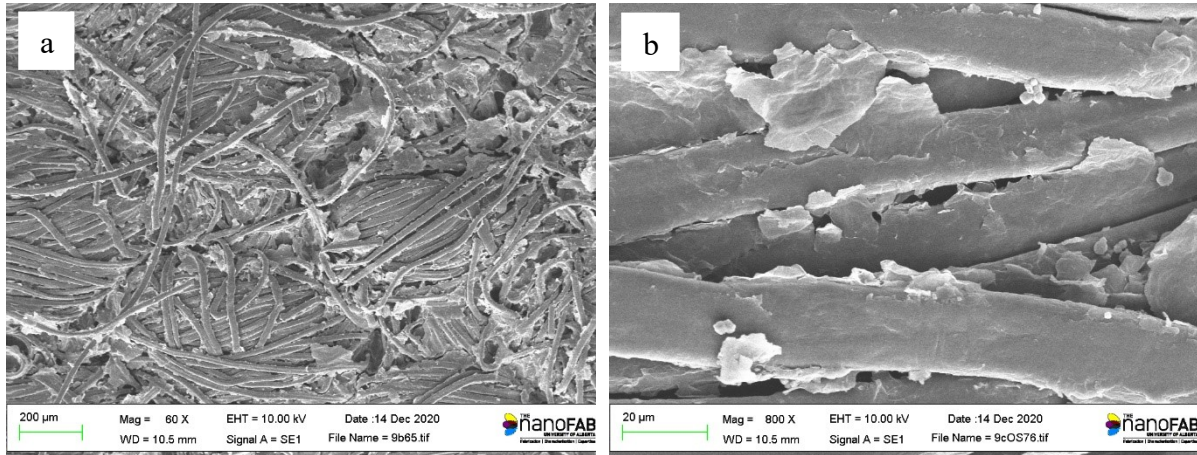


Figure 78. FE-SEM images for specimen coated-9 after one laundering cycle ($60\times$ and $800\times$ magnification).

Specimen coated-11, which had experienced a very high increase in resistance as a result of the first laundering cycle, was also imaged by FE-SEM (Figure 79). It is noticeable that the shape of the fibres is more pronounced with distinct edges. The rGO coating has more cracks with few sheets attached to the surface of the fibres (Figure 79 (a)). Moreover, fibrils seem to appear on the surface of the fibres (Figure 79 (b)). The very high R_s values obtained for coated-11 after the first laundering cycle can be associated with the high number of rGO coating peel offs and the damage reaching the fibres.

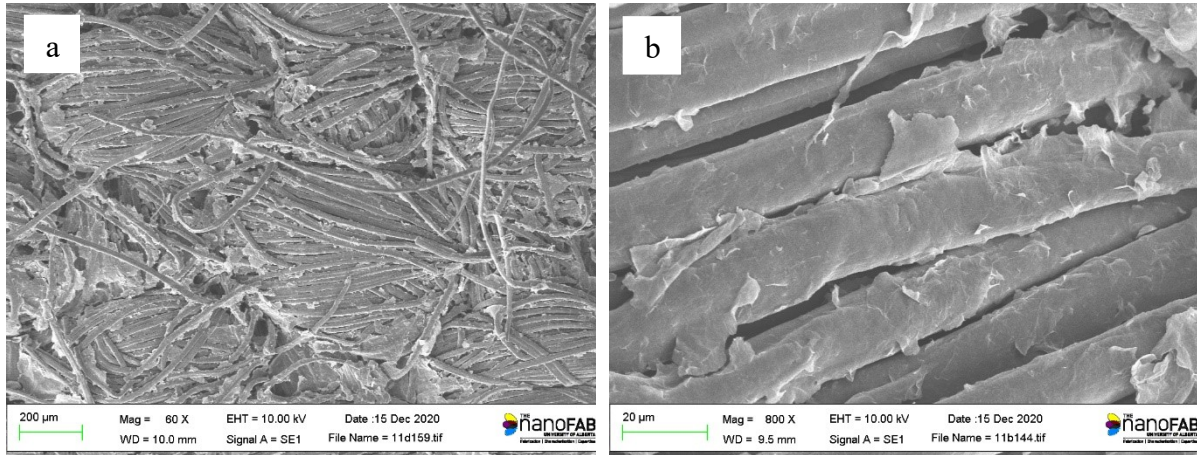


Figure 79. FE-SEM images for specimen coated-11 after one laundering cycle (60 × and 800 × magnification).

Nine rGO-coated (coated-1, -2, -3, -4, -5, -6, -7, -8 and -12) specimens underwent the second laundering cycle. Figure 80 shows the variation in the R_s values for both faces for all 9 rGO-coated specimens after the second laundering cycle. Specimens coated-2, -3, -5 and -6 demonstrated a moderate increase in R_s values (between 18 and 67%) (see Figure 80). Other specimens (coated-1, -7 and -8) exhibited a massive increase in R_s values. Two specimens (coated-4 and -12) showed a moderate increase in R_s values on one face and a massive increase on the other face.

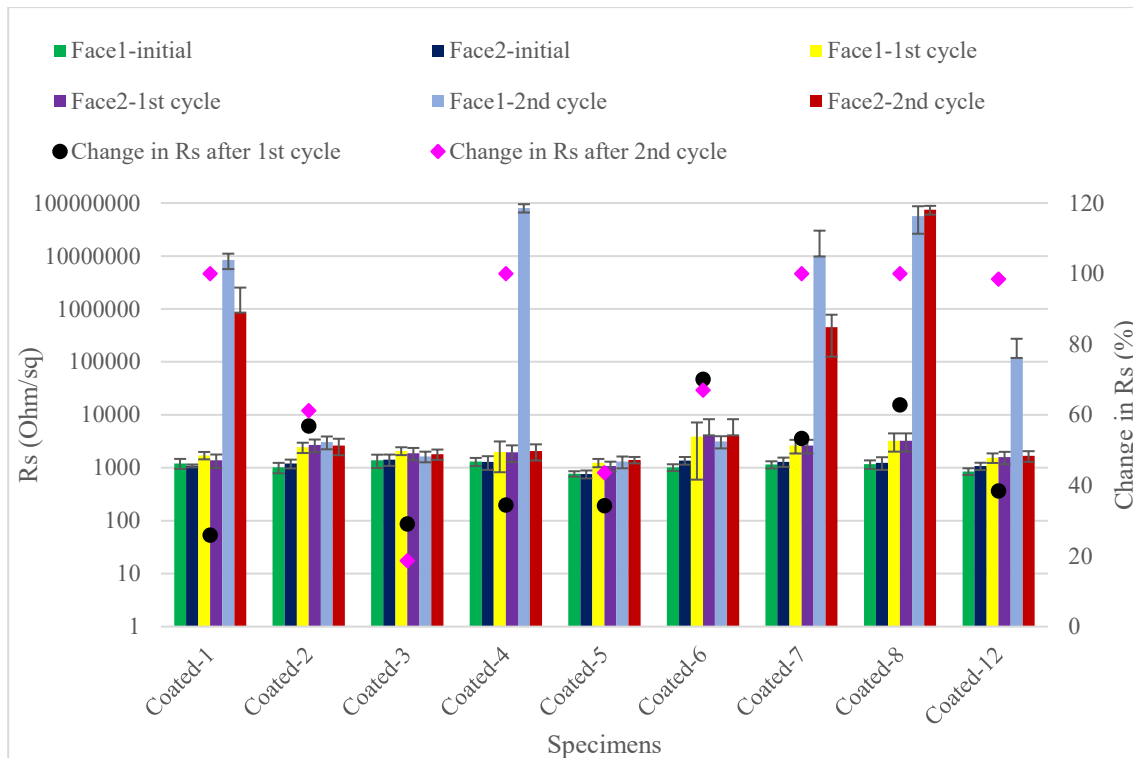


Figure 80. Average initial R_s values for both faces, average residual R_s values for both faces after the first laundering cycle, average residual R_s values for both faces after the second laundering cycle, and corresponding percent change in R_s values for 9 rGO-coated specimens.

Specimen coated-3 was chosen for FE-SEM imaging for comparison with coated-10 (initial) and coated-9 (after first laundering cycle). Figure 81 shows the corresponding FE-SEM images. The fibres look more visible with fewer rGO coating flakes remaining on the surface of the fabric (Figure 81 (a)). A smaller number of rGO coating flakes are attached to the fibres, yet with no signs of cracking (Figure 81 (b)).

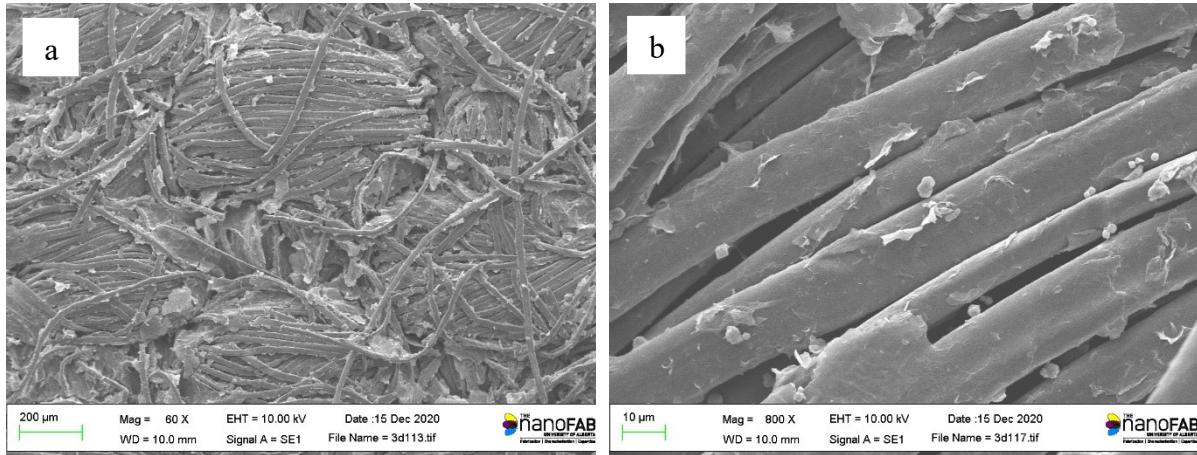


Figure 81. FE-SEM images for specimen coated-3 after two laundering cycles (60 × and 800 × magnification).

Figure 82 shows FE-SEM images of specimen coated-4, which exhibited very high R_s values on one face (Face 1) after the second laundering cycle whereas the other face (Face 2) remained conductive. The fibres are more visible in the picture of face-1 with less rGO coating on the surface in comparison with face-2 (Figure 82 (a,c)). The fibres on face-1 look more individualized with distinct ridges between them (Figure 82 (d)), whereas the fibres on face-2 seem to be still covered by rGO flakes with fewer cracks (Figure 82 (d)). This explains the large difference in R_s values exhibited by face-1 in comparison to face-2.

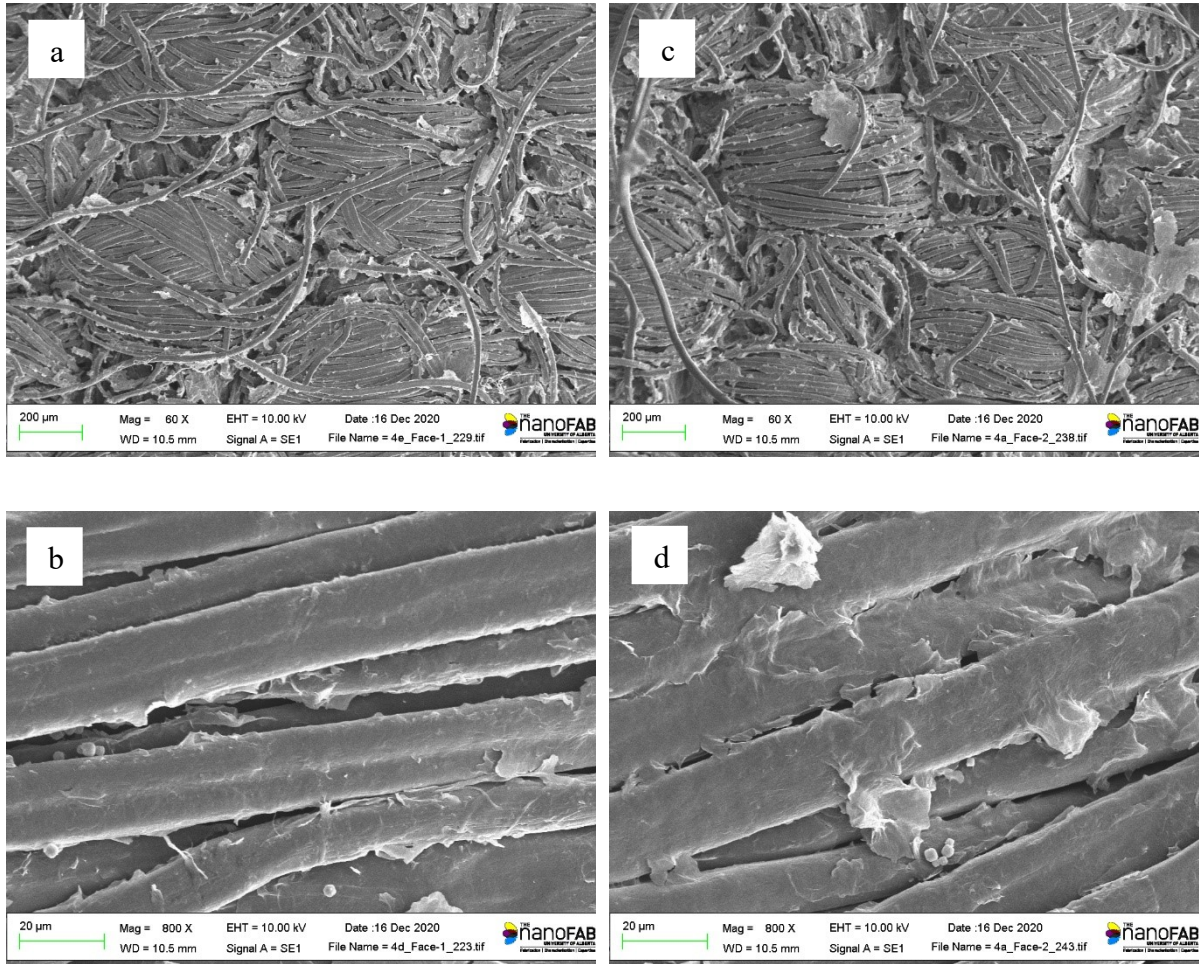


Figure 82. FE-SEM images of specimen coated-4 after two laundering cycles: (left column/a and b) Face-1, and (right column/c and d) Face-2 (60 × and 800 × magnification).

Three rGO-coated specimens (coated-2, -5 and -6) underwent the third laundering cycle. Figure 83 shows the variation in the R_s values for both faces for all 3 rGO-coated specimens after the third laundering cycle. All 3 rGO-coated specimens exhibited very high R_s values after the third laundering cycle, which indicates the failure of the rGO coating to maintain electrical conductivity. None of the specimens was able to maintain its electrical conductivity through three accelerated laundering cycles corresponding to 15 domestic washings.

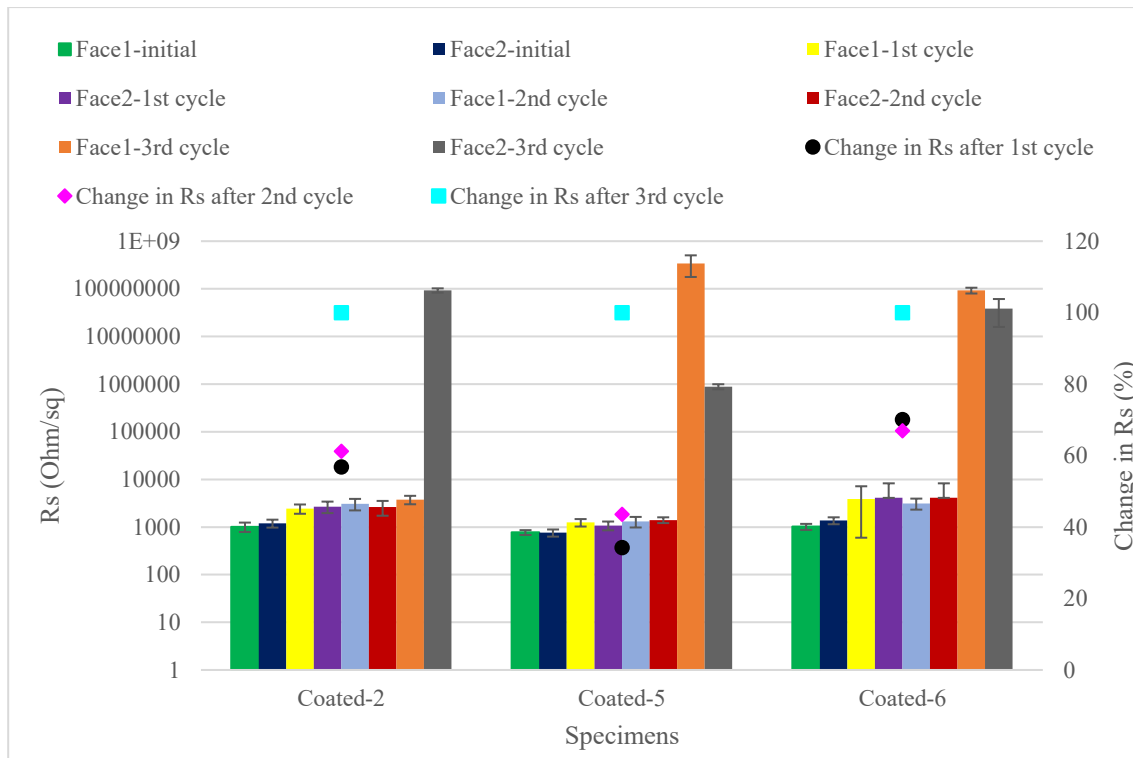


Figure 83. Average initial R_s values for both faces, average residual R_s values for both faces after the first laundering cycle, average residual R_s values for both faces after the second laundering cycle, average residual R_s values for both faces after the third laundering cycle, and corresponding percent change in R_s values for 3 rGO-coated specimens.

The initial R_s values obtained for rGO coating on Fabric A were similar to what have been obtained in a previous study where an rGO coating was applied to a Nomex woven fabric (Cho et al., 2019). After 10 laundering cycles, these authors reported that the R_s values increased only by 3.3 and 11.2 % for specimens coated with 10 and 15 layers of rGO, respectively. By comparison, only 3 accelerated laundering cycles were enough to cause an unstable electrical conductivity and severely damage the 10 rGO layer coating in this study. Several reasons can explain this apparent discrepancy in the results between the two studies. The main reason is related to the severity of the laundering applied. While the temperature was

40 °C in both cases, one laundering cycle only lasted 6 minutes and each canister contained 150 mL of washing solution with 10 metal balls in the study by Cho et al. (2019), while it lasted 30 minutes and each canister contained 50 mL of washing solution with 50 metal balls in my study. The higher mechanical stress caused by the greater number of metal balls and the longer duration of exposure to this higher stress can thus explain in a large part the faster failure of the rGO layers observed in this study.

Another factor may have also played a role in the difference in the durability of the rGO coating observed between the two studies. In the study by Cho et al. (2019), the fabric specimens were cleaned in DI water and 2-propanol then dried at 65 °C for 15 min before the first rGO coating application process and between each dip-reduce-dry procedure. Such cleaning of the specimens before applying the rGO layers was not implemented in my study. However, Cho et al. (2019) did not observe any major difference in the R_s values between rGO applied on the as-received fabric and after subjecting the fabric to a pre-washing treatment involving 50 washing/drying cycles according to CAN/CGSB 4.2 No 58 - Procedure III E (50°C, tumble dry). The R_s value was initially lower in the case of the pre-washed fabric indicating that the pre-washing treatment was efficient at removing the non-permanent textile finishes, impurities, and hydrophobic contaminants from the fabric surface. However, the difference in the R_s between as-received and pre-washed fabrics disappeared after the second rGO coating layer.

5. SUMMARY AND RECOMMENDATIONS

5.1. Summary

A series of fabrics were obtained for the study aimed at identifying a fabric support for the EOL sensor for fire protective fabrics. Some of these fabrics assessed are currently used as an outer shell in firefighters' protective clothing. They are made of blends of meta- and para-aramid, PBI and PBO fibres. Others were identified as potential candidates for the substrate of the graphene-based EOL sensors. These fabrics include glass fibres, cotton, regenerated cellulosic fibres, polyester, PAN, and novoloid fibres. All of the selected fabrics were either inherently FR or treated to be FR.

The fabrics investigated as potential candidates for the sensor substrate were subjected to accelerated ageing conditions selected to simulate conditions that are encountered by firefighters while on duty and their residual mechanical strength measured. The purpose of this assessment was to identify the fabrics that can resist ageing conditions that are known to be damaging to the FR clothing to ensure that the sensor fabric substrate does not interfere with the operation of the sensor over the life of the garment. The criterion used to determine the accelerated ageing conditions for the fabric assessment was the point at which the performance of the outer shell fabrics reaches the minimum strength requirement established in NFPA 1971 (2018) for structural firefighting and proximity firefighting protective ensembles when exposed to the accelerated ageing conditions. The effect of different accelerated ageing conditions on the mechanical performance of fire protective fabrics used as an outer shell of firefighters' clothing was also characterized for comparison purposes.

The fabrics reacted differently to the four types of ageing conditions applied: thermal ageing for 42 h at 235 °C, photochemical ageing for 243 h at 1 W/m² at 340 nm at a

temperature of 80 °C, hydrothermal ageing by immersion in 80 °C water for 15, 24 and 31 days, and accelerated laundering with 10 washing/drying cycles at 60 °C in a Launder-Ometer[®]. Some ageing conditions did not affect some of the fabrics while other conditions left them severely damaged. Based on the behaviour observed for the different fabrics tested, Nomex[®] IIIA was identified as the best material candidate because of its superior performance after exposure to accelerated thermal ageing and good resistance to hydrothermal ageing and accelerated laundering. It exhibits a high sensitivity to UV radiation but may be protected by a surface treatment.

The last step of the study involved verifying the quality of the bond between the rGO coating and the selected substrate fabric. A good conductivity was obtained after the application of a 10-layer rGO coating. However, the coating failed after the third cycle of an accelerated laundering treatment at 40 °C. By comparison, satisfactory results in terms of resistance of an rGO coating to laundering have been reported with a similar Nomex fabric, yet involving shorter cycles and less severe laundering conditions.

5.2. Recommendations

In future studies, a surface treatment to protect the Nomex[®] IIIA fabric selected as a substrate for the EOL sensor from UV degradation should be investigated. Possible solutions include the use of UV blockers and absorbers such as carbon black or titanium dioxide nanoparticles.

Work also needs to be pursued to improve the rGO coating protocol to increase its resistance to the service conditions of the protective garments, including laundering. In

addition, an accelerated laundering protocol more representative of what is experienced by fire protective clothing should be employed.

BIBLIOGRAPHY

- AATCC TM20 (2018). Standard Test Method for Fiber Analysis: Qualitative. AATCC Committee RA24. Retrieved from: <https://members.aatcc.org/store/tm20/485/>
- AATCC TM135 (2018). Dimensional Changes of Fabrics after Home Laundering. AATCC Committee RA64. <https://members.aatcc.org/store/tm135/543/>
- AATCC TM186 (2015). Standard Test Method for Weather Resistance: UV Light and Moisture Exposure. AATCC Committee RA64. <https://members.aatcc.org/store/tm186/582/>
- Abe, Y., & Yabuki, K. (2012). Lyotropic Polycondensation including Fibers. In *Polymer Science: A Comprehensive Reference* (pp. 469–495). Elsevier. <https://doi.org/10.1016/B978-0-444-53349-4.00150-3>
- Abu Obaid, A., Yarlagadda, S., & Gillespie, J. (2015). Combined effects of kink bands and hygrothermal conditioning on tensile strength of polyarylate liquid crystal co-polymer and aramid fibers. *Journal of Composite Materials*, 50(3), 339–350. <https://doi.org/10.1177/0021998315574754>
- Alagirusamy, R., & Das, A. (2015). Chapter 8—Conversion of Fibre to Yarn: An Overview. In R. Sinclair (Ed.), *Textiles and Fashion* (pp. 159–189). Woodhead Publishing. <https://doi.org/10.1016/B978-1-84569-931-4.00008-8>
- Alebeid, O. K., & Zhao, T. (2017). Review on: Developing UV protection for cotton fabric. *The Journal of The Textile Institute*, 108(12), 2027–2039. <https://doi.org/10.1080/00405000.2017.1311201>
- Alongi, J., Frache, A., Malucelli, G., & Camino, G. (2013). 4—Multi-component flame resistant coating techniques for textiles. In F. S. Kilinc (Ed.), *Handbook of Fire Resistant Textiles* (pp. 68–93). Woodhead Publishing. <https://doi.org/10.1533/9780857098931.1.68>
- Arrieta, C., David, E., Dolez, P., & Vu-Khanh, T. (2010). Thermal aging of a blend of high-performance fibers. *Journal of Applied Polymer Science*, 115(5), 3031–3039. <https://doi.org/10.1002/app.30825>

- Arrieta, C., David, É., Dolez, P., & Vu-Khanh, T. (2011a). Hydrolytic and photochemical aging studies of a Kevlar[®]-PBI blend. *Polymer Degradation and Stability*, 96(8), 1411–1419. <https://doi.org/10.1016/j.polymdegradstab.2011.05.015>
- Arrieta, C., David, E., Dolez, P., & Vu-Khanh, T. (2011b). X-ray diffraction, Raman, and differential thermal analyses of the thermal aging of a Kevlar[®]-PBI blend fabric. *Polymer Composites*, 32(3), 362–367. <https://doi.org/10.1002/pc.21041>
- ASTM D1777 (2019). Standard Test Method for Thickness of Textile Materials. ASTM International. <https://doi.org/10.1520/D1777-96R19>
- ASTM D3776 /D3776M (2020). Standard Test Methods for Mass Per Unit Area (Weight) of. ASTM International. <https://doi.org/10.1520/D3776-96>
- ASTM D3775 (2017). Standard Test Method for Fabric Count of Woven Fabric. ASTM International. <https://doi.org/10.1520/D3775-03>
- ASTM D5035 (2019). Standard test Method for Breaking Force and Elongation of Textile Fabrics (Strip Method). ASTM International. <https://doi.org/10.1520/D5035-06>
- ASTM D5587 (2015). Standard test method for the tearing Strength of Fabrics by Trapezoidal method, ASTM International. <https://doi.org/10.1520/D5587-15R19>
- Aveston, J., Kelly, A., & Sillwood, J. M. (1980). Long term strength of glass reinforced plastics in wet environments. In A. R. Bunsell, C. Bathias, A. Martrenchar, D. Menkes, & G. Verchery (Eds.), *Advances in Composite Materials* (pp. 556–568). Elsevier. <https://doi.org/10.1016/B978-1-4832-8370-8.50046-2>
- Bajaj, P., & Sengupta, A. K. (1992). Protective clothing. *Textile Progress*, 22(2–4), 1–110. <https://doi.org/10.1080/00405169208688856>
- Bajaj, P. (2000). 10- Heat and flame protection. In A.R. Horrocks and S.C. Anand (Eds.), *Handbook of Technical Textiles* (pp. 223–263). Woodhead Publishing. <https://doi.org/10.1533/9781855738966.223>
- Barker, R S., Drews, M. J. (1985). 11—Flame retardants for cellulose materials. In T. P. Navell & S. Haig Zeronian (Eds.), *Cellulose chemistry and its application* (pp. 423–454). Chichester, West Sussex, England. <http://hdl.handle.net/2027/umn.31951000333946z>
- Barker, R. L. (2005). *A Review of gaps and limitations in test methods for first responder protective clothing and equipment: A final report presented to National Personal*

- Protection Technology Laboratory, National Institute for Occupational Safety and Health (NIOSH)* (cdc:25330). <https://stacks.cdc.gov/view/cdc/25330>
- Beers, D., Young, R. J., SO, C. L., Sikkema, D. J., Perepelkin, K. E., & Weedon, G. (2001). 4-Other high modulus-high tenacity (HM-HT) fibres from linear polymers. In J. W. S. Hearle (Ed.), *High-Performance Fibres* (pp. 93–155). Woodhead Publishing. <https://doi.org/10.1533/9781855737549.93>
- Bhat, G. S. (2013). 12—Flame resistant nonwoven fabrics. In F. S. Kilinc (Ed.), *Handbook of Fire Resistant Textiles* (pp. 322–348). Woodhead Publishing. <https://doi.org/10.1533/9780857098931.2.322>
- Bellenger, V., Ganem, M., Mortaigne, B., & Verdu, J. (1995). Lifetime prediction in the hydrolytic ageing of polyesters. *Polymer Degradation and Stability*, 49(1), 91–97. [https://doi.org/10.1016/0141-3910\(95\)00049-R](https://doi.org/10.1016/0141-3910(95)00049-R)
- Bendak, A., & El-Marsafi, S. M. (1991). Effects of Chemical Modifications on Polyester Fibres. *Medical Journal of Islamic World Academy of Sciences*, 4(4), 275–284.
- Bourbigot, S., Flambard, X., & Poutch, F. (2001). Study of the thermal degradation of high performance fibres—Application to polybenzazole and p-aramid fibres. *Polymer Degradation and Stability*, 74(2), 283–290. [https://doi.org/10.1016/S0141-3910\(01\)00159-8](https://doi.org/10.1016/S0141-3910(01)00159-8)
- Bourbigot, S., & Flambard, X. (2002). Heat resistance and flammability of high performance fibres: A review. *Fire and Materials*, 26(4–5), 155–168. <https://doi.org/10.1002/fam.799>
- Bourbigot, S. (2008). 2—Flame retardancy of textiles: New approaches. In A. R. Horrocks & D. Price (Eds.), *Advances in Fire Retardant Materials* (pp. 9–40). Woodhead Publishing. <https://doi.org/10.1533/9781845694701.1.9>
- Brennan, P., Fedo, C. (1994). Sunlight, UV, & Accelerated Weathering. *Weathering-LU-0822. Q-Panel Lab Products*. Cleveland, OH. <http://www.q-lab-corporation.ru/doc/Weathering-LU-0822.pdf>
- Brinsko, K. M., Sparena, S. B., & King, M. B. (2016). Examining the Effects of Environmental Degradation on the Optical Properties of Manufactured Fibers of Natural Origin. *McCrone Research Institute*, 37.

- Brooks, N. W., Duckett, R. A., Rose, J., Ward, I. M., & Clements, J. (1993). An n.m.r. study of absorbed water in polybenzimidazole. *Polymer*, 34(19), 4038–4042.
[https://doi.org/10.1016/0032-3861\(93\)90664-V](https://doi.org/10.1016/0032-3861(93)90664-V)
- Brown, J. R., Burchill, P. J., George, G. A., & Power, A. J. (1975). The photodegradation of poly 2,2'-(m-phenylene)-5,5'-bibenzimidazole. *Journal of Polymer Science: Polymer Symposia*, 49(1), 239–247. <https://doi.org/10.1002/polc.5070490124>
- Burrow, T. (2013). 8—Flame resistant manmade cellulosic fibres. In F. S. Kilinc (Ed.), *Handbook of Fire Resistant Textiles* (pp. 221–244). Woodhead Publishing.
<https://doi.org/10.1533/9780857098931.2.221>
- Cameron, N. (1968). Effect of Environment and Temperature on Strength of E-Glass Fibres .2. Heating and Ageing. *Glass Technology*, 9(5), 121-+.
- Chen, J. (2015). Chapter 4—Synthetic Textile Fibers: Regenerated Cellulose Fibers. In R. Sinclair (Ed.), *Textiles and Fashion* (pp. 79–95). Woodhead Publishing.
<https://doi.org/10.1016/B978-1-84569-931-4.00004-0>
- Chin, J., Forster, A., Clerici, C., Sung, L., Oudina, M., & Rice, K. (2007). Temperature and humidity aging of poly(p-phenylene-2,6-benzobisoxazole) fibers: Chemical and physical characterization. *Polymer Degradation and Stability*, 92(7), 1234–1246.
<https://doi.org/10.1016/j.polymdegradstab.2007.03.030>
- Cho, C., Elias, A., Batcheller, J., Dolez, P., & Chung, H.-J. (2019). Electrical conduction of reduced graphene oxide coated meta-aramid textile and its evolution under aging conditions. *Journal of Industrial Textiles*, 1528083719869387.
<https://doi.org/10.1177/1528083719869387>
- Choudhury, A. K. R. (2017). 8—Flame- and fire-retardant finishes. In A. K. Roy Choudhury (Ed.), *Principles of Textile Finishing* (pp. 195–244). Woodhead Publishing.
<https://doi.org/10.1016/B978-0-08-100646-7.00008-4>
- Coffin, D. R., Serad, G. A., Hicks, H. L., & Montgomery, R. T. (1982). Properties and Applications of Celanese PBI—Polybenzimidazole Fiber. *Textile Research Journal*, 52(7), 466–472. <https://doi.org/10.1177/004051758205200706>
- Collier, D. J., Tortora, P. G. (2001). 23-Finishes That Affect Performance. In D. J. Collier & SP. J. Tortora (Eds.), *Understanding Textiles, 6th Edition*. New Jersey. Pearson Education.

- Couvrette, S. T. (2015). The effect of wear and laundering on the moisture management performance of Nomex base layer garments. *Oregon State University*, Corvallis, OR.
- Crown, E. M., & Dale, J. D. (2005). 25—Protection for workers in the oil and gas industries. In R. A. Scott (Ed.), *Textiles for Protection* (pp. 699–713). Woodhead Publishing. <https://doi.org/10.1533/9781845690977.3.699>
- Crown, E. M., & Batcheller, J. C. (2016). 9—Technical textiles for personal thermal protection. In A. R. Horrocks & S. C. Anand (Eds.), *Handbook of Technical Textiles (Second Edition)* (pp. 271–285). Woodhead Publishing. <https://doi.org/10.1016/B978-1-78242-465-9.00009-4>
- Davis, R., Chin, J., Lin, C.-C., & Petit, S. (2010). Accelerated weathering of polyaramid and polybenzimidazole firefighter protective clothing fabrics. *Polymer Degradation and Stability*, 95(9), 1642–1654. <https://doi.org/10.1016/j.polymdegradstab.2010.05.029>
- Dawkins, B. G., Qin, F., Gruender, M., & Copeland, G. S. (2014). 7—Polybenzimidazole (PBI) high temperature polymers and blends. In M. T. DeMeuse (Ed.), *High Temperature Polymer Blends* (pp. 174–212). Woodhead Publishing. <https://doi.org/10.1533/9780857099013.174>
- Deopura, B. L., & Padaki, N. V. (2015). Chapter 5—Synthetic Textile Fibres: Polyamide, Polyester and Aramid Fibres. In R. Sinclair (Ed.), *Textiles and Fashion* (pp. 97–114). Woodhead Publishing. <https://doi.org/10.1016/B978-1-84569-931-4.00005-2>
- Dolez, P. I. (2019a). Unpublished data.
- Dolez, P. I. (2019b). Chapter 6—Application of nanomaterials in textile coatings and finishes. In P. Nguyen Tri, S. Rtimi, & C. M. Ouellet Plamondon (Eds.), *Nanomaterials-Based Coatings* (pp. 139–169). Elsevier. <https://doi.org/10.1016/B978-0-12-815884-5.00006-5>
- Dolez, P. I., Tomer, N. S., & Malajati, Y. (2019). A quantitative method to compare the effect of thermal aging on the mechanical performance of fire protective fabrics. *Journal of Applied Polymer Science*, 136(6), 47045. <https://doi.org/10.1002/app.47045>
- Dolez P, Malajati Y. (2020). Resistance of Fire Protective Fabrics to Repeated Launderings. Performance of Protective Clothing and Equipment: Innovative Solutions to Evolving Challenges. (STP 1624): 1-26. In Press, *ASTM International*. <https://doi.org/10.1520/STP162420190079>

- Dupont Inc. (2019). Nomex[®] fire - Technical guide. Retrieved from:
[https://www.dupont.com/content/dam/dupont/amer/us/en/personal-protection/public/documents/en/Nomex\(R\)%20Fiber%20Technical%20Guide.pdf](https://www.dupont.com/content/dam/dupont/amer/us/en/personal-protection/public/documents/en/Nomex(R)%20Fiber%20Technical%20Guide.pdf)
- Dupont Inc. (2017). Kevlar[®] aramid fire - Technical guide. Retrieved from:
https://www.dupont.com/content/dam/dupont/amer/us/en/safety/public/documents/en/Kevlar_Technical_Guide_0319.pdf
- DuPont Inc. (2001). Technical guide for Nomex - brand fibre. Virginia. Retrieved from:
<https://docplayer.net/23919360-Technical-information-h-revised-july-2001-replaces-h-april-1999.html>
- El Aidani, R., Dolez, P. I., & Vu-Khanh, T. (2011). Effect of thermal aging on the mechanical and barrier properties of an e-PTFE/Nomex[®] moisture membrane used in firefighters' protective suits. *Journal of Applied Polymer Science*, *121*(5), 3101–3110.
<https://doi.org/10.1002/app.33991>
- El Aidani, R., Nguyen-Tri, P., Malajati, Y., Lara, J., & Vu-Khanh, T. (2013). Photochemical aging of an e-PTFE/NOMEX[®] membrane used in firefighter protective clothing. *Polymer Degradation and Stability*, *98*(7), 1300–1310.
<https://doi.org/10.1016/j.polymdegradstab.2013.04.002>
- Fabian T., Kerber S. I., Gandhi P. D., Baxter C. S., Ross C. S., Lockey J. E., and Dalton J.M. (2010). *Firefighter exposure to smoke particulates*. Northbrook, IL: Underwriters Laboratories.
- Fette, R. B., & Sovinski, M. F. (2004). *Vectran Fiber Time-Dependent Behavior and Additional Static Loading Properties*. NASA TM-2004-212773, 2004.
- FiberLine, Co. (n.d.). *Novoloid: High Temperature Packing Yarn*. Gunei Chemical Industry Co. Ltd.; Kynol, Inc. Retrieved from <https://www.fiber-line.com/en/fibers/novoloid/>
- Forster, A. L., Pintus, P., Messin, G. H. R., Riley, M. A., Petit, S., Rossiter, W., Chin, J., & Rice, K. D. (2011). Hydrolytic stability of polybenzobisoxazole and polyterephthalamide body armor. *Polymer Degradation and Stability*, *96*(2), 247–254.
<https://doi.org/10.1016/j.polymdegradstab.2010.10.004>
- Frank, E., Ingildeev, D., & Buchmeiser, M. R. (2017). 2—High-performance PAN-based carbon fibers and their performance requirements. In G. Bhat (Ed.), *Structure and*

- Properties of High-Performance Fibers* (pp. 7–30). Woodhead Publishing.
<https://doi.org/10.1016/B978-0-08-100550-7.00002-4>
- Fei, B. (2018). 2—High-performance fibers for textiles. In M. Miao & J. H. Xin (Eds.), *Engineering of High-Performance Textiles* (pp. 27–58). Woodhead Publishing.
<https://doi.org/10.1016/B978-0-08-101273-4.00002-0>
- Fung, W. (2000). 18—Textiles in transportation. In A. R. Horrocks & S. C. Anand (Eds.), *Handbook of Technical Textiles* (pp. 490–528). Woodhead Publishing.
<https://doi.org/10.1533/9781855738966.490>
- Fynn, P. J., and J. D. Dean. (1951). Effect of light on cotton textiles. *In Yearbook of Agriculture 1950-1951*, (pp. 436-40). U.S. Department of Agriculture.
<https://naldc.nal.usda.gov/download/IND43894097/PDF>
- Gabara, V., Hartzler J, D., Lee, Kiu-Seung., Rodini, J, D., and Yang, H.H. (2007). 13-Aramid Fibers. In M. Lewin (Ed.), *Handbook of Fiber Chemistry* (p. 975–1029). Boca Raton: CRC Press, <https://doi-org.login.ezproxy.library.ualberta.ca/10.1201/9781420015270>
- Geim, A. K., & Novoselov, K. S. (2007). The rise of graphene. *Nature Materials*, 6(3), 183–191. <https://doi.org/10.1038/nmat1849>
- Giwa, A., Isa, M. T., & Idris, U. A. (2013). Analysis of Some Physical and Mechanical Properties of Selected Fabrics. *International Journal of Textile Science*, 2(3), 49–58.
- Gong, R. H., & Chen, X. (2000). 3—Technical yarns. In A. R. Horrocks & S. C. Anand (Eds.), *Handbook of Technical Textiles* (pp. 42–61). Woodhead Publishing.
<https://doi.org/10.1533/9781855738966.42>
- Gu, H. (2005). Ultraviolet treatment on high performance filaments. *Materials & Design*, 26(1), 47–51. <https://doi.org/10.1016/j.matdes.2004.04.009>
- Gu, H. (2009). Research on thermal properties of Nomex/Viscose FR fibre blended fabric. *Materials & Design*, 30(10), 4324–4327. <https://doi.org/10.1016/j.matdes.2009.04.012>
- Guo, X., Zhu, Z., Wang, J., Lin, Y., & Chen, G. (2020). Dimensional stability of glass fiber reinforced poplar scrimber. *Materialwissenschaft Und Werkstofftechnik*, 51(10), 1364–1371. <https://doi.org/10.1002/mawe.202000001>
- Gupta, A. (2005). *Improving UV resistance of high strength fibers*. North Carolina State University, Raleigh.

- Hall, M. E., Zhang, J., & Horrocks, A. R. (1994a). The flammability of polyacrylonitrile and its copolymers. *Polymer Degradation and Stability*, 44(3), 379-386. ISSN 0141-3910, [https://doi.org/10.1016/0141-3910\(94\)90097-3](https://doi.org/10.1016/0141-3910(94)90097-3)
- Hall, M. E., Zhang, J., & Horrocks, A. R. (1994b). The flammability of polyacrylonitrile and its copolymers III. Effect of flame retardants. *Fire and Materials*, 18(4), 231-241. <https://doi.org/10.1002/fam.810180406>
- Hansora, D. P., Shimpi, N. G., & Mishra, S. (2015). Performance of hybrid nanostructured conductive cotton materials as wearable devices: An overview of materials, fabrication, properties and applications. *RSC Advances*, 5(130), 107716-107770. <https://doi.org/10.1039/C5RA16478H>
- Hao, W., Zhang, X., & Tian, Y. (2019). Thermal, Mechanical, and Microstructural Study of PBO Fiber during Carbonization. *Materials*, 12, 608. <https://doi.org/10.3390/ma12040608>
- Hart, S. V. (2005). *Third Status Report to the Attorney General on Body Armor Safety Initiative Testing and Activities*. Washington, DC. National Institute of Justice.
- Hawkins, W. L. (1984). Polymer Degradation. In W. L. Hawkins (Ed.), *Polymer Degradation and Stabilization* (pp. 3-34). Springer. https://doi.org/10.1007/978-3-642-69376-2_2
- Hearle, J. W. S. (2009). 13—Thermally and chemically resistant fibres: Structure and properties. In S. J. Eichhorn, J. W. S. Hearle, M. Jaffe, & T. Kikutani (Eds.), *Handbook of Textile Fibre Structure* (Vol. 2, pp. 450-457). Woodhead Publishing. <https://doi.org/10.1533/9781845697310.3.450>
- Holcombe, B. V. (1981). The evaluation of protective clothing. *Fire Safety Journal*, 4(2), 91-101. [https://doi.org/10.1016/0379-7112\(81\)90008-4](https://doi.org/10.1016/0379-7112(81)90008-4)
- Horrocks, A. R., & Kandola, B. K. (1998). Flame retardant cellulosic textiles. In M. Le Bras, G. Camino, S. Bourbigot, & R. Delobel (Eds.), *Fire Retardancy of Polymers* (pp. 343-362). Woodhead Publishing. <https://doi.org/10.1533/9781845698584.4.341>
- Horrocks, A. R., Eichhorn, H., Schwaenke, H., Saville, N., & Thomas, C. (2001). 9—Thermally resistant fibres. In J. W. S. Hearle (Ed.), *High-Performance Fibres* (pp. 281-324). Woodhead Publishing. <https://doi.org/10.1533/9781855737549.281>

- Horrocks, A. R. (2011). Flame retardant challenges for textiles and fibres: New chemistry versus innovatory solutions. *Polymer Degradation and Stability*, 96(3), 377–392. <https://doi.org/10.1016/j.polymdegradstab.2010.03.036>
- Horrocks, A. R., & Kandola, B. K. (2013). 11—Flame resistant composites and nanocomposites. In F. S. Kilinc (Ed.), *Handbook of Fire Resistant Textiles* (pp. 283–321). Woodhead Publishing. <https://doi.org/10.1533/9780857098931.2.283>
- Horrocks, A. R. (2014). 4—High performance textiles for heat and fire protection. In C. A. Lawrence (Ed.), *High Performance Textiles and their Applications* (pp. 144–175). Woodhead Publishing. <https://doi.org/10.1533/9780857099075.144>
- Horrocks, A. R. (2016). 8—Technical fibres for heat and flame protection. In A. R. Horrocks & S. C. Anand (Eds.), *Handbook of Technical Textiles (Second Edition)* (pp. 237–270). Woodhead Publishing. <https://doi.org/10.1016/B978-1-78242-465-9.00008-2>
- Hoschke, B. N. (1981). Standard and specifications for firefighters' clothing. *Fire Safety Journal*, 4(2), 125–137. [https://doi.org/10.1016/0379-7112\(81\)90011-4](https://doi.org/10.1016/0379-7112(81)90011-4)
- Houshyar, S., Padhye, R., Nayak, R., & Shanks, R. (2016). Deterioration of polyaramid and polybenzimidazole woven fabrics after ultraviolet irradiation. *Journal of Applied Polymer Science*, 121(5), 3101–3110. <https://doi.org/10.1002/app.43073>
- Houshyar, S., Padhye, R., Ranjan, S., Tew, S., & Nayak, R. (2018). The impact of ultraviolet light exposure on the performance of polybenzimidazole and polyaramid fabrics: Prediction of end-of-life performance. *Journal of Industrial Textiles*, 48(1), 77–86. <https://doi.org/10.1177/1528083717725112>
- Hu, J., Jahid, M. A., Kumar, N. H., & Harun, V. (2020). 1- Fundamentals of the Fibrous Materials. In *Handbook of Fibrous Materials, Volume 1—Production and Characterization/Volume 2—Applications in Energy, Environmental Science and Healthcare*. John Wiley & Sons. <https://app.knovel.com/hotlink/pdf/id:kt012ER0E5/handbook-fibrous-materials/what-fibrous-materials>
- Huson, M. G. (2017). 3—High-performance pitch-based carbon fibers. In G. Bhat (Ed.), *Structure and Properties of High-Performance Fibers* (pp. 31–78). Woodhead Publishing. <https://doi.org/10.1016/B978-0-08-100550-7.00003-6>

- International Association of Firefighters (2001). 2000 Death and Injury Survey. International Association of Firefighters, Washington, DC. <https://www.iaff.org/wp-content/uploads/2019/05/2000-DI-1.pdf>
- ISO 105-C06 (2010). Textiles—Tests for colour fastness—Part C06: Colour fastness to domestic and commercial laundering. International Organization for Standardization.
- Izdebska, J. (2016). 22—Aging and Degradation of Printed Materials. In J. Izdebska & S. Thomas (Eds.), *Printing on Polymers* (pp. 353–370). William Andrew Publishing. <https://doi.org/10.1016/B978-0-323-37468-2.00022-1>
- Jaffe, M., East, A. J. (2007). 1-Polyester fibers. In M. Lewin, (Ed.). *Handbook of Fiber Chemistry* (p. 2–26). Boca Raton: CRC Press, <https://doi.org.login.ezproxy.library.ualberta.ca/10.1201/9781420015270>
- Jain, A., & Vijayan, K. (2002). Thermally induced structural changes in Nomex fibres. *Bulletin of Materials Science*, 25. <https://doi.org/10.1007/BF02704129>
- Jassal, M., Agrawal, A. K., Gupta, D., & Panwar, K. (2020). 8- Aramid fibres. In In J, Hu., B, Kumar., & J, Lu. (Eds), *Handbook of Fibrous Materials, Volume 1—Production and Characterization/Volume 2—Applications in Energy, Environmental Science and Healthcare*. John Wiley & Sons. <https://app.knovel.com/hotlink/pdf/id:kt012ER5C1/handbook-fibrous-materials/preparation-aromatic>
- Jiang, F. (2020). 4- Cellulose Fibers. In J, Hu., B, Kumar., & J, Lu. (Eds), *Handbook of Fibrous Materials, Volume 1—Production and Characterization/Volume 2—Applications in Energy, Environmental Science and Healthcare*. John Wiley & Sons. <https://app.knovel.com/hotlink/pdf/id:kt012ER0E5/handbook-fibrous-materials/what-fibrous-materials>
- Jones, F. R. (2001). 6—Glass fibres. In J. W. S. Hearle (Ed.), *High-Performance Fibres* (pp. 191–238). Woodhead Publishing. <https://doi.org/10.1533/9781855737549.191>
- Jones, F. R., & Huff, N. T. (2009). 9—The structure and properties of glass fibres. In S. J. Eichhorn, J. W. S. Hearle, M. Jaffe, & T. Kikutani (Eds.), *Handbook of Textile Fibre Structure* (Vol. 2, pp. 307–352). Woodhead Publishing. <https://doi.org/10.1533/9781845697310.3.307>

- Joseph, P., & Tretsiakova-McNally, S. (2013). 3—Chemical modification of natural and synthetic textile fibres to improve flame retardancy. In F. S. Kilinc (Ed.), *Handbook of Fire Resistant Textiles* (pp. 37–67). Woodhead Publishing.
<https://doi.org/10.1533/9780857098931.1.37>
- Keir, J. L. A., Akhtar, U. S., Matschke, D. M. J., Kirkham, T. L., Chan, H. M., Ayotte, P., White, P. A., & Blais, J. M. (2017). Elevated Exposures to Polycyclic Aromatic Hydrocarbons and Other Organic Mutagens in Ottawa Firefighters Participating in Emergency, On-Shift Fire Suppression. *Environmental Science & Technology*, 51(21), 12745–12755. <https://doi.org/10.1021/acs.est.7b02850>
- Khazanov V.E., Kolesov Y.I., Trofimov N.N. (1995). 1-Glass fibres. In V.I. Kostikov (Ed.), *Fibre Science and Technology*. Soviet Advanced Composites Technology Series, vol 5. Springer, Dordrecht. https://doi-org.login.ezproxy.library.ualberta.ca/10.1007/978-94-011-0565-1_2
- King, A. L. (2012). Influence of Trace-Metals on the Colour and Photostability of Wool. PhD thesis, 2012, Deakin University. <https://dro.deakin.edu.au/eserv/DU:30043933/king-thesis-2011.pdf>
- Kotek, R. (2007). 10-Regenerated Cellulose Fibers. In M. Lewin, (Ed.), *Handbook of Fiber Chemistry* (p. 668–764). Boca Raton: CRC Press. <https://doi-org.login.ezproxy.library.ualberta.ca/10.1201/9781420015270>
- Kunadharaju, K., Smith, T. D., & DeJoy, D. M. (2011). Line-of-duty deaths among U.S. firefighters: An analysis of fatality investigations. *Accident Analysis & Prevention*, 43(3), 1171–1180. <https://doi.org/10.1016/j.aap.2010.12.030>
- Kuraray, Co. (2014). *Vectran™ (Enhance • Transform • Discover), LIQUID CRYSTAL POLYMER FIBER TECHNOLOGY*. America, Inc, Houston, Kuraray Company.
Retrieved from
https://www.kuraray.eu/fileadmin/product_ranges/vectran/downloads/2017_VECTRAN_Product_Brochure.pdf
- Lavin, J. G. (2001). 5—Carbon fibres. In J. W. S. Hearle (Ed.), *High-Performance Fibres* (pp. 156–190). Woodhead Publishing. <https://doi.org/10.1533/9781855737549.156>
- Lawson, L. K., Crown, E. M., Ackerman, M. Y., & Douglas Dale, J. (2004). Moisture Effects in Heat Transfer Through Clothing Systems for Wildland Firefighters. *International*

- Journal of Occupational Safety and Ergonomics*, 10(3), 227–238.
<https://doi.org/10.1080/10803548.2004.11076610>
- Lecoeur, E., Vroman, I., Bourbigot, S., Lam, T. M., & Delobel, R. (2001). Flame retardant formulations for cotton. *Polymer Degradation and Stability*, 74(3), 487–492.
[https://doi.org/10.1016/S0141-3910\(01\)00172-0](https://doi.org/10.1016/S0141-3910(01)00172-0)
- Lee, T., Lee, W., Kim, S. W., Kim, J. J., & Kim, B. S. (2016). Flexible Textile Strain Wireless Sensor Functionalized with Hybrid Carbon Nanomaterials Supported ZnO Nanowires with Controlled Aspect Ratio. *Advanced Functional Materials*, 26(34), 6206–6214. <https://doi.org/10.1002/adfm.201601237>
- Li, C.-S., Zhan, M.-S., Huang, X.-C., & Zhou, H. (2012). The evolution of structure and properties of poly(p-phenylene terephthalamide) during the hydrothermal aging. *Journal of Applied Polymer Science*, 126(2), 552–558. <https://doi.org/10.1002/app.36822>
- Li, P., Wang, B., Xu, Y.-J., Jiang, Z., Dong, C., Liu, Y., & Zhu, P. (2019a). Ecofriendly Flame-Retardant Cotton Fabrics: Preparation, Flame Retardancy, Thermal Degradation Properties, and Mechanism. *ACS Sustainable Chemistry & Engineering*, 7(23), 19246–19256. <https://doi.org/10.1021/acssuschemeng.9b05523>
- Li, L., Song, J., Lei, Z., Kang, A., Wang, Z., Men, R., & Ma, Y. (2019b). Effects of ambient humidity and thermal aging on properties of Nomex insulation in mining dry-type transformer. *High Voltage*. <https://digital-library.theiet.org/content/journals/10.1049/hve.2019.0293>
- Liu, S., Han, K., Chen, L., Zheng, Y., & Yu, M. (2015). Influence of air circulation on the structure and properties of melt-spun PAN precursor fibers during thermal oxidation. *RSC Advances*, 5(47), 37669–37674. <https://doi.org/10.1039/C5RA00476D>
- Liu, P., Mullins, M., Bremner, T., Browne, J. A., & Sue, H. J. (2016). Hygrothermal behavior of polybenzimidazole. *Polymer*, 93, 88–98.
<https://doi.org/10.1016/j.polymer.2016.04.020>
- Mäkinen, H. (1992). The Effect of Wear and Laundering on Flame-Retardant Fabrics. In J. McBriarty & N. Henry (Eds.), *Performance of Protective Clothing: Fourth Volume* (pp. 754-754–12). ASTM International. <https://doi.org/10.1520/STP19203S>

- Mäkinen, H. (2005). 22—Firefighters' protective clothing. In R. A. Scott (Ed.), *Textiles for Protection* (pp. 622–647). Woodhead Publishing.
<https://doi.org/10.1533/9781845690977.3.622>
- Mandal, S., Song, G., & Gholamreza, F. (2016). A novel protocol to characterize the thermal protective performance of fabrics in hot-water exposure. *Journal of Industrial Textiles*, 46(1), 279–291. <https://doi.org/10.1177/1528083715580522>
- Martynova, E., & Cebulla, H. (2018). Chapter 7—Glass Fibers. In B. Mahltig & Y. Kyosev (Eds.), *Inorganic and Composite Fibers* (pp. 131–163). Woodhead Publishing.
<https://doi.org/10.1016/B978-0-08-102228-3.00007-4>
- McQuerry, M., Klausning, S., Cotterill, D., & Easter, E. (2015). A Post-use Evaluation of Turnout Gear Using NFPA 1971 Standard on Protective Ensembles for Structural Fire Fighting and NFPA 1851 on Selection, Care and Maintenance. *Fire Technology*, 51(5), 1149–1166. <https://doi.org/10.1007/s10694-014-0446-x>
- Millington, K. R. (2018). 7—Colorfastness. In M. Miao & J. H. Xin (Eds.), *Engineering of High-Performance Textiles* (pp. 155–186). Woodhead Publishing.
<https://doi.org/10.1016/B978-0-08-101273-4.00029-9>
- Miraftab, M. (2000). 2—Technical fibres. In A. R. Horrocks & S. C. Anand (Eds.), *Handbook of Technical Textiles* (pp. 24–41). Woodhead Publishing.
<https://doi.org/10.1533/9781855738966.24>
- Munevar, L., Batcheller, J., Dolez, P. (2020). Effect of Specimen Size on the trapezoidal tear strength procedure. 119th Scientific Session of the Institute of Textile Science. Edmonton, AB, & Montréal (QC), March 3-4, 2020.
- Musto, P., Karasz, F. E., & MacKnight, W. J. (1993). Fourier transform infra-red spectroscopy on the thermo-oxidative degradation of polybenzimidazole and of a polybenzimidazole/polyetherimide blend. *Polymer*, 34(14), 2934–2945.
[https://doi.org/10.1016/0032-3861\(93\)90618-K](https://doi.org/10.1016/0032-3861(93)90618-K)
- Nazaré, S., Davis, R. D., Peng, J. S., & Chin, J. (2012). Accelerated Weathering of Firefighter Protective Clothing: Delineating the impact of Thermal, Moisture, and Ultraviolet Light Exposures (NIST TN 1746). *National Institute of Standards and Technology*.
<https://doi.org/10.6028/NIST.TN.1746>

- NFPA 1851 (2018). Standard on Selection, Care, and Maintenance of Protective Ensembles for Structural Fire Fighting and Proximity Fire Fighting. Retrieved from: <https://www-nfpa-org.login.ezproxy.library.ualberta.ca/codes-and-standards/all-codes-and-standards/list-of-codes-and-standards/detail?code=1851>
- NFPA 1851 (2020). Standard on Selection, Care, and Maintenance of Protective Ensembles for Structural Fire Fighting and Proximity Fire Fighting. Retrieved from: <https://www-nfpa-org.login.ezproxy.library.ualberta.ca/codes-and-standards/all-codes-and-standards/list-of-codes-and-standards/detail?code=1851>
- NFPA 1971 (2018). Standard on Protective Ensembles for Structural Fire Fighting and Proximity Fire Fighting. Retrieved from: <https://www-nfpa-org.login.ezproxy.library.ualberta.ca/codes-and-standards/all-codes-and-standards/list-of-codes-and-standards/detail?code=1971>
- Nguyen-Tri, P., El Aidani, R., Leborgne, É., Pham, T., & Vu-Khanh, T. (2014). Chemical aging of a polyester nonwoven membrane used in aerosol and drainage filter. *Polymer Degradation and Stability*, *101*, 71–80.
<https://doi.org/10.1016/j.polymdegradstab.2014.01.001>
- Ng, S. F., Hui, C. L., & Ip, C. (2012). 3—Dimensional stability of fabrics: Resistance to shrinkage and other dimensional changes. In P. A. Annis (Ed.), *Understanding and Improving the Durability of Textiles* (pp. 59–69). Woodhead Publishing.
<https://doi.org/10.1533/9780857097644.1.59>
- Niu, R., Han, K., Walsh, R. P., Buchholz, K., Goddard, R. E., Besara, T., & Siegrist, T. M. (2018). Aging Effect of Zylon. *IEEE Transactions on Applied Superconductivity*, *28*(3), 1–4. <https://doi.org/10.1109/TASC.2017.2783362>
- Ozgen, B., & Pamuk, G. (2014). Effects of Thermal Aging on Kevlar and Nomex Fabrics. *Industria Textilă*, *65*, 254–262.
- Parimala, H. V., & Vijayan, K. (1993). Effect of thermal exposure on the tensile properties of Kevlar fibres. *Journal of Materials Science Letters*, *12*(2).
<https://doi.org/10.1007/BF00241860>
- Pegoretti, A., & Traina, M. (2018). 17—Liquid crystalline organic fibers and their mechanical behavior. In A. R. Bunsell (Ed.), *Handbook of Properties of Textile and*

- Technical Fibres (Second Edition)* (pp. 621–697). Woodhead Publishing.
<https://doi.org/10.1016/B978-0-08-101272-7.00017-1>
- Pei, S., & Cheng, H.-M. (2012). The reduction of graphene oxide. *Carbon*, *50*(9), 3210–3228.
<https://doi.org/10.1016/j.carbon.2011.11.010>
- Perez, R. M., Sandler, J. K. W., Altstädt, V., Hoffmann, T., Pospiech, D., Ciesielski, M., & Döring, M. (2006). Effect of DOP-based compounds on fire retardancy, thermal stability, and mechanical properties of DGEBA cured with 4,4'-DDS. *Journal of Materials Science*, *41*(2), 341–353. <https://doi.org/10.1007/s10853-005-2720-2>
- Polymer Properties Database (n.d.). Phenolic Fibers. Retrieved from:
<https://polymerdatabase.com/Fibers/Novoloid.html>
- Pritchard, M., Sarsby, R. W., & Anand, S. C. (2000). 14—Textiles in civil engineering. Part 2 – natural fibre geotextiles. In A. R. Horrocks & S. C. Anand (Eds.), *Handbook of Technical Textiles* (pp. 372–406). Woodhead Publishing.
<https://doi.org/10.1533/9781855738966.372>
- Rebouillat, S. (2001). 2—Aramids. In J. W. S. Hearle (Ed.), *High-Performance Fibres* (pp. 23–61). Woodhead Publishing. <https://doi.org/10.1533/9781855737549.23>
- Rezazadeh, M., & Torvi, D. A. (2011). Assessment of Factors Affecting the Continuing Performance of Firefighters' Protective Clothing: A Literature Review. *Fire Technology*, *47*(3), 565–599. <https://doi.org/10.1007/s10694-010-0188-3>
- Rossi, R. (2003). Fire fighting and its influence on the body. *Ergonomics*, *46*, 1017–1033.
<https://doi.org/10.1080/0014013031000121968>
- Rossi, R., Bolli, W., & Stämpfli, R. (2008). Performance of Firefighters' Protective Clothing After Heat Exposure. *International Journal of Occupational Safety and Ergonomics : JOSE*, *14*, 55–60. <https://doi.org/10.1080/10803548.2008.11076747>
- Rossi, R. (2014). 3—Clothing for protection against heat and flames. In F. Wang & C. Gao (Eds.), *Protective Clothing* (pp. 70–89). Woodhead Publishing.
<https://doi.org/10.1533/9781782420408.1.70>
- Rowell, R., & Stout, H. (2007). 7-Jute and Kenaf. In M. Lewin, (Ed.), *Handbook of Fiber Chemistry* (p. 405–452). Boca Raton: CRC Press, <https://doi-org.login.ezproxy.library.ualberta.ca/10.1201/9781420015270>

- Rubeziene, V., Varnaite, S., Baltusnikaite, J., & Padleckiene, I. (2012). 6—Effects of light exposure on textile durability. In P. A. Annis (Ed.), *Understanding and Improving the Durability of Textiles* (pp. 104–125). Woodhead Publishing.
<https://doi.org/10.1533/9780857097644.1.104>
- Salavagione, H. J., Gómez-Fatou, M. A., Shuttleworth, P. S., & Ellis, G. J. (2018). New Perspectives on Graphene/Polymer Fibers and Fabrics for Smart Textiles: The Relevance of the Polymer/Graphene Interphase. *Frontiers in Materials*, 5, 18.
<https://doi.org/10.3389/fmats.2018.00018>
- Saville, B. P. (1999). 5—Strength and elongation tests. In B. P. Saville (Ed.), *Physical Testing of Textiles* (pp. 115–167). Woodhead Publishing.
<https://doi.org/10.1533/9781845690151.115>
- Senthil Kumar, P., & Suganya, S. (2017). 1—Introduction to sustainable fibres and textiles. In S. S. Muthu (Ed.), *Sustainable Fibres and Textiles* (pp. 1–18). Woodhead Publishing.
<https://doi.org/10.1016/B978-0-08-102041-8.00001-9>
- Shafizadeh, F. (1985). 11—Thermal degradation of cellulose. In T. P. Navell & S. H. Zeronian (Eds.), *Cellulose chemistry and its application* (pp. 266-289). West Sussex, England: <http://hdl.handle.net/2027/umn.31951000333946z>
- Shaw, A. (2012). 9- Durability of protective clothing. In P. Dolez & A. Annis (Eds.), *Understanding and Improving the Durability of Textiles*, Elsevier Science & Technology, ProQuest Ebook Central,
<https://ebookcentral.proquest.com/lib/ualberta/detail.action?docID=1575036>
- Shubha, M., Parimala, H. V., & Vijayan, K. (1993). Moisture uptake by kevlar fibres. *Journal of Materials Science Letters*, 12(1), 60–62. https://nal-ir.nal.res.in/2997/1/Moisture_Uptake.pdf
- Sinclair, R. (2015). Chapter 1—Understanding Textile Fibres and Their Properties: What is a Textile Fibre?. In Rose Sinclair (Ed.), *Textiles and Fashion* (pp. 3–27). Woodhead Publishing. <https://doi.org/10.1016/B978-1-84569-931-4.00001-5>
- Slater, K. (1991). Textile degradation. *Textile Progress*, 21, 1–150.
<https://doi.org/10.1080/00405169108688851>
- Sloan, F. (2017). 5—Liquid crystal aromatic polyester-arylate (LCP) fibers: Structure, properties, and applications. In G. Bhat (Ed.), *Structure and Properties of High-*

- Performance Fibers* (pp. 113–140). Woodhead Publishing.
<https://doi.org/10.1016/B978-0-08-100550-7.00005-X>
- Song, G., & Lu, Y. (2013). 19—Flame resistant textiles for structural and proximity fire fighting. In F. S. Kilinc (Ed.), *Handbook of Fire Resistant Textiles* (pp. 520–548). Woodhead Publishing. <https://doi.org/10.1533/9780857098931.4.520>
- Song, G., Mandal, S., & Rossi, R. M. (Eds.). (2017a). 1—Introduction. In *Thermal Protective Clothing for Firefighters* (pp. 1–4). Woodhead Publishing. <https://doi.org/10.1016/B978-0-08-101285-7.00001-0>
- Song, G., Mandal, S., & Rossi, R. M. (Eds.). (2017b). 4—Development of high performance thermal protective clothing. In *Thermal Protective Clothing for Firefighters* (pp. 27–55). Woodhead Publishing. <https://doi.org/10.1016/B978-0-08-101285-7.00004-6>
- Song, G., Mandal, S., & Rossi, R. M. (Eds.). (2017c). 5—Performance evaluation of thermal protective clothing. In *Thermal Protective Clothing for Firefighters* (pp. 57–144). Woodhead Publishing. <https://doi.org/10.1016/B978-0-08-101285-7.00005-8>
- Song, G., Mandal, S., & Rossi, R. M. (Eds.). (2017d). 7—Effects of various factors on performance of thermal protective clothing. In *Thermal Protective Clothing for Firefighters* (pp. 163–182). Woodhead Publishing. <https://doi.org/10.1016/B978-0-08-101285-7.00007-1>
- Song, G., & Su, Y. (2020). 30-Fibrous Materials for Thermal Protection. *Handbook of Fibrous Materials, Volume 1—Production and Characterization/Volume 2—Applications in Energy, Environmental Science and Healthcare*.
<https://app.knovel.com/hotlink/toc/id:kpHFMVPCV1/handbook-fibrous-materials/handbook-fibrous-materials>
- Stephenson, C. V., Lacey, J. C., & Wilcox, W. S. (1961a). Ultraviolet irradiation of plastics III. Decomposition products and mechanisms. *Journal of Polymer Science*, 55(162), 477–488. <https://doi.org/10.1002/pol.1961.1205516206>
- Stephenson, C. V., Moses, B. C., & Wilcox, W. S. (1961b). Ultraviolet irradiation of plastics. I. Degradation of physical properties. *Journal of Polymer Science*, 55(162), 451–464. <https://doi.org/10.1002/pol.1961.1205516204>
- Stull, J., & Stull, G. G. (2018). Fundamental changes needed to address turnout gear contamination. PPE101 Team. *FireRescue*. Retrieved from:

<http://web.archive.org/web/20190610002417/https://www.ppe101.com/2018/03/fundamental-changes-needed-to-address-turnout-gear-contamination/>

- Stull, J., & Stull, G. G. (2019). PPE advanced cleaning requirements in the new NFPA 1851. *FireRescue*. Retrieved from: <https://www.firerescue1.com/fire-products/personal-protective-equipment-ppe/articles/ppe-advanced-cleaning-requirements-in-the-new-nfpa-1851-pPhJ6VAAM3mPogIK/>
- Sun, X., Song, J., Zhang, J., Liu, J., Ke, H., Wei, Q., & Cai, Y. (2020). Effects of chemical pre-treatment on structure and property of polyacrylonitrile based pre-oxidized fibers. *Journal of Engineered Fibers and Fabrics*, 15, 1558925019898946. <https://doi.org/10.1177/1558925019898946>
- Tamargo-Martínez, K., Villar-Rodil, S., Paredes, J. I., Montes-Morán, M. A., Martínez-Alonso, A., & Tascón, J. M. D. (2004). Thermal decomposition of poly(p-phenylene benzobisoxazole) fibres: Monitoring the chemical and nanostructural changes by Raman spectroscopy and scanning probe microscopy. *Polymer Degradation and Stability*, 86(2), 263–268. <https://doi.org/10.1016/j.polymdegradstab.2004.05.004>
- Tanaka, K., Mizuno, S., Honda, H., Katayama, T., & Enoki, S. (2013). Effect of Water Absorption on the Mechanical Properties of Carbon Fiber/Polyamide Composites. *Journal of Solid Mechanics and Materials Engineering*, 7(5), 520–529. <https://doi.org/10.1299/jmmp.7.520>
- Testa, G., Sardella, A., Rossi, E., Bozzi, C., & Seves, A. (1994). The kinetics of cellulose fiber degradation and correlation with some tensile properties. *Acta Polymerica*, 45(1), 47–49. <https://doi.org/10.1002/actp.1994.010450109>
- TEXTECH. (n.d.). CarbonXRepel CR-80. Retrieved from: https://www.tradingsolutionsw.com/wp-content/uploads/2020/03/Data_Sheet_CR-80-1.pdf
- Textor, T., Derksen, L., Bahners, T., Gutmann, J. S., & Mayer-Gall, T. (2019). Abrasion resistance of textiles: Gaining insight into the damaging mechanisms of different test procedures. *Journal of Engineered Fibers and Fabrics*, 14, 1558925019829481. <https://doi.org/10.1177/1558925019829481>
- Thomas, W. F. (1960). An investigation of the factors likely to affect the strength and properties of glass fibres. *Phys Chem Glasses*, 1(1), 4–18.

- Toyobo. (2005). PBO fiber ZYLON. Retrieved from: https://www.toyobo-global.com/seihin/kc/pbo/zylon-p/bussei-p/technical_201118.pdf
- Tucker, P., Kerr, N., & Hersh, S.P. (1985). Photochemical damage of textiles. *In Textiles and Museum Lighting*, Symposium, Washington, DC, December 1980 (pp. 23-40). Harpers Ferry, WV: Harpers Ferry Regional Textile Group.
- Udayraj, Talukdar, P., Das, A., & Alagirusamy, R. (2016). Heat and mass transfer through thermal protective clothing – A review. *International Journal of Thermal Sciences*, 106, 32–56. <https://doi.org/10.1016/j.ijthermalsci.2016.03.006>
- Vanderschaaf, C.J., J.C. Batcheller, and D.A. Torvi. (2015). Combined effects of laundering and abrasion on the protective performance of flame resistant fabrics. Proceedings of Combustion Institute - Canadian Section, Spring Technical Meeting. Saskatoon, SK. FS6 - FS11.
- Vigneswaran, C., Ananthasubramanian, M., & Kandhavadi, P. (2014). 4—Bioprocessing of synthetic fibres. In C. Vigneswaran, M. Ananthasubramanian, & P. Kandhavadi (Eds.), *Bioprocessing of Textiles* (pp. 189–250). Woodhead Publishing India. <https://doi.org/10.1016/B978-93-80308-42-5.50004-4>
- Wakelyn, P. J., Bertoniere, N. R., French, A. D., Thibodeaus, D. P., Triplett, B. A., Rousselle, M., Goynes, W. R., Edwards, J. V., Hunter, L., Mcalister, D. D., Gamble, G. R. (2007). 9- Cotton fibres. In M. Lewin, (Ed.). *Handbook of Fiber Chemistry* (p. 521–666). Boca Raton: CRC Press, <https://doi-org.login.ezproxy.library.ualberta.ca/10.1201/9781420015270>
- Walsh, P. J., Hu, X., Cunniff, P., & Lesser, A. J. (2006). Environmental effects on poly-p-phenylenebenzobisoxazole fibers. I. Mechanisms of degradation. *Journal of Applied Polymer Science*, 102(4), 3517–3525. <https://doi.org/10.1002/app.24788>
- Wall, M. J., & Frank, G. C. (1971). A Study of the Spectral Distributions of Sun-Sky and Xenon-Arc Radiation in Relation to the Degradation of Some Textile Yarns: . Part I: Yarn Degradation. *Textile Research Journal*, 41(1), 32–38. <https://doi.org/10.1177/004051757104100106>
- XLANCE. (n.d.). XLANCE®. Retrieved from: <https://www.xlancefibre.com/about/>
- Yang, C., & He, Q. (2011). Applications of micro-scale combustion calorimetry to the studies of cotton and nylon fabrics treated with organophosphorus flame retardants. *Journal of*

Analytical and Applied Pyrolysis, 91, 125–133.

<https://doi.org/10.1016/j.jaap.2011.01.012>

Yang, C. Q. (2013). 7—Flame resistant cotton. In F. S. Kilinc (Ed.), *Handbook of Fire Resistant Textiles* (pp. 177–220). Woodhead Publishing.

<https://doi.org/10.1533/9780857098931.2.177>

Yang, H. M. (2018). 1.8 Aramid Fibers. In *Comprehensive Composite Materials II* (pp. 187–217). Elsevier. <https://doi.org/10.1016/B978-0-12-803581-8.10303-0>

Yao, L., Wu, L., Wu, H., Koo, J. H., & Krifa, M. (2019). Design and characterization of flame resistant blended nondrip PA6/Lenzing FR[®]/PBI fiber nonwoven fabrics. *Flame Retardancy and Thermal Stability of Materials*, 2(1), 49–59.

<https://doi.org/10.1515/flret-2019-0005>

Yatagai, M., & Zeronian, S. H. (1994). Effect of ultraviolet light and heat on the properties of cotton cellulose. *Cellulose*, 1(3), 205–214. <https://doi.org/10.1007/BF00813508>

Zambrano, M. C., Pawlak, J. J., Daystar, J., Ankeny, M., Cheng, J. J., & Venditti, R. A. (2019). Microfibers generated from the laundering of cotton, rayon and polyester based fabrics and their aquatic biodegradation. *Marine Pollution Bulletin*, 142, 394–407.

<https://doi.org/10.1016/j.marpolbul.2019.02.062>

Zhang, H., Song, G., Ren, H., & Cao, J. (2017). The effects of moisture on the thermal protective performance of firefighter protective clothing under medium intensity radiant exposure. *Textile Research Journal*, 88(8), 847–862.

<https://doi.org/10.1177/0040517517690620>

APPENDICES

Appendix A: Fabrics' characteristics

Table A1. Fabric A characteristics.


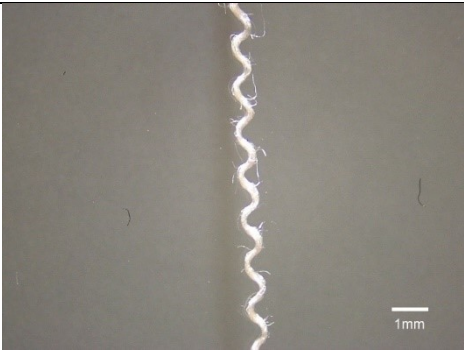
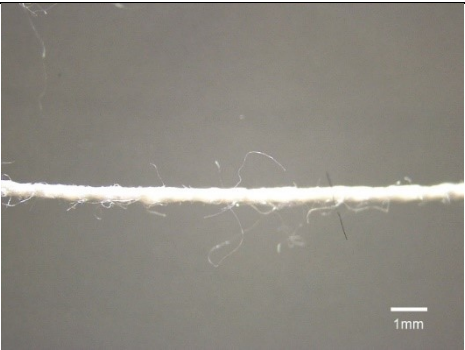
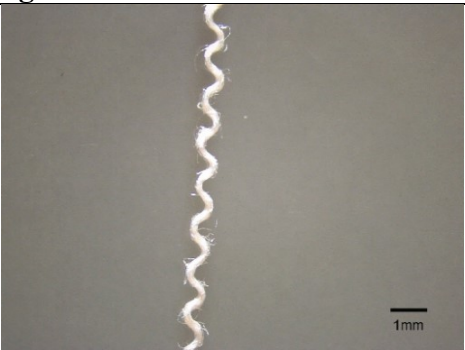
Code:	A		
Name:	Brigade™ 750 – natural		
Structure:	plain weave		
Mass:	257 g/m ²		
Thickness:	0.6 mm		
Origin:	Innotex, Inc.		
Fibre content:	93% Nomex [®] , 5% Kevlar [®] and 2% anti-static carbon		
Fabric count:	28 wa × 17 we		
Yarn			
Warp		Weft	
			
Yarn #1			
Colour:	white		
Ply:	2-ply		
Twist:	zzS		
Structure:	staple spun yarn		
Fibre content:	Nomex [®] and Kevlar [®]		
Microscopic images			
Fibre 1:	Nomex [®]	Fibre 2:	Kevlar [®]



Table A2. Fabric B characteristics.

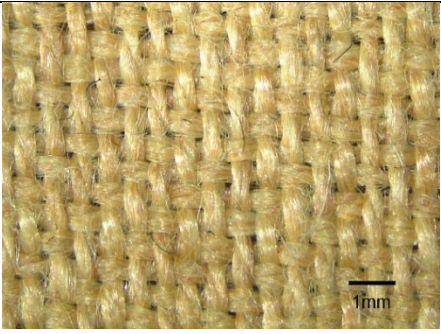






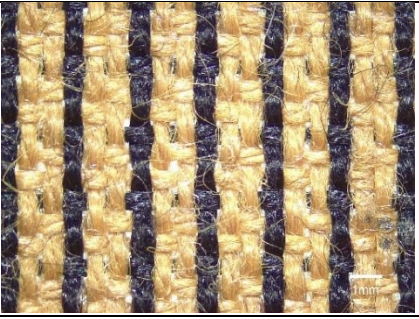




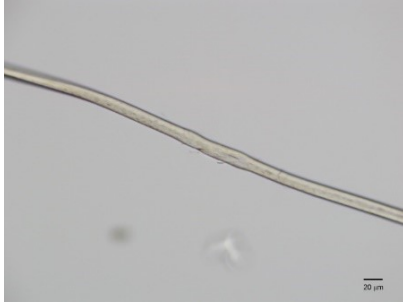
Code:	B				
Name:	Agility™ – light gold				
Structure:	2/1 twill weave				
Mass:	226 g/m ²				
Thickness:	0.5 mm				
Origin:	Innotex, Inc.				
Fibre content:	60% Kevlar®, 20% Nomex® and 20% PBO				
Fabric count:	19 wa × 18 we				
Yarn					
Warp		Weft			
					
Yarn #1					
Colour:	yellow				
Ply:	2-ply				
Twist:	zzS				
Structure:	staple spun yarn				
Fibre content:	Kevlar®, Nomex® and PBO				
Microscopic images					
Fibre 1:	Kevlar®	Fibre 2:	Nomex®	Fibre 3:	PBO
					

Table A3. Fabric C characteristics.

Code:	C		
Name:	Pioneer™ – gold		
Structure:	2/1 twill weave		
Mass:	227 g/m ²		
Thickness:	0.48 mm		
Origin:	Innotex, Inc.		
Fibre content:	60% Kevlar® and 40% Nomex®		
Fabric count:	18 wa × 18 we		
Yarn			
Warp		Weft	
			
Yarn #1			
Colour:	golden		Image: 
Ply:	2-ply		
Twist:	zzS		
Structure:	staple spun yarn		
Fibre content:	Kevlar® and Nomex®		
Microscopic images			
Fibre 1:	Kevlar®	Fibre 2:	Nomex®
			

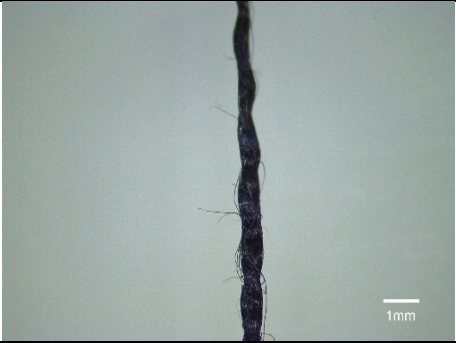

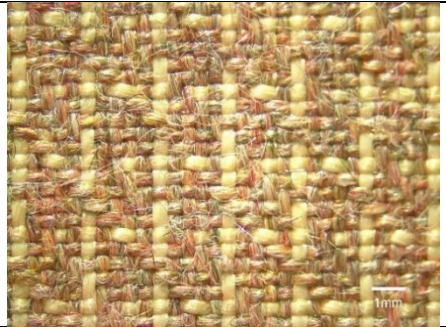





Yarn #2		
Colour:	black	Image: 
Ply:	2-ply	
Twist:	zzS	
Structure:	staple spun yarn	
Fibre content:	Kevlar [®]	
Microscopic images		
Fibre 1:	Kevlar [®]	

Table A4. Fabric D characteristics.

Code:	D		
Name:	Armor AP™ – gold		
Structure:	broken twill weave		
Mass:	222 g/m ²		
Thickness:	0.4 mm		
Origin:	Innotex, Inc.		
Fibre content:	75% Kevlar® and 25% Nomex®		
Fabric count:	24 wa × 24 we		
Yarn			
Warp		Weft	
			
Yarn #1			
Colour:	brown		Image: 
Ply:	2-ply		
Twist:	zzS		
Structure:	staple spun yarn		
Fibre content:	Kevlar® and Nomex®		
Microscopic images			
Fibre 1:	Kevlar®	Fibre 2:	Nomex®
			

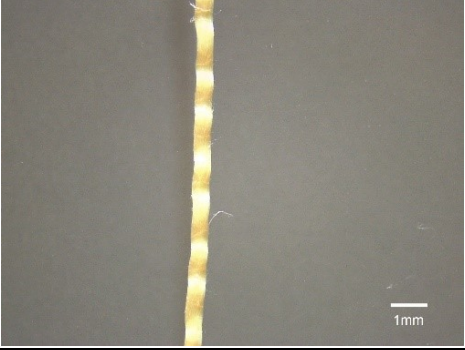








Yarn #2		
Colour:	yellow	Image: 
Ply:	single	
Twist:	S	
Structure:	continuous filament yarn	
Fibre content:	Kevlar [®]	
Microscopic images		
Fibre 1:		Kevlar [®]

Table A5. Fabric E characteristics.

Code:	E				
Name:	Gemini™ XT – naturel				
Structure:	plain weave				
Mass:	246 g/m ²				
Thickness:	0.48 mm				
Origin:	Innotex, Inc.				
Fibre content:	55% Kevlar®, 37% PBI and 8% LCP				
Fabric count:	16 wa × 15 we				
Yarn					
Warp		Weft			
					
Yarn #1					
Colour:	white & brown				
Ply:	2-ply				
Twist:	zzS				
Element:	Element 1	Element 2			
Structure:	Continuous filament yarn	Staple spun yarn			
Fibre content:	LCP	Kevlar® and PBI			
Microscopic images					
Fibre 1:	Kevlar®	Fibre 2:	PBI	Fibre 3:	LCP
					



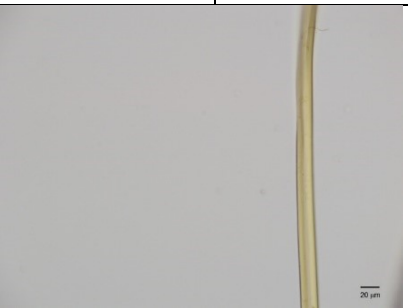
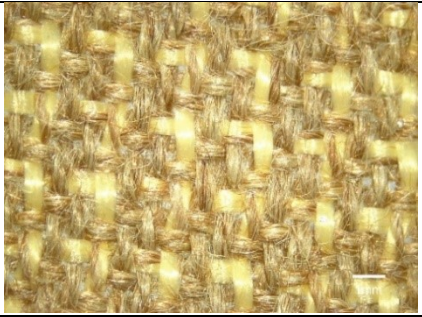




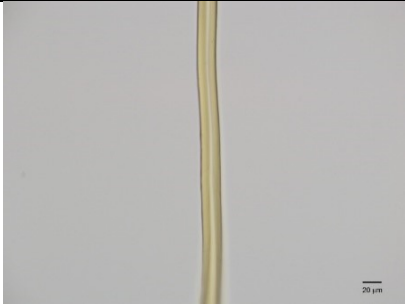
Yarn #2			
Colour:	brown	Image:	
Ply:	2-ply		
Twist:	zzS		
Structure:	staple spun yarn		
Fibre content:	Kevlar [®] and PBI		
Microscopic images			
Fibre 1:	Kevlar [®]	Fibre 2:	PBI
			

Table A6. Fabric F characteristics.

Code:	F		
Name:	Kombat™ Flex – gold		
Structure:	2/1 twill weave		
Mass:	234 g/m ²		
Thickness:	0.5 mm		
Origin:	Innotex, Inc.		
Fibre content:	64% Kevlar® & 36% PBI		
Fabric count:	18 wa × 17 we		
Yarn			
Warp		Weft	
			
Yarn #1			
Colour:	yellow & brown		Image: 
Ply:	2-ply		
Twist:	zzS		
Element:	Element 1	Element 2	
Structure:	continuous filament yarn	staple spun yarn	
Fibre content:	Kevlar®	Kevlar® and PBI	
Microscopic images			
Fibre 1:	Kevlar®	Fibre 2:	PBI
			



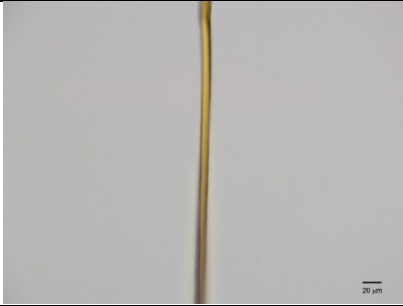
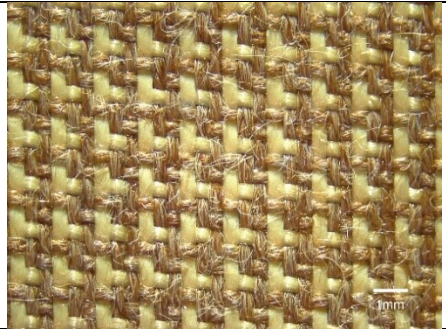


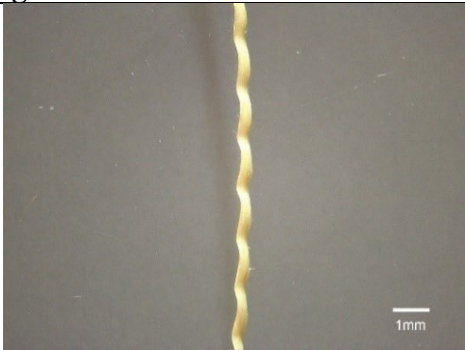

Yarn #2			
Colour:	brown	Image:	
Ply:	2-ply		
Twist:	zzS		
Structure:	staple spun yarn		
Fibre content:	Kevlar [®] and PBI		
Microscopic images			
Fibre 1:	Kevlar [®]	Fibre 2:	PBI
			

Table A7. Fabric G characteristics.

Code:	G		
Name:	PBI Max™ – gold (6.0 oz)		
Structure:	2/1 twill weave		
Mass:	214 g/m ²		
Thickness:	0.38 mm		
Origin:	Innotex, Inc.		
Fibre content:	65% Kevlar® and 35% PBI		
Fabric count:	24 wa × 22 we		
Yarn			
Warp		Weft	
			
Yarn #1			
Colour:	yellow	Image: 	
Ply:	single		
Twist:	S		
Structure:	continuous filament yarn		
Fibre content:	Kevlar®		
Microscopic images			
Fibre 1:		Kevlar®	
			




Yarn #2			
Colour:	brown	Image:	
Ply:	2-ply		
Twist:	zzS		
Structure:	staple spun yarn		
Fibre content:	Kevlar [®] and PBI		
Microscopic images			
Fibre 1:	Kevlar [®]	Fibre 2:	PBI
			

Table A8. Fabric I characteristics.

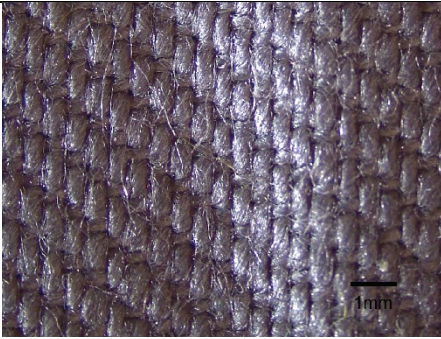


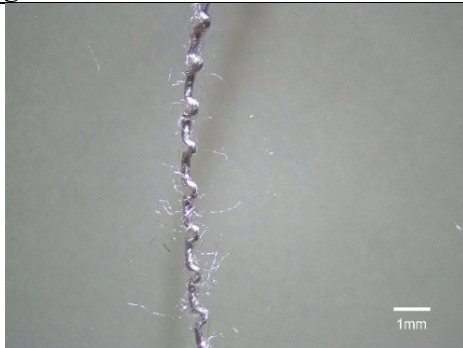


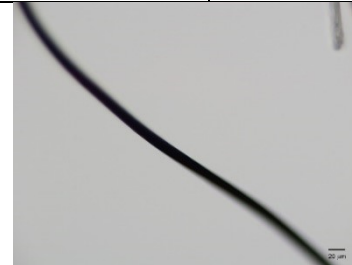
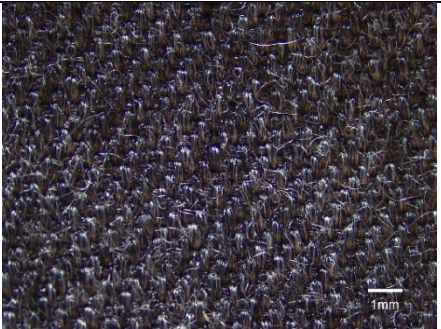
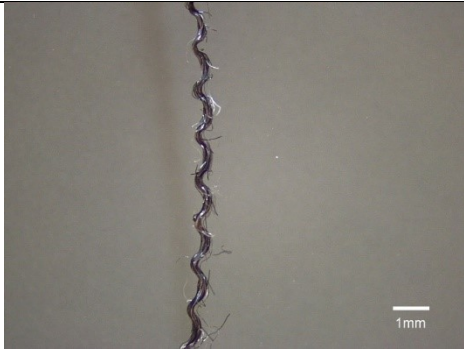
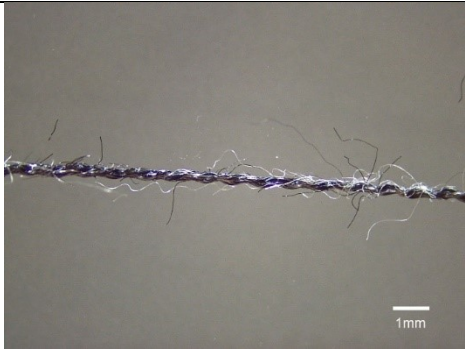



Code:	I				
Name:	Flameflex – graphite				
Structure:	2/1 twill weave				
Mass:	284 g/m ²				
Thickness:	0.5 mm				
Origin:	Carrington Textiles Ltd.				
Fibre content:	63% cotton, 34% polyester and 3% EOL (XLANCE®)				
Fabric count:	28 wa × 17 we				
Yarn					
Warp			Weft		
					
Yarn #1					
Colour:	grey	Image:			
Ply:	single				
Twist:	S				
Structure:	staple spun yarn				
Fibre content:	cotton, polyester and EOL				
Microscopic images					
Fibre 1:	cotton	Fibre 2:	polyester	Fibre 3:	EOL
					

Table A9. Fabric L characteristics.

Code:	L		
Name:	CarbonX Repel		
Structure:	2/1 twill weave		
Mass:	278 g/m ²		
Thickness:	0.58 mm		
Origin:	TexTech Industries, Inc.		
Fibre content:	50% oxidized PAN, 30% FR rayon, 17% para-aramid and 3% anti-static polyester		
Fabric count:	25 wa × 25 we		
Yarn			
Warp		Weft	
			
Yarn #1			
Colour:	grey		
Ply:	2-ply		
Twist:	zzS		
Structure:	staple spun yarn		
Fibre content:	oxidized PAN, FR rayon para-aramid and anti-static polyester		
Microscopic images			
Fibre 1:	oxidized PAN	Fibre 2:	FR rayon
			





Fibre 3:	para-aramid	Fibre 4:	anti-static polyester
	 <p data-bbox="673 506 706 538">20 µm</p>		 <p data-bbox="1307 506 1339 538">20 µm</p>

Table A10. Fabric M characteristics.



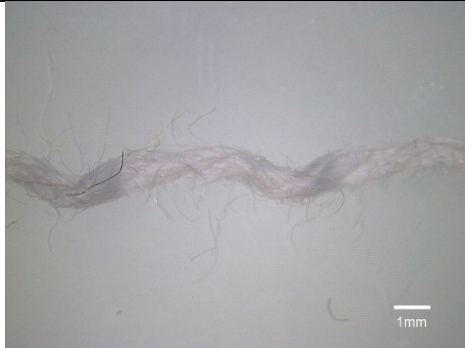


Code:	M	
Name:	LENZING™ FR	
Structure:	3/1 reverse twill weave	
Mass:	556 g/m ²	
Thickness:	1.7 mm	
Origin:	Ivodex Enterprises, Inc.	
Fibre content:	100 % FR viscose	
Fabric count:	13 wa × 7 we	
Yarn		
Warp		Weft
		
Yarn #1		
Colour:	White	Image: 
Ply:	3-ply	
Twist:	zzzS	
Structure:	staple spun yarn	
Fibre content:	FR viscose	
Microscopic images		
FR viscose		
		

Table A11. Fabric N characteristics.






Code:	N		
Name:	Zylon [®]		
Structure:	2/1 twill weave		
Mass:	333 g/m ²		
Thickness:	0.55 mm		
Origin:	Toyobo CO., Ltd.		
Fibre content:	100% PBO		
Fabric count:	27 wa × 22 we		
Yarn			
Warp		Weft	
			
Yarn #1			
Colour:	golden	Image: 	
Ply:	2-ply		
Twist:	zzS		
Structure:	staple spun yarn		
Fibre content:	PBO		
Microscopic images			
Fibre 1:		PBO	
			

Table A12. Fabric O characteristics.




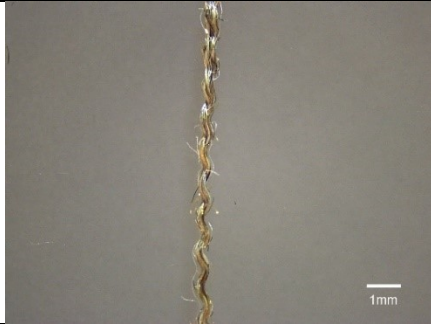



Code:	O				
Name:	NF Arc™				
Structure:	plain weave				
Mass:	170 g/m ²				
Thickness:	0.33 mm				
Origin:	Norfab Corporation.				
Fibre content:	30% novoloid, 30% pre-oxidized PAN, and 40% para-aramid				
Fabric count:	32 wa × 22 we				
Yarn					
Warp			Weft		
					
Yarn #1					
Colour:	green				
Ply:	3-ply				
Twist:	zzzS				
Structure:	staple spun yarn				
Fibre content:	oxidized PAN, para-aramid and novoloid				
Microscopic images					
Fibre 1:	oxidized PAN	Fibre 2:	para-aramid	Fibre 3:	novoloid
					

Table A13. Fabric T characteristics.

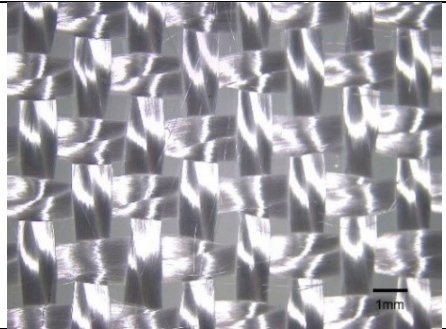
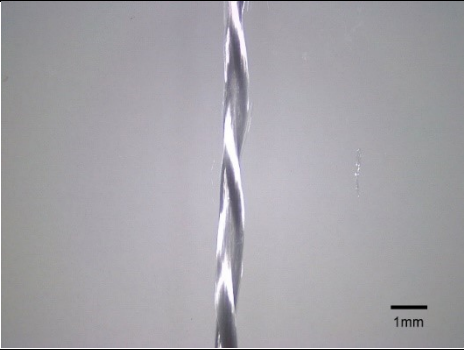

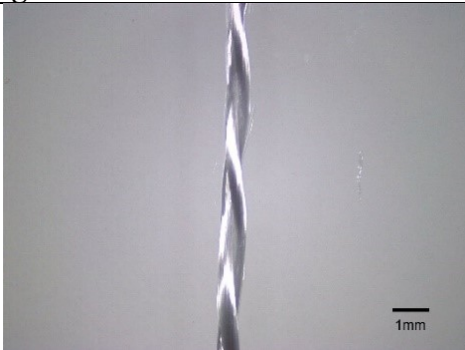

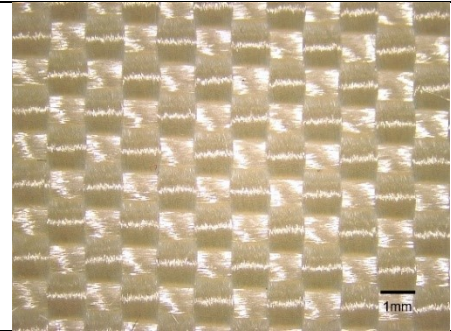
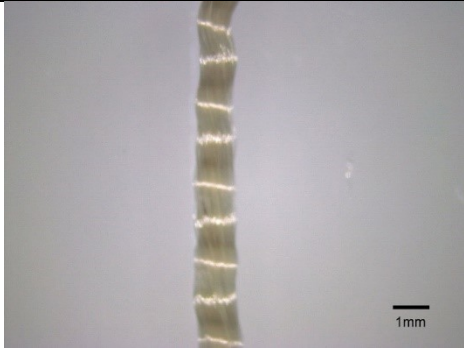
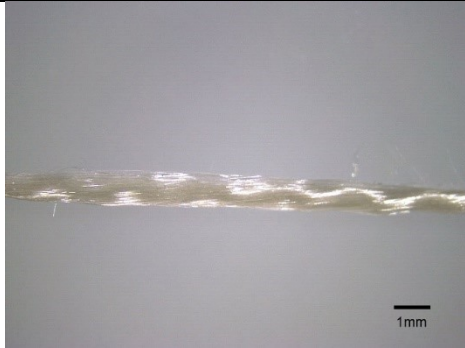
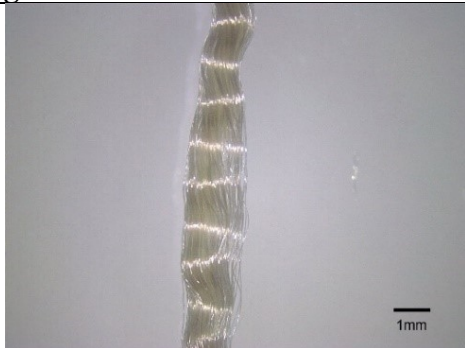
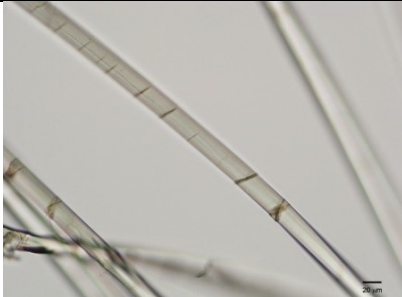
Code:	T		
Name:	Fiberglass Cloth (Style 7500)		
Structure:	plain weave		
Mass:	317 g/m ²		
Thickness:	0.45 mm		
Origin:	Freeman Mfg. & Supply Co.		
Fibre content:	100% fiberglass		
Fabric count:	7 wa × 6 we		
Yarn			
Warp		Weft	
			
Yarn #1			
Colour:	White		
Ply:	2-ply		
Twist:	zzS		
Structure:	continuous filament yarn		
Fibre content:	fibreglass		
Microscopic images			
Fibre 1:		fibreglass	
			

Table A14. Fabric U characteristics.

Code:	U	
Name:	Vectran™	
Structure:	plain weave	
Mass:	289 g/m ²	
Thickness:	0.68 mm	
Origin:	Kuraray CO., Ltd.	
Fibre content:	100% LCP	
Fabric count:	10 wa × 10 we	
Yarn		
Warp		Weft
		
Yarn #1		
Colour:	yellow	Image: 
Ply:	single	
Twist:	S	
Structure:	continuous filament yarn	
Fibre content:	LCP	
Microscopic images		
Fibre 1:		LCP
		

Appendix B: Paired samples test and One-way ANOVA test for all fabrics tested after accelerated thermal ageing

Table B1. Paired samples test for Fabric A.

Strength		Difference
Before	After	
231	185	46
269	143	126
265	195	70
189	192	-3
Mean of difference		60
Std. of difference		53.6
N		4
df		3
t		2.23
p-value		0.036

Table B2. Paired samples test for Fabric B.

Strength		Difference
Before	After	
297	71	226
257	71	185
293	82	210
287	85	202
292	87	204
Mean of difference		206
Std. of difference		14.6
N		5
df		4
t		31.2
p-value		< .001

Table B3. Paired samples test for Fabric C.

Strength		Difference
Before	After	
190	32	158
185	32	153
224	30	194
218	33	185
208	34	174
Mean of difference		173
Std. of difference		17.4
N		5
df		4
t		22.1
p-value		< .001

Table B4. Paired samples test for Fabric D.

Strength		Difference
Before	After	
340	72	268
347	79	268
357	76	281
333	68	265
357	77	280
Mean of difference		272
Std. of difference		7.38
N		5
df		4
t		82.4
p-value		< .001

Table B5. Paired samples test for Fabric E.

Strength		Difference
Before	After	
274	240	34
250	346	-95
256	280	-24
274	321	-47
275	292	-17
Mean of difference		-30
Std. of difference		47.1
N		5
df		4
t		-1.40
p-value		0.153

Table B6. Paired samples test for Fabric F.

Strength		Difference
Before	After	
504	55	449
538	57	482
471	54	416
486	52	434
475	54	421
Mean of difference		440
Std. of difference		26.4
N		5
df		4
t		37.2
p-value		< .001

Table B7. Paired samples test for Fabric G.

Strength		Difference
Before	After	
707	65	642
645	74	571
751	71	680
681	67	614
692	63	628
Mean of difference		627
Std. of difference		39.5
N		5
df		4
t		35.4
p-value		< .001

Table B8. Paired samples test for Fabric I.

Strength		Difference
Before	After	
54	6	48
61	6	55
59	6	53
54	6	49
57	7	50
Mean of difference		51
Std. of difference		2.92
N		5
df		4
t		39.1
p-value		< .001

Table B9. Paired samples test for Fabric L.

Strength		Difference
Before	After	
79	16	63
84	17	67
75	17	58
84	17	67
78	17	61
Mean of difference		63
Std. of difference		3.85
N		5
df		4
t		36.6
p-value		< .001

Table B10. Paired samples test for Fabric N.

Strength		Difference
Before	After	
500	253	246
470	237	233
473	242	231
492	246	246
461	248	213
Mean of difference		234
Std. of difference		13.7
N		5
df		4
t		37.9
p-value		< .001

Table B11. Paired samples test for Fabric T.

Strength		Difference
Before	After	
747	858	-112
619	874	-254
746	822	-76
691	780	-88
718	741	-23
Mean of difference		-111
Std. of difference		86.7
N		5
df		4
t		-2.85
p-value		0.012

Table B12. Paired samples test for Fabric U.

Strength		Difference
Before	After	
2951	2094	857
2636	2655	-20
2679	2220	460
2809	2618	191
2568	2809	-240
Mean difference		250
Std. of difference		427
N		5
df		4
t		1.31
p-value		0.141

Table B13. One-way ANOVA test (Descriptive Statistics).

Dependent Variable: Change in strength

Fabric	Mean	Std. Deviation	N
A	-25.05582	10.180715	4
B	-72.12734	2.692123	5
C	-84.32236	.713198	5
D	-78.54712	1.303011	5
E	11.13318	15.127387	5
F	-88.99416	.377093	5
G	-90.21088	.610166	5
I	-89.66710	.721867	5
L	-79.07964	.582209	5
N	-48.79422	1.282440	5
T	15.69271	7.802924	5
U	-9.14755	11.213631	5
Total	-58.67654	38.834470	59

Table B14. One-way ANOVA test (Levene's Test of Equality of Error Variances^{a,b,c}).

		Levene Statistic	df1	df2	Sig.
Change in strength	Based on Mean	8.258	13	55	.000
	Based on Median	3.770	13	55	.000
	Based on Median and with adjusted df	3.770	13	13.408	.011
	Based on trimmed mean	7.934	13	55	.000

Tests the null hypothesis that the error variance of the dependent variable is equal across groups.

a. Dependent variable: Change in strength

b. Design: Intercept + Specimen#

Tests the null hypothesis that the error variance of the dependent variable is equal across groups.

Table B15. One-way ANOVA test (Tests of Between-Subjects Effects^a).

Dependent Variable: Change in strength

Source	Type III Sum of Squares	df	Mean Square	F	Sig.
Corrected Model	100520.271 ^a	13	7732.329	209.329	.000
Intercept	232916.946	1	232916.946	6,305.517	.000
Time	100520.271	13	7732.329	209.329	.000
Error	2031.623	55	36.939		
Total	340114.482	69			
Corrected Total	102551.894	68			

Tests the null hypothesis that the error variance of the dependent variable is equal across groups.

a. Dependent variable: Change in strength

Table B16. One-way ANOVA test (Multiple Comparisons).

Dependent Variable: Change in strength
Tamhane

(I) Specimen #	(J) Specimen #	Mean Difference (I-J)	Std. Error	Sig.	95% Confidence Interval	
					Lower Bound	Upper Bound
A	B	47.07152	5.230798	.157	-21.00553	115.14856
	C	59.26654	5.100340	.113	-19.56261	138.09570
	D	53.49131	5.123603	.141	-23.11627	130.09888
	E	-36.18900	8.466363	.295	-87.25311	14.87512
	F	63.93834	5.093150	.093	-15.60868	143.48535
	G	65.15506	5.097666	.087	-13.93930	144.24943
	I	64.61128	5.100584	.089	-14.19379	143.41635
	L	54.02382	5.097012	.148	-25.13572	133.18336
	N	23.73840	5.122565	.807	-52.96514	100.44194
	T	-40.74852	6.171618	.069	-84.31437	2.81732
U	-15.90827	7.145687	.997	-59.20046	27.38393	
B	A	-47.07152	5.230798	.157	-115.14856	21.00553
	C	12.19503*	1.245486	.028	1.54414	22.84592
	D	6.41979	1.337562	.262	-2.72993	15.56951
	E	-83.26051*	6.871468	.017	-146.87824	-19.64278
	F	16.86682*	1.215708	.011	5.29445	28.43919
	G	18.08355*	1.234490	.006	7.12773	29.03937
	I	17.53976*	1.246485	.006	6.91475	28.16477
	L	6.95230	1.231787	.286	-4.08440	17.98900
	N	-23.33311*	1.333580	.000	-32.52032	-14.14591
	T	-87.82004*	3.691427	.000	-116.86583	-58.77425
U	-62.97978*	5.157384	.012	-108.17277	-17.78680	
C	A	-59.26654	5.100340	.113	-138.09570	19.56261
	B	-12.19503*	1.245486	.028	-22.84592	-1.54414
	D	-5.77524*	.664302	.010	-10.07844	-1.47203
	E	-95.45554*	6.772688	.013	-162.74931	-28.16177
	F	4.67179*	.360791	.001	2.29884	7.04474
	G	5.88852*	.419751	.000	3.54349	8.23355
	I	5.34473*	.453816	.000	2.84162	7.84785
	L	-5.24273*	.411733	.000	-7.56306	-2.92239
	N	-35.52814*	.656247	.000	-39.74980	-31.30648
	T	-100.01507*	3.504120	.001	-134.29670	-65.73344
U	-75.17481*	5.025021	.010	-124.87195	-25.47768	
D	A	-53.49131	5.123603	.141	-130.09888	23.11627
	B	-6.41979	1.337562	.262	-15.56951	2.72993
	C	5.77524*	.664302	.010	1.47203	10.07844
	E	-89.68030*	6.790223	.016	-156.26597	-23.09464
	F	10.44703*	.606636	.002	5.38701	15.50706
	G	11.66376*	.643450	.000	7.19716	16.13036

	I	11.11997*	.666173	.000	6.82733	15.41262
	L	.53251	.638248	1.000	-3.99030	5.05533
	N	-29.75290*	.817617	.000	-34.26290	-25.24290
	T	-94.23983*	3.537894	.001	-127.27624	-61.20342
	U	-69.39957*	5.048631	.012	-118.16903	-20.63012
E	A	36.18900	8.466363	.295	-14.87512	87.25311
	B	83.26051*	6.871468	.017	19.64278	146.87824
	C	95.45554*	6.772688	.013	28.16177	162.74931
	D	89.68030*	6.790223	.016	23.09464	156.26597
	F	100.12733*	6.767275	.011	32.60975	167.64492
	G	101.34406*	6.770674	.010	33.96733	168.72079
	I	100.80027*	6.772871	.010	33.51406	168.08649
	L	90.21281*	6.770182	.016	22.81574	157.60989
	N	59.92740	6.789440	.075	-6.68935	126.54415
	T	-4.55953	7.612141	1.000	-55.17710	46.05804
	U	20.28073	8.421204	.985	-28.33787	68.89932
F	A	-63.93834	5.093150	.093	-143.48535	15.60868
	B	-16.86682*	1.215708	.011	-28.43919	-5.29445
	C	-4.67179*	.360791	.001	-7.04474	-2.29884
	D	-10.44703*	.606636	.002	-15.50706	-5.38701
	E	-100.12733*	6.767275	.011	-167.64492	-32.60975
	G	1.21673	.320781	.492	-.75750	3.19096
	I	.67294	.364223	1.000	-1.73542	3.08131
	L	-9.91452*	.310215	.000	-11.78907	-8.03996
	N	-40.19993*	.597805	.000	-45.16242	-35.23745
	T	-104.68686*	3.493646	.001	-139.38988	-69.98384
	U	-79.84661*	5.017723	.008	-129.84305	-29.85016
G	A	-65.15506	5.097666	.087	-144.24943	13.93930
	B	-18.08355*	1.234490	.006	-29.03937	-7.12773
	C	-5.88852*	.419751	.000	-8.23355	-3.54349
	D	-11.66376*	.643450	.000	-16.13036	-7.19716
	E	-101.34406*	6.770674	.010	-168.72079	-33.96733
	F	-1.21673	.320781	.492	-3.19096	.75750
	I	-.54379	.422704	1.000	-2.91013	1.82256
	L	-11.13125*	.377166	.000	-13.21387	-9.04862
	N	-41.41666*	.635131	.000	-45.79454	-37.03879
	T	-105.90359*	3.500227	.001	-140.33980	-71.46738
	U	-81.06333*	5.022307	.008	-130.87107	-31.25560
I	A	-64.61128	5.100584	.089	-143.41635	14.19379
	B	-17.53976*	1.246485	.006	-28.16477	-6.91475
	C	-5.34473*	.453816	.000	-7.84785	-2.84162
	D	-11.11997*	.666173	.000	-15.41262	-6.82733
	E	-100.80027*	6.772871	.010	-168.08649	-33.51406
	F	-.67294	.364223	1.000	-3.08131	1.73542
	G	.54379	.422704	1.000	-1.82256	2.91013

	L	-10.58746*	.414743	.000	-12.93079	-8.24413
	N	-40.87288*	.658140	.000	-45.08463	-36.66112
	T	-105.35980*	3.504475	.001	-139.62746	-71.09215
	U	-80.51955*	5.025268	.008	-130.20663	-30.83246
L	A	-54.02382	5.097012	.148	-133.18336	25.13572
	B	-6.95230	1.231787	.286	-17.98900	4.08440
	C	5.24273*	.411733	.000	2.92239	7.56306
	D	-.53251	.638248	1.000	-5.05533	3.99030
	E	-90.21281*	6.770182	.016	-157.60989	-22.81574
	F	9.91452*	.310215	.000	8.03996	11.78907
	G	11.13125*	.377166	.000	9.04862	13.21387
	I	10.58746*	.414743	.000	8.24413	12.93079
	N	-30.28542*	.629860	.000	-34.71781	-25.85302
	T	-94.77234*	3.499274	.001	-129.24674	-60.29794
	U	-69.93209*	5.021643	.013	-119.76700	-20.09717
N	A	-23.73840	5.122565	.807	-100.44194	52.96514
	B	23.33311*	1.333580	.000	14.14591	32.52032
	C	35.52814*	.656247	.000	31.30648	39.74980
	D	29.75290*	.817617	.000	25.24290	34.26290
	E	-59.92740	6.789440	.075	-126.54415	6.68935
	F	40.19993*	.597805	.000	35.23745	45.16242
	G	41.41666*	.635131	.000	37.03879	45.79454
	I	40.87288*	.658140	.000	36.66112	45.08463
	L	30.28542*	.629860	.000	25.85302	34.71781
	T	-64.48693*	3.536390	.003	-97.57531	-31.39854
	U	-39.64667	5.047577	.110	-88.45624	9.16290
T	A	40.74852	6.171618	.069	-2.81732	84.31437
	B	87.82004*	3.691427	.000	58.77425	116.86583
	C	100.01507*	3.504120	.001	65.73344	134.29670
	D	94.23983*	3.537894	.001	61.20342	127.27624
	E	4.55953	7.612141	1.000	-46.05804	55.17710
	F	104.68686*	3.493646	.001	69.98384	139.38988
	G	105.90359*	3.500227	.001	71.46738	140.33980
	I	105.35980*	3.504475	.001	71.09215	139.62746
	L	94.77234*	3.499274	.001	60.29794	129.24674
	N	64.48693*	3.536390	.003	31.39854	97.57531
	U	24.84026	6.109520	.342	-11.14055	60.82106
U	A	15.90827	7.145687	.997	-27.38393	59.20046
	B	62.97978*	5.157384	.012	17.78680	108.17277
	C	75.17481*	5.025021	.010	25.47768	124.87195
	D	69.39957*	5.048631	.012	20.63012	118.16903
	E	-20.28073	8.421204	.985	-68.89932	28.33787
	F	79.84661*	5.017723	.008	29.85016	129.84305
	G	81.06333*	5.022307	.008	31.25560	130.87107
	I	80.51955*	5.025268	.008	30.83246	130.20663

	L	69.93209*	5.021643	.013	20.09717	119.76700
	N	39.64667	5.047577	.110	-9.16290	88.45624
	T	-24.84026	6.109520	.342	-60.82106	11.14055

Based on observed means.

The error term is Mean Square(Error) = 36.939.

*. The mean difference is significant at the .05 level.

Appendix C: Paired samples test and One-way ANOVA test for all fabrics tested after accelerated UV ageing

Table C1. Paired samples test for Fabric A.

Strength		Difference
Before	After	
231	75	156
269	66	202
265	72	193
189	67	122
	70	
Mean of difference		168
Std. of difference		36.8
N		4
df		3
t		9.15
p-value		< .001

Table C2. Paired samples test for Fabric B.

Strength		Difference
Before	After	
297	160	138
257	131	126
293	122	171
287	121	166
292	108	183
Mean of difference		157
Std. of difference		24.0
N		5
df		4
t		14.5
p-value		< .001

Table C3. Paired samples test for Fabric C.

Strength		Difference
Before	After	
190	154	36
185	136	49
224	138	85
218	154	65
208	142	65
Mean of difference		60
Std. of difference		18.6
N		5
df		4
t		7.17
p-value		< .001

Table C4. Paired samples test for Fabric D.

Strength		Difference
Before	After	
340	81	258
347	82	265
357	83	274
333	78	254
357	98	259
Mean of difference		262
Std. of difference		7.62
N		5
df		4
t		76.8
p-value		< .001

Table C5. Paired samples test for Fabric E.

Strength		Difference
Before	After	
274	77	197
250	67	183
256	73	184
274	73	201
275	69	206
Mean of difference		194
Std. of difference		10.2
N		5
df		4
t		42.2
p-value		< .001

Table C6. Paired samples test for Fabric F.

Strength		Difference
Before	After	
504	318	187
538	204	334
471	121	350
486	151	335
475	129	346
Mean of difference		310
Std. of difference		69.5
N		5
df		4
t		9.98
p-value		< .001

Table C7. Paired samples test for Fabric G.

Strength		Difference
Before	After	
707	219	488
645	110	535
751	102	649
681	107	574
692	112	580
Mean of difference		565
Std. of difference		59.4
N		5
df		4
t		21.2
p-value		< .001

Table C8. Paired samples test for Fabric I.

Strength		Difference
Before	After	
54	46	8
61	41	19
59	43	16
54	39	16
57	44	14
Mean of difference		15
Std. of difference		4.02
N		5
df		4
t		8.14
p-value		< .001

Table C9. Paired samples test for Fabric L.

Strength		Difference
Before	After	
79	48	30
84	51	32
75	51	25
84	49	35
78	48	30
Mean of difference		31
Std. of difference		3.99
N		5
df		4
t		17.1
p-value		< .001

Table C10. Paired samples test for Fabric M.

Strength		Difference
Before	After	
380	103	277
359	121	239
360	117	243
377	112	265
372	111	261
Mean of difference		257
Std. of difference		15.7
N		5
df		4
t		36.4
p-value		< .001

Table C11. Paired samples test for Fabric N.

Strength		Difference
Before	After	
500	126	374
470	145	325
473	158	315
492	122	371
461	113	347
Mean of difference		347
Std. of difference		26.2
N		5
df		4
t		29.4
p-value		< .001

Table C12. Paired samples test for Fabric T.

Strength		Difference
Before	After	
747	850	-103
619	802	-182
746	716	30
691	711	-20
718	613	105
Mean of difference		-34
Std. of difference		112
N		5
df		4
t		-0.68
p-value		0.491

Table C13. Paired samples test for Fabric U.

Strength		Difference
Before	After	
2951	495	2457
2636	596	2040
2679	655	2025
2809	657	2152
2568	636	1932
Mean of difference		2121
Std. of difference		203
N		5
df		4
t		23.3
p-value		< .001

Table C14. One-way ANOVA test (Descriptive Statistics).

Dependent Variable: Change in strength

Fabric	Mean	Std. Deviation	N
A	-70.64411	1.456786	5
B	-54.93554	6.734177	5
C	-29.27197	4.144927	5
D	-75.65011	2.207129	5
E	-73.01381	1.395920	5
F	-62.71859	16.420127	5
G	-81.32269	7.203095	5
I	-25.62958	4.799717	5
L	-38.34307	1.971817	5
M	-69.49666	1.782903	5
N	-72.31423	3.793876	5
T	4.83147	12.954784	5
U	-73.11731	3.002056	5
Total	-50.40369	28.083311	65

Table C15. One-way ANOVA test (Levene's Test of Equality of Error Variances^{a,b,c}).

		Levene Statistic	df1	df2	Sig.
Change in strength	Based on Mean	3.996	15	62	.000
	Based on Median	1.643	15	62	.088
	Based on Median and with adjusted df	1.643	15	16.783	.163
	Based on trimmed mean	3.698	15	62	.000

Tests the null hypothesis that the error variance of the dependent variable is equal across groups.

a. Dependent variable: Change in strength

b. Design: Intercept + Specimen#

Tests the null hypothesis that the error variance of the dependent variable is equal across groups.

Table C16. One-way ANOVA test (Tests of Between-Subjects Effects^a).

Dependent Variable: Change in strength

Source	Type III Sum of Squares	df	Mean Square	F	Sig.
Corrected Model	57805.286 ^a	15	3853.686	81.755	.000
Intercept	197951.760	1	197951.760	4,199.511	.000
Time	57805.286	15	3853.686	81.755	.000
Error	2922.485	62	47.137		
Total	258889.228	78			
Corrected Total	60727.771	77			

Tests the null hypothesis that the error variance of the dependent variable is equal across groups.

a. Dependent variable: Change in strength

Table C17. One-way ANOVA test (Multiple Comparisons).

Dependent Variable: Change in strength

Tamhane

(I) Specimen #	(J) Specimen #	Mean Difference (I-J)	Std. Error	Sig.	95% Confidence Interval	
					Lower Bound	Upper Bound
A	B	-15.70857	3.081278	.483	-45.19669	13.77956
	C	-41.37214*	1.964823	.001	-57.66434	-25.07994
	D	5.00600	1.182679	.379	-2.42680	12.43880
	E	2.36970	.902310	.975	-2.82691	7.56631
	F	-7.92552	7.372147	1.000	-85.39537	69.54433
	G	10.67858	3.286542	.967	-21.18987	42.54703
	I	-45.01453*	2.243190	.001	-64.62693	-25.40213
	L	-32.30104*	1.096384	.000	-38.92540	-25.67668
	M	-1.14745	1.029657	1.000	-7.20564	4.91074
	N	1.67012	1.817455	1.000	-12.86937	16.20961
	T	-75.47558*	5.830071	.021	-135.98714	-14.96402
U	2.47320	1.492285	1.000	-8.27440	13.22080	

B	A	15.70857	3.081278	.483	-13.77956	45.19669
	C	-25.66357*	3.536370	.026	-48.52717	-2.79997
	D	20.71457	3.169245	.156	-6.26436	47.69349
	E	18.07826	3.075638	.321	-11.60696	47.76348
	F	7.78304	7.936872	1.000	-53.93852	69.50461
	G	26.38715*	4.409846	.039	.95131	51.82299
	I	-29.30596*	3.698281	.010	-51.91076	-6.70116
	L	-16.59247	3.138063	.376	-44.35105	11.16610
	M	14.56111	3.115378	.564	-13.83632	42.95855
	N	17.37868	3.456664	.220	-5.85442	40.61179
	T	-59.76702*	6.529557	.011	-105.30803	-14.22600
	U	18.18177	3.297317	.209	-6.51712	42.88065
C	A	41.37214*	1.964823	.001	25.07994	57.66434
	B	25.66357*	3.536370	.026	2.79997	48.52717
	D	46.37814*	2.100088	.000	31.89362	60.86265
	E	43.74183*	1.955966	.000	27.25691	60.22676
	F	33.44661	7.573651	.654	-36.48053	103.37376
	G	52.05072*	3.716584	.001	27.30737	76.79407
	I	-3.64239	2.836113	1.000	-20.15545	12.87066
	L	9.07110	2.052729	.453	-5.85040	23.99259
	M	40.22468*	2.017878	.000	24.86212	55.58725
	N	43.04225*	2.512923	.000	28.52111	57.56340
	T	-34.10345	6.082875	.288	-86.33361	18.12672
	U	43.84533*	2.288788	.000	29.92950	57.76117
D	A	-5.00600	1.182679	.379	-12.43880	2.42680
	B	-20.71457	3.169245	.156	-47.69349	6.26436
	C	-46.37814*	2.100088	.000	-60.86265	-31.89362
	E	-2.63630	1.167905	.999	-10.10220	4.82960
	F	-12.93152	7.409345	1.000	-88.78579	62.92274
	G	5.67258	3.369154	1.000	-23.69079	35.03595
	I	-50.02053*	2.362571	.000	-67.46679	-32.57426
	L	-37.30704*	1.323592	.000	-44.97627	-29.63781
	M	-6.15345	1.268870	.159	-13.63813	1.33122
	N	-3.33588	1.962902	1.000	-16.34058	9.66882
	T	-80.48158*	5.877037	.014	-139.06049	-21.90268
	U	-2.53280	1.666359	1.000	-12.61618	7.55058
E	A	-2.36970	.902310	.975	-7.56631	2.82691
	B	-18.07826	3.075638	.321	-47.76348	11.60696
	C	-43.74183*	1.955966	.000	-60.22676	-27.25691
	D	2.63630	1.167905	.999	-4.82960	10.10220
	F	-10.29522	7.369792	1.000	-87.87130	67.28086
	G	8.30888	3.281255	.999	-23.75145	40.36922
	I	-47.38423*	2.235436	.001	-67.20075	-27.56770
	L	-34.67074*	1.080431	.000	-41.28971	-28.05176
	M	-3.51715	1.012653	.669	-9.53596	2.50166

	N	-.69958	1.807876	1.000	-15.41968	14.02052
	T	-77.84528*	5.827092	.019	-138.48694	-17.20362
	U	.10350	1.480604	1.000	-10.77381	10.98081
F	A	7.92552	7.372147	1.000	-69.54433	85.39537
	B	-7.78304	7.936872	1.000	-69.50461	53.93852
	C	-33.44661	7.573651	.654	-103.37376	36.48053
	D	12.93152	7.409345	1.000	-62.92274	88.78579
	E	10.29522	7.369792	1.000	-67.28086	87.87130
	G	18.60411	8.018792	1.000	-41.90418	79.11239
	I	-37.08900	7.650593	.489	-104.80114	30.62313
	L	-24.37552	7.396061	.970	-100.79362	52.04259
	M	6.77807	7.386465	1.000	-70.05634	83.61248
	N	9.59564	7.536764	1.000	-61.50934	80.70062
	T	-67.55006*	9.353577	.014	-123.03621	-12.06391
	U	10.39872	7.465024	1.000	-63.24043	84.03788
	G	A	-10.67858	3.286542	.967	-42.54703
B		-26.38715*	4.409846	.039	-51.82299	-.95131
C		-52.05072*	3.716584	.001	-76.79407	-27.30737
D		-5.67258	3.369154	1.000	-35.03595	23.69079
E		-8.30888	3.281255	.999	-40.36922	23.75145
F		-18.60411	8.018792	1.000	-79.11239	41.90418
I		-55.69311*	3.870965	.000	-79.93239	-31.45383
L		-42.97962*	3.339839	.011	-73.13496	-12.82429
M		-11.82603	3.318533	.904	-42.62065	18.96858
N		-9.00846	3.640826	.997	-34.24711	16.23018
T		-86.15416*	6.628891	.001	-130.97523	-41.33310
U		-8.20538	3.489897	1.000	-35.15257	18.74181
I		A	45.01453*	2.243190	.001	25.40213
	B	29.30596*	3.698281	.010	6.70116	51.91076
	C	3.64239	2.836113	1.000	-12.87066	20.15545
	D	50.02053*	2.362571	.000	32.57426	67.46679
	E	47.38423*	2.235436	.001	27.56770	67.20075
	F	37.08900	7.650593	.489	-30.62313	104.80114
	G	55.69311*	3.870965	.000	31.45383	79.93239
	L	12.71349	2.320575	.240	-5.31904	30.74601
	M	43.86708*	2.289804	.001	25.29520	62.43895
	N	46.68465*	2.736084	.000	30.46157	62.90772
	T	-30.46105	6.178409	.395	-80.62531	19.70320
	U	47.48773*	2.531783	.000	31.22874	63.74672
	L	A	32.30104*	1.096384	.000	25.67668
B		16.59247	3.138063	.376	-11.16610	44.35105
C		-9.07110	2.052729	.453	-23.99259	5.85040
D		37.30704*	1.323592	.000	29.63781	44.97627
E		34.67074*	1.080431	.000	28.05176	41.28971
F		24.37552	7.396061	.970	-52.04259	100.79362

	G	42.97962*	3.339839	.011	12.82429	73.13496
	I	-12.71349	2.320575	.240	-30.74601	5.31904
	M	31.15359*	1.188848	.000	24.27489	38.03228
	N	33.97116*	1.912148	.000	20.63368	47.30863
	T	-43.17454	5.860281	.166	-102.41813	16.06904
	U	34.77424*	1.606263	.000	24.66018	44.88830
M	A	1.14745	1.029657	1.000	-4.91074	7.20564
	B	-14.56111	3.115378	.564	-42.95855	13.83632
	C	-40.22468*	2.017878	.000	-55.58725	-24.86212
	D	6.15345	1.268870	.159	-1.33122	13.63813
	E	3.51715	1.012653	.669	-2.50166	9.53596
	F	-6.77807	7.386465	1.000	-83.61248	70.05634
	G	11.82603	3.318533	.904	-18.96858	42.62065
	I	-43.86708*	2.289804	.001	-62.43895	-25.29520
	L	-31.15359*	1.188848	.000	-38.03228	-24.27489
	N	2.81757	1.874686	1.000	-10.88733	16.52247
	T	-74.32813*	5.848165	.021	-134.06922	-14.58704
	U	3.62065	1.561479	.999	-6.63099	13.87230
N	A	-1.67012	1.817455	1.000	-16.20961	12.86937
	B	-17.37868	3.456664	.220	-40.61179	5.85442
	C	-43.04225*	2.512923	.000	-57.56340	-28.52111
	D	3.33588	1.962902	1.000	-9.66882	16.34058
	E	.69958	1.807876	1.000	-14.02052	15.41968
	F	-9.59564	7.536764	1.000	-80.70062	61.50934
	G	9.00846	3.640826	.997	-16.23018	34.24711
	I	-46.68465*	2.736084	.000	-62.90772	-30.46157
	L	-33.97116*	1.912148	.000	-47.30863	-20.63368
	M	-2.81757	1.874686	1.000	-16.52247	10.88733
	T	-77.14570*	6.036885	.010	-130.54381	-23.74759
	U	.80308	2.163600	1.000	-12.02214	13.62830
T	A	75.47558*	5.830071	.021	14.96402	135.98714
	B	59.76702*	6.529557	.011	14.22600	105.30803
	C	34.10345	6.082875	.288	-18.12672	86.33361
	D	80.48158*	5.877037	.014	21.90268	139.06049
	E	77.84528*	5.827092	.019	17.20362	138.48694
	F	67.55006*	9.353577	.014	12.06391	123.03621
	G	86.15416*	6.628891	.001	41.33310	130.97523
	I	30.46105	6.178409	.395	-19.70320	80.62531
	L	43.17454	5.860281	.166	-16.06904	102.41813
	M	74.32813*	5.848165	.021	14.58704	134.06922
	N	77.14570*	6.036885	.010	23.74759	130.54381
	U	77.94878*	5.947079	.012	21.87940	134.01816
U	A	-2.47320	1.492285	1.000	-13.22080	8.27440
	B	-18.18177	3.297317	.209	-42.88065	6.51712
	C	-43.84533*	2.288788	.000	-57.76117	-29.92950

	D	2.53280	1.666359	1.000	-7.55058	12.61618
	E	-.10350	1.480604	1.000	-10.98081	10.77381
	F	-10.39872	7.465024	1.000	-84.03788	63.24043
	G	8.20538	3.489897	1.000	-18.74181	35.15257
	I	-47.48773*	2.531783	.000	-63.74672	-31.22874
	L	-34.77424*	1.606263	.000	-44.88830	-24.66018
	M	-3.62065	1.561479	.999	-13.87230	6.63099
	N	-.80308	2.163600	1.000	-13.62830	12.02214
	T	-77.94878*	5.947079	.012	-134.01816	-21.87940

Based on observed means.

The error term is Mean Square(Error) = 47.137.

*. The mean difference is significant at the .05 level.

Appendix D: Paired samples test and One-way ANOVA test for all fabrics tested after accelerated hydrothermal ageing

Table D1. Paired samples test for Fabric A.

Strength				Difference after 15 Days	Difference after 24 Days	Difference after 31 Days
Before	After 15 Days	After 24 Days	After 31 Days			
231	240	266	272	-9	-35	-42
269		266	258	269	3	11
265		290	250	265	-24	15
189		243	234	189	-54	-45
		219	211			
Mean of difference				178	-28	-15
Std. of difference				130	24	33
N				4	4	4
df				3	3	3
t				3	-2	-1
p-value					0.236	0.486

Table D2. Paired samples test for Fabric B.

Strength				Difference after 15 Days	Difference after 24 Days	Difference after 31 Days
Before	After 15 Days	After 24 Days	After 31 Days			
297	274	291	279	23	6	19
257	307	291	231	-50	-34	26
293	323	269	224	-30	24	69
287	339	250	282	-52	37	5
292	252	247	323	39	44	-32
Mean of difference				-14	15	17
Std. of difference				42	31	36
N				5	5	5
df				4	4	4
t				-1	1	1
p-value				0.449	0.232	0.403

Table D3. Paired samples test for Fabric C.

Strength				Difference after 15 Days	Difference after 24 Days	Difference after 31 Days
Before	After 15 Days	After 24 Days	After 31 Days			
190	193	218	229	-3	-28	-39
185	215	219	199	-30	-34	-15
224	199	213	210	25	10	14
218	223	209	211	-5	10	8
208	215	194	203	-7	13	5
Mean of difference				-4	-6	-5
Std. of difference				19	23	22
N				5	5	5
df				4	4	4
t				0	-1	-1
p-value				0.689	0.535	0.568

Table D4. Paired samples test for Fabric D.

Strength				Difference after 15 Days	Difference after 24 Days	Difference after 31 Days
Before	After 15 Days	After 24 Days	After 31 Days			
340	335	274	309	4	65	31
347	320	274	307	27	73	40
357	330		319	27	357	38
333	331	305	301	2	28	31
357	363	335	312	-6	22	45
Mean of difference				11	109	37
Std. of difference				15	140	6
N				5	4	5
df				4	3	4
t				2	2	14
p-value				0.248	0.037	< .001

Table D5. Paired samples test for Fabric E.

Strength				Difference after 15 Days	Difference after 24 Days	Difference after 31 Days
Before	After 15 Days	After 24 Days	After 31 Days			
274	265	268	231	9	6	44
250	239	216	298	12	35	-47
256	247	241	237	9	15	19
274	245	255	260	29	19	14
275	275	273	249	0	2	26
Mean of difference				12	15	11
Std. of difference				11	13	35
N				5	5	5
df				4	4	4
t				3	3	1
p-value				0.207	0.218	0.416

Table D6. Paired samples test for Fabric F.

Strength				Difference after 15 Days	Difference after 24 Days	Difference after 31 Days
Before	After 15 Days	After 24 Days	After 31 Days			
504	93	55	45	411	449	459
538	82	51	53	456	488	485
471	72	49	45	398	421	426
486	64	48	54	422	438	432
475	85	55	44	390	419	431
Mean of difference				415	443	446
Std. of difference				26	28	25
N				5	5	5
df				4	4	4
t				36	36	40
p-value				< .001	< .001	< .001

Table D7. Paired samples test for Fabric G.

Strength				Difference after 15 Days	Difference after 24 Days	Difference after 31 Days
Before	After 15 Days	After 24 Days	After 31 Days			
707	119	97	69	588	610	638
645	160	76	97	485	569	548
751	102	98	78	648	652	673
681	195	82	68	486	599	613
692	141	77	91	551	614	600
Mean of difference				552	609	614
Std. of difference				70	30	46
N				5	5	5
df				4	4	4
t				18	46	30
p-value				< .001	< .001	< .001

Table D8. Paired samples test for Fabric I.

Strength				Difference after 15 Days	Difference after 24 Days	Difference after 31 Days
Before	After 15 Days	After 24 Days	After 31 Days			
54	58	57	57	-3	-3	-2
61	68	71	62	-7	-11	-1
59	75	57	62	-17	2	-3
54	74	57	56	-20	-2	-1
57	67	66	62	-10	-9	-5
Mean of difference				-11	-4	-2
Std. of difference				7	5	1
N				5	5	5
df				4	4	4
t				-4	-2	-4
p-value				0.010	0.209	0.218

Table D9. Paired samples test for Fabric L.

Strength				Difference after 15 Days	Difference after 24 Days	Difference after 31 Days
Before	After 15 Days	After 24 Days	After 31 Days			
79	62	69	77	16	10	2
84	83	75	63	0	9	21
75	86	71	80	-11	4	-5
84	64	73	66	20	11	18
78	72	74	79	6	4	-1
Mean of difference				6	7	7
Std. of difference				12	3	12
N				5	5	5
df				4	4	4
t				1	5	1
p-value				0.257	0.008	0.115

Table D10. Paired samples test for Fabric M.

Strength				Difference after 15 Days	Difference after 24 Days	Difference after 31 Days
Before	After 15 Days	After 24 Days	After 31 Days			
380		326	267	380	54	113
359	266	279		93	80	359
360	320	263	252	40	98	108
377	387	265	254	-11	112	123
372	335	271	372	37	101	0
Mean of difference				108	89	141
Std. of difference				157	22	132
N				4	5	4
df				3	4	3
t				1	9	2
p-value				0.100	< .001	0.014

Table D11. Paired samples test for Fabric N.

Strength				Difference after 15 Days	Difference after 24 Days	Difference after 31 Days
Before	After 15 Days	After 24 Days	After 31 Days			
500	404	380	362	95	119	138
470	431	409	461	39	61	9
473	380	535	423	93	-62	50
492	379	416	369	114	76	124
461	439	524	447	22	-63	14
Mean of difference				73	26	67
Std. of difference				40	84	61
N				5	5	5
df				4	4	4
t				4	1	2
p-value				0.001	0.445	0.014

Table D12. Paired samples test for Fabric T.

Strength				Difference after 15 Days	Difference after 24 Days	Difference after 31 Days
Before	After 15 Days	After 24 Days	After 31 Days			
747	597	662	699	150	85	47
619	609	558	551	10	62	69
746	644	706	590	102	40	156
691	601	470	416	91	222	275
718	613	676	520	105	42	198
Mean of difference				92	90	149
Std. of difference				51	76	94
N				5	5	5
df				4	4	4
t				4	3	4
p-value				0.006	0.109	0.021

Table D13. Paired samples test for Fabric U.

Strength						
Before	After 15 Days	After 24 Days	After 31 Days	Difference after 15 Days	Difference after 24 Days	Difference after 31 Days
2951	3402	3248	3085	-451	-297	-134
2636	3257	3401	3000	-621	-765	-364
2679	3206	2976	3266	-526	-297	-586
2809	3410	2975	3324	-601	-165	-515
2568	3219	3134	3086	-650	-566	-518
Mean of difference				-570	-418	-423
Std. of difference				81	243	181
N				5	5	5
df				4	4	4
t				-16	-4	-5
p-value				< .001	0.004	0.002

Appendix E: Paired samples test and One-way ANOVA test for all fabrics tested after accelerated laundering

Table E1. Paired samples test for Fabric A.

Strength		Difference
Before	After	
231	223	7
269	230	39
265	212	53
189		189
Mean of difference		72
Std. of difference		80.2
N		4
df		3
t		1.79
p-value		0.496

Table E2. Paired samples test for Fabric B.

Strength		Difference
Before	After	
297	288	10
257	308	-51
293	259	33
287	284	2
292	277	14
Mean of difference		2
Std. of difference		31.5
N		5
df		4
t		0.13
p-value		0.869

Table E3. Paired samples test for Fabric C.

Strength		Difference
Before	After	
190	222	-33
185	239	-55
224	232	-9
218	216	2
208	274	-66
Mean of difference		-32
Std. of difference		29.
N		5
df		4
t		-2.47
p-value		0.035

Table E4. Paired samples test for Fabric D.

Strength		Difference
Before	After	
340	276	64
347	268	79
357	267	90
333	274	58
357	261	96
Mean of difference		78
Std. of difference		16.4
N		5
df		4
t		10.5
p-value		< .001

Table E5. Paired samples test for Fabric E.

Strength		Difference
Before	After	
274	225	50
250	247	4
256	218	39
274	201	73
275	229	47
Mean of difference		42
Std. of difference		25.0
N		5
df		4
t		3.77
p-value		0.002

Table E6. Paired samples test for Fabric F.

Strength		Difference
Before	After	
504	644	-140
538	471	67
471	635	-165
486	618	-133
475	651	-176
Mean of difference		-109
Std. of difference		100
N		5
df		4
t		-2.44
p-value		0.016

Table E7. Paired samples test for Fabric G.

Strength		Difference
Before	After	
707	690	17
645	720	-75
751	787	-37
681	770	-89
692	789	-97
Mean of difference		-56
Std. of difference		47.0
N		5
df		4
t		-2.66
p-value		0.065

Table E8. Paired samples test for Fabric I.

Strength		Difference
Before	After	
54	48	7
61	57	4
59	52	7
54	58	-3
57	54	3
Mean of difference		4
Std. of difference		4.22
N		5
df		4
t		1.89
p-value		0.144

Table E9. Paired samples test for Fabric L.

Strength		Difference
Before	After	
79	66	13
84	53	31
75	57	18
84	57	27
78	52	26
Mean of difference		23
Std. of difference		7.31
N		5
df		4
t		7.01
p-value		< .001

Table E10. Paired samples test for Fabric N.

Strength		Difference
Before	After	
500	429	70
470	417	53
473	379	94
492	403	89
461	410	51
Mean of difference		71
Std. of difference		20.0
N		5
df		4
t		7.97
p-value		< .001

Table E11. Paired samples test for Fabric T.

Strength		Difference
Before	After	
747	391	355
619	505	115
746	409	337
691	425	266
718	384	335
Mean of difference		281
Std. of difference		99.2
N		5
df		4
t		6.34
p-value		< .001

Table E12. Paired samples test for Fabric U.

Strength		Difference
Before	After	
2951	3278	-326
2636	3171	-536
2679	3460	-780
2809	3049	-240
2568	3754	-1185
Mean of difference		-614
Std. of difference		381
N		5
df		4
t		-3.60
p-value		0.002

Table E13. One-way ANOVA test (Descriptive Statistics).

Dependent Variable: Change in strength

Fabric	Mean	Std. Deviation	N
A	-6.91224	3.808138	3
B	-.63630	6.117372	5
C	15.65107	10.974826	5
D	-22.38307	1.755591	5
E	-15.89842	6.260807	5
F	22.09166	15.225877	5
G	8.07098	6.372216	5
I	-6.26253	7.151926	5

L	-28.67046	6.609436	5
N	-14.88824	3.889231	5
T	-39.95144	6.899257	5
U	22.48563	10.070715	5
Total	-6.09737	20.654440	59

Table E14. One-way ANOVA test (Levene's Test of Equality of Error Variances^{a,b,c}).

		Levene Statistic	df1	df2	Sig.
Change in strength	Based on Mean	2.626	12	50	.008
	Based on Median	.988	12	50	.473
	Based on Median and with adjusted df	.988	12	19.144	.493
	Based on trimmed mean	2.373	12	50	.017

Tests the null hypothesis that the error variance of the dependent variable is equal across groups.

a. Dependent variable: Change in strength

b. Design: Intercept + Specimen#

Tests the null hypothesis that the error variance of the dependent variable is equal across groups.

Table E15. One-way ANOVA test (Tests of Between-Subjects Effects^a).

Dependent Variable: Change in strength

Source	Type III Sum of Squares	df	Mean Square	F	Sig.
Corrected Model	22240.653 ^a	12	1853.388	22.017	.000
Intercept	2317.624	1	2317.624	27.532	.000
Time	22240.653	12	1853.388	22.017	.000
Error	4208.913	50	84.178		
Total	28791.771	63			
Corrected Total	26449.565	62			

Tests the null hypothesis that the error variance of the dependent variable is equal across groups.

a. Dependent variable: Change in strength

Table E16. One-way ANOVA test (Multiple Comparisons).

Dependent Variable: Change in strength
Tamhane

(I) Specimen #	(J) Specimen #	Mean Difference (I-J)	Std. Error	Sig.	95% Confidence Interval	
					Lower Bound	Upper Bound
A	B	-6.27594	3.509761	1.000	-29.18477	16.63289
	C	-22.56331	5.378042	.440	-60.69560	15.56898
	D	15.47083	2.334608	.603	-34.03533	64.97699
	E	8.98618	3.559988	.973	-14.15817	32.13053
	F	-29.00390	7.155378	.570	-85.30525	27.29746
	G	-14.98322	3.599305	.376	-38.32574	8.35930
	I	-.64971	3.881234	1.000	-25.69965	24.40022
	L	21.75822	3.683871	.079	-2.04741	45.56386
	N	7.97600	2.803426	.963	-15.94229	31.89430
	T	33.03921*	3.788657	.010	8.59854	57.47988
U	-29.39787	5.011769	.108	-63.98926	5.19352	
B	A	6.27594	3.509761	1.000	-16.63289	29.18477
	C	-16.28737	5.619058	.873	-51.40496	18.83021
	D	21.74677	2.846202	.063	-1.23360	44.72714
	E	15.26212	3.914587	.300	-5.82535	36.34959
	F	-22.72796	7.338250	.863	-75.43552	29.97961
	G	-8.70728	3.950376	.991	-30.00005	12.58550
	I	5.62623	4.208854	1.000	-17.32662	28.57907
	L	28.03416*	4.027577	.009	6.27652	49.79181
	N	14.25195	3.241862	.235	-4.96299	33.46688
	T	39.31515*	4.123639	.001	16.94091	61.68938
U	-23.12193	5.269564	.251	-54.91247	8.66861	
C	A	22.56331	5.378042	.440	-15.56898	60.69560
	B	16.28737	5.619058	.873	-18.83021	51.40496
	D	38.03414	4.970491	.095	-6.87757	82.94586
	E	31.54949	5.650566	.086	-3.42339	66.52237
	F	-6.44059	8.393737	1.000	-54.09219	41.21102
	G	7.58009	5.675420	1.000	-27.29078	42.45097
	I	21.91360	5.858273	.444	-12.49155	56.31875
	L	44.32153*	5.729423	.012	9.63790	79.00517
	N	30.53932	5.207167	.149	-8.70825	69.78688
	T	55.60252*	5.797354	.003	21.09317	90.11187
D	A	-15.47083	2.334608	.603	-64.97699	34.03533
	B	-21.74677	2.846202	.063	-44.72714	1.23360
	C	-38.03414	4.970491	.095	-82.94586	6.87757
	E	-6.48465	2.907914	.999	-30.11786	17.14856
	F	-44.47473	6.854334	.187	-108.18963	19.24017
	G	-30.45405*	2.955917	.018	-54.59448	-6.31362
	I	-16.12054	3.293392	.376	-43.81032	11.56924

	L	6.28739	3.058325	1.000	-18.93323	31.50801
	N	-7.49483	1.908309	.505	-20.55402	5.56437
	T	17.56838	3.183767	.249	-8.97173	44.10848
	U	-44.86870*	4.571682	.034	-85.73918	-3.99822
E	A	-8.98618	3.559988	.973	-32.13053	14.15817
	B	-15.26212	3.914587	.300	-36.34959	5.82535
	C	-31.54949	5.650566	.086	-66.52237	3.42339
	D	6.48465	2.907914	.999	-17.14856	30.11786
	F	-37.99008	7.362405	.209	-90.37676	14.39660
	G	-23.96940*	3.995068	.025	-45.48787	-2.45093
	I	-9.63589	4.250829	.987	-32.73857	13.46679
	L	12.77204	4.071421	.665	-9.18768	34.73177
	N	-1.01018	3.296174	1.000	-20.72132	18.70097
	T	24.05303*	4.166472	.033	1.50493	46.60112
	U	-38.38405*	5.303150	.016	-70.08738	-6.68072
F	A	29.00390	7.155378	.570	-27.29746	85.30525
	B	22.72796	7.338250	.863	-29.97961	75.43552
	C	6.44059	8.393737	1.000	-41.21102	54.09219
	D	44.47473	6.854334	.187	-19.24017	108.18963
	E	37.99008	7.362405	.209	-14.39660	90.37676
	G	14.02068	7.381497	1.000	-38.12317	66.16452
	I	28.35418	7.522996	.553	-22.25746	78.96583
	L	50.76212	7.423099	.054	-.88398	102.40822
	N	36.97990	7.027851	.292	-21.54998	95.50978
	T	62.04310*	7.475655	.019	10.96807	113.11814
	U	-.39397	8.163904	1.000	-48.08277	47.29483
G	A	14.98322	3.599305	.376	-8.35930	38.32574
	B	8.70728	3.950376	.991	-12.58550	30.00005
	C	-7.58009	5.675420	1.000	-42.45097	27.29078
	D	30.45405*	2.955917	.018	6.31362	54.59448
	E	23.96940*	3.995068	.025	2.45093	45.48787
	F	-14.02068	7.381497	1.000	-66.16452	38.12317
	I	14.33351	4.283811	.555	-8.89616	37.56318
	L	36.74144*	4.105844	.002	14.61449	58.86840
	N	22.95922*	3.338600	.023	2.85590	43.06255
	T	48.02243*	4.200116	.000	25.32883	70.71603
	U	-14.41465	5.329624	.917	-46.06111	17.23181
I	A	.64971	3.881234	1.000	-24.40022	25.69965
	B	-5.62623	4.208854	1.000	-28.57907	17.32662
	C	-21.91360	5.858273	.444	-56.31875	12.49155
	D	16.12054	3.293392	.376	-11.56924	43.81032
	E	9.63589	4.250829	.987	-13.46679	32.73857
	F	-28.35418	7.522996	.553	-78.96583	22.25746
	G	-14.33351	4.283811	.555	-37.56318	8.89616
	L	22.40794	4.355105	.068	-1.12196	45.93783

	N	8.62572	3.640773	.987	-14.36783	31.61926
	T	33.68892*	4.444092	.005	9.73962	57.63821
	U	-28.74816	5.523936	.085	-60.25205	2.75574
L	A	-21.75822	3.683871	.079	-45.56386	2.04741
	B	-28.03416*	4.027577	.009	-49.79181	-6.27652
	C	-44.32153*	5.729423	.012	-79.00517	-9.63790
	D	-6.28739	3.058325	1.000	-31.50801	18.93323
	E	-12.77204	4.071421	.665	-34.73177	9.18768
	F	-50.76212	7.423099	.054	-102.40822	.88398
	G	-36.74144*	4.105844	.002	-58.86840	-14.61449
	I	-22.40794	4.355105	.068	-45.93783	1.12196
	N	-13.78222	3.429600	.373	-34.73913	7.17469
	T	11.28098	4.272807	.905	-11.75182	34.31379
	U	-51.15609*	5.387095	.003	-82.71252	-19.59967
	N	A	-7.97600	2.803426	.963	-31.89430
B		-14.25195	3.241862	.235	-33.46688	4.96299
C		-30.53932	5.207167	.149	-69.78688	8.70825
D		7.49483	1.908309	.505	-5.56437	20.55402
E		1.01018	3.296174	1.000	-18.70097	20.72132
F		-36.97990	7.027851	.292	-95.50978	21.54998
G		-22.95922*	3.338600	.023	-43.06255	-2.85590
I		-8.62572	3.640773	.987	-31.61926	14.36783
L		13.78222	3.429600	.373	-7.17469	34.73913
T		25.06320*	3.541917	.025	3.03190	47.09450
U		-37.37387*	4.827948	.038	-72.59973	-2.14802
T		A	-33.03921*	3.788657	.010	-57.47988
	B	-39.31515*	4.123639	.001	-61.68938	-16.94091
	C	-55.60252*	5.797354	.003	-90.11187	-21.09317
	D	-17.56838	3.183767	.249	-44.10848	8.97173
	E	-24.05303*	4.166472	.033	-46.60112	-1.50493
	F	-62.04310*	7.475655	.019	-113.11814	-10.96807
	G	-48.02243*	4.200116	.000	-70.71603	-25.32883
	I	-33.68892*	4.444092	.005	-57.63821	-9.73962
	L	-11.28098	4.272807	.905	-34.31379	11.75182
	N	-25.06320*	3.541917	.025	-47.09450	-3.03190
	U	-62.43708*	5.459287	.001	-93.93949	-30.93467
	U	A	29.39787	5.011769	.108	-5.19352
B		23.12193	5.269564	.251	-8.66861	54.91247
C		6.83456	6.661323	1.000	-29.17722	42.84633
D		44.86870*	4.571682	.034	3.99822	85.73918
E		38.38405*	5.303150	.016	6.68072	70.08738
F		.39397	8.163904	1.000	-47.29483	48.08277
G		14.41465	5.329624	.917	-17.23181	46.06111
I		28.74816	5.523936	.085	-2.75574	60.25205
L		51.15609*	5.387095	.003	19.59967	82.71252

	N	37.37387*	4.827948	.038	2.14802	72.59973
	T	62.43708*	5.459287	.001	30.93467	93.93949

Based on observed means.

The error term is Mean Square(Error) = 84.178.

*. The mean difference is significant at the .05 level.

Appendix F: Summary of Descriptive Statistics, Levene's Test of Equality of Error Variances, Tests of Between-Subjects Effects, and Multiple Comparisons for shrinkage for all fabrics tested

Table F1. One-way ANOVA test for Fabric A.

Descriptive Statistics^a

Dependent Variable: shrinkage

Time	Mean	Std. Deviation	N
0	,0000	,00000	5
2	1,7500	,68465	5
4	2,2500	,55902	5
6	3,5000	,55902	5
8	3,7500	,00000	5
10	3,8750	,27951	5
Total	2,5208	1,45407	30

a. Fabric # = A

Levene's Test of Equality of Error Variances^{a,b,c}

		Levene Statistic	df1	df2	Sig.
change in shrinkage	Based on Mean	6,474	5	24	,001
	Based on Median	,920	5	24	,485
	Based on Median and with adjusted df	,920	5	13,043	,498
	Based on trimmed mean	5,015	5	24	,003

Tests the null hypothesis that the error variance of the dependent variable is equal across groups.a,b,c

a. Fabric = A

b. Dependent variable: shrinkage

c. Design: Intercept + Time

Tests of Between-Subjects Effects^a

Dependent Variable: shrinkage

Source	Type III Sum of Squares	df	Mean Square	F	Sig.
Corrected Model	56,628 ^b	5	11,326	57,987	,000
Intercept	190,638	1	190,638	976,067	,000
Time	56,628	5	11,326	57,987	,000
Error	4,688	24	,195		
Total	251,953	30			
Corrected Total	61,315	29			

a. Specimen # = A

b. R Squared = ,924 (Adjusted R Squared = ,908)

Multiple Comparisons^a

Dependent Variable: shrinkage							
	(I) Time	(J) Time	Mean Difference (I-J)	Std. Error	Sig.	95% Confidence Interval	
						Lower Bound	Upper Bound
Tamhane	0	2	-1,7500	,30619	,067	-3,6526	,1526
		4	-2,2500*	,25000	,013	-3,8034	-,6966
		6	-3,5000*	,25000	,002	-5,0534	-1,9466
		8	-3,7500	,00000	000.	-3,7500	-3,7500
		10	-3,8750*	,12500	,000	-4,6517	-3,0983

Based on observed means.

The error term is Mean Square(Error) = .195.^a

*. The mean difference is significant at the .05 level.

a. Fabric = A

Table F2. One-way ANOVA test for Fabric B.

Descriptive Statistics^a

Dependent Variable: shrinkage

Time	Mean	Std. Deviation	N
0	,0000	,00000	5
2	,0000	,00000	5
4	,2500	,34233	5
6	,7500	,52291	5
8	1,0000	,55902	5
10	1,0000	,55902	5
Total	,5000	,57797	30

a. Specimen # = B

Levene's Test of Equality of Error Variances^{a,b,c}

		Levene Statistic	df1	df2	Sig.
change in shrinkage	Based on Mean	3,860	5	24	,010
	Based on Median	,818	5	24	,549
	Based on Median and with adjusted df	,818	5	13,260	,558
	Based on trimmed mean	3,073	5	24	,028

Tests the null hypothesis that the error variance of the dependent variable is equal across groups.a,b,c

a. Fabric = B

b. Dependent variable: shrinkage

c. Design: Intercept + Time

Tests of Between-Subjects Effects^a

Dependent Variable: shrinkage

Source	Type III Sum of Squares	df	Mean Square	F	Sig.
Corrected Model	5,625 ^b	5	1,125	6,646	,001
Intercept	7,500	1	7,500	44,308	,000
Time	5,625	5	1,125	6,646	,001
Error	4,063	24	,169		
Total	17,188	30			
Corrected Total	9,688	29			

a. Specimen # = B

b. R Squared = ,581 (Adjusted R Squared = ,493)

Multiple Comparisons^a

Dependent Variable: shrinkage

	(I) Time	(J) Time	Mean Difference (I-J)	Std. Error	Sig.	95% Confidence Interval	
						Lower Bound	Upper Bound
Tamhane	0	2	,0000	,00000	1,000	,0000	,0000
		4	-,2500	,15309	,947	-1,2013	,7013
		6	-,7500	,23385	,392	-2,2031	,7031
		8	-1,0000	,25000	,216	-2,5534	,5534
		10	-1,0000	,25000	,216	-2,5534	,5534

Based on observed means.

The error term is Mean Square(Error) = .169.^a

*. The mean difference is significant at the .05 level.

a. Fabric = B

Table F3. One-way ANOVA test for Fabric C.

Descriptive Statistics^a

Dependent Variable: shrinkage

Time	Mean	Std. Deviation	N
0	,0000	,00000	5
2	,1250	,27951	5
4	,1250	,27951	5
6	,1250	,27951	5
8	,6250	,62500	5
10	,6250	,62500	5
Total	,2500	,45248	30

a. Specimen # = C

Levene's Test of Equality of Error Variances^{a,b,c}

		Levene Statistic	df1	df2	Sig.
change in shrinkage	Based on Mean	7,153	5	24	,000
	Based on Median	5,200	5	24	,002
	Based on Median and with adjusted df	5,200	5	16,000	,005
	Based on trimmed mean	6,785	5	24	,000

Tests the null hypothesis that the error variance of the dependent variable is equal across groups.a,b,c

a. Fabric = C

b. Dependent variable: shrinkage

c. Design: Intercept + Time

Tests of Between-Subjects Effects^a

Dependent Variable: shrinkage

Source	Type III Sum of Squares	df	Mean Square	F	Sig.
Corrected Model	2,187 ^b	5	,437	2,800	,040
Intercept	1,875	1	1,875	12,000	,002
Time	2,188	5	,438	2,800	,040
Error	3,750	24	,156		
Total	7,813	30			
Corrected Total	5,937	29			

a. Specimen # = C

b. R Squared = ,368 (Adjusted R Squared = ,237)

Multiple Comparisons^a

Dependent Variable: shrinkage

	(I) Time	(J) Time	Mean Difference (I-J)	Std. Error	Sig.	95% Confidence Interval	
						Lower Bound	Upper Bound
Tamhane	0	2	,0000	,00000	,999	,0000	,0000
		4	-,1250	,12500	,999	-,9017	,6517
		6	-,1250	,12500	,999	-,9017	,6517
		8	-,6250	,27951	,753	-2,3618	1,1118
		10	-,6250	,27951	,753	-2,3618	1,1118

Based on observed means.

The error term is Mean Square(Error) = .156.^a

*. The mean difference is significant at the .05 level.

a. Fabric = C

Table F4. One-way ANOVA test for Fabric D.

Descriptive Statistics^a

Dependent Variable: shrinkage

Time	Mean	Std. Deviation	N
0	,0000	,00000	5
2	,2500	,55902	5
4	1,0000	,55902	5
6	1,2500	,00000	5
8	1,6250	,55902	5
10	1,6250	,55902	5
Total	,9583	,76517	30

a. Specimen # = D

Levene's Test of Equality of Error Variances^{a,b,c}

		Levene Statistic	df1	df2	Sig.
change in shrinkage	Based on Mean	4,247	5	24	,007
	Based on Median	,700	5	24	,629
	Based on Median and with adjusted df	,700	5	16,000	,631
	Based on trimmed mean	3,339	5	24	,020

Tests the null hypothesis that the error variance of the dependent variable is equal across groups.a,b,c

a. Fabric = D

b. Dependent variable: shrinkage

c. Design: Intercept + Time

Tests of Between-Subjects Effects^a

Dependent Variable: shrinkage

Source	Type III Sum of Squares	df	Mean Square	F	Sig.
Corrected Model	11,979 ^b	5	2,396	11,500	,000
Intercept	27,552	1	27,552	132,250	,000
Time	11,979	5	2,396	11,500	,000
Error	5,000	24	,208		
Total	44,531	30			
Corrected Total	16,979	29			

a. Specimen # = D

b. R Squared = ,706 (Adjusted R Squared = ,644)

Table F5. One-way ANOVA test for Fabric E.

Descriptive Statistics^a

Dependent Variable: shrinkage

Time	Mean	Std. Deviation	N
0	,0000	,00000	5
2	,7500	,68465	5
4	,8750	,55902	5
6	1,6250	,55902	5
8	1,6250	,55902	5
10	2,0000	,68465	5
Total	1,1458	,85418	30

a. Specimen # = E

Levene's Test of Equality of Error Variances^{a,b,c}

		Levene Statistic	df1	df2	Sig.
change in shrinkage	Based on Mean	6,783	5	24	,000
	Based on Median	,542	5	24	,743
	Based on Median and with adjusted df	,542	5	19,200	,742
	Based on trimmed mean	5,879	5	24	,001

Tests the null hypothesis that the error variance of the dependent variable is equal across groups.a,b,c

a. Fabric = E

b. Dependent variable: shrinkage

c. Design: Intercept + Time

Tests of Between-Subjects Effects^a

Dependent Variable: shrinkage

Source	Type III Sum of Squares	df	Mean Square	F	Sig.
Corrected Model	13,659 ^b	5	2,732	8,742	,000
Intercept	39,388	1	39,388	126,042	,000
Time	13,659	5	2,732	8,742	,000
Error	7,500	24	,313		
Total	60,547	30			
Corrected Total	13,659 ^b	5	2,732	8,742	,000

a. Specimen # = E

b. R Squared = ,646 (Adjusted R Squared = ,572)

Multiple Comparisons^a

Dependent Variable: shrinkage

	(I) Time	(J) Time	Mean Difference (I-J)	Std. Error	Sig.	95% Confidence Interval	
						Lower Bound	Upper Bound
Tamhane	0	2	-,7500	,30619	,666	-2,6526	1,1526
		4	-,8750	,25000	,315	-2,4284	,6784
		6	-1,6250*	,25000	,042	-3,1784	-,0716
		8	-1,6250*	,25000	,042	-3,1784	-,0716
		10	-2,0000*	,30619	,042	-3,9026	-,0974

Based on observed means.

The error term is Mean Square(Error) = .200.^a

*. The mean difference is significant at the .05 level.

a. Fabric = E

Table F6. One-way ANOVA test for Fabric E.

Descriptive Statistics^a

Dependent Variable: shrinkage

Time	Mean	Std. Deviation	N
0	,0000	,00000	5
2	,0000	,00000	5
4	,0000	,00000	5
6	,5000	,68465	5
8	1,0000	1,04583	5
10	1,7500	,68465	5
Total	,5417	,84864	30

a. Specimen # = F

Levene's Test of Equality of Error Variances^{a,b,c}

		Levene Statistic	df1	df2	Sig.
change in shrinkage	Based on Mean	12,558	5	24	,000
	Based on Median	2,356	5	24	,071
	Based on Median and with adjusted df	2,356	5	12,000	,104
	Based on trimmed mean	12,653	5	24	,000

Tests the null hypothesis that the error variance of the dependent variable is equal across groups.a,b,c

a. Fabric = F

b. Dependent variable: shrinkage

c. Design: Intercept + Time

Tests of Between-Subjects Effects^a

Dependent Variable: shrinkage

Source	Type III Sum of Squares	df	Mean Square	F	Sig.
Corrected Model	12,760 ^b	5	2,552	7,538	,000
Intercept	8,802	1	8,802	26,000	,000
Time	12,760	5	2,552	7,538	,000
Error	8,125	24	,339		
Total	29,688	30			
Corrected Total	20,885	29			

a. Specimen # = F

b. R Squared = ,611 (Adjusted R Squared = ,530)

Multiple Comparisons^a

Dependent Variable: shrinkage

	(I) Time	(J) Time	Mean Difference (I-J)	Std. Error	Sig.	95% Confidence Interval	
						Lower Bound	Upper Bound
Tamhane	0	2	,0000	,00000	.	,0000	,0000
		4	,0000	,00000	.	,0000	,0000
		6	-,5000	,30619	,947	-2,4026	1,4026
		8	-1,0000	,46771	,792	-3,9062	1,9062
		10	-1,7500	,30619	,067	-3,6526	,1526

Based on observed means.

The error term is Mean Square(Error) = .339.^a

*. The mean difference is significant at the .05 level.

a. Fabric = F

Table F7. One-way ANOVA test for Fabric G.

Descriptive Statistics^a

Dependent Variable: shrinkage

Time	Mean	Std. Deviation	N
0	,0000	,00000	5
2	,2500	,55902	5
4	,5000	,68465	5
6	1,3750	,27951	5
8	1,3750	,27951	5
10	1,3750	,27951	5
Total	,8125	,69925	30

a. Specimen # = G

Levene's Test of Equality of Error Variances^{a,b,c}

		Levene Statistic	df1	df2	Sig.
change in shrinkage	Based on Mean	5,936	5	24	,001
	Based on Median	,877	5	24	,511
	Based on Median and with adjusted df	,877	5	12,291	,524
	Based on trimmed mean	4,738	5	24	,004

Tests the null hypothesis that the error variance of the dependent variable is equal across groups.a,b,c

a. Fabric = G

b. Dependent variable: shrinkage

c. Design: Intercept + Time

Tests of Between-Subjects Effects^a

Dependent Variable: shrinkage

Source	Type III Sum of Squares	df	Mean Square	F	Sig.
Corrected Model	10,117 ^b	5	2,023	11,954	,000
Intercept	19,805	1	19,805	117,000	,000
Time	10,117	5	2,023	11,954	,000
Error	4,063	24	,169		
Total	33,984	30			
Corrected Total	14,180	29			

a. Specimen # = G

b. R Squared = ,713 (Adjusted R Squared = ,654)

Multiple Comparisons^a

Dependent Variable: shrinkage

	(I) Time	(J) Time	Mean Difference (I-J)	Std. Error	Sig.	95% Confidence Interval	
						Lower Bound	Upper Bound
Tamhane	0	2	-,2500	,25000	,999	-1,8034	1,3034
		4	-,5000	,30619	,947	-2,4026	1,4026
		6	-1,3750*	,12500	,006	-2,1517	-,5983
		8	-1,3750*	,12500	,006	-2,1517	-,5983
		10	-1,3750*	,12500	,006	-2,1517	-,5983

Based on observed means.

The error term is Mean Square(Error) = .169.^a

*. The mean difference is significant at the .05 level.

a. Fabric = G

Table F8. One-way ANOVA test for Fabric I.

Descriptive Statistics^a

Dependent Variable: shrinkage

Time	Mean	Std. Deviation	N
0	,0000	,00000	5
2	,0000	,00000	5
4	,3750	,55902	5
6	1,3750	,68465	5
8	1,8750	,62500	5
10	2,1250	,71261	5
Total	,9583	1,00823	30

a. Specimen # = I

Levene's Test of Equality of Error Variances^{a,b,c}

		Levene Statistic	df1	df2	Sig.
change in shrinkage	Based on Mean	4,023	5	24	,009
	Based on Median	1,664	5	24	,182
	Based on Median and with adjusted df	1,664	5	13,812	,209
	Based on trimmed mean	3,777	5	24	,012

Tests the null hypothesis that the error variance of the dependent variable is equal across groups.a,b,c

a. Fabric = I

b. Dependent variable: shrinkage

c. Design: Intercept + Time

Tests of Between-Subjects Effects^a

Dependent Variable: shrinkage

Source	Type III Sum of Squares	df	Mean Square	F	Sig.
Corrected Model	22,760 ^b	5	4,552	16,260	,000
Intercept	27,552	1	27,552	98,419	,000
Time	22,760	5	4,552	16,260	,000
Error	6,719	24	,280		
Total	57,031	30			
Corrected Total	29,479	29			

a. Specimen # = I

b. R Squared = ,772 (Adjusted R Squared = ,725)

Multiple Comparisons^a

Dependent Variable: shrinkage

	(I) Time	(J) Time	Mean Difference (I-J)	Std. Error	Sig.	95% Confidence Interval	
						Lower Bound	Upper Bound
Tamhane	0	2	,0000	,00000	.	,0000	,0000
		4	-,3750	,25000	,970	-1,9284	1,1784
		6	-1,3750	,30619	,152	-3,2776	,5276
		8	-1,8750*	,27951	,038	-3,6118	-,1382
		10	-2,1250*	,31869	,039	-4,1053	-,1447

Based on observed means.

The error term is Mean Square(Error) = .280.^a

*. The mean difference is significant at the .05 level.

a. Fabric = I

Table F9. One-way ANOVA test for Fabric L.

Descriptive Statistics^a

Dependent Variable: shrinkage

Time	Mean	Std. Deviation	N
0	,0000	,00000	5
2	,3750	,55902	5
4	,8750	,55902	5
6	1,3750	,68465	5
8	1,6250	,83853	5
10	1,6250	,83853	5
Total	,9792	,86359	30

a. Specimen # = N

Levene's Test of Equality of Error Variances^{a,b,c}

		Levene Statistic	df1	df2	Sig.
change in shrinkage	Based on Mean	3,806	5	24	,011
	Based on Median	,918	5	24	,486
	Based on Median and with adjusted df	,918	5	19,755	,490
	Based on trimmed mean	3,658	5	24	,013

Tests the null hypothesis that the error variance of the dependent variable is equal across groups.a,b,c

a. Fabric = N

b. Dependent variable: shrinkage

c. Design: Intercept + Time

Tests of Between-Subjects Effects^a

Dependent Variable: shrinkage

Source	Type III Sum of Squares	df	Mean Square	F	Sig.
Corrected Model	11,628 ^b	5	2,326	5,581	,002
Intercept	28,763	1	28,763	69,031	,000
Time	11,628	5	2,326	5,581	,002
Error	10,000	24	,417		
Total	50,391	30			
Corrected Total	21,628	29			

a. Specimen # = N

b. R Squared = ,538 (Adjusted R Squared = ,441)

Multiple Comparisons^a

Dependent Variable: shrinkage

	(I) Time	(J) Time	Mean Difference (I-J)	Std. Error	Sig.	95% Confidence Interval	
						Lower Bound	Upper Bound
Tamhane	0	2	-,3750	,25000	,970	-1,9284	1,1784
		4	-,8750	,25000	,315	-2,4284	,6784
		6	-1,3750	,30619	,152	-3,2776	,5276
		8	-1,6250	,37500	,170	-3,9552	,7052
		10	-1,6250	,37500	,170	-3,9552	,7052

Based on observed means.

The error term is Mean Square(Error) = .417.^a

*. The mean difference is significant at the .05 level.

a. Fabric = N